Interactions of the *Treponema pallidum* adhesin Tp0751 with the human vascular endothelium

by

Karen V. Lithgow
BSc, University of Alberta, 2013

A Dissertation Submitted in Partial Fulfillment
of the Requirements for the Degree of

DOCTOR OF PHILOSOPHY

in the Department of Biochemistry & Microbiology

Supervisory Committee

Interactions of the *Treponema pallidum* adhesin Tp0751 with the human vascular endothelium

by

Karen V. Lithgow
BSc, University of Alberta, 2013

Supervisory Committee

Dr. Caroline E. Cameron, Department of Biochemistry & Microbiology
Supervisor

Dr. Perry Howard, Department of Biochemistry & Microbiology
Departmental Member

Dr. John E. Burke, Department of Biochemistry & Microbiology
Departmental Member

Dr. Fraser Hof, Department of Chemistry
Outside Member

Abstract

Treponema pallidum ssp. *pallidum* is the causative agent of syphilis, a sexually transmitted infection characterized by multi-stage disease and diverse clinical manifestations. *Treponema pallidum* undergoes rapid vascular dissemination to penetrate tissue, placental, and blood-brain barriers and gain access to distant tissue and organ sites. The rapidity and extent of *T. pallidum* dissemination is well documented, but the molecular mechanisms that underlie this process have yet to be fully elucidated. Tp0751 is a *T. pallidum* adhesin that interacts with vascular factors and mediates adherence to endothelial cells under shear flow. This dissertation explores the molecular interactions and functional outcomes of Tp0751-mediated vascular endothelium adhesion.

The findings presented herein demonstrate that recombinant Tp0751 adheres to human macrovascular and microvascular endothelial cells, including cerebral brain endothelial cells. This interaction is confirmed using live *T. pallidum,* where spirochete-endothelial cells interactions are disrupted with Tp0751-specific antiserum. Further, the 67 kDa laminin receptor (LamR) is identified as an endothelial receptor using affinity chromatography coupled with mass spectrometry to isolate and identify Tp0751-interacting proteins from endothelial cells membrane extracts. Notably, LamR is a brain endothelial cell receptor for other neurotropic invasive pathogens. Evaluation of endothelial intercellular junctions reveals that recombinant Tp0751 and live *T. pallidum* disrupt junctional architecture. However, transwell solute flux assays reveal that Tp0751 and *T. pallidum* do not alter endothelial barrier integrity. The transendothelial migration of *T. pallidum* can be partially abrogated with an endocytosis inhibitor, implying a transcellular route for barrier traversal. However, a subpopulation of *T. pallidum* localizes to intercellular junctions, indicating paracellular traversal may also be employed. These findings enhance our understanding of the mechanics of *T. pallidum* attachment to endothelial cells and suggest that *T. pallidum* may use both paracellular and transcellular mechanisms to traverse the vascular endothelium without altering barrier permeability. A more complete understanding of this process will facilitate vaccine development for syphilis.

Table of Contents

List of Tables

List of Figures

List of Abbreviations

Abbreviation	Meaning
ACN	Acetonitrile
Amiloride	5-(*N*-ethyl-*N*-isopropyl)amiloride
ANOVA	Analysis of Variance
Arf6	Adenosine diphosphate-ribosylation factor 6
ATP	Adenosine triphosphate
B. burgdorferi	*Borrelia burgdorferi*
BBB	Blood-brain barrier
Bb-Tp0751	Tp0751-expressing *Borrelia burgdorferi*
BCA	Bicinchoninic acid
bEC	Brain endothelial cells (hCMEC/d3)
BS^3	bis(sulfosuccinimidyl)suberate
BSA	Bovine serum albumin
BSK II	Barbour-Stoenner-Kelly-II
CCAC	Canadian Council on Animal Care
Cdk5	Cyclin-dependent kinase 5
CHAPS	(3-((3-chloamidopropyl) dimethylammonio-1-propanesulfonate)
CNF1	Cytotoxic necrotizing factor
CNS	Central nervous system
DALY	Disability-adjusted life year
DAPI	4',6-diamidino-2-phenylindole
dFBS	Dialyzed fetal bovine serum
DMEM	Dulbecco's modified Eagle's medium
DMSO	Dimethyl sulfoxide
DOC	Deoxycholate
DTT	Dithiothreitol
E. coli	*Escherichia coli*
ECIS	Electrical cell-substrate impedance sensing
ECM	Extracellular matrix
EGM-2	Endothelial growth medium 2
ERK1/2	Extracellular signal-regulated kinase 1/2
F-actin	Filamentous actin
fHbp	Factor H binding protein
FITC	Fluorescein isothiocyanate
FOV	Field of view
GAPDH	Glyceraldehyde 3-phosphate dehydrogenase
gDNA	Genomic DNA
GFP	Green fluorescent protein
Gpd	Glycerophosphodiester phosphodiesterase
GRAF1	GTPase regulator associated with focal adhesion kinase-1
H. influenzae	*Haemophilus influenzae*
HBSS	HEPES buffered saline solution

hCMEC/d3	Human cerebral microvascular endothelial cells
HIV	Human immunodeficiency virus
hMVECd	Human dermal microvascular endothelial cells
HPLC	HPLC
HUVEC	Human umbilical vein endothelial cells
IB	Immunoblotting
IP	Immunoprecipitation
JAMs	Junctional adhesion molecules
LamR	67 kDa laminin receptor
LC-MS/MS	Liquid chromatography tandem mass spectrometry
LPS	lipopolysaccharide
MMP9	Matrix metallopeptidase 9
MSM	Men-who-have-sex-with-men
MTCT	Mother-to-child tranmission
MW	Molecular weight
MWCO	Molecular weight cut off
N. meningitidis	*Neisseria meningitidis*
NGAL	Neutrophil gelatinase-associated lipocalin
Ni-HRP	Nickel horseradish peroxidase
NRS	Normal rabbit serum
N-WASP	Neural Wiskott-Aldrich syndrome protein
p10	Synthetic Tp0751 peptide spanning amino acids R172-F196
p11	Synthetic Tp0751 peptide spanning amino acids S185-V209
p4	Synthetic Tp0751 peptide spanning amino acids G88-A112
p6	Synthetic Tp0751 peptide spanning amino acids Q117-I141
PAR3	Partitioning-defective 3
PAR6	Partitioning-defective 6
Parent	Non-infectious, adhesion-attenuated, GFP-expressing strain of *B. burgdorferi*
PBS	Phosphate buffered saline
PFA	Paraformaldehyde
pFN	Plasma fibronectin
PrEP	Pre-exposure prophylaxis
qPCR	Quantitative real-time polymerase chain reaction
RT	Room temperature
S. pneumoniae	*Streptococcus pneumoniae*
Scr	Scrambled
SDS	Sodium dodecyl sulfate
SDS-PAGE	Sodium dodecyl sulfate polyacrylamide gel electrophoresis
SEM	Standard error of the mean
sFN	Super fibronectin
SILAC	Stabile Isotope Labeling by Amino Acids in Cell Culture
SP	Signal peptide
Super FN	Super fibronectin

T. pallidum	*Treponema pallidum* subspecies *pallidum*
TBS	Tris buffered saline
TEER	Transendothelial electrical resistance
TEx	Testicular extract
TFA	Trifluoroacetic acid
TiO_2	Titanium dioxide
TLR2	Toll like receptor 2
TMB	3,3’,5,5’-Tetramethylbenzidine
Tp	*T. pallidum*
TX-100	Triton X-100
VE-cadherin	Vascular endothelial-cadherin
VVO	Vesiculo-vacuolar organelle
WHO	World Health Organization

Acknowledgments

To my incredible supervisor: Dr. Caroline Cameron. You have been a huge inspiration to me since day one and I can't think of a better mentor to have guided me through this experience. Thank you for providing me with every opportunity to learn, grow and succeed. Your guidance and support have been invaluable; I am so grateful for everything you have invested in me.

A sincere thank you to my supervisory committee members: Dr. Fraser Hof, Dr. John Burke and Dr. Perry Howard. Your guidance has been instrumental to my degree progress and I genuinely appreciate the time and intellectual contributions each of you has made to my thesis work.

I have had the pleasure of working with wonderful collaborators during my degree. Thank you to: Dr. Tara Moriarty for your insight and guidance on my project over the years; Dr. Leigh Anne Swayne for your scientific enthusiasm, positive energy and for always making the time to discuss my work; Dr. Leonard Foster and Jenny (Kyung-Mee) Moon for your contributions to the phosphoproteomics project.

There have been so many fantastic members of the Cameron Lab over the years and each person has shaped my experience and contributed to my development as a scientist in unique ways. Thank you to: Becky and Charmaine for welcoming me into the lab, training me and guiding my work; Simon Houston for all your intellectual input; the wonderful undergraduate students who have provided invaluable support and input on various projects: Anita Weng, Nina Radisavljevic, Emily Tsao, and Sean Waugh. You all have bright futures ahead of you; Brigette Church for keeping me company on long experimental days and always providing unique perspectives on science and the world. Finally, thank you to Alloysius Martin for your constant support, incredible work ethic, and willingness to go to great lengths to make sure my experiments succeed.

To my wonderful family: thank you for your endless support and encouragement over the years. Mom and Chris: for your willingness to learn about my research has meant the world to me; Dad: for highlighting the importance of my education from a young age; Kirstie: your intense dedication continues to inspire me to succeed; Trent your compassion does not go unnoticed.

To the Thomson family: Jane, Callum, Dugald, Meg, Maisie (in no particular order) and Jimmy. Thank you for helping me keep things in perspective, for supporting my work and distracting me with family dinners, ski weekends and epic adventures when I need it the most.

To the other band members of The Copper Lights: Euan Thomson, Jill Hesser, and Brem Smith: thank you for the comradery, jams, and the endless laughter. This artistic outlet has kept me grounded and has been a highlight of my time in Victoria.

My sanity would surely be in question without the beloved dogs in my life. To the late Buddy Mahkesis – you were a best friend that brought joy to even the hardest days. You have been dearly missed. And to our GSD: Iggy Pup, you've taught me so much about patience and perseverance. Your (mostly) well-timed distractions have kept me mentally and physically healthy during the last 6 months of my degree.

Euan: it's impossible to put into words what your support has meant to me over the years. Thank you for being my champion, inspiring me to think outside the box, and reminding me about the important things in life. Most importantly, thank you for keeping me sufficiently caffeinated.

Dedication

For my partner Euan, who has been my co-pilot on adventures of all varieties.

Your unwavering support and encouragement have kept me afloat during this particularly challenging intellectual adventure.

Chapter 1: Introduction

1.1 Syphilis

Syphilis is a chronic human-specific sexually transmitted infection caused by the spirochete bacterium *Treponema pallidum* subsp. *pallidum* that presents in multiple stages with diverse clinical manifestations (Lafond and Lukehart 2006). Despite continued sensitivity to penicillin, syphilis remains a global health concern for which no vaccine is available (World Health Organization 2016a).

1.1.1 Epidemiology

The World Health Organization (WHO) estimates there are 18 million syphilis cases worldwide, with 5.6 million new cases emerging per annum (Newman et al. 2015). Although syphilis rates are highest in low- and middle-income regions (World Health Organization 2016a), high-income settings including Canada (Public Health Agency of Canada 2017), Europe (Herbert and Middleton 2012; Savage et al. 2009), the United Kingdom (Savage et al. 2012; Simms et al. 2005), China (Tucker and Cohen 2011; Tucker, Chen, and Peeling 2010; Newman et al. 2015; Chen et al. 2017), and the United States (Patton et al. 2014; Centers for Disease Control and Prevention 2019) are experiencing increasing syphilis rates. In the United States there was a 73% increase in syphilis cases between 2013 and 2017. It is estimated that 68% of syphilis cases in the United States occur in the men-who-have-sex-with-men (MSM) population and recent reports reveal trends toward increasing rates among women. In fact, the rates of syphilis in the United States are increasing among all racial and Hispanic ethnicity groups and in 72% of states across the country (Centers for Disease Control and Prevention 2019). In Canada, syphilis rates increased by 86% between 2010 and 2015, corresponding to a 90.2% increase in males and a 27.8% increase amongst females (Choudhri et al. 2018). Of utmost concern is the increasing predominance of congenital syphilis, which continues to contribute substantially to adverse pregnancy outcomes including stillbirth, early neonatal death, and pre-term birth (Newman et al. 2013). In 2012 the WHO estimated that more than 900,000 pregnant women had an active syphilis infection, resulting in 200,000 cases of stillbirth or neonatal death (Wijesooriya et al. 2016). Rates of congenital syphilis in the United States have

increased yearly since 2013, with a 153.3% increase between 2013 and 2017 (Centers for Disease Control and Prevention 2019). Additionally, active syphilis infections increase the risk of HIV acquisition and transmission by three to five-fold (Greenblatt et al. 1988; Stamm et al. 1988; Centers for Disease Control and Prevention 1998) and have been associated with increased HIV viral loads (Jarzebowski et al. 2012; Buchacz et al. 2004). Based on the observed global increases in rates of active syphilis infections (World Health Organization 2016a), it is clear that current screening and treatment protocols are not adequate for controlling spread of the disease. An improved understanding of syphilis disease progression and *T. pallidum* pathogenicity is essential to finding better strategies to curb syphilis infections globally.

1.1.2 Disease progression

The disease progression of syphilis is complicated with diverse clinical manifestations and multiple stages of active disease interspersed with periods of asymptomatic latency Variability in the presentation of symptoms at each stage of the disease coupled with unpredictable durations of active and latent stages can confound diagnosis. Early syphilis includes the primary, secondary, and early latent stage of the disease, while late syphilis encompasses late latent and tertiary stages (Figure 1).

Transmission and Local Infection

Transmission

Infection with *T. pallidum* most commonly occurs via sexual transmission at mucous membranes or dermal microabrasions of genital regions (Stoltey and Cohen 2015), but can also be transmitted vertically from a pregnant woman to her fetus, via blood transfusions, through sharing infected needles, or by contact between lesions and mucous membranes or broken skin. It is thought that sexual transmission can only occur during primary and secondary stages, while congenital transmission can occur at any stage of the disease progression including latency (Hook 2017).

Primary syphilis

Primary lesions typically present as single, painless, ulcerative lesions at the site of infection and heal spontaneously after four to six weeks (Lafond and Lukehart 2006; Chapel 1978). Multiple primary lesions can also manifest, most commonly in HIV-positive patients (Rompalo et al. 2001; Hourihan et al. 2004) as can non-classical presentations of the chancres (Chapel 1978). Regional lymphadenopathy, in which lymph nodes localized near the site of infection undergo moderate inflammation may also occur during the primary stage (Lafond and Lukehart 2006). The development of primary lesions can be attributed to localized inflammatory immune reactions to proliferating *T. pallidum* (Carlson et al. 2011) and local clearance of *T. pallidum* is mediated by antibody-dependent phagocytosis by macrophages, also known as opsonophagocytosis (Hawley et al. 2017; Lukehart and Miller 1978; Baker-Zander, Shaffer, and Lukehart 1993).

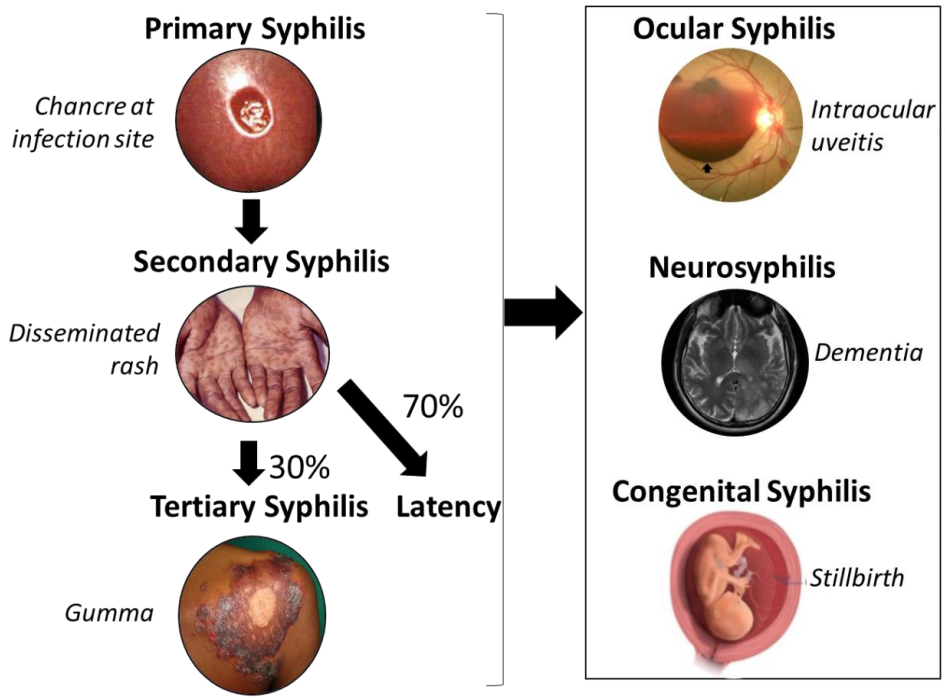

Figure 1: The disease progression of untreated syphilis. Early syphilis encompasses primary, secondary and early latent (<2 years post-infection) stages of the disease, while late syphilis includes tertiary syphilis and late latency (>2 years post-infection). Characteristic symptoms of each stage are shown. At any point during the disease progression patients can experience ocular or neurological involvement, or vertical transmission from a pregnant woman to the unborn fetus.

Disseminated Infection

Secondary syphilis

Within hours of infection *T. pallidum* gains access to the host circulatory and lymphatic systems to mediate widespread dissemination, invading into distant tissue and organ sites (Stokes 1944; Cumberland MC 1949; Raiziss GW 1937). Progression to secondary syphilis occurs in 90% of untreated patients (Gjestland 1955) and is typified by systemic lymphadenopathy and an infectious disseminated mucocutaneous rash. Disseminated *T. pallidum* accesses epidermal and subepidermal locales via blood vessels and perivascular lymphatics where organisms multiply, inducing host immune cellular infiltration and inflammation that underlies the formation of the secondary lesion. Additional systemic symptoms of the secondary stage include fever, malaise, weight loss, sore throat, headache, and muscle aches (Baughn and Musher 2005). Less frequently, glomerulonephritis (Bansal et al. 1978; O'Regan et al. 1976; Tourville et al. 1976), arthritis, alopecia and ocular involvement can also occur (Hira et al. 1987; Mindel et al. 1989). Similar to the primary stage, secondary lesions heal spontaneously within three to eight weeks (Baughn and Musher 2005), and other symptoms generally resolve within three months (Lafond and Lukehart 2006).

Latent syphilis

Following the secondary stage, untreated patients enter a latent stage of varying duration. Within two years post-infection this is classified as early latent syphilis (World Health Organization 2016a), wherein 25% of patients may revert back to the secondary stage (Gjestland 1955). Asymptomatic infection beyond two years post-infection is classified as late latent syphilis (World Health Organization 2016a), and 70% percent of patients will remain in asymptomatic latency with no further complications (Lafond and Lukehart 2006).

Tertiary syphilis

The onset of tertiary syphilis is typically 20-40 years post-infection and occurs in 30% of untreated patients. Tertiary syphilis includes some of the most severe clinical manifestations of the disease including gumma and cardiovascular and neurological

complications (Gjestland 1955; Kampmeier 1972). Since the introduction of penicillin as an effective treatment, progression to tertiary syphilis is rare (Hook 2017). Localized bone and tissue damage (gumma) is the most common symptom of tertiary syphilis, occurring in 15% of untreated patients. Gumma are predominantly localized to bone or skin but can also present on internal organs (Gjestland 1955; Kampmeier 1972). Gumma formation on critical organs such as the heart and brain underlie some of the most severe cardiovascular and neurological complications including aneurysm and paralysis or dementia, respectively (Byard 2018). Treponemes can be detected in gummateous lesions (Handsfield et al. 1983) but unlike lesions of early syphilis, resolution typically does not occur without antibiotic treatment (Lafond and Lukehart 2006). Prior to the introduction of penicillin therapy, cardiovascular involvement during tertiary syphilis was a major contributor to patient mortality. Cardiovascular complications arose in up to 10% of untreated patients, with aortic inflammation (aortitis) of varying severity being the most common symptom. The most severe cardiovascular manifestations associated with tertiary syphilis include aortic regurgitation (valve failure in the aorta), ostial stenosis (blood vessel narrowing in the heart), saccular brain aneurysm and ischemic stroke (Kampmeier 1946, 1948, 1972; Weinstein, Kampmeier, and Harwood 1957; Kampmeier 1964).

Disseminated Infection in Immune Privileged Sites

The widespread dissemination of treponemes during syphilis extends to immune privileged sites including the central nervous system (CNS), placenta, and ocular structures (Lukehart SA 1988; Chawla, Gupta, and Raghu 1985; Woolston, Dhanireddy, and Marrazzo 2016). These sites have highly protected blood-tissue barriers with specialized ultrastructure that prevents the entry of circulating immune cells and most infectious diseases (Shechter, London, and Schwartz 2013). Unique from the clinical manifestations that arise during primary and secondary syphilis, neurosyphilis, congenital syphilis and ocular syphilis can occur at any point during the disease progression, including latent stages (Figure 1) (Lukehart SA 1988; Chawla, Gupta, and Raghu 1985; Woolston, Dhanireddy, and Marrazzo 2016).

Neurosyphilis

Neuroinvasion can occur at any point during the disease progression of syphilis, including the primary stage, and may not be associated with apparent neurological symptoms (Hook and Marra 1992). Central nervous system invasion occurs in 40% of patients during early syphilis, resulting in asymptomatic neurosyphilis, acute early meningitis, or immune clearance (Ghanem 2010). Asymptomatic neurosyphilis or clearance are the most common clinical outcomes; however up to 6% of untreated patients progress to early meningeal syphilis and patients with asymptomatic neurosyphilis are more likely to develop late neurological complications. Early meningeal syphilis is characterized by diffuse inflammation of the meninges with clinical presentations of meningitis including fever, headache, nausea, vomiting, stiff neck, and occasionally seizures (Ghanem 2010; Lafond and Lukehart 2006). Outcomes of late neurosyphilis include meningovascular syphilis, tabes dorsalis, and general paresis. Meningovascular syphilis is predicted to occur in up to 10% of modern neurosyphilis cases (Perdrup, Jorgensen, and Pedersen 1981; Danielsen et al. 2004) and presents as headache, vertigo, insomnia or ischemic stroke resulting from inflammation of arterial blood vessels in the CNS accompanied by blood clotting and vessel obstruction (Ghanem 2010). Tabes dorsalis is the degeneration of the spinal cord causing abnormal gait and paralysis; general paresis is a progressive dementia with symptoms ranging from a change in personality or sleeping habits and forgetfulness to psychiatric manifestations including depression and hallucinations. However, tabes dorsalis and paresis are not common in the post-antibiotic era (Ghanem 2010; Hook 2017).

Congenital syphilis

At any point during the disease progression of syphilis, *T. pallidum* can be transmitted via the bloodstream from a pregnant woman to the fetus, though the risk of transmission is much higher for pregnant women with early syphilis. Congenital syphilis can result in spontaneous abortion, stillbirth and premature delivery, and infants born with syphilis are often underweight and vulnerable to pulmonary hemorrhage, secondary bacterial infections and hepatitis. Within the two first years after birth, rhinitis (snuffles), disseminated rash, and gummateous lesions may occur. Even with treatment, clinical manifestations persist and worsen beyond 2 years of age and can include blindness, neurosyphilis, deafness, and tooth deformities (Chawla, Gupta, and Raghu 1985). Importantly, the disability-adjusted

life years (DALY; sum of lost years of healthy life) for congenital syphilis is 3.6 million, representing an associated medical cost of $309 million in United States Dollars (World Health Organization 2012). The estimated DALY for syphilis is 8.9 million, thus congenital syphilis represents a substantial portion of this metric (GBD DALYs and Hale Collaborators 2016).

Ocular syphilis

Treponema pallidum traversal of retinal barriers can take place during early or late syphilis and leads to permanent visual impairment in 10% of patients (Woolston, Dhanireddy, and Marrazzo 2016). Ocular involvement can affect almost any structure of the eye (Woolston, Dhanireddy, and Marrazzo 2016) and is often associated with meningovascular syphilis, especially in HIV-infected patients (Tucker et al. 2011).

1.1.3 Complicating factors in the incidence, diagnosis and treatment of syphilis

Penicillin is a highly effective and inexpensive treatment for syphilis, yet in the post-antibiotic era syphilis remains a global health concern (World Health Organization 2016a). This contradiction can be explained by a complex interplay of social and biological factors that contribute to the continued global incidence of syphilis.

Social Factors

In high income settings such as Canada and the United States the burden of syphilis infections is most prominent among the MSM population (Choudhri et al. 2018; Centers for Disease Control and Prevention 2019), which is concerning as syphilis infections increase the risk of HIV acquisition and transmission (Greenblatt et al. 1988; Stamm et al. 1988; Centers for Disease Control and Prevention 1998). Harm reduction strategies for preventing HIV acquisition include serosorting (selection of a partner based on concordant HIV status), differential selection of sexual act based on HIV-status (for example, lower risk of transmission with oral sex versus anal sex), HIV-status based condom use (Cassels and Katz 2013; Marcus, Schmidt, and Hamouda 2011; Truong et al. 2006), as well as the use of preventative intervention therapies like pre-exposure prophylaxis (PrEP): a daily

dosing of antiretroviral drugs (Sidebottom, Ekstrom, and Stromdahl 2018). While there are conflicting reports, serosorting and status-based condom use have been shown to be protective behavioral modifications to reduce HIV acquisition in MSM populations, though consistent and proper use of condoms is still the best preventative measure (Cassels and Katz 2013; Purcell et al. 2017). Similarly, the use of PrEP has been highly effective at reducing HIV acquisition in high-risk MSM populations (Sidebottom, Ekstrom, and Stromdahl 2018). Such behavioral modifications and preventative therapies combined with nonadherence to condom use are predicted to be contributing to the increasing rates of other sexually transmitted infections, including syphilis. While it is difficult to establish causation between PrEP usage and increased STI incidence, a meta-analysis study from 2016 found that within MSM populations, individuals taking PrEP were 44.6 times more likely to acquire syphilis than those not using PrEP. Similarly, PrEP usage increased the incidence of other sexually transmitted infections including *Neisseria gonorrhoeae* and *Chlamydia trachomatis* (Kojima, Davey, and Klausner 2016). Furthermore, during large-scale PrEP implementation in the United States, it was found that 50% of patients were diagnosed with a sexually transmitted infection during follow-up within 12 months after initiating PrEP usage (Liu et al. 2016; Volk et al. 2015). Other examples of social factors associated with an increased risk of acquiring syphilis include female sex work (Ouedraogo et al. 2018), the use of geosocial networking applications for finding sexual partners (Wang et al. 2018), and the usage of methamphetamines and intravenous drugs (Kidd et al. 2019). Individuals living in poverty or with limited access to health care, as well as and racial and ethnic minorities also have a higher risk of acquiring syphilis (Centers for Disease Control and Prevention 2019; Public Health England 2015).

In low-income and middle-income countries, limited access to screening and treatment for syphilis has historically been a contributing factor to the continued incidence of syphilis. Previously, diagnostic testing for syphilis required specialized equipment such that the majority of testing had to be done offsite in low-income and middle-income settings. This presents barriers to diagnosis and treatment that may include delays in testing and treatment and lack of patient compliance for return visits (Casas et al. 2018; Fears and Pope 2001). The development of point-of-care testing has improved screening and treatment in low-income and middle-income settings, particularly with regard to the

prevention of congenital syphilis through antenatal screening (World Health Organization 2016a; Perez and Mayaud 2019). Despite the improvements in screening for syphilis, low-middle- and high-income countries are all being affecting by global shortages of penicillin (Nurse-Findlay et al. 2017). Penicillin G is the drug of choice for treating all stages of syphilis, typically via a large intramuscular dose. To date there are no documented cases of *T. pallidum* resistance to penicillin, although resistance to the macrolide antibiotic azithromycin has been observed (Lukehart et al. 2004; Stamm and Bergen 2000). Alternatives to penicillin treatment include oral doxycycline and tetracycline, but these antibiotics are only recommended for patients with penicillin allergies. Benzathine penicillin G is the only recommended treatment to prevent congenital transmission (World Health Organization 2016a) and pregnant women with penicillin allergies must undergo desensitization prior to treatment with benzathine penicillin G (Workowski 2015). The treatment regimen can vary depending upon the disease stage and clinical manifestations. For example, patients with late latent or tertiary syphilis undergo prolonged treatment with benzathine penicillin G to ensure clearance of *T. pallidum* (Workowski 2015). Benzathine penicillin G is an inexpensive off-patent medication yet is costly to manufacture; driving production freezes by many suppliers (Nurse-Findlay et al. 2017). Benzathine penicillin G is currently recognized by the World Health Assembly as an essential medicine at high-risk for stock out (World Health Organization 2016b). A recent study found that 39 out of 91 countries surveyed reported shortages of benzathine penicillin G, including six high-income countries and 18 countries that had experienced a full stock-out of benzathine penicillin G (Nurse-Findlay et al. 2017). These global shortages are concerning given that benzathine penicillin G is the only antibiotic known to cross the placental barrier and prevent transmission of syphilis from a pregnant woman to her fetus (Workowski 2015). Equal access to this antibiotic will be critical for the success of WHO initiatives to reduce the global incidence of congenital syphilis (Taylor et al. 2016).

Biological Factors

Diagnosis at the primary and secondary stages of syphilis can be complicated by the variable appearances of lesions (Chapel 1978; Baughn and Musher 2005), particularly in patients co-infected with HIV (Rompalo et al. 2001; Hourihan et al. 2004). The internal

location of primary chancres common to both women (cervix and labia) and MSM (anal canal, rectum, and oral cavity) in concert with the painless nature of the lesions often allows for the primary stage to go unnoticed, precluding early diagnosis and treatment of the infection (Watts, Greenberg, and Khachemoune 2016; Lafond and Lukehart 2006). Furthermore, clinical manifestations at all stages of the disease progression can mimic other conditions which may result in misdiagnosis. As an example, primary chancres often mimic the presentation of chancroid or genital herpes, while secondary lesions can be mistaken for eczema or Rocky mountain spotted fever (Hook 2017). Localization of secondary lesions to the palms of the hands and soles of the feet is a distinguishing feature of secondary syphilis that occurs in up to 11% of patients (Baughn and Musher 2005). Repeat episodes of syphilis are increasingly common and often present clinical manifestations and immune responses that are distinct from the initial infection (Kenyon et al. 2014; Kenyon et al. 2018). Furthermore, HIV-infected patients are more likely to experience asymptomatic syphilis upon re-infection (Kenyon, Osbak, and Apers 2018).

1.1.4 Strategies for the elimination of syphilis

There are numerous confounding biological and social factors contributing to the increasing global rates of syphilis that need to be considering when developing a strategic approach to reduce incidence. Curbing the global burden of syphilis will require a combinatorial approach that addresses the need for improved screening protocols, increased awareness and education in vulnerable populations, mending the pipeline for penicillin production as well as advancements in basic research of *T. pallidum* biology to facilitate preventative therapies including vaccine development. Toward realizing these goals antenatal screening and treatment programs to reduce mother-to-child transmission (MTCT) of syphilis and HIV have been successfully implemented by the World Health Organization (WHO). These programs have resulted in decreased rates of congenital syphilis in low- and middle-income countries. Based on the WHO criteria of less than 50 cases of HIV infections and congenital syphilis cases per 100,000 live births, MTCT has been eliminated in numerous countries including Cuba, Thailand and Belarus (World Health Organization 2016a; Sidibe and Singh 2016; Zhang et al. 2019).

1.2 *Treponema pallidum* subspecies *pallidum*: causative agent of syphilis

1.2.1 Biology of *T. pallidum*

Treponema pallidum is a spiral-shaped bacterium ranging from 6-15 µm in length and 0.2 µm in diameter (Jepsen, Hougen, and Birch-Andersen 1968). The unique cell envelope of *T. pallidum* includes a loosely associated outer membrane and a thin layer of peptidoglycan in the periplasm in close proximity to the cytoplasmic membrane. Endoflagella localized to the periplasmic space facilitate the characteristic corkscrew motility of the bacterium (Wolgemuth 2015). While the outer leaflet of the *T. pallidum* cytoplasmic membrane is decorated with lipoproteins (Radolf 1995), the cell surface has a paucity of outer membrane proteins (Radolf, Norgard, and Schulz 1989; Walker et al. 1989) and lacks lipopolysaccharide (LPS), a common inflammatory glycolipid of Gram-negative bacteria (Fraser et al. 1998).

Treponema pallidum is an obligate human pathogen that is highly sensitive to both temperature and oxygen. The inability to survive outside of a host is exemplified by the minimalist genome of *T. pallidum*, which lack the genes required for *de novo* synthesis of nucleotides, fatty acids, vitamins, amino acids (AAs) and co-factors (Fraser et al. 1998). These metabolic insufficiencies likely underlie the slow replication rate of *T. pallidum*, observed to be 30 hours *in vivo* (Magnuson, Eagle, and Fleischman 1948). At ~1.1 million base pairs, *T. pallidum* has the smallest genome amongst spirochetes and encodes for roughly one-third of the open reading frames of the classically studied pathogen *Escherichia coli* (Radolf et al. 2016; Fraser et al. 1998). While there is still a limited understanding of the specific mechanisms for *T. pallidum* nutrient acquisition, 5% of the genome encodes transporters and symporters suggesting that nutrients are scavenged from the host environment (Radolf et al. 2016). Recent structural biology-based approaches have greatly improved the understanding of *T. pallidum* metabolism through the identification of transporters for AAs (Bian et al. 2015; Deka et al. 2004) and long chain fatty acids (Brautigam, Deka, Ouyang, et al. 2012; Brautigam, Deka, Schuck, et al. 2012).

1.2.2 Challenges confronting *T. pallidum* investigations

The limited knowledge regarding *T. pallidum* biology and pathogenesis can be attributed to the significant technical challenges associated with studying this organism, the most substantial of which being the historical inability to culture *T. pallidum in vitro.* Recently,

long-term *in vitro* cultivation of *T. pallidum* was demonstrated for the first time using a co-culture system with rabbit epithelial cells (Edmondson, Hu, and Norris 2018). While this represents a major development to the field of study, the adhesion of *T. pallidum* to mammalian cells in the co-culture presents a significant challenge for obtaining pure treponemes for downstream experimentation. To date, treponemes grown in the co-culture system have not been utilized in any published *in vitro* host-pathogen investigations. Live *T. pallidum* can be propagated *in vivo* in rabbits for use in downstream experiments (Lukehart and Marra 2007). Aside from the obvious ethical and economical issues associated with *in vivo* cultivation of *T. pallidum*, it has been demonstrated that the bacteria do not retain infectious capabilities for extended periods after harvest, although survival can be prolonged by maintaining the organisms at 34°C in an atmosphere of 1.5% O_2 (Norris and Edmondson 1986). The use of *in vivo* and *in vitro* propagated organisms is further complicated by the uniquely fragile outer membrane of *T. pallidum* which is susceptible to shearing during routine manipulations such as centrifugation, making it extraordinarily difficult to separate the bacteria from rabbit host components (Cox et al. 1992). Concurrent with the difficulties of culturing *T. pallidum* is the genetic intractability of the organism, precluding classical genetic approaches for studying microbial pathogenesis. To overcome these barriers, researchers use recombinant treponemal proteins or heterologous expression systems to study *T. pallidum* biology. However, the general lack of classical virulence factors in the genome presents a challenge for identifying candidate proteins that contribute to disease progression (Lafond and Lukehart 2006; Fraser et al. 1998).

1.2.3 Systemic dissemination

Treponema. pallidum dissemination is central to the disease progression of syphilis. Following acquisition, organisms rapidly gain entry to the bloodstream, facilitating extensive invasion into distant tissue and organ sites (Mahoney 1934; Stokes 1944; Cumberland MC 1949; Raiziss GW 1937). The invasive capability of *T. pallidum* is exemplified by the widespread disease manifestations associated with syphilis, including the development of disseminated lesions and generalized lymphadenopathy during secondary syphilis (Chapel 1981, 1980; Hira et al. 1987; Baughn and Musher 2005) and

the gummatous lesions, cardiovascular complications (Kampmeier 1946, 1948; Weinstein, Kampmeier, and Harwood 1957), and bone destruction that can occur during the tertiary stage of the disease (Gjestland 1955; Kampmeier 1972; Lafond and Lukehart 2006). Further, invasion into immune privileged areas (Woolston et al. 2015), vertical transmission from a pregnant woman to her fetus (Chawla, Gupta, and Raghu 1985; Sheffield et al. 2002), and entry into the CNS (Lukehart SA 1988; Marra et al. 2004) can all occur during early syphilis. In a rabbit infection model, *T. pallidum* invades into the lymphatic system within minutes of infection and into the cerebrospinal fluid within hours (Raiziss GW 1937; Collart, Franceschini, and Durel 1971). While the rapid and widespread nature of *T. pallidum* dissemination is well documented, the molecular mechanisms underlying this process have not been fully elucidated, largely owing to the difficulty associated with studying this organism.

1.2.4 Mechanisms of *T. pallidum* persistence and dissemination

Dissemination and immune evasion are key elements of *T. pallidum* pathogenesis. The clinical course of infection includes active stages with localized inflammatory reactions balanced with asymptomatic stages of latency, during which *T. pallidum* demonstrates a remarkable capacity to evade the immune system and persist within the host. The varied clinical manifestations observed throughout infection can be attributed to *T. pallidum* dissemination and invasion into diverse sites within the host.

Persistence

The scarcity of outer membrane proteins and lack of LPS causes the cell surface of *T. pallidum* to be antigenically inert, which is thought to be a major contributor to immune evasion (Penn, Cockayne, and Bailey 1985; Cox et al. 1992). This lack of antigenicity may explain why repeated rounds of *T. pallidum* vascular dissemination can occur without inducing systemic inflammation. Previous investigations have identified subpopulations of *T. pallidum* that are resistant to immune clearance in lesion sites (Cruz et al. 2012; Lukehart, Shaffer, and Baker-Zander 1992), which has been attributed to the variable sequences and expression of the *Treponema pallidum* repeat proteins (Tprs). The Tpr family proteins are *T. pallidum* outer membrane proteins that are targets of the host immune

system but can facilitate immune evasion via phase variation and antigenic variation. Antibody responses to different members of the Tpr family change throughout the course of infection, implying that *T. pallidum* alters expression of these genes to avoid recognition by the immune system (Sun et al. 2004; Leader et al. 2003). Further to this, a subset of the Tpr family proteins (*tprE, tprJ/I, tpr G/F*) contain homopolymeric repeats of guanosine in their promoter region that regulate gene expression through slipped-strand mispairing (Giacani, Lukehart, and Centurion-Lara 2007). The antigenic variation of TprK plays a key role in *T. pallidum* immune evasion. This protein contains seven variable regions that are targeted by the host antibody response. Gene conversion is used to introduce sequence diversity in the variable regions, which accumulates throughout the course of infection and slight changes to the AA sequence can abolish antibody binding (Morgan, Lukehart, and Van Voorhis 2003; Morgan et al. 2002). Treponemes that escape immune clearance in lesions undergo vascular dissemination and recognition by the immune system may be precluded by *T. pallidum* seeding into diverse anatomical sites including immune privileged areas (Chawla, Gupta, and Raghu 1985; Woolston, Dhanireddy, and Marrazzo 2016; Lukehart SA 1988) in combination with the slow replication rate of *T. pallidum* in tissues (Magnuson, Eagle, and Fleischman 1948).

Dissemination

Treponema pallidum can interact with numerous host-derived ECM components (Fitzgerald et al. 1984) and mammalian cell types (Fitzgerald et al. 1977; Hayes et al. 1977; Sandok et al. 1976; Thomas, Baseman, and Alderete 1985) including endothelial cells (Thomas et al. 1989; Thomas et al. 1988; Lee et al. 2003). Intriguingly, a recent study visualized *T. pallidum* merging with the membranes of brain endothelial cells using scanning electron microscopy (Wu, Zhang, and Wang 2017). *Treponema pallidum* has also been observed to localize to intercellular junctions of endothelial cells implying a paracellular route of transendothelial migration. *In vitro, T. pallidum* traversal of endothelial barriers occurs without a discernible disruption of barrier integrity (Thomas et al. 1989; Thomas et al. 1988). Additionally, *T. pallidum* can activate endothelial cells, promoting activation marker upregulation and adhesion of leukocytes and monocytes to endothelial surfaces (Riley et al. 1992; Riley et al. 1994). This cellular activation has been

attributed to the *T. pallidum* proteins Tp17 [Tp0435] (Zhang et al. 2015), Tp47 kDa lipoprotein [Tp0574] (Riley et al. 1992) and Tp0965 (Zhang, Zhang, and Wang 2014). However, the implications of *T. pallidum* activating endothelial cells, localizing to endothelial intercellular junctions, and merging with endothelial membranes has not been explored in the context of dissemination.

The identification of *T. pallidum* host-binding adhesins that facilitate interactions with cells or ECM components has been hampered by the many technical challenges associated with studying this pathogen. A common method for virulence factor discovery in pathogenic bacteria is *in silico* genome evaluation to find orthologs of characterized virulence factors in other pathogens. However, the genome of *T. pallidum* contains very few classical virulence factors and approximately 30% of the *T. pallidum* genome encodes for proteins without an assigned function or known ortholog (Fraser et al. 1998; Petrosova et al. 2013). The *T. pallidum* genome also lacks pathogenicity islands, horizontally transferred genetic elements enriched in virulence factors and commonly found in pathogenic bacteria (Gal-Mor and Finlay 2006). A tertiary structure protein modelling program has been used to explore the *T. pallidum* proteome and infer protein functions, proposing putative functions for approximately 80% of *T. pallidum* proteins. This study identified 21 proteins of unknown function with structural similarity to characterized virulence factors from other pathogens (Houston et al. 2018), presenting an exciting new avenue for the identification of *T. pallidum* proteins involved in pathogenesis. However, experimental validation will be required to confirm the proposed function of these putative virulence factors. Mutagenesis followed by high throughput screening for loss of virulence in animal, plant and insect infection models are also commonly employed methods for virulence factor identification, but the genetic intractability of *T. pallidum* precludes this approach (Mahajan-Miklos, Rahme, and Ausubel 2000). Genomic and proteomic approaches are also frequently utilized to identify proteins that are secreted or localize to the bacterial cell surface and therefore appropriately poised to interact with the host (Wu, Wang, and Jennings 2008). The paucity of proteins on the cell surface of *T. pallidum* and the inherent fragility of the outer membrane (Cox et al. 1992) present a significant challenge for confirming protein localization to the outer membrane.

The identification and validation of *T. pallidum* outer membrane proteins has been a challenging and controversial endeavor in the field of study due to the inherent fragility and low protein content of the outer membrane (Cox et al. 1992). This controversy largely stems from a lack of consensus on the technical approaches that should be utilized to characterize *T. pallidum* outer membrane proteins. Further to this, early investigations into the nature of the *T. pallidum* outer membrane relied on misconceptions that led to incorrect identification of outer membrane components. Such investigations postulated that the *T. pallidum* outer membrane was a host-derived coat of serum proteins and mucopolysaccharide (Alderete and Baseman 1979; Christiansen 1963; Fitzgerald and Johnson 1979). This theory was later refuted with a combination of high resolution imaging techniques that demonstrated the existence of *T. pallidum* outer membrane layer distinct from the treponemal-associated host components (Johnson et al. 1973, Radolf et al. 1986). Another misconception was that heterologous expression of *T. pallidum* proteins in *E. coli* could provide information about the outer membrane localization of the endogenous proteins, but the inherent differences in cellular ultrastructure and transport machinery of the bacteria called the validity of such findings into question (Norgard and Miller 1983; Stamm et al. 1982; Walfield et al. 1982). Additionally, the perception that reactivity of host serum with *T. pallidum* proteins was a direct demonstration of outer membrane localization also resulted in incorrect identification of *T. pallidum* outer membrane proteins (Norgard and Miller 1983; Stamm et al. 1982; Walfield et al. 198).

As the main mechanism of *T. pallidum* clearance in the host, opsonophagocytosis has been harnessed as a technique for exploring *T. pallidum* outer membrane proteins. The *T. pallidum* glycerophosphodiester phosphodiesterase (Gpd), TprK and BamA (Tp0326) are all targets of opsonizing antibodies as demonstrated by opsonophagocytosis of *T. pallidum* by rabbit peritoneal macrophages in the presence of Gpd-, TprK- and BamA-reactive serum. Furthermore, immunization with these antigens provides partial protection against *T. pallidum* challenge in a rabbit model of infection (Stebeck et al. 1997; Cameron et al. 1998; Centurion-Lara et al. 1999; Cameron et al. 2000). Taken together, these findings support the outer membrane localization of Gpd, TprK and BamA.

Beta-barrels are common structural folds of outer membrane proteins in prokaryotes and eukaryotes (Wimley 2003). Structural modelling programs have been utilized to

identify *T. pallidum* proteins predicted to form beta-barrels revealing eighteen candidate proteins including members of the Tpr family and numerous proteins of unknown function (Radolf and Kumar 2018; Cox et al. 2010). Complementary experimental approaches have been employed to confirm the localization of proteins to the outer membrane, including immunofluorescence (Cox et al. 1995; Luthra, Anand, and Radolf 2015), proteinase K accessibility, and opsonophagocytosis assays (Anand et al. 2012; Desrosiers et al. 2011; Hazlett et al. 2005; Radolf and Kumar 2018). The outer membrane localization of TprC/D, TprI and BamA was validated using these computational and experimental approaches (Anand et al. 2012), while TprF and TprK were found to localize to the periplasm of *T. pallidum* (Cox et al. 2010). However, this is in direct conflict with a large body of work that demonstrates TprK is a *T. pallidum* outer membrane protein that facilitates immune evasion through antigenic variation (LaFond et al. 2006; LaFond et al. 2003; Morgan et al. 2002; Centurion-Lara et al. 2004; Centurion-Lara et al. 1999). The discrepancy in experimental evidence for TprK localization exemplifies the challenge of determining true outer membrane proteins in *T. pallidum.* Although there remains no gold standard, the validation of *T. pallidum* outer membrane proteins should combine functional *in vivo* data with biochemical determination of protein localization.

Attachment to host ECM components is a common strategy for disseminating pathogens (Singh et al. 2012; Lemichez et al. 2010) and metastatic tumors (Venning, Wullkopf, and Erler 2015). The ECM is a dynamic meshwork composed of fibrous proteins including collagen, elastin and laminin; soluble glycoproteins such as fibronectin; and proteoglycans such as heparin sulfate (White 2015; Patti et al. 1994). These complex matrices function as structural scaffolds that surround cells and participate in cellular signaling and migration (Hynes 2009). The basement membrane is a specific ECM structure that anchors endothelial cells and surrounds blood vessels; laminin and collagen are the main constituents of the basement membrane (Singh et al. 2012). Plasma fibronectin circulates through the bloodstream and can deposit on vascular surfaces using integrins as receptors. Cell surface deposition results in fibrillogenesis, or the unfolding of compact fibronectin into a matrix-like conformation, which can initiate endothelial cell signaling cascades. Conversely, tissue fibronectin is a structural component of the ECM and can be found in basement membranes (To and Midwood 2011). Previous bioinformatic analysis

of the *T. pallidum* genome identified ten putative adhesins based on a predicted outer membrane locale (Cameron 2003). Functional characterization of these proteins revealed that three out of ten proteins (Tp0751, Tp0155, and Tp0483) possessed the capacity for binding to host extracellular matrix components (Cameron 2003; Cameron et al. 2004). Additional investigations also identified Tp0136 as a *T. pallidum* fibronectin binding adhesin (Brinkman et al. 2008; Ke et al. 2015). While Tp0155, Tp0483 and Tp0136 adhere to both plasma and tissue fibronectin (Cameron et al. 2004; Brinkman et al. 2008; Ke et al. 2015), Tp0751 has been confirmed to interact with numerous ECM components including laminin, fibronectin, and collagens (Cameron 2003; Cameron et al. 2005; Cameron et al. 2008; Houston et al. 2015; Parker et al. 2016).

The interactions of Tp0751 with laminin, collagen and fibronectin implicate this protein in basement membrane adhesion. Furthermore, Tp0751-mediated fibronectin binding could facilitate host cell attachment through bridged interactions with integrin, a common strategy for pathogen-host cell adhesion (Cameron 2003; Cameron et al. 2005; Cameron et al. 2008; Houston et al. 2015; Parker et al. 2016; Lemichez et al. 2010). Taken together, these findings suggest that Tp0751 may bring *T. pallidum* in close proximity to the vascular endothelium via interactions with luminal fibronectin depositions and ECM components of the subluminal basement membrane. A role for this protein in *T. pallidum* dissemination is further supported by evidence of Tp0751 localization to the host-interacting, surface-exposed outer membrane of *T. pallidum.* Tp0751 is the target of opsonic antibodies (Houston et al. 2012) and heterologous expression of Tp0751 in model spirochetes including *Treponema phagedenis* and *Borrelia burgdorferi* results in cell surface localization (Parker et al. 2016; Cameron et al. 2008). There is also evidence that Tp0751 is a *T. pallidum* lipoprotein. The Tp0751 open reading frame contains a lipoprotein signal sequence and heterologous expression in *T. phagedenis* results in palmitoylation (Houston et al. 2011).

Structural determination of Tp0751 reveals a compact eight-stranded beta-barrel that adopts a unique lipocalin fold with an extended N-terminal alpha helix (Parker et al. 2016). Biochemical investigations with Tp0751 peptides demonstrate that one face of the lipocalin barrel and N-terminal helix confer binding to ECM components (Parker et al. 2016). Members of the lipocalin protein family typically coordinate small hydrophobic molecules

in a central cavity and eukaryotic lipocalins are involved in diverse cellular processes such as cell adhesion, immune modulation and cancer metastases (Du et al. 2015). In humans, neutrophil gelatinase-associated lipocalin (NGAL) is highly expressed in numerous cancer types including pancreatic and liver cancer (Wurmbach et al. 2007; Pei et al. 2005). While NGAL can contribute to cancer progression by complexing with the matrix metallopeptidase 9 (MMP9) to promote ECM degradation and tumor invasion (Yan et al. 2001; Leng et al. 2008), NGAL also has anti-oncogenic effects in certain cancer types exhibiting protective effects against tumor invasion. These divergent roles for NGAL highlight the diverse functionality of lipocalins (Venkatesha et al. 2006; Tong et al. 2008). Although there is limited knowledge regarding the role of prokaryotic lipocalins, Tp0751 displays structural similarity to the *Neisseria meningitdis* factor H binding protein (fHbp) as both proteins lack the characteristic lipocalin hydrophobic binding pocket (Bishop 2000; Cantini et al. 2009; Cendron et al. 2011; Veggi et al. 2012). The *N. meningitidis* lipocalin fHbp is a key virulence factor that allows the bacteria to resist killing by human serum via factor H binding (Veggi et al. 2012). Intriguingly, the host molecule binding interface of Tp0751 and fHbp both map along one face of the lipocalin barrel (Parker et al. 2016; Cantini et al. 2009; Cendron et al. 2011; Veggi et al. 2012).

The ECM-binding adhesin, Tp0751, has also been characterized as a metalloprotease that can degrade human fibrinogen and laminin based on *in vitro* degradation assays with recombinant Tp0751 (Houston et al. 2011; Houston et al. 2012). This proteolytic capacity has been attributed to a metal-coordinating HEXXH motif localized to the C-terminal region of Tp0751 (Houston et al. 2012). Importantly, the Tp0751 proteolytic and adhesive activities function independently as Tp0751 active site mutants retain their ability to bind to host component despite the loss of protease activity (Houston et al. 2012). Although structural characterization of Tp0751 did not reveal a clear mechanism for metal coordination in the previously characterized HEXXH active site (Parker et al. 2016; Houston et al. 2012), these studies were performed with a Tp0751 active site mutant, Tp0751 S78-P237 with an E199A mutation (HAXXH), which could provide a possible explanation for the apparent lack of metal coordination (Parker et al. 2016). Heterologous expression of Tp0751 in the model treponeme, *T. phagedenis*, revealed a gain-of-function for fibrin clot degradation *in vitro (*Houston et al. 2012), however, to date there is no

evidence that endogenous Tp0751 participates in degradation of host components in the context of live *T. pallidum.* Despite the experimental limitations of characterizing the host interactions of *T. pallidum*, the functional characterization of endogenous Tp0751 will be a critical future experiment for validating the protease activity of this protein.

Tp0751 has been identified as a central host binding adhesin driving *T. pallidum* dissemination through its interactions with extracellular matrix (ECM) components such as laminin (Cameron et al. 2005; Cameron et al. 2008; Houston et al. 2015; Parker et al. 2016) and fibronectin (Parker et al. 2016; Houston et al. 2015). Tp0751-mediated interactions with host cells have also been confirmed. Heterologous expression of Tp0751 in a non-infectious *B. burgdorferi* model system confers a gain-of-function phenotype for endothelial attachment *in vitro* in a particle-tracking flow chamber and *in vivo* in mouse post-capillary venules (Parker et al. 2016; Kao et al. 2017). These functional roles support the finding that immunization with Tp0751 partially inhibits treponemal dissemination to distant organ sites upon infectious *T. pallidum* challenge in an animal infection model (Lithgow et al. 2017). Taken together, these functional characterizations indicate that Tp0751 is an important mediator of *T. pallidum* dissemination.

1.3 Vascular dissemination

1.3.1 The vascular endothelium

The vascular endothelium is a dynamic cellular barrier that lines the luminal surfaces of blood vessels and separates the circulatory system from surrounding extravascular tissue and organ sites. Endothelial barriers play a critical role in regulating vascular haemostasis as well as innate and adaptive intravascular immune reactions in response to signals of inflammation, damage, or infection. Distinct structural and phenotypic heterogeneities are exhibited by endothelial cells throughout the circulatory system that correspond to the functional requirements of a given vascular layer (Aird 2007a, 2007b). The macrovasculature is comprised of arteries and veins and is continuous and non-fenestrated (lacking transcellular pores) with a limited capacity for modulation of vascular permeability. While the microvasculature, including arterioles, capillaries, and venules is variable and can be continuous, fenestrated or discontinuous. Capillaries are particularly specialized for the requirements of the underlying tissue (Aird 2007a). The capillary

endothelium of the heart, lungs, and skin is continuous, whereas the capillary endothelium of the liver, kidney glomeruli, and endocrine system are discontinuous or fenestrated, such that the cells are separated by pores or gaps in the endothelium allowing for increased filtration or transendothelial transport (Figure 2) (Fung, Fairn, and Lee 2018; Aird 2007b).

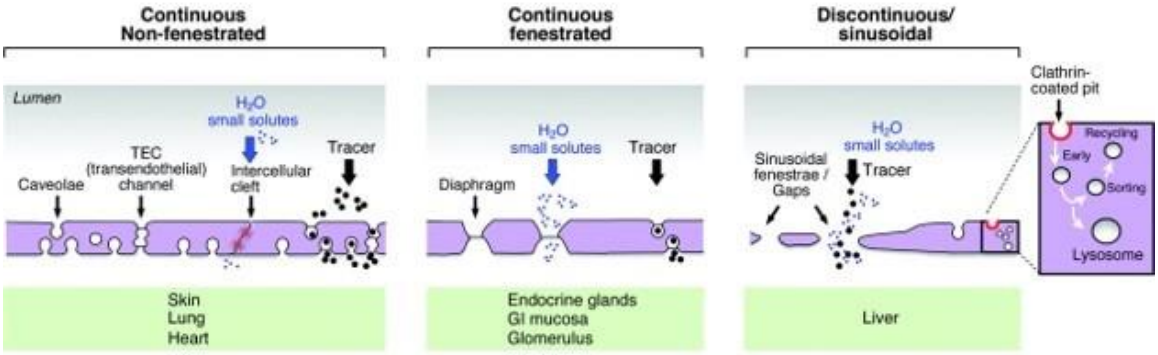

Figure 2: Structural heterogeneity of endothelial barriers. Capillary endothelial barriers can be **continuous and non-fenestrated** exhibiting enrichment in caveolae and vesiculo-vacuolar organelles (VVOs; intercellular clefts), **fenestrated** with small gaps (with diaphragms) and transendothelial channels, or **discontinuous** with large gaps (without diaphragms) between endothelial cells. Discontinuous endothelial barriers are also enriched in clathrin-coated pits for receptor-mediated endocytosis and transcytosis. Larger solutes ('tracer') traverse the endothelium through transcytosis pathways including caveolae or transendothelial channels, whereas small solutes traverse through VVOs or via gaps between endothelial cells. The differences in endothelial ultrastructure reflects the requirements of the underlying extravascular tissue or organ site. Image printed with permission (Aird 2007b).

The ultrastructure of a vascular barrier is composed of endothelial cells attached to a basolateral substratum known as the basement membrane, composed of glycoproteins, proteoglycans extracellular matrix proteins including laminin (Aird 2007b). The surface of endothelial cells are protected from the mechanical forces of the blood flow by a luminal exclusion layer called the glycocalyx, comprised of membrane-bound proteoglycans and glycoproteins (Reitsma et al. 2007). The composition of endothelial barriers is not uniform throughout the vasculature with variation in thickness of the basement membrane and glycocalyx, composition of intercellular junctions, and predominance of components that

support transcytosis or endocytosis pathways. This heterogeneity of the vascular endothelium reflects the functional requirements of a given vascular barrier (Aird 2007b). Endothelial barriers facilitate the exchange of blood proteins and cells between the circulatory system and underlying tissue sites. Traversal of the vascular endothelium can occur via three distinct mechanisms (1) coordinated opening and closing of intercellular junctions (2) transcellular transport vesicles and (3) endocytic pathways.

Endothelial intercellular junctions are made up of tight and adherens junctions which are interspersed along cell-cell borders. Junctional complexes are formed via homophilic interactions between transmembrane proteins of neighboring cells (Figure 3). The cytoplasmic tails of junctional proteins interact with adaptor proteins and the cytoskeleton to stabilize junctions as well as signaling proteins to coordinate the opening and closing of junctions. Adherens junctions are comprised of nectins and vascular endothelial-cadherin (VE-cadherin), an endothelial-specific protein that is ubiquitous throughout the vasculature. Tight junctions are made up of junction adhesion molecules (JAMs) and claudins (Figure 3). Tight junctions are abundant in tightly regulated vascular barriers, such as the blood-brain barrier, and poorly organized in barriers that undergo significant exchange between blood and tissue such as post-capillary venules (Dejana 2004).

Transcytosis, the transcellular movement of molecules across endothelial barriers, is facilitated by vesiculo-vacuolar organelles (VVOs) and caveolae (Aird 2007b). Caveolae are membrane-bound flask-shaped 70 nm vesicles that coordinate luminal or abluminal uptake of molecules to traffic across the endothelium (Bendayan 2002). Vesiculo-vacuolar organelles allow for extravasation of small macromolecules via interconnected clusters of uncoated vacuoles and vesicles within endothelial cells, but this traversal route is limited to solutes with a molecular radius <3 nm (Dvorak et al. 1996; Aird 2007b). Caveolae are most abundant in the capillary endothelium and continuous endothelial barriers (skin, heart, skeletal muscle), while VVOs predominate venular regions (Aird 2007b). Endothelial endocytosis can occur via receptor-mediated endocytosis or nonspecific uptake into clathrin-coated pits or vesicles, caveolae-mediated endocytosis, or macropinocytosis (Muro, Koval, and Muzykantov 2004). Unique from transcytosis, molecules that undergo

endocytosis are generally targeted to the lysosome for degradation, though transcellular traversal can also occur (Aird 2007b).

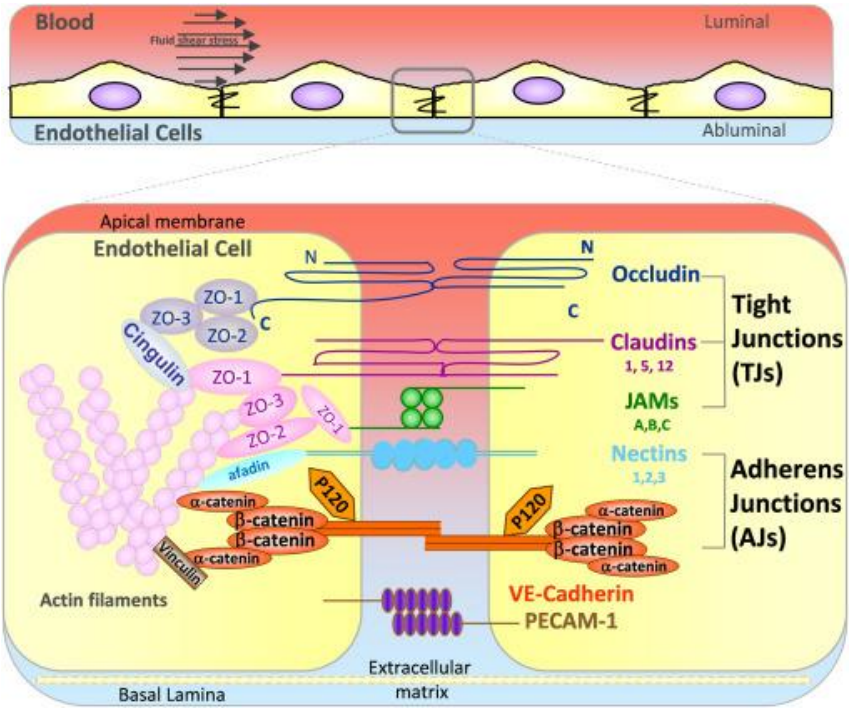

Figure 3: The composition of endothelial intercellular junctions. Junctions at endothelial cell-cell borders are made up of homophilic interactions between transmembrane proteins on neighboring cells. This includes two types of junctional complexes: adherens junctions (VE-cadherin, nectins) and tight junctions (claudins, occludins, JAMs). The cytoplasmic tails of junctional proteins bind to adaptor proteins including catenins and afadins (adherens junctions) and zona-occludins (tight junctions), which link the junctional complexes to the actin cytoskeelton. Image printed with permission (Cerutti and Ridley 2017).

1.3.2. Leukocyte transendothelial migration

The process of endothelial barrier traversal is best described for the extravasation of immune cells, however there is still a limited understanding of this highly complicated process. Leukocyte transendothelial migration is initiated by the honing of leukocytes to areas of tissue damage or infection. Recruitment is facilitated by activation of endothelial cells which promotes chemokine release and upregulation of cell surface adhesion molecules. Adhesion to vascular surface occurs in a multi-stage process that includes

rolling, arrest, crawling and firm adhesion prior to endothelial barrier transmigration. A variety of leukocyte adhesins and endothelial receptors participate in these adhesive interactions which function to help leukocytes overcome the shear forces of the blood flow to mediate stable interactions with vascular surface (Schimmel, Heemskerk, and van Buul 2017). The current understanding of leukocyte transendothelial migration is that traversal occurs without modulation of vascular permeability (Valeski and Baldwin 1999; Kim, Curry, and Simon 2009; Lewis and Granger 1988; Lewis, Miller, and Granger 1989), supported by the finding that different tyrosine residues on VE-cadherin in endothelial barriers control leukocyte extravasation and vascular permeability *in vivo* (Wessel et al. 2014). Leukocytes preferentially cross endothelial barriers at post-capillary venules where the barrier ultrastructure is simplified with fewer intercellular junctions, a thinner basement membrane and larger pores between endothelial cells (Aird 2007a). There are two mechanisms for transendothelial migration: transcellular and paracellular traversal, and the structural and functional heterogeneity of the vasculature results in different traversal mechanisms at different sites in the body. For example, transcellular traversal mechanisms are utilized for immune cell entry into the blood-brain barrier and lymph nodes, whereas a paracellular route is preferentially used for entry into the lungs or skin (Schimmel, Heemskerk, and van Buul 2017; Schulte et al. 2011; Kuppers, Vestweber, and Schulte 2013).

The molecular mechanisms that allow for leukocyte transcellular and paracellular traversal without increasing vascular permeability are not fully understood. The predominant hypotheses for transendothelial migration mechanisms are as follows. As depicted in Figure 4A, during paracellular traversal, endothelial junctions are transiently destabilized via dephosphorylation of VE-cadherin tyrosine 731, triggering clathrin-dependent endocytosis of VE-cadherin at localized sites to allow for leukocyte passage between endothelial cells (Wessel et al. 2014). The transcellular migration of leukocytes (Figure 4B) is initiated by clustering of ICAM-1 and caveolin on vascular surfaces at sites of leukocyte adhesion followed by F-actin depolymerization which allows for the formation of a transcellular pore (Millan et al. 2006). In both processes, movement across the barrier is confined by the formation of a contractile pore in the endothelium. This pore is formed via protrusions of filamentous actin (F-actin) around the leukocyte producing a

contractile ring that immune cells must squeeze through. This contractile ring has been proposed to underlie the maintenance of barrier integrity during traversal (Heemskerk et al. 2016).

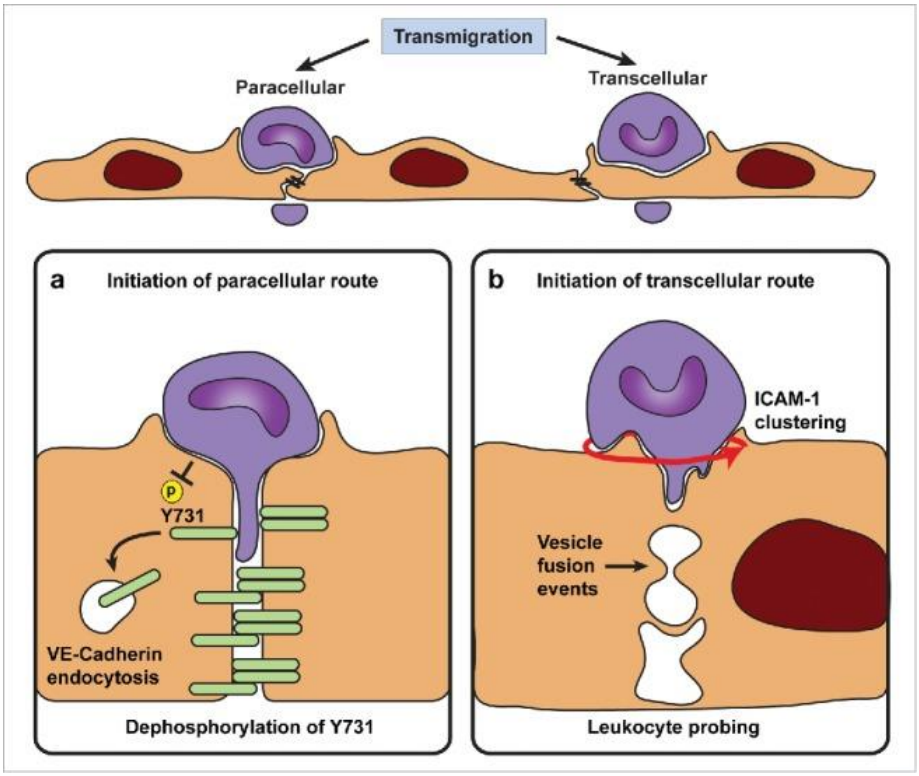

Figure 4: Mechanisms of leukocyte transendothelial migration. (A) Leukocytes can cross endothelial barriers using a paracellular route in which the immune cells induce dephosphorylation of tyrosine 731 of VE-cadherin, inducing endocytosis of the junctional protein to open a paracellular transmigration route. (B) Leukocytes can cross endothelial barriers using a transcellular route in which leukocytes probe the cell surface to promote ICAM-1 clustering at the cell surface, leukocyte uptake and traversal across the endothelial through vesicle fusion events. Image printed with permission (Schimmel, Heemskerk, and van Buul 2017).

1.3.3 Bacterial traversal of the vascular endothelium

Systemic dissemination via the circulatory system is a strategy utilized by many bacterial pathogens to invade secondary infection sites. Bacteria that can survive and migrate through the host bloodstream must be equipped with the necessary molecular machinery to overcome the complex microenvironment of the vasculature. Disseminating pathogens are exposed to the shear forces of the blood flow as well as patrolling immune cells and

intravascular immune factors and must interact directly with the vascular endothelium in order to gain access to underlying tissues and organs. Furthermore, pathogens must adhere to vascular surfaces and traverse endothelial barriers to access extravascular tissue sites, which can be accomplished by inducing changes in endothelial signaling and cytoskeletal organization to create membrane protrusions, mediate cellular invasion, or increase barrier permeability to penetrate intercellular junctions (Lemichez et al. 2010).

While vascular extravasation mechanisms for bacterial pathogens are not fully understood it is hypothesized that the general mechanism mimics leukocyte extravasation with multi-stage adhesion events followed by paracellular and/or transcellular migration across the endothelium (Doulet et al. 2006; Ebady et al. 2016). Supporting this hypothesis, during hematogenous dissemination of the highly invasive Lyme disease spirochete, *Borrelia burgdorferi*, bacteria mediate vascular interactions in capillaries, postcapillary venules, and large veins via a multistage attachment process that parallels leukocyte transendothelial migration (Norman et al. 2008; Moriarty et al. 2008; Ebady et al. 2016). The vascular adhesion of *B. burgdorferi* can be divided into two stages: (1) transient tethering and dragging interactions that initiate contact with vascular surface and promote deceleration of the bacteria in the blood stream and (2) stationary adhesion during which the bacteria intimately attach to receptors on endothelial cells. The bacterial stationary adhesion phase occurs directly within the glycocalyx exclusion layer at endothelial surfaces, providing a protective niche for the bacteria to avoid the shear forces of the blood flow (Reitsma et al. 2007; Moriarty et al. 2012)

The entry of bacterial pathogens into highly protected areas such as the brain, eye, or placenta is impeded due to specialized endothelial barriers with differential vessel ultrastructure, junctional architecture, and immune surveillance (Aird 2007a). *Treponema pallidum* is one of the few pathogens capable of crossing these specialized barriers to mediate vertical transmission (Chawla, Gupta, and Raghu 1985) and invade the CNS (Lukehart SA 1988; Marra et al. 2004) and other immunologically privileged sites in infected hosts. Other pathogens known to exhibit this ability include *Streptococcus pneumoniae, Neisseria meningitidis,* and *Haemophilus influenzae* (Coureuil et al. 2017); intriguingly, these three meningitis-causing organisms all interact with the 67 kDa laminin receptor (LamR) on the surface of cerebral endothelial cells to initiate CNS entry (Orihuela

et al. 2009). This presents the exciting possibility that there may be a common mechanism for attachment of extracellular bacterial pathogens to the brain microvasculature.

Amongst bacterial pathogens, transendothelial migration is best understood for *N. meningitis* which can traverse brain endothelial barriers via transcellular and paracellular routes (Lemichez et al. 2010). Adhesion of *N. meningitidis* to brain endothelial cells induces F-actin polymerization whereby localized cytoskeletal protrusions are formed around the adherent bacteria (Hoffmann, Eugene, et al. 2001; Eugene et al. 2002; Lambotin et al. 2005; Doulet et al. 2006). These protrusions are proposed to enable bacterial resistance to shear stress within the vasculature (Mikaty et al. 2009; Mairey et al. 2006). Adhesion results in recruitment of endothelial intracellular proteins (ezrin and moesin) and receptor clustering (endothelial adhesion molecule ICAM1 and tyrosine kinase ERBB2) at the site of bacterial attachment (Hoffmann, Eugene, et al. 2001; Eugene et al. 2002). Subsequent activation of ERBB2 and phosphorylation of cortactin mediates *N. meningitidis* internalization and transcellular traversal (Hoffmann, Eugene, et al. 2001; Lambotin et al. 2005). Additionally, polarity complex proteins (partitioning-defective 3 [PAR3], PAR6 and protein kinase Cζ) and junctional proteins (VE-cadherin, claudin) can be recruited to the bacterial adhesion site which results in the formation of new intercellular junctions below the bacteria, opening up a paracellular route of traversal (Coureuil et al. 2009).

The overarching themes of *N. meningitidis* include cytoskeletal modulation, altered signaling pathways, recruitment of host adaptor proteins, and endocytosis or junctional disruption; these themes are common to other disseminating pathogens (Lemichez et al. 2010). Furthermore, the signaling events initiated during endothelial traversal of *N. meningitidis* mimic leukocyte transendothelial migration signaling mechanisms (Doulet et al. 2006), demonstrating that parallels also exist between barrier traversal of immune cells and bacteria.

1.4 Research objectives:

Treponema pallidum dissemination is critical to the persistence and dissemination of the organism that underlies the clinical manifestations that occur during the course of infection. The rapid and widespread nature of *T. pallidum* vascular dissemination is well documented,

however knowledge of the molecular mechanisms is limited. A complete understanding of this process will provide opportunities to prevent *T. pallidum* attachment to the host vasculature and impede treponemal modulation of the vascular endothelium. Furthermore, improved knowledge regarding *T. pallidum* pathogenesis will facilitate vaccine development for syphilis. Given the lack of molecular characterization of *T. pallidum*-host interactions, the investigations in this dissertation explore the mechanics of *T. pallidum* interactions with the vascular endothelium, a fundamental step in the process of *T. pallidum* vascular dissemination and the disease progression of syphilis. With the knowledge that Tp0751 can mediate adhesion to ECM components and vascular surfaces under physiological shear stress, this body of work aims to explore the role of Tp0751 in the dissemination of *T. pallidum.* The three objectives, corresponding goals and main conclusions of this dissertation project are as follows:

(1) Characterize the adhesive interaction between Tp0751 and human endothelial cells.

a. Does Tp0751 mediate adherence to the human macrovascular and microvascular endothelial cells?

b. Do ECM components facilitate Tp0751-mediated adherence to human endothelial cells?

c. What region of Tp0751 mediates endothelial interactions?

d. Does Tp0751 attach to specific host endothelial cell receptors?

In chapter 2 of this dissertation, three distinct approaches are used to demonstrate that Tp0751 functions as an endothelial adhesin and mediates interactions with endothelial cells of microvascular and macrovascular origin including a brain microvascular endothelial cell line. This chapter also identifies the 67 kDa laminin receptor (LamR) as an endothelial receptor for Tp0751. Importantly, LamR is targeted by meningitis-causing bacterial pathogens *Neisseria meningitidis*, *Haemophilus influenzae*, and *Streptococcus pneuomoniae*, suggesting a common molecular strategy for tissue invasion by these neuroinvasive pathogens (Orihuela et al. 2009). Inhibition studies using antibodies targeting discrete regions of LamR show that *Tp* interacts with the same LamR region as these other pathogens.

(2) Discern whether Tp0751 can induce alterations in endothelial junctional integrity and vascular permeability to facilitate bacterial transendothelial migration.

a. Do Tp0751 and *T. pallidum* modify endothelial intercellular junctions?

b. Does *T. pallidum* localize to intercellular junctions?

c Do Tp0751 and *T. pallidum* alter endothelial permeability?

d. Does *T. pallidum* cross endothelial barriers via the paracellular pathway, transcellular pathway, or both?

The results presented in chapter 3 of this dissertation reveal that *T. pallidum* and Tp0751 disrupt the architecture of human cell-cell junctions in endothelial cells without altering the overall endothelial barrier integrity. Despite the lack of disruption to barrier permeability, *T. pallidum* can still traverse across endothelial barriers. Using inhibitors of different pathways of endocytosis the results in chapter 3 reveal that *T. pallidum* may utilize a lipid raft-dependent mechanism of transcellular traversal. Furthermore, evidence for treponemal localization to intercellular junctions implies a paracellular route of traversal. Taken together these results suggest that *T. pallidum* may use two distinct mechanisms for transendothelial migration.

(3) Explore Tp0751-induced alterations of signaling pathways in human endothelial cells.

a. How does recombinant Tp0751 alter signalling in host endothelial cells?

Chapter 4 of this dissertation explores methodology development for a large scale phosphoproteome analysis of endothelial cells using stabile isotope labeling by amino acids in cell culture (SILAC). A small scale phosphoproteome analysis reveals that endothelial cells exposed to Tp0751 exhibit increased phosphorylation of drebrin and cortactin. These proteins are involved in modulation of the host cytoskeleton, primarily with respect to the polymerization of F-actin (Tanabe et al. 2014; Worth et al. 2013; Campbell, Sutherland and Daly 1999; Kelley et al. 2010; Martinez-Quiles et al. 2004). Notably, phoshphorylation of cortactin is common to the host cell invasion pathways of many other pathogenic bacteria (Lambotin et al. 2005; Slanina et al. 2012; Hoffmann, Eugene, et al. 2001; Martinez and Cossart 2004; Agerer et al. 2003; Fawaz et al. 1997;

Bougneres et al. 2004; Dumenil, Sansonetti, and Tran Van Nhieu 2000; Cantarelli et al. 2000; Cantarelli et al. 2006; Cantarelli et al. 2002; Bougneres et al. 2004; Zettl and Way 2001; Frischknecht and Way 2001; Sousa et al. 2007).

Chapter 2: Adhesive interactions of Tp0751 with the human vascular endothelium

Contributions: KL performed all experiments and data analysis with the exception of the affinity chromatography mass spectrometry repeat using hCMEC/d3 cells, which was performed by Brigette Church.

Figure 10B-E is printed with permission (Appendix I) and adapted from the previously published manuscript:

Parker, M. L., S. Houston, H. Petrosova, K. V. Lithgow, R. Hof, C. Wetherell, W. C. Kao, Y. P. Lin, T. J. Moriarty, R. Ebady, C. E. Cameron, and M. J. Boulanger. 2016. 'The Structure of Treponema pallidum Tp0751 (Pallilysin) Reveals a Non-canonical Lipocalin Fold That Mediates Adhesion to Extracellular Matrix Components and Interactions with Host Cells', *PLoS Pathog*, 12: e1005919.

Figure 11A is printed with permission (Appendix I) and adapted from the previously published manuscript:

Kao, W. A., H. Petrosova, R. Ebady, K. V. Lithgow, P. Rojas, Y. Zhang, Y. E. Kim, Y. R. Kim, T. Odisho, N. Gupta, A. Moter, C. E. Cameron, and T. J. Moriarty. 2017. 'Identification of Tp0751 (Pallilysin) as a *Treponema pallidum* Vascular Adhesin by Heterologous Expression in the Lyme disease Spirochete', *Sci Rep*, 7: 1538.

2.1 Introduction

Treponema pallidum undergoes rapid vascular dissemination to penetrate tissue, placental, and blood-brain barriers and gain access to distant tissue and organ sites. The rapidity and extent of *T. pallidum* dissemination is well documented, but the molecular mechanisms underlying this process have yet to be fully elucidated. One protein that has been shown to play a role in treponemal dissemination is Tp0751, a *T. pallidum* adhesin that interacts with host components found within the vasculature and mediates bacterial adherence to endothelial cells under shear flow conditions (Kao et al. 2017; Parker et al. 2016; Houston et al. 2011; Houston et al. 2015). In this chapter the molecular interactions of Tp0751-mediated adhesion to the vascular endothelium are further explored, demonstrating that recombinant Tp0751 adheres to human endothelial cells of macrovascular and microvascular origin, including a cerebral brain microvascular endothelial cell line.

Adhesion assays using N-terminal truncations of recombinant Tp0751 reveal that endothelial binding is localized to the lipocalin structural domain of the protein. This interaction is also confirmed using live *T. pallidum* to show that spirochete attachment to endothelial monolayers is disrupted by Tp0751-specific antiserum. Further, the 67 kDa laminin receptor (LamR) is identified as an endothelial receptor for Tp0751 using affinity chromatography coupled with mass spectrometry. Notably, LamR has been identified as a receptor for adhesion of other neurotropic invasive bacterial pathogens to brain endothelial cells, including *Neisseria meningitidis, Haemophilus influenzae,* and *Streptococcus pneumoniae*, suggesting the existence of a common mechanism for extravasation of invasive extracellular bacterial pathogens.

2.2 Materials & Methods

Ethics Statements

All animal studies were approved by the local institutional review board at the University of Victoria and were conducted in strict accordance with standard accepted principles as set forth by the Canadian Council on Animal Care (CCAC), National Institutes of Health and the United States Department of Agriculture in facilities accredited by the American Association for the Accreditation of Laboratory Animal Care and the CCAC.

Cloning and purification of recombinant proteins

The treponemal protein Tp0327 [I23-S172] and N-terminal truncations of Tp0751 [C24-P237], Tp0751 [V99-P237] and Tp0751 [E115-P237] were cloned in previous studies (Parker et al. 2016; Houston et al. 2011; Houston et al. 2014). Tp0327 and Tp0751 constructs were purified from *Escherichia coli* BL21-A1 or BL21*DE3, respectively, and subject to nickel affinity chromatography with HisTrap FF columns (GE Healthcare, Mississauga, ON) and further purified with size exclusion and cation exchange chromatography (HiLoad 16/60 Superdex 75; GE Healthcare, GE Healthcare) on an AKTA Prime Plus FPLC system (GE Healthcare) in a final buffer of 20 mM HEPES pH 7.0, 150 mM NaCl, 1% glycerol as previously described (Parker et al. 2016; Houston et al. 2011; Houston et al. 2014).

Endothelial cell culturing

Human umbilical vein endothelial cells (HUVECs) were cultured as previously described (Parker et al. 2016). Human dermal microvascular endothelial cells (HMVECds) from pooled donors (Lonza, Mississauga, ON) and human brain endothelial cells hCMEC/d3 (Millipore, Etobicoke, ON) were cultured at 37°C in an atmosphere of 5% CO_2 in endothelial growth medium-2 microvascular (EGM-2 MV) and EndoGro (Millipore, Etobicoke, ON) supplemented with basic fibroblast growth factor (Millipore), respectively.

Treponema pallidum *propagation*

Treponema pallidum subsp. *pallidum* (Nichols strain) was propagated in, and extracted from, New Zealand White rabbits as previously described (Lukehart and Marra 2007). Testicular extractions were performed in 10% normal rabbit serum (NRS) in 0.9% NaCl at room temperature in an atmosphere of 3-5% O_2 in a modified anaerobic chamber (Coy Laboratories, Grass Lake, MI). Oxygen levels were monitored using a LabQuest2 oxygen meter (Vernier, Beaverton, ON) and maintained with gas injections carbon dioxide balanced with nitrogen.

Borrelia burgdorferi *strains and growth*

Borrelia burgdorferi strains utilized in this chapter included: an adhesion attenuated GFP-expressing B31-A-derived high passage strain of *Borrelia burgdorferi* (GCB706 designated as 'Parent'), a GCB706 background strain containing the Tp0751-3XFLAG plasmid constructs (designated *Bb-Tp0751*; Parker et al. 2016), and the infectious GFP-expressing *B. burgdorferi* strain GCB726 (B31 5A4 NP1 background designated as 'Infectious'). All *B. burgdorferi* strains were cultivated in Barbour-Stoenner-Kelly-II (BSK-II) medium supplemented with gentamicin (100 µg/mL) and/or kanamycin (200 µg/mL) at 37°C in 5% CO_2. The selection of *B. burgdorferi* strains was based on a previously established model system for gain-of-function studies in GCB706, an adhesion attenuated background strain of *B. burgdorferi* (Moriarty et al. 2008).

Endothelial cell attachment assays: recombinant treponemal proteins

Endothelial cells were seeded into 96-well plates (Sarstedt, Newtown, NC) that had been coated with phenol red-free Matrigel (Corning, Tewsbury, MA) by incubating with 500 μg/mL Matrigel for one hour at room temperature and grown for 48 h at 37°C in 5% CO_2 to form confluent monolayers. Endothelial cells were washed with warm HEPES buffered saline (HBSS; Lonza, Mississauga, ON) and incubated with recombinant negative control protein Tp0327 or N-terminal truncations of Tp0751 for 90 minutes at 37°C in an atmosphere of 5% CO_2. To calculate the concentration of the protein constructs, UV absorbance at 280 nm was measured prior to each experiment using a spectrophotometer. Molar concentrations of proteins were calculated based on the molecular weight of each recombinant protein construct in a defined volume to ensure the addition of equimolar amounts of protein. Monolayers were gently washed three times with warm HBSS to remove non-adherent protein, fixed in 2% paraformaldehyde (PFA), and blocked for 30 minutes in 1% bovine serum albumin (BSA) in phosphate buffered saline (PBS) at 37°C in an atmosphere of 5% CO_2. Attachment of recombinant proteins to endothelial monolayers was evaluated by detecting the N-terminal hexa-histidine tags on recombinant proteins as previously described (Cameron et al. 2005; Parker et al. 2016; Houston et al. 2011) using nickel-labeled horseradish peroxidase (Ni-HRP; Mandel Scientific, Guelph, ON). Plates were developed with a 3,3',5,5'-Tetramethylbenzidine (TMB) substrate system (Mandel Scientific) and read at OD600 nm on a BioTek Synergy HT (Biotek, Nepean, ON).

Tp0751-expressing B. burgdorferi *attachment assays*

HUVECs were grown to confluence in 4-well chamber slides (Nalgene Nunc International, Rochester, NY, USA) coated with 500 μg/mL phenol red-free Matrigel (Corning, Tewksbury, MA, USA). For fibronectin competitive inhibition experiments, bacteria or HUVEC were pre-incubated with 8 μg of plasma fibronectin (pFn; Sigma, Oakville, Canada) for 1 hour. *Borrelia burgdorferi* strains were added to each well ($1.4x10^7$ cells/well) and incubated for 12 hours at 36°C/1.5% CO_2. For synthetic peptide inhibition assays, synthetic Tp0751 peptides (p4, p6, p10, p11, p8, p4scr, p6scr, and p10scr1) were diluted to 500 μg/ml in HBSS (Lonza) and HUVECs were pre-incubated with 0.1 μg of Tp0751 peptide per well for 3 h at 37°C in 5% CO_2. Peptide solutions were

removed from HUVECs prior to the addition of bacteria. *Borrelia burgdorferi* strains were added to each well ($1.4x10^7$ cells/well) and incubated for 12 hours at 36°C/1.5% CO_2. For fibronectin adhesion assays, 4-well chamber slides (Nalgene) were coated with 8 μg/well of pFN or super fibronectin (super FN) for 16 hours at 4°C, then washed 2X with HBSS; *B. burgdorferi* strains were added to each well (1.4×10^7 cells/well) and incubated for 20 hours at 36°C/1.5% CO_2.

Two days prior to the experiment, *B. burgdorferi* cultures were passaged to $6x10^5$ cells/mL and grown for 48 h to reach a concentration of $2x10^7$ cells/mL; cultures were then centrifuged and resuspended in a 3:1 mixture of BSK-II:EGM-2 and $1.4x10^7$ cells of each biological replicate were added to HUVECs or fibronectin-coated slides in duplicate wells. Bacteria were co-incubated with HUVECs (12 hours) or fibronectin-coated chamber slides (20 hours) at 36°C in 1.5% CO_2, washed three times with warm HBSS to remove non-adherent bacteria, and fixed in 10% formalin (Fischer Scientific, Ottawa, ON). To determine the effect of increasing concentrations of p10 and a negative control peptide (p8) on adherence of Parent and *Bb*-Tp0751 to HUVECs, cell binding assays were performed as above with cells preincubated with increasing concentrations of peptide (0 nM, 0.54 nM, 5.45 nM, 54.5 nM, and 545 nM). Quantitation of *B. burgdorferi* adhesion to HUVECs was performed by counting GFP-expressing bacteria in ten fields of view (FOV) from duplicate wells for each biological replicate under 400X magnification on a Nikon 80i fluorescence microscope (Meridian Instrument Company, Inc., Kent, WA) fitted with a monochrome digital camera, a dark-field condenser, and fluorescein filter (Excelitas Technologies, Mississauga, ON). Endothelial monolayers were evaluated by darkfield microscopy in each field of view to ensure there had not been any disruptions to the monolayer that could affect spirochete attachment.

T. pallidum-*endothelial attachment assays*

Eight-well chamber slides were coated with phenol red-free Matrigel (Corning) by incubating with 500 μg/mL Matrigel for one hour at room temperature. Human umbilical vein endothelial cells or hCMEC/d3 were seeded into Matrigel coated 8-well chamber slides (LabTek) and grown for 48 hours at 37°C in 5% CO_2 to form confluent monolayers. *Treponema pallidum* was isolated from rabbit testicular extractions and quantified using a

Petroff-hauser counting chamber (Hausser Scientific, Horsham, PA), and $5x10^6$ *T. pallidum* were added to each well of endothelial cells. For Tp0751 serum inhibition assays, *T. pallidum* isolated from testicular extractions was incubated with a 1:2 dilution of heat inactivated antiserum for 90 minutes at 34°C in an atmosphere of 3-5% O_2, and then added to HBSS-washed endothelial monolayers and incubated for 60 minutes at 34°C in an atmosphere of 3-5% O_2. Each well was washed four times with 10% NRS/0.9% NaCl (warmed to 34°C) and then fixed in 10% formalin and permeabilized with 0.05% Triton X-100 (TX-100). Endothelial attachment of *T. pallidum* was assessed by quantifying adherent cells using immunofluorescent detection of the major flagellar protein FlaA. Monolayers were blocked with 4% BSA in PBS and incubated with chicken anti-*T. pallidum* FlaA serum (1/1000; pre-adsorbed with testicular extract and NRS; Cameron et al. 2008) and mouse anti-human VE-Cadherin (0.5 µg/mL; R&D Systems, Minneapolis, MN) for 1 hour at room temperature (RT), washed three times in PBS, and incubated with goat anti-chicken A568 (1/1000; ThermoFisher Scientific Inc, Burnaby, BC) and goat anti-mouse A488 (1/1000; ThermoFisher Scientific) for 1 hour at RT. Monolayers were counterstained with 3 µM DAPI (4',6-diamidino-2-phenylindole; Sigma Aldrich) for 5 minutes at RT, washed with PBS, and mounted with Vectashield mounting medium (Vector Laboratories, Brockville, ON). Viability and outer membrane integrity of *T. pallidum* was confirmed by sampling from each HUVEC or hCMEC/d3 co-incubated well prior to fixation. Viability was evaluated by visualizing the motility of treponemal samples on glass slides (ThermoFisher Scientific) on a Nikon Eclipse E600 darkfield microscope (Nikon Canada, Mississauga, ON, Canada) with a 40X objective (400 X magnification). Membrane integrity of *T. pallidum* was assessed by fixing samples onto CC^2 8-well chamber slides (ThermoFisher Scientific) using 2% PFA. Samples were either left unpermeabilized or permeabilized with 0.05% TX-100, followed by immunofluorescent detection using FlaA-specific antibodies as described above. Visualization was carried out on a Nikon 80i fluorescence microscope (Meridian Instrument Company, Inc., Kent, WA) fitted with a monochrome digital camera, a dark-field condenser, and fluorescein, DAPI and Texas Red filters. Images were acquired with a 100× oil immersion objective (×1000). For LamR inhibition assays, hCMEC/d3 monolayers were pre-incubated with polyclonal LamR or GAPDH antibodies for one hour prior to the addition of *T. pallidum*.

Endothelial cell receptor identification

Affinity chromatography and mass spectrometry were performed as previously described (Houston et al. 2014), with select modifications. Two separate experiments were performed using different endothelial cell lines, recombinant Tp0751 constructs, and mass spectrometry sample preparation methods (Figure 12). Briefly, endothelial membrane and membrane associated proteins were isolated from HUVECs or hCMEC/d3 cell monolayers using a ThermoFisher Scientific Mem-PER eukaryotic membrane protein extraction kit (ThermoFisher Scientific). HUVEC proteins were isolated after endothelial cells were lifted with trypsin and scraping, while hCMEC/d3 cells were physically lifted by scraping. Samples were immediately exposed to protease inhibitor cocktail V (Millipore) and dialyzed three times against 150-fold volumes of Tris buffered saline (TBS) supplemented with 0.05% CHAPS [(3-((3-chloamidopropyl) dimethylammonio-1-propanesulfonate)] at 4°C using Slide-a-Lyzer dialysis cassettes (ThermoFisher). Isolation of Tp0751-interacting endothelial proteins was achieved using a ProFound Pull-Down PolyHis Protein:Protein Interaction kit (ThermoFisher Scientific). Recombinant Tp0751 [C24-P237] or Tp0751 [E115-P237] were dialyzed against TBS/0.05% CHAPS buffer at 4°C, followed by addition of CHAPS to a final concentration of 0.5%, and utilized as bait proteins (Figure 12). Samples were subject to in-gel or in-solution tryptic digestion before analysis by liquid chromatography tandem mass spectrometry (LC-MS/MS) on LTQ Velos Orbitrap with Easy nLC-II (ThermoFisher Scientific). Data analysis was performed using Mascot (Matrix Science, Boston, MA) or Scaffold (Proteome Software, Portland, OR) and candidate endothelial receptors for Tp0751 were identified based upon peptides that achieved a significant mascot score, were found exclusively in the bait-prey sample in both experiments, had greater than one unique significant peptide hit, and were determined through literature analyses to localize to the surface of host cells.

Immunofluorescent detection of LamR

Surface localized LamR was detected from non-permeabilized endothelial monolayers fixed with 4% PFA using mouse anti-LamR (Novus biologicals, Littleton, CO) and goat anti-mouse A568 (ThermoFisher Scientific). Validation of intact endothelial membranes

was achieved with a control immunofluorescence experiment to detect internal protein GAPDH in permeabilized and non-permeabilized endothelial cells using a mouse anti-GAPDH primary antibody (ThermoFisher Scientific) and a secondary goat anti-mouse Alexa 488 (ThermoFisher Scientific).

Co-immunoprecipitation

Live hCMEC/d3 monolayers were co-incubated with 25 µM recombinant Tp0751 [115-237] for 60 minutes at 37°C/5% CO_2. Monolayers were washed with HBSS and lysates were harvested with M-PER Mammalian Protein Extract Reagent (ThermoFisher Scientific) in the presence of the protease inhibitor cocktail set V (Calbiochem, San Diego, CA), incubated on ice for 20 minutes, and centrifuged at 20,000 x g for 15 minutes at 4°C. Protein concentration was determined with a bicinchoninic acid (BCA) assay (ThermoFisher Scientific). Mouse monoclonal anti-LamR antibodies (MLuc5, ThermoFisher Scientific) were covalently coupled to protein G magnetic beads (Dynabeads; ThermoFisher Scientific) using bis(sulfosuccinimidyl)suberate (BS^3; ThermoFisher Scientific) and co-incubated with 75 µg of hCMEC/d3 lysate for 2 hours at 4°C. Beads were washed with M-PER lysis buffer, resuspended in SDS-PAGE loading buffer containing dithiothreitol (DTT, ThermoFisher) and heated to 95°C to elute interacting proteins. Protein interactions were analyzed by SDS-PAGE and immunoblotting with rabbit anti-LamR (R&D Biosystems) and goat anti-rabbit IRdye680 secondary antibodies (LI-COR, Lincoln, NE) to detect LamR and Tp0751-specific mouse monoclonal antibodies (Immunoprecise Antibodies, Victoria, BC) with goat anti-mouse IRdye800 secondary antibodies (LI-COR) to detect Tp0751. Immunoblots were visualized on an Odyssey CLx imaging system (LI-COR) and fold-enrichment of LamR was determined by measuring band intensity using the LI-COR Image Studio Software.

Microscopy and cell counting

Unless otherwise indicated, microscopy images were captured with a Cytation 5 Imaging Reader (BioTek) with a 20X objective at five random FOV per well. For *T. pallidum* adhesion assays, samples were blinded and the number of endothelial nuclei (DAPI; 10-60 µm) and the number of *T. pallidum* cells (FlaA; 2-8 µm) were measured from each field of

view with the Cytation 5 software using size exclusion quantification settings (Biotek). For *B. burgdorferi* adhesion assays, samples were blinded and quantification was performed as described above. To quantify *T. pallidum* cells samples were blinded and the size threshold was set to a minimum of 2 µm and maximum of 8 µm, thereby excluding quantification of background fluorescence from endothelial cells. Endothelial cell quantification was achieved by counting nuclei using a size threshold ranging from 10 – 60 µm. The average count of *T. pallidum* cells was normalized to the number of endothelial cells per field of view.

Statistical Analyses

Statistical analyses were performed in GraphPad Prism (GraphPad, La Jolla, CA) as denoted in figure legends. Graphs were prepared in GraphPad Prism (GraphPad) or Excel (Microsoft, Redmond, WA)

2.3 Results

Tp0751 adheres to endothelial cells of microvascular and macrovascular origin.

With the knowledge that Tp0751 interacts with ECM components that are in close proximity to the vascular endothelium (Cameron et al. 2005; Cameron et al. 2008; Houston et al. 2011; Houston et al. 2015; Parker et al. 2016), the endothelial interactions mediated by this *T. pallidum* adhesin were explored. Attachment of Tp0751 to endothelial cell monolayers of macrovascular and microvascular origin was evaluated using plate-based binding assays with a recombinant protein construct (Tp0751 [V99-P237]) that corresponds to the characterized structural domains of Tp0751 including the extended N-terminal helix and lipocalin domain (Parker et al. 2016). Recombinant Tp0751 binding was compared to the negative control treponemal protein, Tp0327. Tp0751 exhibited dose-dependent binding to two primary human endothelial cell lines: human umbilical vein macrovascular cells (HUVECs; Figure 5A; Tp0751 vs. Tp0327 p=0.017) and human microvascular dermal endothelial cells (HMVECds; Figure 5B; Tp0751 vs. Tp0327 p=0.042). Further, Tp0751 displayed dose-dependent adhesion to a monolayer of immortalized cerebral brain microvascular endothelial cells (hCMEC/d3; Figure 5C; Tp0751 vs. Tp0327 p=0.0033).

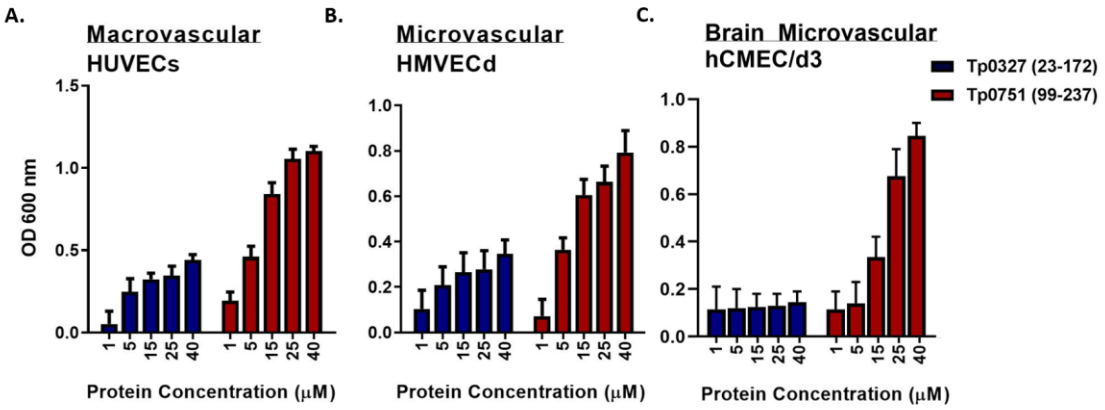

Figure 5: Tp0751 adheres to primary endothelial cells of microvascular and macrovascular origin. Dose-dependent binding assays evaluating attachment of recombinant Tp0751 [V99-P237] or negative control recombinant Tp0327 [I23-S172] to host cell monolayers of **(A)** macrovascular human umbilical vein endothelial cells (HUVECs) **(B)** microvascular human dermal endothelial cells (hMVECd) and **(C)** human cerebral microvascular endothelial cells (hCMEC/d3). Results are presented as mean absorbance at 600 nm ± SEM from triplicate wells in four independent experiments for HUVECs and hMVECd and from duplicate wells in two independent experiments for hCMEC/d3. Statistical analyses were performed using a two-way ANOVA comparing endothelial binding of Tp0751 [V99-P237] to Tp0327 [I23-S172] in HUVECs (p=0.017), hMVECd (p=0.042) and hCMEC/d3 (p=0.0033).

Tp0751 mediates spirochete attachment to endothelial cells

To determine whether Tp0751 facilitates binding to endothelial cells in the biologically relevant context of a live spirochete, a heterologous expression system with the model spirochete *Borrelia burgdorferi* was used. A non-infectious, adhesion-attenuated, GFP-expressing strain of *B. burgdorferi* ('Parent') was transformed with a plasmid carrying Tp0751 ('*Bb*-Tp0751'), resulting in Tp0751 localization to the bacterial surface (Parker et al. 2016) and a gain-of-function for attachment to endothelial cells *in vitro* under conditions of shear flow and *in vivo* in mouse post-capillary venules (Figure 6A; Parker et al. 2016;

Kao et al. 2017). A stationary adhesion assay was optimized (Figure 6B) and a significant gain-of-function for endothelial attachment of *Bb*-Tp0751 was observed compared to the Parent strain after a 12-hour co-incubation with HUVECs (Figure 6C, $p<0.0001$).

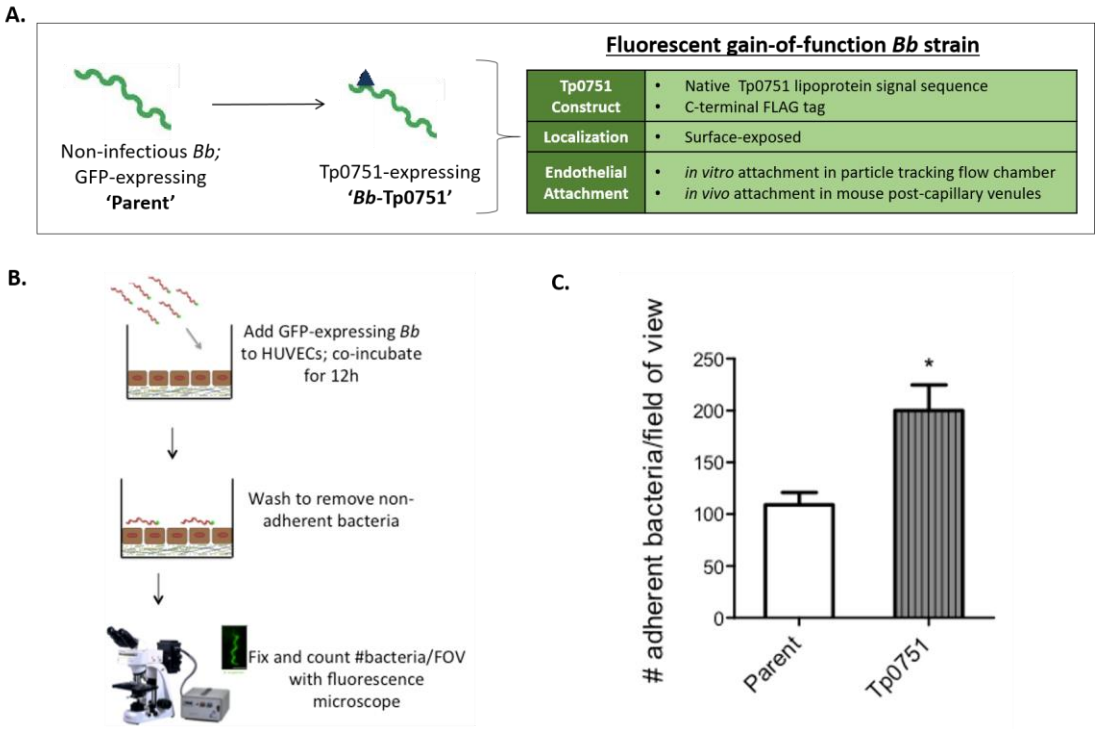

Figure 6: Tp0751-expressing *B. burgdorferi* mediates attachment to endothelial cells. **(A)** Schematic showing the construction of the *B. burgdorferi* heterologous expression system. A non-infectious, adhesion-attenuated, GFP-expressing strain of *B. burgdorferi* ('Parent') was transformed with a C-terminal 3X-FLAG tagged construct of Tp0751 containing the native Tp0751 lipoprotein signal sequence ('*Bb*-Tp0751'). Heterologous expression of Tp0751 resulted in localization to the cell surface of *B. burgdorferi* (Parker et al. 2016) and conferred gain-of-function for adhesion to endothelial cells *in vitro* using a particle tracking flow chamber to mimic the shear flow of the host vasculature as well as adhesion to mouse post-capillary venules *in vivo* during intravital microscopy (Kao et al. 2017). **(B)** Schematic showing the experimental design of the *B. burgdorferi*-HUVEC attachment assay. Confluent HUVEC monolayers seeded on an artificial basement membrane were co-incubated with the non-infectious, adhesion-attenuated Parent strain (negative control) or the Tp0751-expressing *B. burgdorferi* strain to assess gain-of-function for endothelial attachment After washing to remove non-adherent bacteria, *B.*

burgdorferi adhesion to HUVECs was quantified using fluorescence microscopy to count the number of adherent bacteria per field of view (FOV) at 400x magnification. **(C)** Number of adherent Parent or *Bb*-Tp0751 per FOV, presented as mean ± SEM from three independent experiments (three biological replicates and two technical replicates per experiment). Statistical analysis was performed using a Student's two-tailed t-test comparing endothelial binding of the Parent strain with *Bb*-Tp0751 (***; $p<0.001$).

Tp0751-specific serum inhibits attachment of *Treponema pallidum* to endothelial cells

To determine if Tp0751 is involved in the endothelial attachment of live *T. pallidum,* a *T. pallidum* adhesion assay was developed where endothelial-treponemal interactions were detected and quantified via immunofluorescence imaging (Figure 7A-B). Serum-mediated disruption of *T. pallidum*-endothelial interactions was evaluated by incubating *T. pallidum* with normal rabbit serum (NRS), antiserum specific to Tp0751, or antiserum specific to the control treponemal protein Tp0327, prior to co-incubation with endothelial monolayers (Figure 7A). Treponemes were isolated from testicular extractions and maintained in an atmosphere of 34°C, 3-5% O_2. Treponemal motility was monitored throughout the experiment via darkfield microscopy to confirm the ongoing health of the organisms; non-permeabilized controls were incorporated into each experiment to validate *T. pallidum* outer membrane integrity by comparing reactivity of serum specific to the endoflagellar protein, FlaA, between permeabilized and non-permeabilized samples (Figure 8). In these experiments treponemes pre-incubated with Tp0751-specific antiserum showed a statistically significant reduction in endothelial adhesion relative to *T. pallidum* incubated with the NRS and anti-Tp0327 serum negative controls (Figure 7C-D, $p=0.015$ vs. NRS, $p=0.025$ vs. anti-Tp0327 serum).

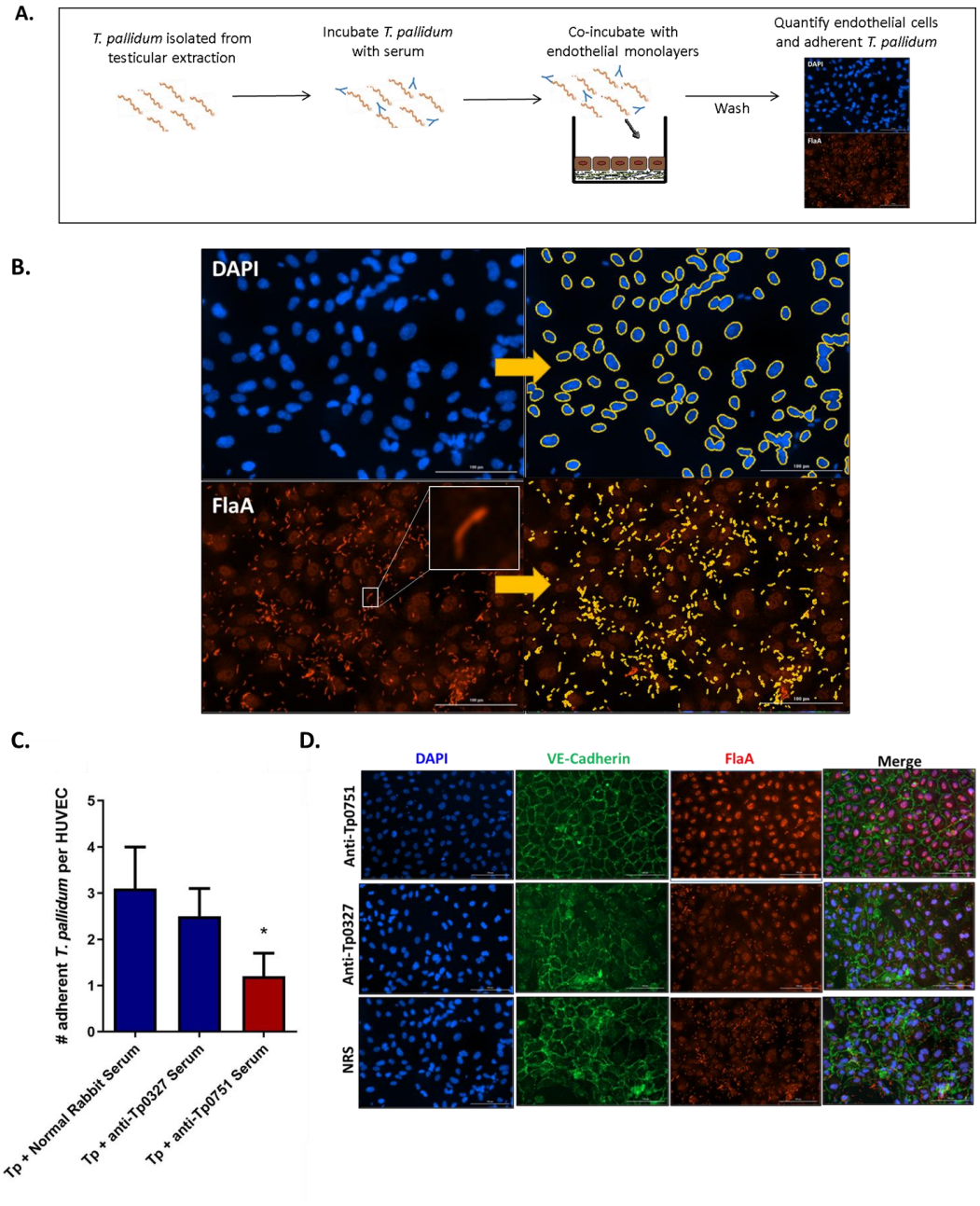

Figure 7: Tp0751-specific antiserum disrupts *T. pallidum* interactions with endothelial cells.**(A)** Schematic illustrating the *T. pallidum*-endothelial cell adhesion assay. *Treponema pallidum* isolated from a rabbit testicular extraction was preincubated with Tp0751-specific serum or control serum (Tp0327-specific or normal rabbit). *Treponema pallidum* was then co-incubated with confluent HUVEC monolayers seeded on an artificial basement membrane to assess the blocking activity of the serum. After washing to remove non-

adherent treponemes, *T. pallidum* endothelial attachment was evaluated using immunofluorescence detection of FlaA (periplasmic flagellar protein) for treponemal quantification and DAPI (nuclear stain) for HUVEC quantification to determine the number of adherent *T. pallidum* per HUVEC at 200X magnification. (B) Representative immunofluorescence images from the *T. pallidum* adhesion assay. HUVEC nuclei were stained with DAPI (blue; upper panel) and quantified by automatic counting of nuclei within the size threshold of 10 – 60 µm (top right panel; yellow outline). *Treponema pallidum* cells (bottom left panel; inset) were stained with anti-FlaA chicken serum followed by goat anti-chicken (Alex568 conjugated, red) and quantified by automatic counting of treponemes within the size threshold of 2-8 µm (bottom right panel; yellow outline). **(C)** Number of adherent *T. pallidum* (Tp) per HUVEC following preincubation with normal rabbit serum or anti-Tp0327 serum (blue, negative control) or Tp0751-specific serum (red). Mean number of *T. pallidum* per HUVEC ± SEM were quantified blinded from five FOV in duplicate wells in four independent experiments**.** Statistical analysis was performed using a Student's two-tailed t-test comparing endothelial binding of *T. pallidum* preincubated with Tp0751-specific serum to *T. pallidum* preincubated with negative control serum (blue; Tp + Normal Rabbit Serum [p=0.015], Tp + anti-Tp0327 serum [p=0.025]). **(D)** Representative immunofluorescence images from *T. pallidum* inhibition assay. HUVEC nuclei were stained with DAPI (blue) and cellular margins were stained with mouse monoclonal anti-VE-cadherin followed by goat anti-mouse (Alexa488-conjugated, green). *Treponema pallidum* was visualized with anti-FlaA chicken serum followed by goat anti-chicken (Alex568 conjugated, red). Quantification of HUVECs and *T. pallidum* were compared between anti-Tp0751 preincubations **(upper panel)**, anti-Tp0327 preincubations **(middle panel)**, and normal rabbit serum preincubations **(lower panel)**. Quantification of *T. pallidum* was achieved using size exclusion software to selectively count *T. pallidum* in the TexasRed filter using a size threshold range between

2-8 µm to exclude background fluorescence from endothelial cells. Endothelial cells were quantified by automatic counting of nuclei within the size threshold of 10 – 60 µm.

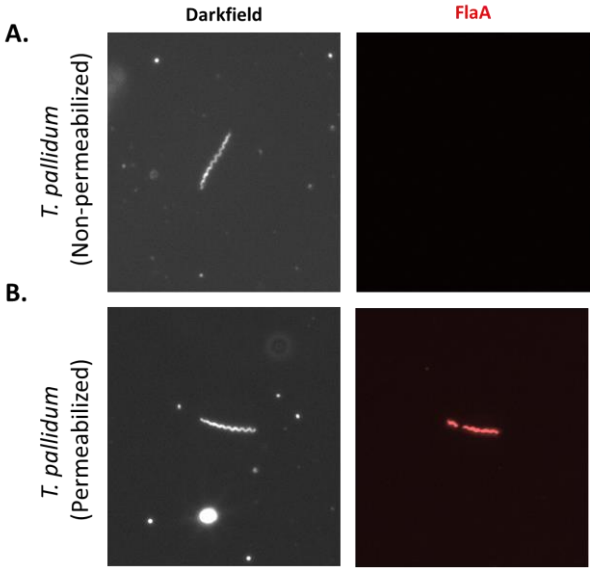

Figure 8: Validation of *T. pallidum o*uter membrane integrity during endothelial attachment assays. Samples taken from *T. pallidum*-endothelial attachment assays were fixed with 4% PFA in 8-well chamber slides and stained for the endoflagellar protein FlaA using anti-Tp0249 (FlaA) chicken serum and goat anti-chicken Alexa568 to confirm that non-permeabilized *T. pallidum* retained outer membrane integrity, as indicated by visualization of treponemes by darkfield microscopy (A, column 1) and absence of signal from FlaA immunofluorescence (A, column 2). These samples were compared to *T. pallidum* intentionally permeabilized with TX-100 to disrupt outer membrane integrity allowing for visualization of treponemes by darkfield microscopy (B, column 1) and FlaA immunofluorescence (B, column 2). Representative epifluorescence images obtained from a Nikon 80i fluorescence microscope at 200X magnification.

Endothelial interactions are mediated by the C-terminal lipocalin region of Tp0751

To delineate the endothelial binding interface of Tp0751, recombinant protein attachment to endothelial monolayers was evaluated using constructs with varying N-terminal truncations. Endothelial binding was compared between Tp0751 [C24-P237] which encompasses the mature lipoprotein sequence; Tp0751 [V99-P237] which includes the lipocalin domain with the N-terminal helix; and Tp0751 [E115-P237] which includes the

lipocalin domain without the N-terminal helix (Figure 9A). Plate-based binding assays were used to evaluate adhesion of Tp0751 truncations or a negative control treponemal protein, Tp0327, to confluent endothelial monolayers of microvascular and macrovascular origin. All three constructs exhibited statistically significant binding to endothelial monolayers when compared to the negative control recombinant protein, Tp0327 (Figure 9B-C, $p<0.0001$), but no difference in binding was observed between the three Tp0751 N-terminal truncation constructs (C24-P237, V99-P237, and E115-P237; Figure 6B-C, not significant [ns]), demonstrating that endothelial binding localizes to the C-terminal lipocalin domain of the protein. To ensure that the endothelial binding capacity of Tp0751 is not due to an abundance of charged residues facilitating non-specific host cell binding, the net charge of each recombinant protein was compared at pH 7 (Table 1). Despite differences in net charge between Tp0751 [C24-P237], Tp0751 [V99-P237] and Tp0751 [E115-P237] (Table 1; +0.09, +0.545, -1.442, respectively), all N-terminal truncations of Tp0751 exhibit the same level of endothelial binding (Figure 9B), indicating that the net charge of the protein is not driving host cell adhesion.

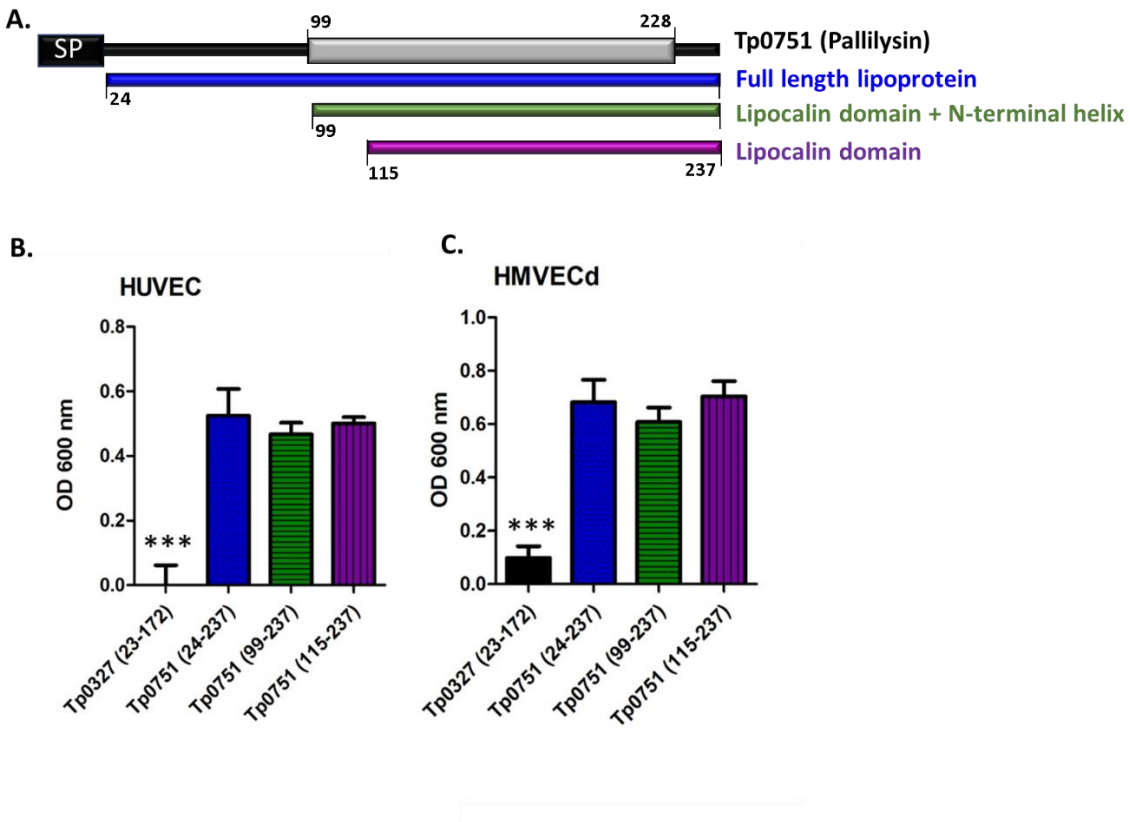

Figure 9: Endothelial binding is localized to the lipocalin domain of Tp0751. **(A)** Schematic of Tp0751 primary sequence including the signal peptide (SP black box M1-S23), defined secondary structure elements (V99 – H228, grey box) (Parker et al. 2016) and N-terminal truncations corresponding to the mature lipoprotein (blue), the lipocalin domain with the N-terminal helix (green), or the lipocalin domain (purple). Plate-based binding assays evaluated attachment of recombinant Tp0751 N-terminal truncations and the negative control Tp0327 I23-S172 to **(B)** HUVECs and **(C)** HMVECd. Proteins were added in equimolar concentration (25 µM) and results are presented as mean ± SEM from three independent experiments performed in triplicate. Statistical analysis was performed using a Student's two-tailed t-test comparing endothelial binding of Tp0751 N-terminal truncations to Tp0327 I23-S172 (***; $p<0.001$)

Table 1 Net charge of treponemal recombinant protein constructs.

Recombinant Protein Construct	# Positively Charged Residues[1]	# Negatively Charged Residues[2]	Net Charge	Net Charge at pH7[3]
Tp0327 [I23-S172]	22	22	0	-0.041
Tp0751 [C24-P237]	19	18	+1	+0.09
Tp0751 [V99-P237]	14	14	0	+0.545
Tp0751 [E115-P237]	14	12	+2	-1.442

[1]Total number of positively charged arginine and lysine residues
[2]Total number of negatively charged aspartic acid and glutamic acid residues
[3]Calculated by prot pI based upon ExPASy pKa values (The UniProt Consortium 2019)

A discrete region of the Tp0751 lipocalin domain mediates endothelial adhesion of *Bb*-Tp0751.

Tp0751 contains four ECM-binding regions that map along a single face of the beta-barrel of the Tp0751 lipocalin domain and N-terminal helix (Figure 10A). It is predicted that these four binding regions synergistically coordinate interactions with large ECM components (Parker et al. 2016; Cameron et al. 2005). To delineate the endothelial interaction region of Tp0751 in the biological context of a live spirochete, a competitive inhibition assay was designed using the *B. burgdorferi* heterologous expression system (Parker et al. 2016) and synthetic peptides from known Tp0751 ECM-binding regions including peptides 4, 6, 10, and 11 spanning amino acids G88-A112, Q117-I141, R172-F196, and S185-V209 respectively **(**Figure 10B**)**. The endothelial binding capacity of *Bb*-Tp0751 was evaluated relative to the non-adherent, non-transformed *B. burgdorferi* strain (Parent), alone or individually preincubated with Tp0751 synthetic peptides (Figure 10C). While peptides p4, p6, and p11 did not alter *Bb*-Tp0751 adhesion, incubation with peptide p10 significantly reduced binding of *Bb*-Tp0751 to HUVEC monolayers compared to the binding levels exhibited following preincubation with the scrambled (scr) peptide, p10scr1 (Figure 10D; *Bb*-Tp0751 p10 vs. *Bb*-Tp0751 p10scr * $p \leq 0.005$). A negative control peptide (p8) that does not bind ECM components (Parker et al. 2016) had no effect on the endothelial adhesion of either *B. burgdorferi* strain (Figure 10D). Furthermore, preincubation of HUVEC monolayers with increasing concentrations of p10 (0 nM– 545 nM) resulted in dose-dependent decrease of *Bb*-Tp0751 attachment to HUVEC monolayers

compared to the levels of binding when preincubated with p8 (Figure 10E; ≥5.45 nM p10; $p \leq 0.005$). These results show that p10 is uniquely capable of inhibiting binding of Tp0751-expressing *B. burgdorferi* to HUVEC monolayers. The potency of p10 (Figure 10F) suggests that Tp0751 is expressed at low levels in the *B. burgdorferi* heterologous expression system since a small amount of peptide is required for inhibition of spirochete attachment.

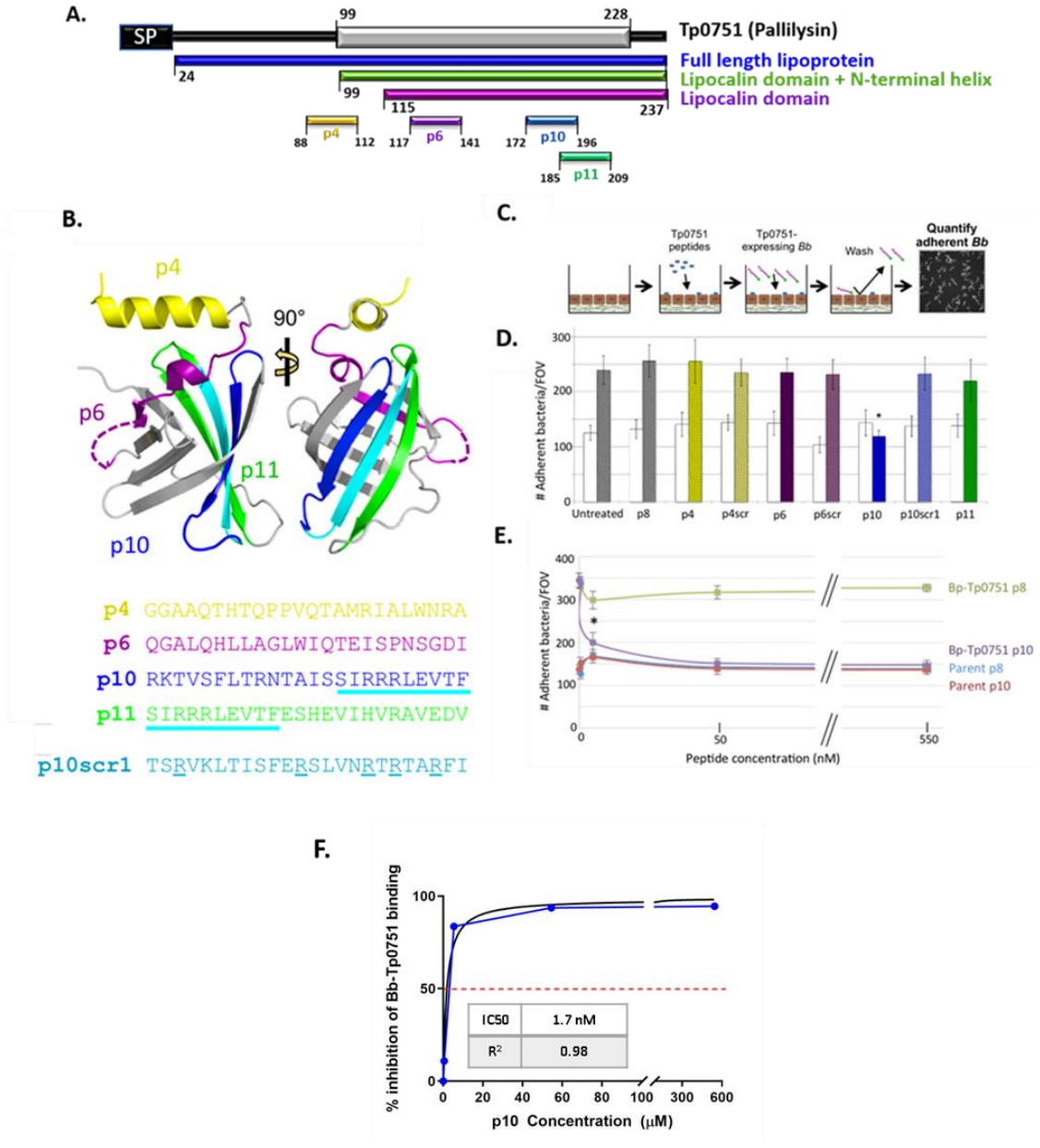

Figure 10: Tp0751 peptide 10 inhibits adhesion of Tp0751-expressing *B. burgdorferi* to HUVEC monolayers. Schematic of Tp0751 primary sequence including the signal peptide

(SP black box M1-S23), defined secondary structure elements (V99 – H228, grey box) (Parker et al. 2016) and N-terminal truncations corresponding to the mature lipoprotein (blue), the lipocalin domain with the N-terminal helix (green), the lipocalin domain (purple), and ECM binding peptides p4 [G88-A112], p6 [Q117-I141], p10 [R172-196F], and p11 [S185-V209]. **(B)** Primary amino acid sequences and corresponding location on the Tp0751 structure of ECM-binding peptides p4, p6, p10, and p11 (Parker et al. 2016; Cameron et al. 2005). The overlapping region between p10 and p11 is highlighted in cyan in the structure and the underlined in cyan in the primary amino acid sequence; the sequence of scrambled p10 (scr1, teal) is shown with the positively charged arginine residues underlined. **(C)** Schematic showing the competitive inhibition assay experimental design. Confluent HUVEC monolayers seeded on artificial basement membrane were preincubated with synthetic Tp0751 peptides (p4, p6, p10, p11, p4scr, p6scr, and p10scr1) to allow for peptide-endothelial cell interactions. HUVECs were then co-incubated with the non-infectious, adhesion-attenuated Parent strain (negative control) or Tp0751-expressing *B. burgdorferi* strains to assess the competitive inhibition capacity of the synthetic Tp0751 peptides. After washing to remove non-adherent bacteria, *B. burgdorferi* adhesion to HUVECs was quantified using fluorescence microscopy to count the number of adherent bacteria per FOV at 400x magnification; samples were blinded during quantification. **(D**) Number of adherent Parent (white bars) or *Bb*-Tp0751 (hatched, colored bars) per FOV. Results presented as mean counts ± SEM from ten FOV for each biological replicate. For statistical analyses, attachment by strain *Bb*-Tp0751 to HUVEC monolayers preincubated with peptides p4, p6, p10 and p11 was compared to the attachment of strain *Bb*-Tp0751 in the presence of corresponding scrambled peptides, using Student's two-tailed t-test. Strain *Bb*-Tp0751 exhibited statistically significant lower levels of binding to HUVEC monolayers preincubated with peptide p10 (*$p \leq 0.005$) when compared to the levels of binding when preincubated with the scrambled version of peptide 10 (p10scr1). A statistically significant increase in endothelial adhesion compared to the Parent strain was observed for *Bb*-Tp0751 under untreated conditions and when monolayers were pre-incubated with all other peptides ($p<0.05$). **(E)** The effect of increasing concentrations (0 nM, 0.54 nM, 5.45 nM, 54.5 nM, and 545 nM) of p10 and negative control peptide p8 on adherence of Parent and *Bb*-Tp0751 to HUVECs. Results are presented as mean bacteria ±

SEM from ten FOV for each biological replicate. Statistical analysis was performed using Student's two-tailed t-test. Strain *Bb*-Tp0751 exhibited significantly lower levels of binding to HUVEC monolayers when preincubated with ≥5.45 nM p10 compared to the levels of binding when preincubated with ≥5.45 nM p8 (*$p \leq 0.005$). (F) Non-linear regression curve was fitted and the IC50 for p10 inhibition of HUVEC binding by *Bb*-Tp0751 was calculated (IC50 = 1.7 nM; red dashed line) using GraphPad Prism data analysis software (San Diego, CA).

The role of fibronectin in Tp0751-mediated endothelial cell adhesion

The *T. pallidum* adhesin, Tp0751, is known to interact with ECM components that associate with luminal and basolateral faces of the vascular endothelium. It has been postulated that Tp0751-mediated attachment to endothelial cells may occur through bridged interactions with ECM molecules. Plasma fibronectin ('pFN') is an abundant blood glycoprotein that exists in a compact globular form in the bloodstream and undergoes conformational changes when deposited on vascular surfaces to form insoluble matrices (Kadler, Hill, and Canty-Laird 2008); cell surface associated fibronectin is a common attachment site for disseminating bacterial pathogens (Lemichez et al. 2010). To explore the role of fibronectin in Tp0751-mediated endothelial attachment, *Bb*-Tp0751 was evaluated for the ability to adhere to endothelial monolayers in the presence of pFN. Attachment of *Bb*-Tp0751 was inhibited by pre-incubation of bacteria with pFN before addition to endothelial cells (Figure 11A; * $p<0.05$). However, no inhibition was observed when HUVECs were pre-incubated with pFN to allow for matrix formation on HUVEC surfaces prior to co-incubation with *Bb*-Tp0751 (Figure 11A). This result suggests that either fibronectin already present on endothelial cells is sufficient to mediate interactions, or that interactions may be occurring directly with endothelial surfaces.

To determine whether Tp0751 facilitates spirochete attachment to immobilized fibronectin, the attachment of the parent strain, *Bb*-Tp0751, and an infectious *B. burgdorferi* strain were compared for adhesion to immobilized pFN or superfibronectin (sFN), which mimics the insoluble fibronectin matrices that form on cell surfaces

(Morla, Zhang, and Ruoslahti 1994). The infectious *B. burgdorferi* strain exhibited significantly higher levels of adhesion to both immobilized pFN and sFN compared to the negative control parent strain or *Bb*-Tp0751 where no fibronectin attachment was observed (Figure 11B; Infectious vs. Parent * p=0.0064, Infectious vs. Tp0571 * p=0.0063).

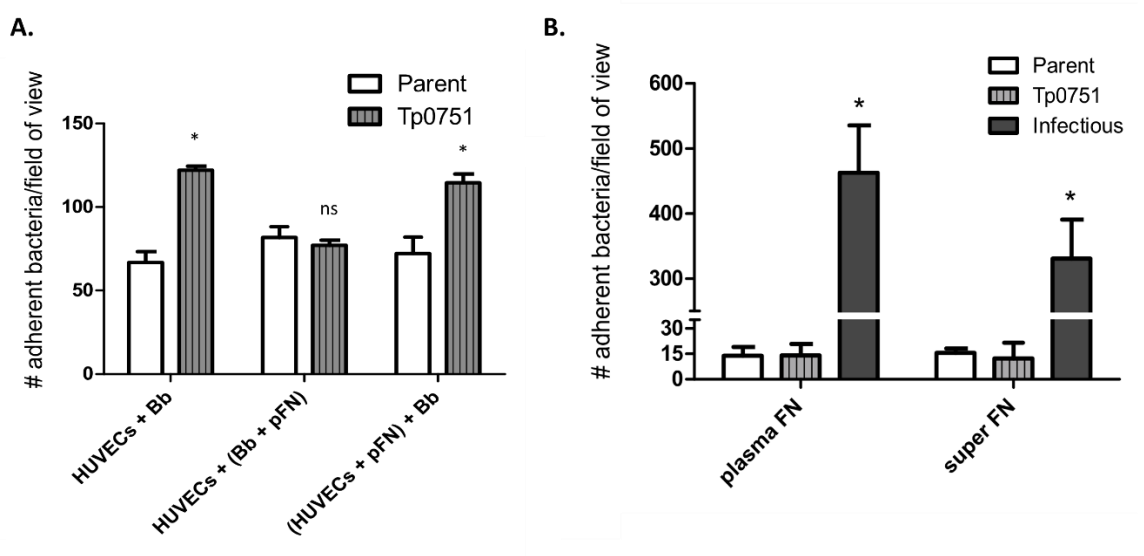

Figure 11: Interactions of *Bb*-Tp0751 with soluble and immobilized fibronectin. Mean ± SEM of Parent and Tp0751-expressing *B. burgdorferi* (*Bb*-Tp0751) cells adhered to primary HUVEC monolayers after 12 h of co-incubation (HUVECs + *Bb*, control). HUVECs + (*Bb* + pFn): binding of bacteria pre-incubated with plasma fibronectin (pFn) to HUVECs. (HUVECs + pFn) + *Bb*: binding of bacteria to HUVEC pre-incubated with pFn. Results from two independent experiments with three biological replicates in technical duplicate per experiment**.** Statistical analysis performed using a one-way Kruskal-Wallis ANOVA with Dunn's post-test * p<0.05 *Bb*-Tp0751 vs. Parent in 'HUVECs + *Bb'* and '(HUVECs + pFN) + *Bb'* treatments. **(B)** Mean ± SEM numbers of Parent, Tp0751-expressing *B. burgdorferi* (*Bb*-Tp0751), and infectious *B. burgdorferi* adhered to immobilized pFN or sFN after 20 hours of co-incubation. Results from two independent experiments with three biological replicates in technical duplicate per experiment. Statistical analysis was performed with a two-way ANOVA strain factor * p=0.0032, fibronectin factor ns p=0.1689 with a Tukey's post-test comparing Parent

vs. Tp0751 ns p=0.996; Parent vs. Infectious * p=0.0064; Tp0751 vs. Infectious * p=0.0063.

Identification of LamR and stomatin as endothelial receptors for Tp0751

The molecular identity of host cell receptors targeted by Tp0751 during the process of vascular adhesion were determined using affinity chromatography coupled with mass spectrometry (Figure 12). Integral membrane proteins and membrane-associated proteins were isolated from HUVECs or hCMEC/d3 and incubated with recombinant Tp0751 immobilized on cobalt chelate columns. Interacting host proteins were eluted from the column and identified by liquid chromatography tandem mass spectrometry (LC-MS/MS). In independent experiments using HUVECs and hCMEC/d3 as prey and Tp0751 [C24-P237] or Tp0751 [E115-P237] as bait, respectively, LamR and stomatin were identified with greater than one significant peptide hit from Tp0751-conjugated, but not control unconjugated, columns (Table 2, Table 3).

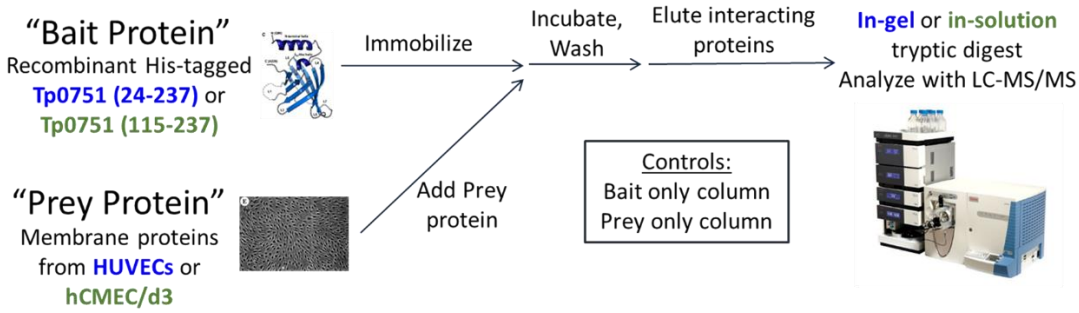

Figure 12: Schematic illustration of affinity chromatography mass spectrometry framework for identification of candidate endothelial cell receptors for Tp0751. Recombinant histidine-tagged Tp0751 was immobilized to a cobalt chelate matrix followed by the addition of membrane proteins and membrane-associated proteins isolated from endothelial cells. Following a series of incubations and washes, interacting proteins were eluted with imidazole and identified with liquid chromatography tandem mass spectrometry following tryptic digestion. Two separate experiments were conducted and differences in the protocol are denoted in blue or green. In parallel, an unconjugated cobalt chelate affinity column was subject to the same conditions to identify endothelial proteins that interact non-specifically with the chelate. Candidate endothelial receptors were

identified from peptides that were found exclusively in the bait-prey sample in both experiments, had greater than one unique significant peptide hit, and were known to localize to the surface of host cells

Table 2 Tp0751 [E115-P237]-reactive hcMEC/d3 membrane and membrane associated proteins identified by affinity chromatography and mass spectrometry.

hCMEC/d3 Protein	Uniprot #	Scaffold Probability[1]	# of Peptides[2,3]	Peptide Sequences	Total Sequence Coverage[4]	Predicted Localization
67 kDa laminin receptor	P08865	98%	4	(K)FLAAGTHLGGTNLDFQMEQYIYK(R) (R)AIVAIENPADVSVISSR(N) (K)FAAATGATPIAGR(F) (R)FTPGTFTNQIQAAFR(E)	23%	Cell surface, cytoplasm, nucleus
Stomatin	P27105	98%	2	(K)EASMVITESPAALQLR(Y) (R)VQNATLAVANITNADSATR(L)	15%	Cell surface (lipid rafts)

[1]Only proteins identified with a Scaffold probability ≥95 % were considered potentially significant.
[2]No. of observed peptides include all peptides that differ only by sequence and that were identified with a Scaffold probability ≥95 %; peptides with the same sequence but modification or charge differences are not included. Proteins that were identified with a Scaffold probability ≥95 % but with only one observed peptide were not considered.
[3]Peptides found exclusively in the Bait-Prey sample; >1 unique, significant peptide hit; localization to the external face of the plasma membrane of host cells
[4]Total Sequence Coverage is based on all identified peptides with unique sequences.

Table 3 Tp0751 [C24-P237]-reactive HUVEC membrane and membrane associated proteins identified by affinity chromatography and mass spectrometry.

HUVEC Protein	Uniprot Accession Number	Mascot Score[1]	# of Peptides[2,3]	Peptide Sequences	Total Sequence Coverage[4]	Predicted Localization
67 kDa laminin receptor	P08865	78	4	(K)SDGIYIINLK(R) (R)FTPGTFTNQIQAAFR(E) (R)AIVAIENPADVSVISSR(N) (R)ADHQPLTEASYVNLPTIALCNTDSPLR(Y)	23%	Cell surface, cytoplasm, nucleus
Stomatin	P27105	157	5	(R)ILQGGAKGPGLFFILPCTDSFIKVDMR(T) (R)ALKEASMVITESPAALQLR(Y) (K)EASMVITESPAALQLR(Y) (K)NSTIVFPLPIDMLQGIIGAK(H) (R)VQNATLAVANITNADSATR(L)	35%	Cell surface (lipid rafts)

[1]Only proteins identified with a significant Mascot score were considered potentially significant.
[2]No. of observed peptides include all peptides that differ only by sequence and that were identified with a significant Mascot score; peptides with the same sequence but modification or charge differences are not included. Proteins that were identified with a significant Mascot score but with only one observed peptide

were not considered.
[3]Peptides found exclusively in the Bait-Prey sample; >1 unique, significant peptide hit; localization to the external face of the plasma membrane of host cells
[4]Total Sequence Coverage is based on all identified peptides with unique sequences.

Recombinant Tp0751 interacts with endogenous LamR from cerebral brain endothelial cells.

The molecular interaction between Tp0751 and LamR was validated using co-immunoprecipitation. Following incubation of recombinant Tp0751 [E115-P237] with live hCMEC/d3 monolayers, specific binding between Tp0751 and endogenous LamR was confirmed by demonstrating that Tp0751 co-precipitates with LamR when LamR-specific antibodies are covalently linked to magnetic beads (Figure 13). An enrichment of LamR of at least 12-fold was observed in co-immunoprecipitations (Figure 13; IP: LamR) compared to controls where lysates were incubated with magnetic beads in the absence of antibodies (Figure 13; Lysate + Bead Controls).

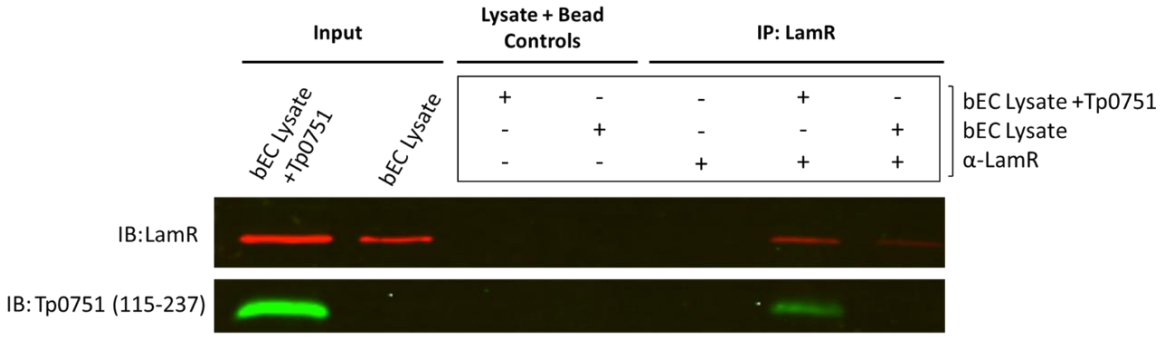

Figure 13: Recombinant Tp0751 interacts with LamR endogenously expressed by brain endothelial cells (bECs). Live hCMEC/d3 monolayers were left untreated (bEC lysate) or co-incubated with exogenous recombinant Tp0751 (bEC lysate + Tp0751). Lysates were incubated with magnetic beads in the absence of antibodies (lysate + bead controls) to control for non-specific interactions between LamR and the beads. LamR was immunoprecipitated (IP) from lysates using mouse anti-LamR antibody covalently coupled to magnetic beads, and co-immunoprecipitation of Tp0751 was evaluated by immunoblotting (IB) against Tp0751 [E115-P237] and LamR. Representative result from three independent experiments.

***T. pallidum* interacts with the C-terminal region of endogenous LamR on cerebral brain endothelial cells.**

LamR contains three distinct interaction regions that are engaged by laminin (Castronovo, Taraboletti, and Sobel 1991; Kazmin et al. 2000; Landowski, Dratz, and Starkey 1995; Landowski, Uthayakumar, and Starkey 1995), prion protein (Kazmin et al. 2000; Hundt et al. 2001) and the neuroinvasive pathogens *S. pneumoniae, H. influenzae,* and *N. meningitidis* (Orihuela et al. 2009) (Figure 14A). The peptide G region (Figure 14A; yellow box, amino acids 161-180) and direct binding site (Figure 14A; orange box, amino acids 205-229) are bound by laminin and the prion protein (Castronovo, Taraboletti, and Sobel 1991; Kazmin et al. 2000; Landowski, Dratz, and Starkey 1995; Landowski, Uthayakumar, and Starkey 1995; Hundt et al. 2001), whereas a discrete region of the LamR C-terminus (Figure 14A; green box, amino acids 263-282) is the attachment site for several neuroinvasive bacterial pathogens (Orihuela et al. 2009). Given the neuroinvasive capability of *T. pallidum*, the *T. pallidum*-endothelial adhesion assay (Figure 7A) was utilized to determine whether attachment to brain endothelial cells could be disrupted by blocking the LamR C-terminal pathogen binding region. Polyclonal antibodies specific to the LamR C-terminus (amino acids 263-282) inhibited *T. pallidum* attachment to hCMEC/d3 cells in a dose-dependent manner (Figure 14B; p=0.0037), while a negative control polyclonal antibody specific to the irrelevant protein glyceraldehyde 3-phosphate dehydrogenase (GAPDH) had no effect on *T. pallidum* endothelial attachment at all antibody dilutions tested (Figure 14B). Surface expression of LamR in endothelial cells was confirmed using immunofluorescence experiments conducted under the same culture conditions (Figure 15).

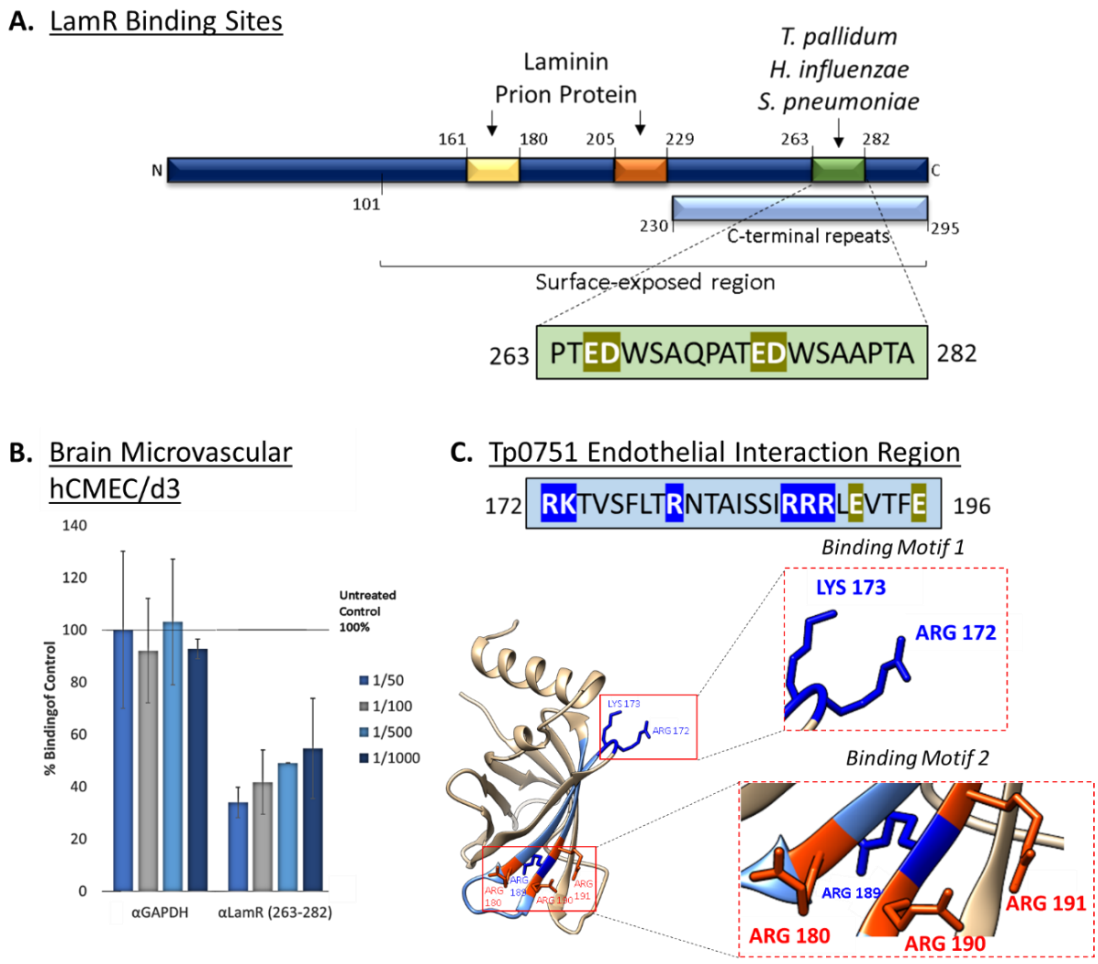

Figure 14: *T. pallidum* interacts with LamR (263-282) on brain endothelial cell surfaces. Schematic illustration of characterized interaction regions of LamR (Orihuela et al. 2009; Castronovo, Taraboletti, and Sobel 1991; Kazmin et al. 2000; Landowski, Uthayakumar, and Starkey 1995; Hundt et al. 2001). Elements include the predicted surface-exposed region (amino acids 101-295), C-terminal repeats (light blue box, amino acids 230-295), binding sites for laminin and the prion protein including the peptide G region (yellow box; amino acids 161-180) and direct binding region (orange box; amino acids 205-229) and the binding site for neuroinvasive bacterial pathogens (green box; amino acids 263-282). **(B)** *Treponema pallidum* attachment to brain endothelial cells hCMEC/d3 was evaluated using immunofluorescence detection of FlaA (periplasmic flagellar protein) for treponemal quantification and DAPI (nuclear stain) for hCMEC/d3 quantification to determine the number of adherent *T. pallidum* per hCMEC/d3 at 200X magnification from five FOV in duplicate from two independent experiments. Inhibition of *T. pallidum* attachment to

hCMEC/d3 cells by antibodies was quantified as a percentage of the untreated no-antibody control (set at 100%). Results are presented as mean ± SEM and statistical analysis was performed using two-way ANOVA with Tukey's post-test comparing *T. pallidum* binding to endothelial cells following hCMEC/d3 preincubation with αGAPDH versus αLamR (263-282) where p=0.0037. **(C)** The Tp0751 endothelial interaction region (Parker et al. 2016) shown as the primary amino acid sequence (light blue box amino acids 172-196; positively charged residues highlighted in blue, negatively charged residues highlighted in dark green) and a structural model (interaction region, light blue). Within the endothelial interaction region of Tp0751 there are two putative binding motifs shown as insets of the ribbon diagram. Binding motif #1 is a looped structure with positively charged amino acids displayed in blue. Binding motif #2 is a clustered region of exposed positively charged amino acids displayed in red.

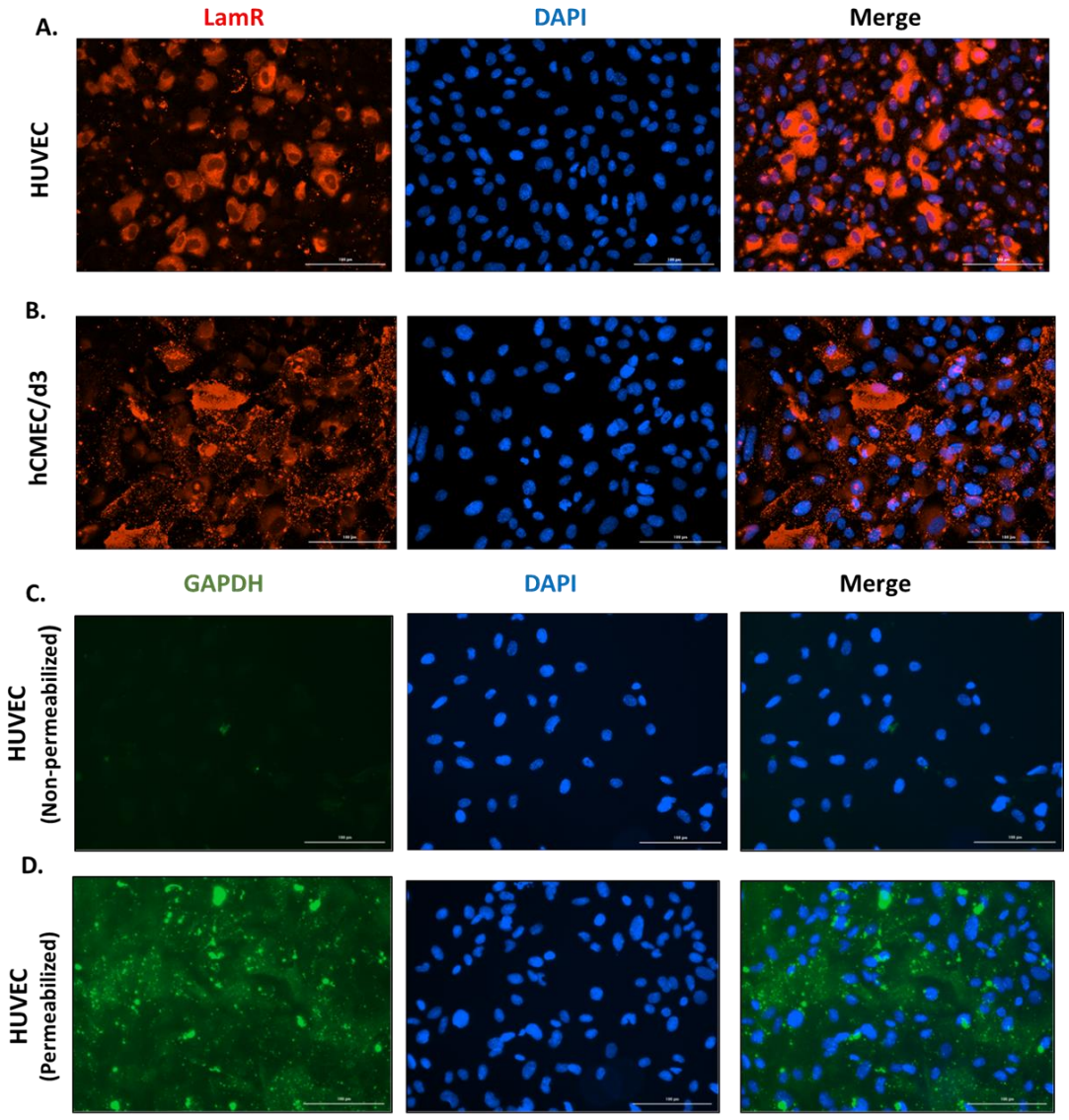

Figure 15: Surface localization of LamR cultured endothelial cells. Endothelial monolayers of **(A)** HUVECs and **(B)** hCMEC/d3 grown under experimental culture conditions were fixed with 4% PFA and stained with a LamR antibody (red) and a nuclear stain (DAPI, blue). Visualization of LamR from non-permeabilized monolayers indicates surface localization of LamR. Validation that cell membranes remained intact was achieved using GAPDH antibody (green) to detect the protein in **(C)** non-permeabilized and **(D)** permeabilized endothelial monolayers. Representative epifluorescence images obtained from a Cytation 5 imager at 200X magnification.

2.4 Discussion

The highly invasive nature of *T. pallidum* is illustrated by its widespread vascular dissemination during early disease progression, with spirochetes traversing across tissue barriers as well as highly protected blood-brain, placental, and retinal barriers (Mahoney 1934; Stokes 1944; Cumberland MC 1949; Raiziss GW 1937). *Treponema pallidum*-endothelial interactions are a critical step in this process, but elucidation of the molecular mechanisms for vascular adhesion has been limited by the challenges associated with studying *T. pallidum.* The findings in this chapter provide evidence to confirm Tp0751 is a vascular adhesin that interacts with microvascular and macrovascular endothelial cells, including cerebral brain endothelial cells. An endothelial receptor for Tp0751 is identified that is targeted by other extracellular neuroinvasive bacterial pathogens, suggesting the existence of a shared invasive strategy amongst neurotropic pathogens.

It has been well established that *T. pallidum* binds to host-derived ECM components (Fitzgerald et al. 1984) as well as a plethora of mammalian cell types (Fitzgerald et al. 1977; Hayes et al. 1977; Sandok et al. 1976), including endothelial cells (Thomas et al. 1988; Thomas et al. 1989; Wu, Zhang, and Wang 2017). While numerous ECM binding interactions with specific *T. pallidum* proteins have been confirmed using *in vitro* assays with live *T. pallidum* (Cameron et al. 2005; Cameron et al. 2004; Ke et al. 2015), the disruption of *T. pallidum*-endothelial attachment with Tp0751-specific antiserum reported herein represents, to our knowledge, the first direct demonstration of a *T. pallidum* protein-host cell interaction. In this work, recombinant Tp0751 in endothelial plate-based binding assays and *T. pallidum* endothelial attachment experiments are used to evaluate the adhesive capabilities of Tp0751. It is also demonstrated that Tp0751 expressed by a non-infectious strain of the model spirochete, *B. burgdorferi,* confers a gain-of-function for attachment to endothelial cells *in vitro* under stationary conditions. Inhibition of *Bb*-Tp0751 binding to endothelial cells with a peptide corresponding to a discrete region within the Tp0751 lipocalin barrel confirms the specificity of this interaction. Taken in the context of previous findings, which show that Tp0751-expressing *B. burgdorferi* facilitates adhesion to endothelial cells under shear flow conditions *in vitro* and *in vivo* in mouse post capillary venules (Parker et al. 2016; Kao et al. 2017), this presents strong evidence using three distinct approaches that Tp0751 is an endothelial adhesin.

Although the precise locations for treponemal extravasation from the vasculature are not known, previous investigations have revealed that Tp0751 facilitates vascular attachment *in vivo* via adherence to post-capillary venules (Kao et al. 2017). The findings presented herein demonstrate that Tp0751 adheres to both microvascular and macrovascular cell lines, suggesting that Tp0751 may mediate vascular adhesion in both the macrovasculature and microvasculature of the host. Further, attachment of Tp0751 to the immortalized blood-brain barrier model cell line hCMEC/d3 is an important first step in investigating the contribution of this adhesin to the process of *T. pallidum* neuroinvasion.

Specialized microvascular regions, including high endothelial venules and post-capillary venules, are common locations for immune cell extravasation. These sites harbor phenotypically distinct endothelial cells with increased propensity to alter permeability, as well as fewer smooth muscle cells underlying the vascular endothelium, lower blood velocity, and decreased shear forces (Aird 2007a; von Andrian and Mempel 2003; Miyasaka and Tanaka 2004; Yuan and Rigor 2010). These areas thus represent the most likely sites for treponemal traversal across the vascular endothelium. Studies of other neuroinvasive pathogens show that vascular interactions of the Lyme disease spirochete, *B. burgdorferi,* occur in capillaries, post-capillary venules, and veins during *in vivo* dissemination (Moriarty et al. 2008), while *N. meningitidis* attaches to the cerebral microvasculature by taking advantage of transient reductions in blood flow and shear stress that occur within the cerebral microcirculation (Hudetz et al. 1994; Villringer et al. 1994; Mairey et al. 2006). The stationary interactions with cerebral endothelial cells demonstrated in this chapter could indicate that *T. pallidum* adhesion to the blood-brain barrier also occurs during these flow reductions in the cerebral microcirculation. Previous investigations using intravital microscopy demonstrate that Tp0751-mediated spirochete-endothelial interactions can occur in the presence of shear forces within the range of 0.75-1 dyn/cm^2 in *in vitro* particle tracking flow chambers or *in vivo* in mouse dermal post-capillary venules (Kao et al. 2017), demonstrating that Tp0751 can maintain vascular interactions in the presence of physiological shear stress. However, it remains to be determined whether Tp0751-endothelial interactions would be stable in the presence of higher levels of shear stress, which can range from 1 to 60 dyn/cm^2 in different areas of the vasculature (Baeyens 2018; Loscalzo and Schafer 2003). Future investigations using

cerebral endothelial cells under flow conditions are needed to reveal whether adhesion occurs exclusively under stationary conditions, or whether this interaction also occurs in the presence of shear forces. Furthermore, evaluation of Tp0751-endothelial interactions in the presence of a wider range of physiological shear stress would provide additional information as to whether this adhesin functions at diverse sites within the vasculature. Overall, the binding of Tp0751 to endothelial cells of diverse origin suggests extravasation could occur at multiple sites within the circulatory system, including areas of the microvasculature and macrovasculature, which could partly explain the diversity of secondary infection sites accessed by treponemes during infection (Mahoney 1934; Stokes 1944; Cumberland MC 1949; Raiziss GW 1937). Structural characterization of Tp0751 has revealed the C-terminal domain adopts a lipocalin fold with a unique extended N-terminal alpha helix, and that attachment to ECM components is mediated by four host binding regions that map along a single face of the protein including these two structural regions (Parker et al. 2016). In this chapter it is demonstrated that the endothelial binding capacity of Tp0751 localizes to the C-terminal lipocalin domain, since identical levels of endothelial binding were observed for three N-terminal truncations of Tp0751. This is further supported by the finding that endothelial binding of Tp0751-expressing *B. burgdorferi* is localized to a discrete region within the lipocalin barrel of Tp0751. Collectively, these results suggest that Tp0751 interacts with a specific endothelial cell receptor via a discrete region of the lipocalin barrel, rather than mediating contact with the vasculature through an ECM bridge. This hypothesis is grounded in the discoveries that only (1) one out of the four ECM binding regions of Tp0751 can disrupt *Bb*-Tp0751 attachment to endothelial cells and (2) that an N-terminal truncation of Tp0751 that excludes the alpha helix ECM-binding region can still facilitate endothelial attachment.

Fibronectin is commonly targeted by invasive bacteria as a molecular bridge for association with endothelial cells (Lemichez et al. 2010). Within the bloodstream fibronectin exists in a compact globular form (plasma FN) that can deposit on the surface of endothelial cells to undergo an integrin-dependent conformational change that exposes sites essential for polymerization and fibril formation with other fibronectin molecules and ECM components such as collagen (Kadler, Hill, and Canty-Laird 2008). *Staphylococcus aureus* uses fibronectin as a bridging molecule to facilitate interactions with α5β1 integrins

on endothelial surfaces to modulate intracellular signaling and cytoskeleton organization (Lemichez et al. 2010; Schroder et al. 2006; Schwarz-Linek et al. 2003). *Treponema pallidum* can attach directly to immobilized fibronectin (Cameron et al. 2004; Fitzgerald et al. 1984; Fitzgerald and Repesh 1985) and host cell binding by *T. pallidum* is inhibited by anti-fibronectin antibodies (Peterson, Baseman, and Alderete 1983; Thomas, Baseman, and Alderete 1985). The fibronectin binding capacity of *T. pallidum* has been attributed to the adhesins Tp0155, Tp0483 (Cameron et al. 2004), Tp0136 (Brinkman et al. 2008; Ke et al. 2015) and Tp0751 (Cameron et al. 2004; Houston et al. 2015) based on recombinant protein studies. Furthermore, pre-treatment of *T. pallidum* with recombinant Tp0136, Tp0155, or Tp0483 disrupts treponemal-fibronectin interactions (Cameron et al. 2004; Brinkman et al. 2008; Ke et al. 2015). While adhesion to insoluble tissue fibronectin may be important for ECM binding in tissues, interactions with plasma FN within the bloodstream could provide opportunities for bridged interactions between *T. pallidum* and luminal endothelial surfaces. It has also been postulated that plasma FN binding by pathogens may facilitate immune evasion by disguising epitopes in adhesins (Dickerson et al. 2012). To explore whether fibronectin plays a role in Tp0751-mediated endothelial attachment, the Tp0751-expressing *B. burgdorferi* heterologous expression system was utilized. Preincubation of HUVECs with pFN to induce ECM deposition and fibril formation on endothelial surfaces had no impact on adherence of *Bb*-Tp0751, whereas pre-incubation of *Bb*-Tp0751 with pFN inhibited spirochete attachment to endothelial cells. There are two possibilities to explain these findings: (1) that cultured HUVECs already produce sufficient fibronectin at the cell surface, such that adding exogenous fibronectin does not enhance available binding sites for *Bb*-Tp0751, or (2) that *Bb*-Tp0751 interacts with soluble pFN but cannot mediate interactions with endothelial-bound fibronectin under stationary conditions. In support of the latter hypothesis, adhesion assays with immobilized fibronectin revealed that *Bb*-Tp0751 was unable to mediate adherence to immobilized pFN or sFN, which mimics the fibronectin matrices found on endothelial surfaces (Morla, Zhang, and Ruoslahti 1994). Investigations into the vascular dissemination of the Lyme disease spirochete, *B. burgdorferi,* reveal that bacterial attachment to vascular surfaces occurs via a multistage mechanism that parallels immune cell extravasation through tethering, dragging, and stationary interactions with the endothelium prior to

transendothelial migration (Moriarty et al. 2012). *Borrelia burgdorferi* initiates contact with glycocalyx layer of vascular surfaces through short-term tethering interactions bridged by plasma fibronectin. These associations function as molecular brakes to help the pathogen overcome the shear forces of the blood flow to decelerate and facilitate more stable dragging interactions with glycocalyx glycosaminoglycans. Subsequently, the spirochetes undergo stable stationary interactions that occur within the glycocalyx exclusion layer, providing a protective niche for the bacteria. Intriguingly, all three steps are coordinated by the same adhesin, BBK32, although the stationary adhesion stage is hypothesized to require additional adhesins and receptors (Moriarty et al. 2008; Moriarty et al. 2012; Norman et al. 2008). The optimized *Bb*-Tp0751 adhesion assay described in this work explores the stationary interaction phase of Tp0751-mediated adhesion that occurs within the protective niche of the endothelial glycocalyx (Reitsma et al. 2007; Moriarty et al. 2012). This work complements previous investigations that demonstrate Tp0751 can facilitate tethering and dragging interactions *in vitro* and *in vivo* (Kao et al. 2017), suggesting that, similar to BBK32, Tp0751 may be involved in tethering, dragging, and stationary interactions with the vascular endothelium. While fibronectin does not appear to be an important bridging molecule for Tp0751 in stationary endothelial attachment assays, the possibility remains that pFN could promote Tp0751-mediated tethering and dragging interactions in the presence of the shear force of the blood flow, but further investigation will be needed to fully elucidate the role of fibronectin in Tp0751-mediated endothelial adhesion.

To further characterize Tp0751 interactions with vascular surfaces, affinity chromatography coupled with mass spectrometry was used with the primary aim of identifying candidate endothelial receptors targeted by Tp0751. This approach identified LamR and stomatin as interaction partners for Tp0751. In epithelial cell membranes, stomatin forms oligomeric structures with the proteins flotillin and caveolin-1 within cholesterol-rich lipid rafts and contributes to membrane organization and regulation of membrane proteins (Snyers, Umlauf, and Prohaska 1999; Snyers, Thines-Sempoux, and Prohaska 1997); conversely knowledge of the role of stomatin in endothelial membranes is minimal. As a fuller body of literature exists for the role of LamR in endothelial cells, attention was focused on this host cell receptor. LamR exists in two distinct forms within

host cells: (1) a low molecular weight 37 kDa laminin receptor precursor (LRP) found primarily in intracellular locations and (2) a high molecular weight 67 kDa laminin receptor (LamR) that localizes to cell surfaces. While LamR participates in a focused set of molecular interactions at the cell surface, LRP exhibits diverse functionality with roles in ribosome biogenesis, cytoskeletal reorganization, and chromatin/histone binding (DiGiacomo and Meruelo 2016). The mechanisms underlying LRP conversion to the high molecular weight 67 kDa LamR species and cell surface localization remain unknown. However, LamR is thought to localize to lipid rafts at the cell surface (Fujimura, Yamada, and Tachibana 2005; Fujimura et al. 2006), and the current hypotheses for precursor conversion to the high molecular weight form of LamR include (1) a large post-translational modification (such as SUMOylation), (2) homo-dimerization, or (3) hetero-dimerization (DiGiacomo and Meruelo 2016). The limited knowledge regarding the composition and orientation of LamR at the cell surface poses a significant challenge for experimental determination of protein-protein interactions involving LamR.

Despite the inherent difficulty of studying this receptor, significant knowledge has been gained regarding its role in host and pathogen invasive processes. At the cell surface, LamR functions as a cell anchor via high affinity interactions with laminin (Lesot, Kuhl, and Mark 1983; Malinoff and Wicha 1983; Rao et al. 1983; Hilario et al. 1996), and increased expression of LamR is associated with increased invasiveness and metastasis of human cancers (DiGiacomo and Meruelo 2016; Menard, Tagliabue, and Colnaghi 1998; Menard et al. 1997). Additionally, LamR has a role in infectious diseases, acting as the receptor for viral pathogens including Dengue virus (Tio, Jong, and Cardosa 2005; Thepparit and Smith 2004), Sindbis virus (Wang et al. 1992), adeno-associated virus (Akache et al. 2006), tick-borne encephalitis virus (Malygin et al. 2009), Venezuelan equine encephalitis virus (Malygin et al. 2009; Bondarenko et al. 2004; Bondarenko et al. 2003; Ludwig, Kondig, and Smith 1996), and Swine fever virus (Chen et al. 2015). Neuroinvasive bacterial pathogens such as *N. meningitidis, S. pneumoniae,* and *H. influenzae* also use LamR as a receptor for attachment to the brain microvascular endothelium (Orihuela et al. 2009), and LamR is targeted by the secreted *E. coli* cytotoxic necrotizing factor (CNF1) during CNS invasion (Chung et al. 2003; Kim, Chung, and Kim 2005). LamR contains three distinct interaction regions (Figure 14A); the direct binding

(AA 205-229) and peptide G (AA 161-180) regions are involved in interactions with the prion protein and laminin (Castronovo, Taraboletti, and Sobel 1991; Kazmin et al. 2000; Landowski, Uthayakumar, and Starkey 1995; Hundt et al. 2001), whereas a discrete site within the C-terminal region corresponding to AA 263-282 is targeted by neuroinvasive pathogenic bacteria (Orihuela et al. 2009). The C-terminal region of LamR is inherently disordered (Ould-Abeih et al. 2012) and contains an abundance of acidic residues and five (D/E)W(S/T) repeats (Kazmin et al. 2000), two of which are contained within the LamR pathogen binding site (AA 263-282).

To validate the interaction between *T. pallidum* and LamR in the biologically relevant context of an endothelial cell membrane, an antibody blocking approach was used with polyclonal antibodies specific to the LamR pathogen binding site (263-282) (Orihuela et al. 2009); these antibodies disrupted *T. pallidum* interactions with cerebral microvascular endothelial cells. Intriguingly, the competitive inhibition assay using Tp0751-expressing *B. burgdorferi* revealed that a discrete region of Tp0751 (Figure 10A-B; p10 amino acids R172-F196) facilitates spirochete attachment to endothelial cells, based on the ability of p10 to uniquely inhibit *Bb*-Tp0751 binding to HUVECs. This endothelial binding region is highly positively charged and contains hydrophobic residues that are buried within the protein core as well as two exposed basic patches at either end of the hydrophobic region (Figure 14C). The most notable element in the primary amino acid sequence of the Tp0751 endothelial interaction region is an arginine triplet corresponding to amino acids R189-R191. However, spirochete attachment to endothelial cells was not inhibited by a scrambled version of p10 (where arginine residues were separated) or with p11 (which overlaps with p10 and contains the arginine triplet), suggesting the endothelial binding cannot be fully attributed to the positively charged residues R189-R191. It is also plausible that spirochete inhibition by p10, but not p11, is due to a difference in secondary structure of the peptides. While p10 may adopt a stable antiparallel beta sheet that recapitulates the structure of this regions in the full length protein, p11 may not form the predicted stable beta sheets that are observed in the Tp0751 structure. Within the arginine triplet of the endothelial interaction region, only the amino acids R190 and R191, but not R189 are appropriately positioned for interactions based on their location within the structure (Figure 14C; binding motif 2). Furthermore, evaluation of the spatial clustering of all positively

charged residues in the Tp0751 endothelial binding region reveals spatial clustering of R172 and K172 in an exposed loop region at the top of the lipocalin barrel near the N-terminal helix (Figure 14C; binding motif 2) as well as spatial clustering of R190, R191, and R180 (Figure 14C; binding motif 2) at the base of the lipocalin domain distal from the N-terminal helix. The bacterial ligands responsible for LamR engagement in *N. meningitidis*, *H. influenzae* and *S. pneumoniae* were identified as PilQ and PorA, OmpP2, and CbpA, respectively (Orihuela et al. 2009). While consensus sequences for the interaction region of the *N. meningitidis* LamR-binding adhesins have yet to be determined (Abouseada et al. 2012), the LamR-binding motifs for CbpA ('EPRNEEK') and OmpP2 ('RNSKNDAGWG') both map to exposed loop regions of the adhesin structures (Orihuela et al. 2009; Abouseada et al. 2012). They do not, however, share an obvious consensus sequence with each other or the Tp0751 host binding region (Figure 14C). The highly negatively charged nature of the LamR pathogen binding site and the abundance of positively charged residues localized to exposed regions within the Tp0751 endothelial binding site (Figure 14C) suggests that electrostatic interactions could underlie the LamR-Tp0751 molecular interface. Spirochete attachment to endothelial cells is uniquely disrupted with p10, but not scr10, demonstrating that the molecular interaction is based on a sequence of amino acids, rather than an abundance of positively charged residues. This suggests that the specific positioning of the positively charged amino acids is important for the adhesive interactions. Furthermore, the comparison of endothelial binding between Tp0751 N-terminal truncations, which have different net charges, demonstrates that the overall charge of the adhesin does not drive receptor interactions. Instead, it is expected that this putative electrostatic interaction between Tp0751-LamR occurs through specific charged residues within a discrete region of Tp0751.

Prior investigations have demonstrated that *T. pallidum* and Tp0751 have the capacity to interact with laminin (Cameron et al. 2005; Cameron et al. 2008; Houston et al. 2011; Fitzgerald et al. 1984); therefore, there is a possibility that the Tp0751-LamR interaction is bridged by this ECM molecule. However, the evidence to date suggests that Tp0751 interacts directly with LamR. If laminin was required for this interaction, one would anticipate co-isolating laminin peptides with LamR during affinity chromatography, yet no laminin peptides were detected during mass spectrometry analyses in either of the

two experiments. Additionally, *T. pallidum* attachment to endothelial cells was disrupted with antibodies specific to the LamR C-terminal pathogen binding region (263-282), which is not known to be a laminin binding site. Finally, laminin localizes to the basement membrane on the basolateral face of the endothelial barrier and thus would not be appropriately poised for apical endothelial cell interactions with Tp0751 (Yousif, Di Russo, and Sorokin 2013). Although laminin is unlikely to be an important bridging molecule for these interactions, it is plausible that traversal across the basement membrane during intravasation or extravasation could involve laminin-bridged interactions with endothelial cells.

With the knowledge that Tp0751 can interact with LamR on endothelial surfaces as well as ECM components found within the vasculature, including fibronectin and fibrinogen (Cameron et al. 2005; Cameron et al. 2008; Houston et al. 2015; Houston et al. 2011; Houston et al. 2012), it appears that Tp0751 participates in a variety of molecular interactions during dissemination. Based on the current findings, it is hypothesized that initial *T. pallidum* interactions with vascular surfaces are mediated by tethering interactions between Tp0751 and ECM components such as fibronectin, followed by stationary adhesion in which Tp0751 interacts directly with LamR. To put this into the broader context of *T. pallidum* dissemination, it is likely that an assortment of *T. pallidum* adhesins contribute to the host-pathogen interaction. Supporting this notion, previous investigations have revealed that the *T. pallidum* protein Tp0750 mediates interactions with the fibrinolytic receptor complex protein Annexin A2, a protein that localizes to endothelial surfaces (Houston et al. 2014). Further, *T. pallidum* attachment to human dermal endothelial cells can be blocked with RGD peptides or antibodies specific to the RGD binding region of the integrin α5 subunit, suggesting that fibronectin likely bridges *T. pallidum*-endothelial interactions (Lee et al. 2003). Candidate fibronectin-binding adhesins include the treponemal proteins Tp0483 (Cameron et al. 2004), Tp0136 (Ke et al. 2015; Brinkman et al. 2008), and Tp0155 (Cameron et al. 2004). A more robust understanding of *T. pallidum* interactions with endothelial cells will be essential for elucidating the underlying mechanisms for the highly invasive nature of this pathogen.

In summary, a growing body of evidence has revealed diverse roles for Tp0751 in the vasculature from endothelial cell adhesion (Parker et al. 2016; Kao et al. 2017) to

basement membrane engagement (Cameron et al. 2005; Cameron et al. 2008). These findings provide support for the previous discovery that Tp0751 immunization partially inhibits *T. pallidum* dissemination in an animal model of infection (Lithgow et al. 2017). Further characterization of *T. pallidum* dissemination will provide mechanistic insight into vascular traversal of *T. pallidum* and other invasive extracellular pathogens. These investigations support the concept of a common invasion strategy employed by neuroinvasive pathogens that supersedes traditional bacterial taxonomic classification.

Chapter 3: Molecular mechanisms of *T. pallidum* junctional disruption and transendothelial migration

Contributions: Sean Waugh and Emily Tsao performed genomic DNA extraction and real-time quantitative polymerase chain reaction (qPCR) on *T. pallidum* samples from transwell endocytosis inhibition assays. The remainder of the experiments and data analysis were performed by KL.

3.1 Introduction

Bacterial pathogens that undergo systemic dissemination to invade secondary infection sites must traverse the vascular endothelium to gain access to underlying tissue and organ sites. There are two recognized routes for transendothelial migration (1) transcellular traversal in which organisms induce endocytosis to cross the barrier or (2) paracellular traversal whereby organisms move in between cell at the sites of cellular junctions to access extravascular areas (Lemichez et al. 2010). While it is appreciated that *T. pallidum* is capable of invading into diverse anatomical sites within its host, the molecular mechanisms that underlie the process of *T. pallidum* transendothelial migration are poorly understood. *In vitro* evaluation of *T. pallidum* interactions with aortic endothelial cells demonstrates that treponemes localize to intercellular junctions and traverse monolayers without disrupting barrier integrity (Thomas et al. 1988). Conversely, scanning electron microscopic imaging of *T. pallidum* interacting with brain microvascular endothelial cells reveals that treponemes can merge with endothelial membranes (Wu, Zhang, and Wang 2017). These divergent findings imply a paracellular and transcellular route for *T. pallidum* transendothelial migration, respectively.

In this chapter, the mechanisms of *T. pallidum* traversal of endothelial barriers are explored. Immunofluorescence microscopy is used to demonstrate that recombinant Tp0751 and live *T. pallidum* disrupt the architecture of VE-cadherin, the main endothelial junctional protein, which plays a key role in regulating vascular permeability. Further to this, a subpopulation of *T. pallidum* cells localize to intercellular junctions. Despite the observation of junctional reorganization in endothelial cells, no changes to endothelial barrier permeability were observed in recombinant Tp0751 treated monolayers or *T.*

pallidum treated monolayers in transwell plate assays. Further investigations revealed that recombinant Tp0751 alone could not traverse endothelial barriers and although *T. pallidum* was able to cross endothelial monolayers, the traversal rate was low. Finally, *T. pallidum* transendothelial migration was partially abrogated by the addition of an inhibitor that blocks cholesterol-mediated endocytosis, but no change in traversal was observed in the presence of inhibitors of micropinocytosis or dynamin-dependent endocytosis. Collectively, these results imply that *T. pallidum* uses a dynamin-independent, cholesterol raft-mediated endocytosis mechanism to traverse endothelial barriers. Further, treponemal localization to intercellular junctions suggests that a paracellular route may also be utilized, a dual traversal strategy that has also been observed for *N. meningitidis* migration across brain endothelial barriers *in vitro* (Hoffmann, Eugene, et al. 2001; Lambotin et al. 2005; Coureuil et al. 2010)

3.2 Materials & Methods

Ethics Statements

All animal studies were approved by the local institutional review board at the University of Victoria and were conducted in strict accordance with standard accepted principles as set forth by the Canadian Council on Animal Care (CCAC), National Institutes of Health and the United States Department of Agriculture in facilities accredited by the American Association for the Accreditation of Laboratory Animal Care and the CCAC.

Cloning and purification of recombinant proteins

Treponemal proteins Tp0327 [I23-S172] and Tp0751 [V99-P237] were cloned as previously described (Parker et al. 2016; Houston et al. 2011; Houston et al. 2014). Tp0327 and Tp0751 constructs were purified from *Escherichia coli* BL21-A1 or BL21*DE3, respectively, and subject to nickel affinity chromatography with HisTrap FF columns (GE Healthcare, Mississauga, ON) and further purified with size exclusion and cation exchange chromatography (HiLoad 16/60 Superdex 75; GE Healthcare, GE Healthcare) on an AKTA Prime Plus FPLC system (GE Healthcare) in a final buffer of 20 mM HEPES, 150 mM NaCl, 1% glycerol, pH 7.0 as previously described(Parker et al. 2016; Houston et al. 2011; Houston et al. 2014).

Recombinant protein FITC labelling

Recombinant Tp0327 [I23-S172] and Tp0751 [V99-P237] were purified as described above, with the following exceptions. Binding buffer, elution buffer, and gel filtration were all prepared without glycerol. A portion of recombinant protein was immediately flash frozen as unlabeled protein and the remaining purified protein was chemically labeled with fluorescein isothiocyanate isomer I (FITC I, SigmaAldrich) after purification. Fluorescein isothiocyanate was dissolved in dimethyl sulfoxide (DMSO) at 10 mg/mL. Five milligrams of recombinant protein was incubated with 0.5 mg of FITC in a final volume of 5 mL of 1M sodium bicarbonate pH 9.1 for 20 minutes at RT (Tp0327 FITC labeling) or 1 hour at RT (Tp0751 FITC labeling). Samples were then buffer exchanged to remove unconjugated FITC into 20 mM HEPES, 150 mM NaCl (pH 7.0) using a 10,000 kDa molecular weight cutoff (MWCO) centricon. Labeling efficiency of each construct was determined by calculating the molar F/P ratio using the equations:

$$\text{Molar F/P} = \frac{A_{495} \times C}{A_{280}-(0.35 \times A_{495})} \quad (1)$$

$$\text{where } C = \frac{\text{MW} \times E^{0.1\%}_{280}}{389 \times 195} \quad (2)$$

Where molar F/P is the ratio of moles of FITC to moles of protein in the conjugate, A_{495} is the absorbance of the sample at 495 nm and A_{280} is absorbance of the sample at 280 nm. C is a constant value given for a protein, MW is the molecular weight of the protein, 389 is the molecular weight of FITC, 195 is the absorption $E^{0.1\%}$ of bound FITC at 490 nm at pH 13.0, and (0.35 X A_{495}) is the correction factor due to the absorbance of FITC at 280 nm. $E^{0.1\%}$ is the absorption at 280 nm of a protein at 1.0 mg/mL.

Endothelial cell culturing

Human umbilical vein endothelial cells (HUVECs, Lonza, Mississauga, ON) were cultured as previously described (Parker et al. 2016) but cells were cultured with Vasculife EnGS Endothelial Medium (Lifeline Cell Technologies, Oceanside, CA) that does not contain vascular endothelial growth factor.

Treponema pallidum *propagation*

Treponema pallidum subsp. *pallidum* (Nichols strain) was propagated in, and extracted from, New Zealand White rabbits as previously described (Lukehart and Marra 2007). Testicular extractions were performed in 10% normal rabbit serum (NRS) in 0.9% NaCl at room temperature in an atmosphere of 3-5% O_2 in a modified anaerobic chamber (Coy Laboratories, Grass Lake, MI). Oxygen levels were monitored using a LabQuest2 oxygen meter (Vernier, Beaverton, ON) and maintained with gas injections carbon dioxide balanced with nitrogen.

Immunofluorescence evaluation of VE-cadherin junctional architecture

Eight well chamber slides were coated with phenol red-free Matrigel (Corning, Tewsbury, MA) by incubating with 500 µg/mL Matrigel for one hour at room temperature. HUVECs were seeded into Matrigel coated 8-well chamber slides (ThermoFisher Scientific, Burnaby, BC) and grown for 48 h at 37°C in 5% CO_2 to form confluent monolayers. For recombinant protein assays, monolayers were treated with gel filtration buffer or equimolar amounts of recombinant Tp0751 [V99-P237] or recombinant Tp0327 [I23-S172] for 30 minutes at 37°C in 5% CO_2. Each well was washed two times with HEPES buffered saline solution (warmed to room temperature), fixed with 4% paraformaldehyde (PFA), and permeabilized with 0.05% Triton X-100 (TX-100). Monolayers were blocked with 4% BSA in PBS and incubated with 0.5 µg/mL mouse anti-human VE-Cadherin (R&D Systems, Minneapolis, MN) for 1 hour at room temperature (RT), washed three times in PBS, and incubated with goat anti-mouse A488 or goat anti-mouse A568 (1/1000; ThermoFisher Scientific) for 1 hour at RT. Monolayers were counterstained with 3 µM DAPI (4',6-diamidino-2-phenylindole; Sigma Aldrich) for 5 minutes at RT, washed with PBS, and mounted with Vectashield mounting medium (Vector Laboratories, Brockville, ON). For treponemal binding assays, *T. pallidum* was isolated from rabbit testicular

extractions and quantified using a Petroff-hauser counting chamber (Hausser Scientific, Horsham, PA). Treponemes were pre-incubated with anti-Tp0751 serum (1:2 dilution) or normal rabbit serum for 60 minutes at 34°C in an atmosphere of 3-5% O_2. *Treponema pallidum* ($5x10^6$ cells/well) were added to endothelial monolayers and co-incubated for 60 minutes at 34°C in an atmosphere of 3-5% O_2. Monolayers were blocked with 4% BSA in PBS and incubated with chicken anti-*T. pallidum* FlaA (Tp0249) serum (1/1000; pre-adsorbed with testicular extract and NRS; Cameron et al. 2008) and mouse anti-human VE-cadherin (0.5 µg/mL; R&D Systems, Minneapolis, MN) for 1 hour at RT, washed three times in PBS, and incubated with goat anti-chicken A568 (1/1000; ThermoFisher Scientific) and goat anti-mouse A488 (1/1000; ThermoFisher Scientific) for 1 hour at RT. Monolayers were counterstained with 3 µM DAPI (4',6-diamidino-2-phenylindole; Sigma Aldrich) for 5 minutes at RT, washed with PBS, and mounted with Vectashield mounting medium (Vector Laboratories, Brockville, ON).

Endothelial transwell assays

Matrigel-coated transwell plates (8 µm pore size, 24 well plate; Corning) were seeded with HUVECs ($3x10^4$/well) and grown to confluence (48 – 72 hours) at 37°C in 5% CO_2. Endothelial cells cultured in transwell plates were removed from normal growth conditions and incubated at RT for 20 minutes prior to evaluation of transendothelial electrical resistance (TEER). Barrier integrity was evaluated using an EndOhm chamber with EVOM-2 voltmeter (World Precision Instrument, Sarasota, FL) to measure resistance and the TEER was calculated using the equation:

$$TEER_{REPORTED} = [R_{TOTAL}\ (\Omega) - R_{BLANK}(\Omega)] \times M_{AREA}(cm^2) \qquad (3)$$

Where $TEER_{REPORTED}$ is the calculated resistance of the barrier in Ω x cm^2, R_{TOTAL} is the resistance measured across a Matrigel-coated insert seeded with HUVECs, R_{BLANK} is the resistance measured across a Matrigel-coated insert without cells, and M_{AREA} is the growth area (0.33 cm^2) of the transwell insert (Srinivasan et al. 2015). Reported TEER values ≥12 Ω x cm^2 were indicative of an intact endothelial barrier (Dewi, Takasaki, and Kurane 2004). For recombinant protein assays, cells were treated as indicated with recombinant proteins (25 µM), FITC-labelled recombinant proteins (25 µM), or control buffer. For *T. pallidum*

assays, each upper well of endothelial cells was treated with rabbit testicular extract from uninfected rabbits (Uninfected TEx, equal volume to *T. pallidum* treatment), $3.2x10^7$ live *T. pallidum,* or $3.2x10^7$ *T. pallidum* that had been heat inactivated by incubating at 56°C for 45 minutes to eliminate treponemal motility (Fitzgerald et al. 1984; Thomas et al. 1988). To the lower compartments in the transwell plates, a mixture of 50% endothelial growth medium and 50% NRS was added. For transwell solute flux assays, FITC-dextran (40 kDa, 1 mg/ml; Sigma Aldrich) was added to the apical side of the endothelial monolayers. At time=0, 10 µl samples were taken from the upper and lower compartments and for the remainder of the time-course 10 µl samples were taken from the lower compartment only and added to 90 µl of distilled water in a black clear bottom 96-well plate (Corning). Fluorescence of the time-course sample was measured on a BioTek Synergy HT plate reader (Biotek, Nepean, ON) using a FITC filter (excitation @ 485nm/emission @ 528 nm) and compared to a standard curve of known concentrations of FITC-dextran to determine the amount of solute present in the lower well. The absolute permeability was calculated with the equation:

$$P = \frac{[C(t) - C(t_0)] \times V}{A \times t \times C_0} \quad (4)$$

Where $C(t)$ is the concentration [µg/ml] of FITC-dextran in the samples that were taken from the lower compartment at each timepoint, $C(t_0)$ is the FITC-dextran concentration [µg/ml] of the samples taken after 0 min, t is the duration of the flux (s), V is the volume [cm^3] in the lower compartment, A is the surface of the Transwell® membrane [cm^2] and C_0 is the initial concentration [µg/ml] of the tracer on the donor side. Results were normalized to the matrigel-only well lacking endothelial cells (set as 100% flux of the fluorescent tracer). Transwell solute flux assays using FITC-recombinant proteins were performed as described above, but fluorescence was compared to a standard curve of known µg amounts of each FITC-labelled recombinant protein construct to determine the traversal of each recombinant protein.

Treponema pallidum *genomic DNA (gDNA) extraction*

Supernatant removed from upper and lower compartments of transwell plates was centrifuged at 10 000 x g for 10 minutes at RT to pellet *T. pallidum.* Cells were resuspended in 200 µl of PBS and lysed by adding buffer AL (DNeasy blood and tissue kit, Qiagen), vortexing for 10 seconds, and incubating at 56°C for 10 minutes; 200 µl of 100% ethanol was added to the mixture and vortexed. Genomic DNA was extracted with the DNeasy blood and tissue kit (Qiagen) as per manufacturer's instructions. Samples were eluted in 30 µl RNAse-free DNAse-free PCR grade distilled water (ThermoFisher Scientific)

Quantitative real-time PCR

Quantitative real-time PCR (qPCR) was performed on gDNA extractions of *T. pallidum* from transwell plate assays using SsoFast™ EvaGreen® Supermix (Bio-rad, Mississauga, ON). Quantification of *T. pallidum* gDNA was determined using HPLC-purified primers (Integrated DNA Technologies, Coralville, IA) targeting the endoflagellar sheath protein (*flaA*) gene (GenBank accession number M63142.1). The sense primer (5′-AACGCAAACGCAATGATAAA-3′) anneals to bases 475 to 494, and the antisense primer (5′-CCAGGAGTCGAACAGGAGATAC-3′) anneals to bases 738 to 759 of *flaA* (Lithgow et al. 2017). A standard curve was generated for *flaA* using 10-fold serial dilutions of 10^5 to 10^1 *T. pallidum* cells isolated from rabbit testicular extractions and spiked into endothelial growth medium (Lonza) and extracted as described for the transwell assay samples. Standard curve samples were extracted in duplicate, and each dilution was run in triplicate for a combined efficiency of 92.4% and an R^2 value of 0.986. All reactions (20 µl) were performed in triplicate with SsoFast™ EvaGreen® Supermix, 700 nM *flaA* primers and 4 µl of template (extracted genomic DNA from transwell assay or control). Assays were run on a Bio-Rad CFX Connect Real-Time PCR Detection System (Bio-Rad Laboratories, Mississauga, ON) using twin.tec™ skirted 96-well plates (Eppendorf, Mississauga, ON) sealed with microseal B film (Bio-Rad Laboratories). PCR conditions for *flaA* were as follows: 95°C for 2 minutes, followed by 40 rounds of 95°C for 10 seconds, and 65°C for 15 seconds. Following 40 cycles, there was a final denaturation step for 10 seconds at 95°C and melt curve analysis from 65°C to 95°C in 0.5°C increments for 5 seconds each. Each assay

was run with the following controls: negative controls including no template control and no amplification control (no primers), and positive control including linearized *flaA* plasmid as the template. Data was analyzed using Bio-Rad Maestro software, version 4.1.2.

Endothelial endocytosis inhibition

Thirty minutes prior to the addition of *T. pallidum*, endothelial cells in transwell plates were treated with endocytosis inhibitors at concentrations based upon previously published results including: filipin III at 5 μM (Schnitzer et al. 1994; Voigt, Christensen, and Shastri 2014; Rothberg et al. 1990), 5-(*N*-ethyl-*N*-isopropyl)amiloride (amiloride) at 1mM (Li et al. 2013; Zhao et al. 2011), Sigma-Aldrich), or Dynasore at 80 μM (Loh, Gao, and Tuomanen 2017; Basagiannis et al. 2017). All endocytosis inhibitors were purchased from Sigma-Aldrich.

Endothelial cell attachment assays using recombinant treponemal proteins

Endothelial cells were seeded into 96-well plates (Sarstedt) that had been coated with phenol red-free Matrigel (Corning) by incubating with 500 μg/mL Matrigel for one hour at room temperature and grown for 48 h at 37°C in 5% CO_2 to form confluent monolayers. Endothelial cells were washed with warm HEPES buffered saline (Lonza) and incubated with recombinant Tp0751 [99-237] or FITC-labelled Tp0751 [99-237] for 90 minutes at 37°C in an atmosphere of 5% CO_2. Protein concentrations were measured with a spectrophotometer at 280 nm prior to each experiment and the concentration of each construct was calculated by dividing the absorbance at 280 nm by the Abs 0.1% extinction coefficient for each protein. Molar concentrations of proteins were calculated based on the molecular weight (kDa) of each recombinant protein construct in a defined volume to ensure the addition of equimolar amounts of protein. Monolayers were gently washed three times with warm HBSS to remove non-adherent protein or peptide, fixed in 2% PFA and blocked for 30 minutes in 1% BSA in PBS at 37°C in an atmosphere of 5% CO_2. Attachment of recombinant proteins to endothelial monolayers was evaluated by detecting the N-terminal hexa-histidine tags on recombinant proteins as previously described (Parker et al. 2016; Cameron et al. 2005; Houston et al. 2011) using nickel-labeled horseradish

peroxidase (Ni-HRP; Mandel Scientific, Guelph, ON) and plates were developed with a 3,3',5,5'-Tetramethylbenzidine (TMB) substrate system (Mandel Scientific) and read at OD600 nm on a BioTek Synergy HT (Biotek, Nepean, ON).

Microscopy and cell counting

Unless otherwise indicated, microscopy images were captured with a Cytation 5 Imaging Reader (BioTek) with a 20X objective using five random fields of view per well. For *T. pallidum* adhesion assays, samples were blinded and the numbers of endothelial nuclei (DAPI; 10-60 µm) and *T. pallidum* cells (FlaA; 2-8 µm) were measured from each field of view with the Cytation 5 software using size exclusion quantification settings (Biotek). To quantify *T. pallidum* cells the size threshold was set to a minimum of 2 µm and maximum of 8 µm, thereby excluding quantification of background fluorescence from endothelial cells. Endothelial cell quantification was achieved by counting nuclei using a size threshold ranging from 10 – 60 µm. Mean fluorescence intensity of VE-cadherin was quantified using the Cytation 5 Imaging Reader (BioTek) with a 20X objective at five random fields of view per well.

Statistical Analysis

Statistical analyses were performed in GraphPad Prism (GraphPad) as denoted in figure legends. Data normality was analyzed using Shapiro-Wilk test (GraphPad). Graphs were prepared in GraphPad Prism (GraphPad) or Excel (Microsoft).

3.3 Results

Tp0751 modifies the architecture of endothelial adherens junctions

With the knowledge that Tp0751 functions as a *T. pallidum* vascular adhesin (Chapter 2: Figure 5, Figure 6, Figure 7) these investigations sought to understand whether Tp0751 could elicit functional changes in endothelial monolayers that promote spirochete dissemination. To this end, the architecture of the adherens intercellular junction protein VE-cadherin, a key structural and regulatory molecule of vascular barriers (Dejana, Orsenigo, and Lampugnani 2008) was evaluated in human umbilical vein endothelial cells

(HUVECs) following exposure to recombinant Tp0751 or the negative control recombinant Tp0327. Previous investigations have characterized morphologies of endothelial intercellular junctions that include: (1) continuous junctions where VE-cadherin is observed in linear arrangement between cells with no obvious disruption; (2) interrupted junctions in which a punctate or discontinuous pattern of VE-cadherin is visualized; (3) adhesion plaques where VE-cadherin localizes to the plasma membrane during an intermediate overlap of plasma membrane between cells; and (4) cytoplasmic VE-cadherin which is indicative of junctional protein internalization and manifests as a punctate pattern at regions clearly discrete from cell-cell borders (Abu Taha and Schnittler 2014; Seebach 2016; Seebach et al. 2015; Cao et al. 2017; Cao and Schnittler 2019). Using these classifications, these investigations revealed that endothelial monolayers treated with the negative control recombinant protein, Tp0327, retained linear VE-cadherin junctional patterns (Figure 16A; inset *ii*) with some VE-cadherin plaques (Figure 16A; inset *i*), while Tp0751-treated monolayers primarily exhibited discontinuous junctions (Figure 16B; inset *ii)* and intracellular VE-cadherin (Figure 16B; inset *iii*) with some instances of linear VE-cadherin junctional morphology (Figure 16B; inset *i*). To further explore Tp0751-mediated disruption of adherens junction architecture, a quantitative immunofluorescence microscopy approach was used to analyze changes in the mean fluorescence intensity per field of view (FOV) of VE-cadherin in HUVEC monolayers following exposure to recombinant proteins and controls. Monolayers were not subject to any permeabilization step to ensure specific immunofluorescence quantification of VE-cadherin at intercellular junctions and exclude intracellular pools of internalized junctional protein. This analysis revealed that Tp0751-treated monolayers had a significant reduction in cell surface junctional VE-cadherin when compared to untreated, gel-filtration buffer-treated, or negative control recombinant Tp0327-treated monolayers (Figure 17; ** p=0.007).

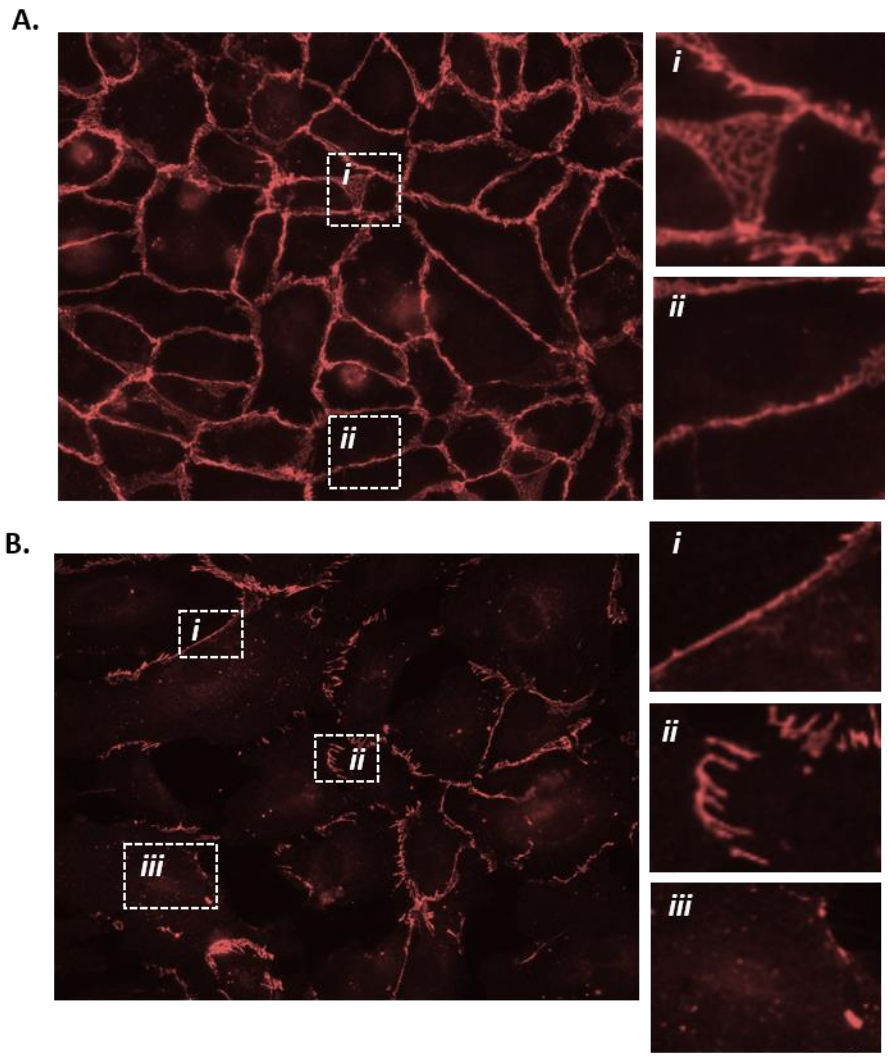

Figure 16: Recombinant Tp0751 disrupts endothelial VE-cadherin intercellular junctions. Immunofluorescence evaluation of the distribution of the adherens junction protein VE-cadherin in human umbilical vein endothelial cells (HUVECs) following a 30-minute co-incubation with 25 μM of recombinant protein. Shown are representative immunofluorescence images of permeabilized endothelial cells stained with mouse anti-VE-cadherin and goat anti-mouse (Alexa568-conjugated) at 200X magnification from three independent experiments. Insets reveal specific junctional architecture. **(A)** HUVECs treated with negative control recombinant Tp0327 [I23-S172] where insets reveal (*i*) VE-cadherin plaque-like junctional structure and (*ii*) linear (continuous) junctions. **(B)** HUVECs treated with recombinant Tp0751 [V99-P237] where insets reveal (*i*) linear

(continuous) junctions, (*ii*) disrupted (discontinuous) junctions, and (*i*) intracellular VE-cadherin.

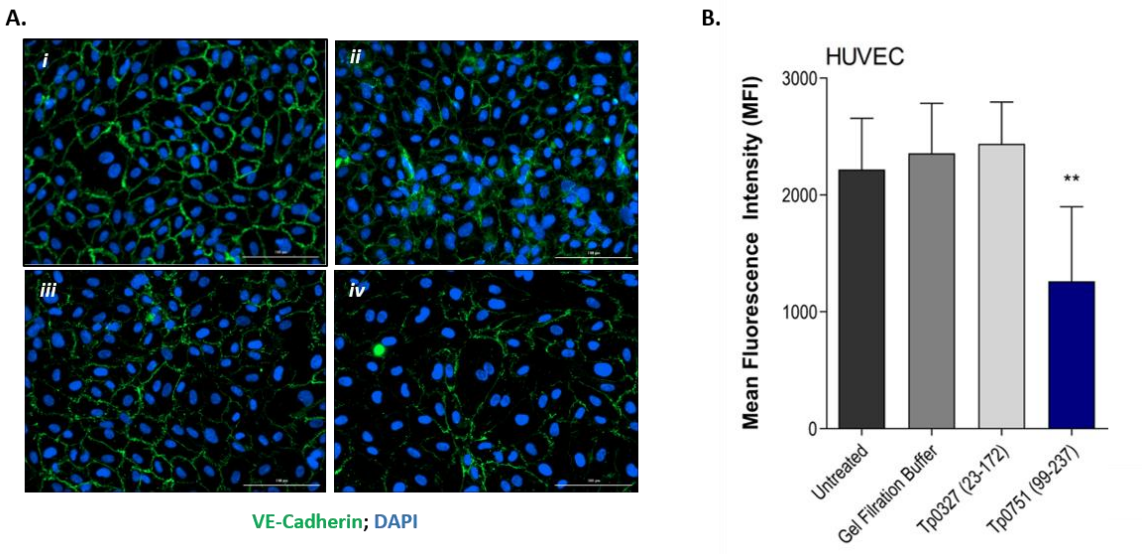

Figure 17: Junctional VE-cadherin is reduced in endothelial cells after exposure to Tp0751. **(A)** Representative immunofluorescence images from HUVECs treated with *(i)* media only, *(ii)* gel filtration buffer, *(iii)* 30 µM negative control recombinant Tp0327 [I23-S172] or *(iv)* 30 µM recombinant Tp0751 [V99-P237]. HUVEC nuclei were stained with DAPI (blue) and cellular margins were stained with mouse monoclonal anti-VE-cadherin followed by goat anti-mouse (Alexa488-conjugated, green). HUVEC membranes remained intact (non-permeabilized) to eliminate intracellular pools of VE-cadherin from the analysis. **(B)** Quantification of junctional architecture in HUVECs using mean fluorescence intensity (MFI) of VE-cadherin per field of view after treatment with media only, gel filtration buffer, negative control recombinant Tp0327 [I23-S172], or recombinant Tp0751 [V99-P237]. Results presented as MFI ± standard error of the mean (SEM) from 3 independent experiments. Statistical significance was evaluated using Student's t-test comparing Tp0751-treated endothelial monolayers to Tp0327-treated endothelial monolayers (** p=0.007).

Treponema pallidum **localizes to intercellular adherens junctions**

Treponema pallidum localization to intercellular junctional regions of endothelial cells has been previously established (Thomas et al. 1988). To further explore this tropism for endothelial junctions, a time course evaluation of *T. pallidum* attachment to HUVECs was employed and treponemal localization to areas overlapping with VE-cadherin in endothelial monolayers was evaluated (Figure 18A). Over a 60 minute time course, *T. pallidum* exhibited increased attachment to HUVEC monolayers at each time point (Figure 18B; p=0.033). Junctional localization was observed in 23.9% of the treponemal population after a 10 minute *T. pallidum*-endothelial co-incubation (Figure 18C) and there was a significant increase in junctional localization between 10 minute co-incubations and subsequent 30 minute and 60 minute co-incubations (Figure 18C; p=0.048). After 30 minutes of *T. pallidum*-HUVEC co-incubations, junctional localization reached a plateau in which half of the treponemal population was localized to intercellular junctions (Figure 18C). Localization to VE-cadherin was determined based on overlapping pixel intensity between *T. pallidum* FlaA and VE-cadherin (Figure 18C; inset, white arrows) and compared to *T. pallidum* attachment in non-junctional regions (Figure 18C; inset, black arrows).

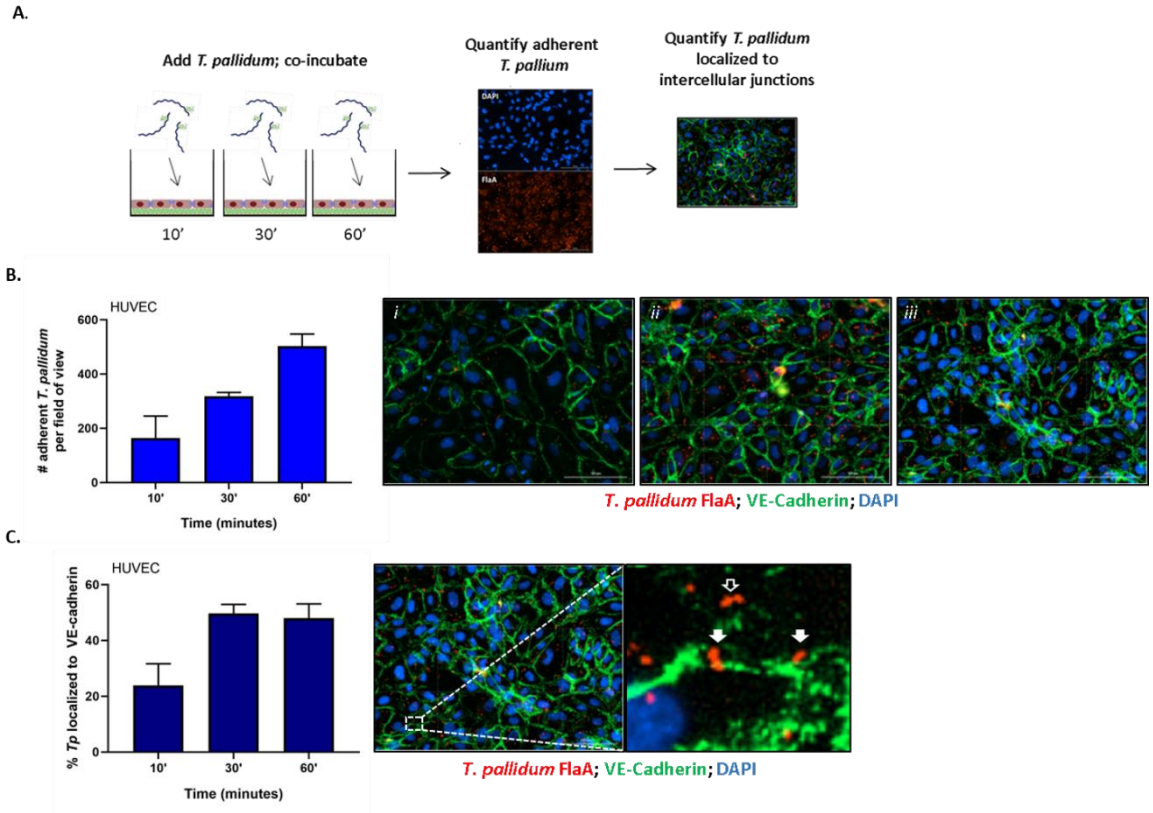

Figure 18: *Treponema pallidum* localizes to endothelial intercellular junctions. **(A)** Schematic illustrating the *T. pallidum* junctional localization assay. *Treponema pallidum* isolated from a rabbit testicular extract was co-incubated with confluent HUVEC monolayers for 10, 30, or 60 minutes. After washing to remove non-adherent treponemes, *T. pallidum* and HUVECs were fixed and permeabilized and *T. pallidum* attachment to endothelial monolayers was assessed via immunofluorescent staining of the *T. pallidum* periplasmic flagellar protein (FlaA, red) for treponemal quantification; HUVEC nuclei (DAPI, blue), and cellular margins (VE-cadherin, green) were stained to evaluate *T. pallidum* localization to cellular margins (green) or non-junctional areas. **(B)** Time course of *T. pallidum* attachment to HUVECs and representative immunofluorescent images after (*i*) 10 minute (*ii*) 30 minutes and (*iii*) 60-minute co-incubations with representative images **(C)** Percent localization of *T. pallidum* to VE-cadherin intercellular junctions. Colocalization with adherens junctions was evaluated by quantifying *T. pallidum* cells attached at sites with overlapping signal between FlaA (red; *T. pallidum*) and intercellular junctions (green; VE-cadherin). Representative immunofluorescence image of *T. pallidum* attached to endothelial cells. Inset reveals *T. pallidum* attached to endothelial cells in non-junctional regions (black arrow) and localized to VE-cadherin (white arrows). Results are presented as mean ± SEM from 3 independent experiments. Statistical significance was evaluated by one-way ANOVA comparing *T. pallidum* attachment to HUVECs between timepoints (p=0.048) and *T. pallidum* localization to junctions between timepoints (p=0.033).

Treponema pallidum modifies endothelial junctional architecture of VE-cadherin

To evaluate whether *T. pallidum* junctional localization results in modification of VE-cadherin architecture, adherent *T. pallidum* were grouped into four categories based on localization of bacteria including (1) linear junctions, (2) disrupted junctions, (3) plaque-like junctions or (4) non-junctional regions (Figure 19A *i-iv*, respectively) and compared between 30 minute and 60 minutes timepoints. Since *T. pallidum* localization to VE-cadherin junctions did not differ between these two timepoints (Figure 18C), this analysis explored whether the junctional architecture in regions of *T. pallidum* adhesion changed over time. Consistent with the junctional co-localization analysis (Figure 18C), there was

no change in the abundance of *T. pallidum* cells localized to non-junctional regions (Figure 19A inset *iv*) at 30 and 60 minute timepoints (Figure 19C, ns p=0.64). Similarly, *T. pallidum* localization to plaque-like junctional regions (Figure 19A inset *iii*) did not differ between the two timepoints (Figure 19C ns p=0.60). *Treponema pallidum* colocalization with linear junctions (Figure 19A inset *i*) decreased from 30.4% to 12.1% between 30 minute and 60 minute timepoints (Figure 19C * p=0.04), while the opposite effect was observed for *T. pallidum* in areas of junctional disruption (Figure 19A inset *ii*) where localization increased from 11.2% at 30 minutes to 23.0% at 60 minutes (Figure 19C ** p=0.002). This shift from a higher proportion of *T. pallidum* observed within linear junctions at 30 minutes to a higher proportion of *T. pallidum* observed within areas of junctional disruption at 60 minutes (Figure 19D) suggests that *T. pallidum* is involved in junctional disruption of VE-cadherin. Furthermore, when treponemal cells were incubated with Tp0751-specific serum prior to the HUVEC co-incubation, decreased *T. pallidum* adhesion to the monolayer was observed (Figure 19B). This replicates the observations in Chapter 2 of this dissertation, which also showed Tp0751-specific serum disrupted *T. pallidum* attachment to HUVECs (Figure 7). Importantly, no areas of junctional disruption were observed when treponemes were pre-incubated with Tp0751-specific serum (Figure 19B), demonstrating that *T. pallidum* attachment to endothelial monolayers is required to promote changes in VE-cadherin architecture. This finding also reveals that host factors present in the *T. pallidum in vivo* propagation extraction mixture are not driving junctional modification in HUVECs, as junctional changes are only observed in samples with adherent treponemes.

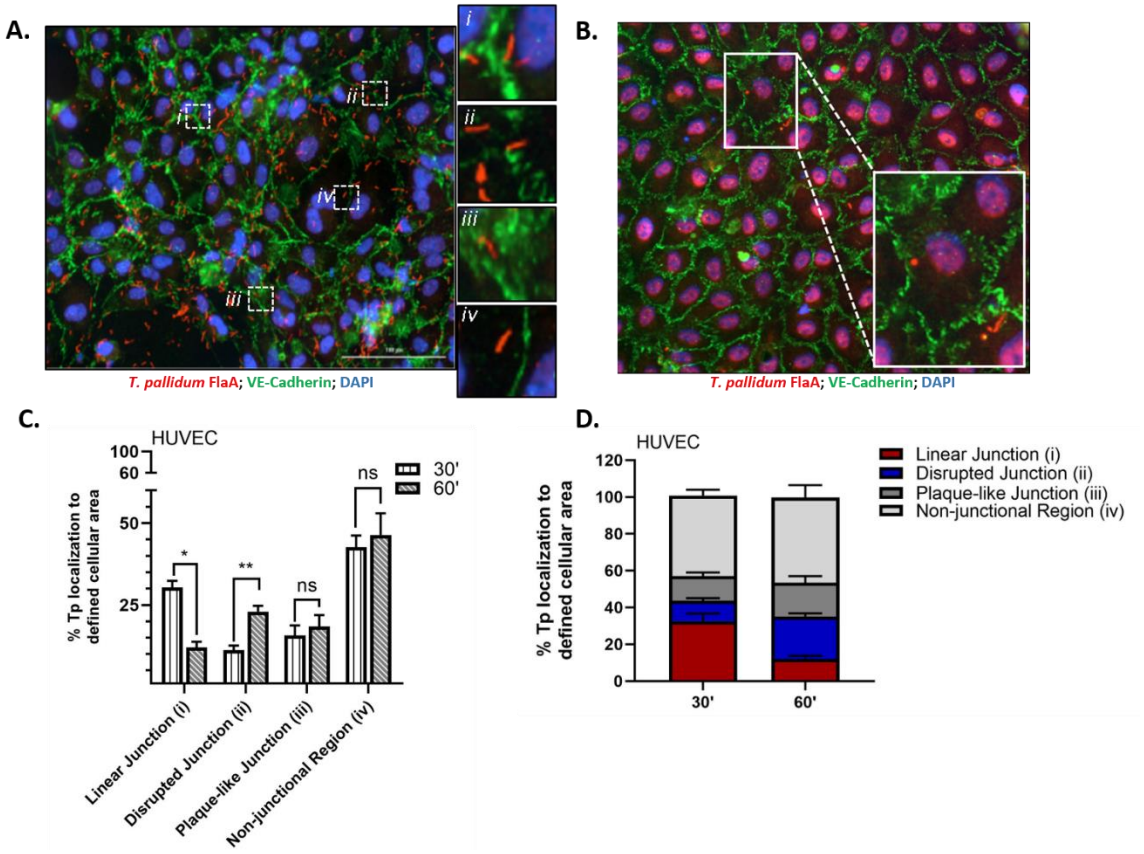

Figure 19: *Treponema pallidum* modifies endothelial VE-cadherin architecture. **(A)** Immunofluorescence image of *T. pallidum* attached to a HUVEC monolayer after a 60 minute co-incubation. Immunofluorescence of FlaA (*T. pallidum;* red), DAPI (nuclear stain, blue), and intercellular junctions (VE-cadherin, green) shown at 200X magnification. Insets highlight *T. pallidum* localized to defined regions including (*i*) linear (undisrupted junctions), (*ii*) disrupted junctions, (*iii*) plaque-like junctions, and (*iv*) non-junctional areas. **(B)** Immunofluorescence image of *T. pallidum* attached to HUVECs following treponemal pre-incubation with Tp0751-specific serum to inhibit adhesion to the monolayers. Representative images at 200X from 3 independent experiments. **(C,D)** Percent localization of *T. pallidum* to defined cellular regions at 30 minute and 60 minute timepoints. Results presented as mean ± SEM from 3 independent experiments; statistical significance was assessed with Student's t-tests comparing percent localization to cellular structures between 30 minute and 60 minute timepoints for linear junction (* p=0.04), disrupted junction (** p=0.002), plaque-like junction (ns p=0.60), and non-junctional area (ns p=0.64)

Recombinant Tp0751 does not alter the permeability of endothelial barriers

To assess the effect of Tp0751-mediated junctional remodeling on endothelial permeability, solute flux was measured across endothelial monolayers after Tp0751 exposure. Human umbilical vein endothelial cells were seeded into transwell plates coated with an artificial basement membrane and barrier integrity was confirmed via transendothelial electrical resistance (TEER) measurements. Monolayers were incubated with recombinant Tp0751, recombinant Tp0327 (negative control), or thrombin (positive control), a known vasoactive agent that increases the permeability of endothelial barriers (Gavard 2014). Flux of the fluorescent tracer, fluorescein isothiocyanate-dextran (FITC-dextran), across the endothelial barrier was monitored over the time course of the experiment (Figure 20A). Monolayers exposed to the positive control thrombin exhibited elevated permeability within the first 50 minutes compared to monolayers exposed to either recombinant protein (Figure 20B; Thrombin vs. Tp0751 *** p=0.0003; or vs. Tp0327 *** p=0.0002). Conversely, Tp0751 did not elicit any change in endothelial barrier permeability when compared to monolayers exposed to the negative control recombinant protein Tp0327 (Figure 20B; ns Tp0751 vs. Tp0327 p=0.720) demonstrating that recombinant Tp0751 does not affect barrier integrity of HUVEC monolayers at the timepoints measured.

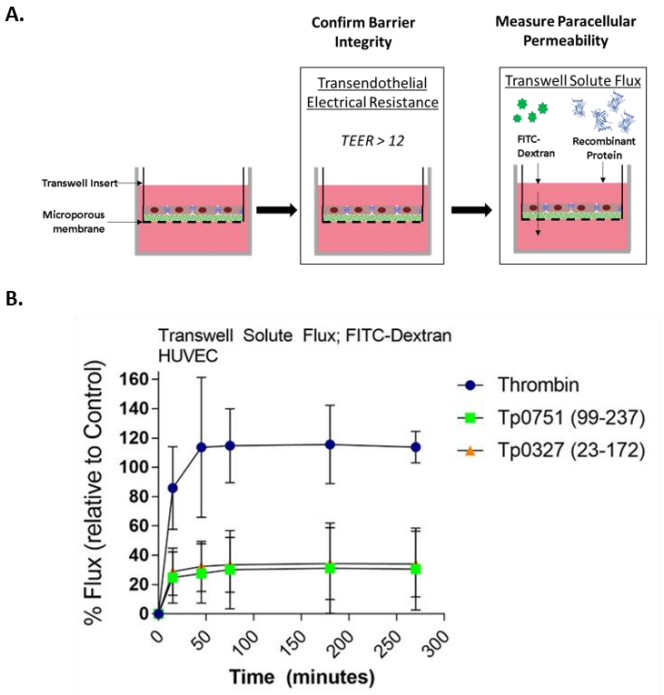

Figure 20: Tp0751 does not alter endothelial barrier integrity**. (A)** Schematic of transwell solute flux assay of endothelial monolayers exposed to recombinant treponemal proteins. HUVECs were seeded onto an artificial basement membrane in transwell inserts and grown to confluence. Barrier integrity was confirmed using transendothelial electrical resistance (TEER), where monolayer resistance >12Ωxcm^2 dictated an intact monolayer. Paracellular permeability was assessed using a transwell solute flux assay, where endothelial permeability in the presence of recombinant treponemal proteins was monitored with a FITC-dextran fluorescent tracer by sampling from the bottom compartment of the transwell for fluorescence measurements throughout the time course of the experiments. **(B)** Solute permeability of HUVEC monolayers was evaluated with the fluorescent tracer FITC-dextran in the presence of recombinant Tp0751 [V99-P237], negative control recombinant Tp0327 [I23-S172], and compared to the vasoactive agent thrombin (positive control) over 4.5 hours. Results are normalized to transwells containing artificial basement membrane without endothelial cells (set as 100% flux of FITC-dextran) and presented as mean ± SEM from 3 independent experiments. Statistical significance was assessed by two-way ANOVA ns p=0.559 [time factor], * p=0.0212 [treatment factor] with Tukey's post-test, Thrombin vs. Tp0751 *** p=0.0003; Thrombin vs. Tp0327 *** p=0.0002, Tp0751 vs. Tp0327 ns p=0.720.

Recombinant Tp0751 does not traverse endothelial barriers

Since recombinant Tp0751 does not impact the paracellular permeability of endothelial monolayers (Figure 20B), the capability for recombinant Tp0751 to traverse monolayers through paracellular or transcellular routes independent of barrier permeability alteration was explored. Recombinant Tp0327 and recombinant Tp0751 were chemically labelled with FITC (Table 4) to allow for fluorescent tracking of recombinant protein traversal across the monolayers (Figure 22A). Plate-based endothelial binding assays confirmed that FITC-labeling did not affect the cell binding capacity of Tp0751 (Figure 21; ns p=0.116). Confluent monolayers were co-incubated with FITC-labelled recombinant protein and protein flux into the bottom compartment was monitored throughout the 4.5 hour time course (Figure 22A). Neither FITC-Tp0751 nor FITC-Tp0327 traversed across the endothelial barrier (Figure 22B; ns p=0.499), while thrombin still increased barrier permeability as demonstrated by increased flux of FITC-dextran across the monolayer (Figure 22B).

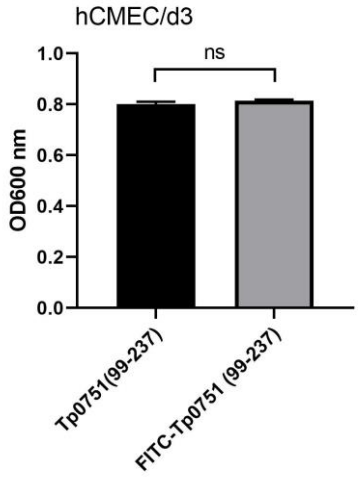

Figure 21: Endothelial binding by Tp0751 is not affected by chemical labeling with FITC. Binding assays evaluating attachment of recombinant Tp0751 [V99-P237] or FITC-labelled Tp0751 [V99-P237] to a host cell monolayer of human cerebral microvascular endothelial cells (hCMEC/d3). Results are presented as mean absorbance at 600 nm ± SEM from triplicate wells in two independent experiments. Statistical analyses were performed

using a Student's *t*-test comparing endothelial binding of Tp0751 [V99-P237] to FITC-labelled Tp0751 [V99-P237] ns p=0.116.

Table 4 Fluorescein isothiocyanate labeling of recombinant treponemal proteins.

Protein Construct[1]	Residues Available for Labeling[2]	Molar F/P Ratio[3]
Tp0751 [V99-P237]	Histidine terminal amine (1) Lysine (2)	0.86
Tp0327 [I23-S172]	Histidine terminal amine (1) Lysine (11)	1.50

[1]Recombinant protein construct used for FITC labeling
[2]Number and identity of amino acids in the sequence of the recombinant protein construct with amine residues available for chemical labeling with FITC
[3]Ratio of moles of FITC to moles of protein in the conjugate calculated using equations (1) and (2).

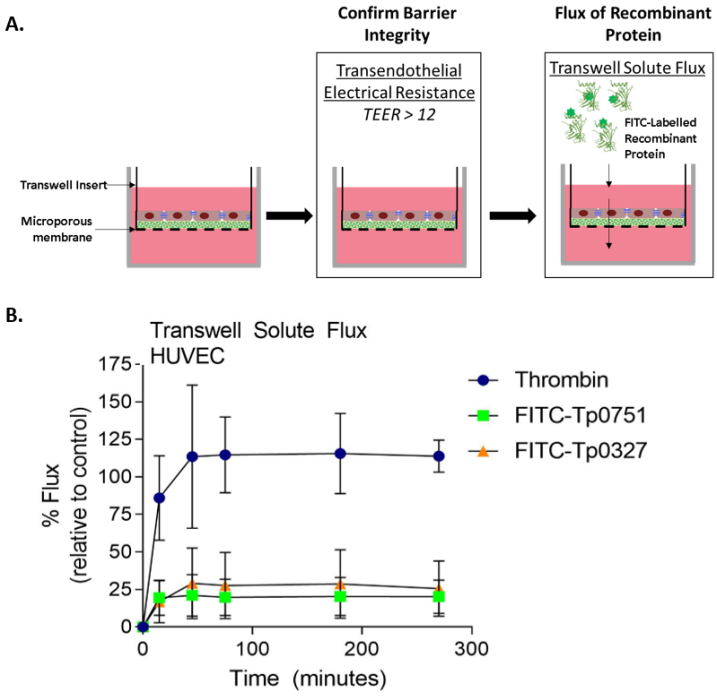

Figure 22: Recombinant Tp0751 does not traverse endothelial barriers. **(A)** Schematic of transwell solute flux assay of endothelial monolayers exposed to FITC-labelled recombinant treponemal proteins. HUVECs were seeded onto an artificial basement membrane in transwell inserts and grown to confluence. Barrier integrity was confirmed using transendothelial electrical resistance (TEER), where monolayer resistance >12Ωxcm^2 dictated an intact monolayer. Permeability was assessed with a transwell solute

flux assay, where the flux of FITC-labelled recombinant treponemal proteins across the monolayer was monitored by sampling from the bottom compartment of the transwell for fluorescence measurements throughout the time course of the experiments. **(B)** Solute permeability of HUVEC monolayers was evaluated by monitoring the flux of FITC-Tp0751 and FITC-Tp0327 (negative control) across the monolayer, compared to flux of FITC-dextran across monolayers in the presence of the vasoactive agent thrombin (positive control) over 4.5 hours. Results are normalized to transwells containing artificial basement membrane without endothelial cells (set as 100% flux of FITC-dextran) and presented as mean ± SEM from 3 independent experiments. Statistical analyses were performed using a two-way ANOVA ns p=0.577 [time factor], * p=0.0277 [treatment factor] with Tukey's post-test, Thrombin vs. Tp0751 **** p<0.0001; Thrombin vs. Tp0327 *** p<0.0001, Tp0751 vs. Tp0327 ns p=0.090.

Treponema pallidum **traverses endothelial monolayers without disrupting barrier permeability**

To explore the functional consequence of *T. pallidum* junctional remodeling and investigate the mechanisms of *T. pallidum* transendothelial migration, barrier permeability was monitored during *T. pallidum* traversal across endothelial monolayers. Paracellular permeability was evaluated via transwell solute flux of FITC-dextran across endothelial monolayers during exposure to live *T. pallidum*, heat-killed *T. pallidum*, or testicular extract from uninfected rabbits (Figure 23A). While darkfield microscopic analysis of samples from the bottom chamber revealed that live *T. pallidum* traversed endothelial barriers (Figure 23C), no significant changes in barrier permeability were observed in endothelial barriers exposed to any of the treatments over the 390 minute (6.5 hour) time course (Figure 23B; A ns p=0.707 [treatment factor]).

A.

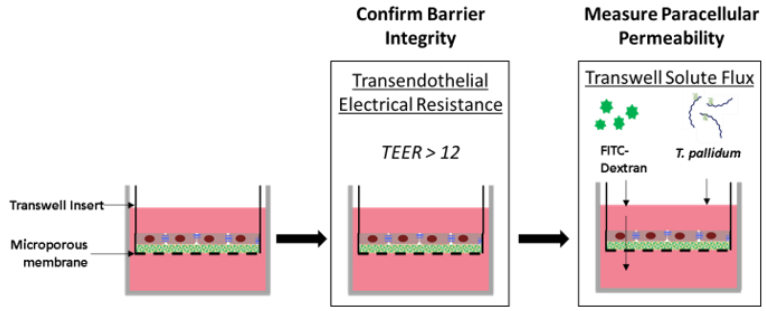

B.

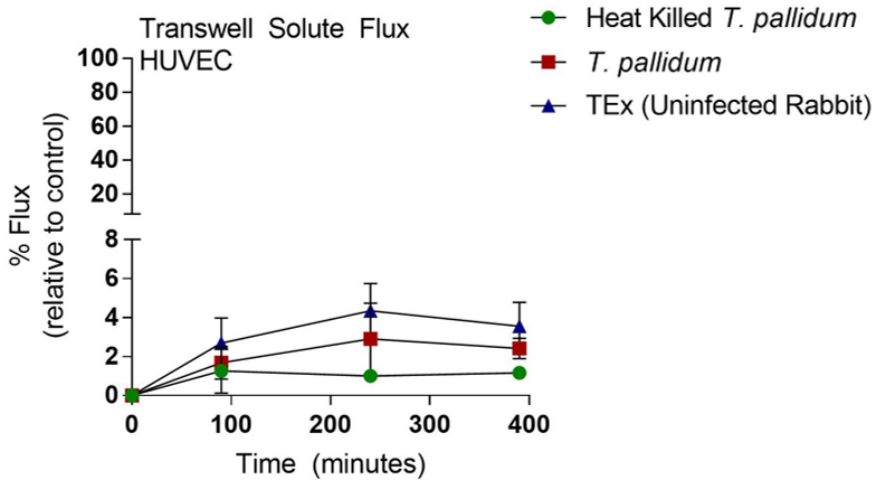

C.

		Time (minutes)		
		00'	240'	390'
Heat-Killed *T. pallidum*	*Exp1*	-/-	-/-	-/-
	Exp2	-/-	-/-	-/-
	Exp3	-/-	-/-	-/-
Live *T. pallidum*	*Exp1*	-/-	-/-	+/+
	Exp2	-/-	+/-	+/+
	Exp3	+/+	+/+	+/+
TEx (Uninfected Rabbit)	*Exp1*	-/-	-/-	-/-
	Exp2	-/-	-/-	-/-
	Exp3	-/-	-/-	-/-

Figure 23: *Treponema pallidum* traverses endothelial monolayers without disrupting barrier integrity. **(A)** Schematic of transwell solute flux assay of endothelial monolayers exposed to *T. pallidum*. HUVECs were seeded onto an artificial basement membrane in transwell inserts and grown to confluence. Barrier integrity was confirmed using transendothelial electrical resistance (TEER), where monolayer resistance >12**Ω**xcm^2 dictated an intact monolayer. Barrier permeability was assessed with a transwell solute flux assay, where endothelial permeability in the presence of *T. pallidum* was monitored with a FITC-dextran fluorescent tracer by sampling from the bottom compartment of the transwell for fluorescence measurements throughout the time course. **(B)** Solute permeability of HUVEC monolayers was evaluated with the fluorescent tracer FITC-dextran in the presence of *T. pallidum*, heat-killed *T. pallidum*, or testicular extract from uninfected rabbits over 6.5 hours. Results are normalized to transwells containing artificial basement membrane without endothelial cells (set as 100% flux of FITC-dextran) and presented as mean ± SEM from 3 independent experiments. Statistical significance was analyzed by two-way ANOVA comparing *T. pallidum*, heat killed *T. pallidum*, and testicular extract from uninfected rabbits ['TEx (Uninfected Rabbit)']; treatment factor ns p=0.707; time factor ** p=0.004. **(C)** Darkfield analysis of duplicate 10 µl samples taken from the bottom chambers from endothelial cells treated with live *T. pallidum*, heat-killed *T. pallidum*, or TEx (Uninfected Rabbit) from three separate experiments at each timepoint. Technical replicates are separated by forward slashes, a negative sign (-) indicates no *T. pallidum* observed in the darkfield sample, while a positive sign (+) indicates *T. pallidum* was visualized in the darkfield sample. Slides were scanned for ten different fields of view and the presence of ≥1 *T. pallidum* was recorded as a positive.

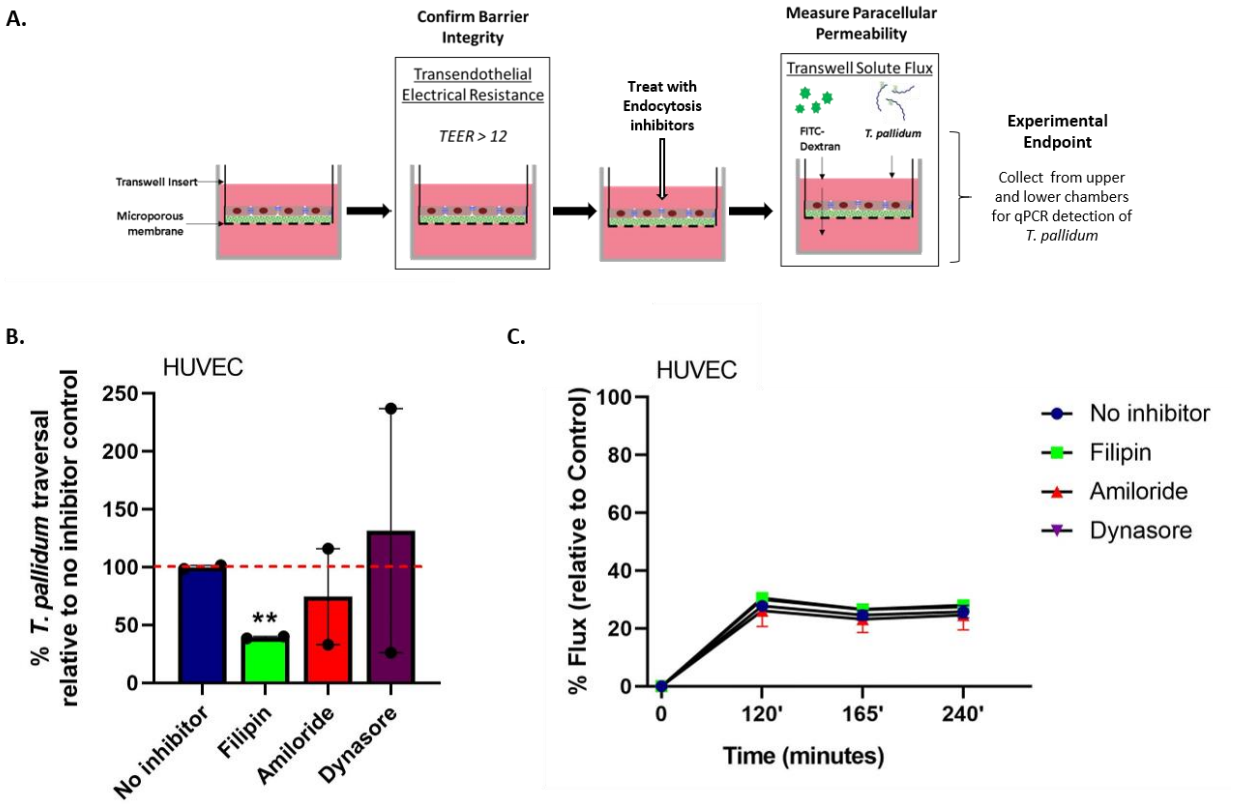

Figure 24: *Treponema pallidum* traversal of endothelial barriers is partially abrogated with an inhibitor of lipid raft-mediated endocytosis. Schematic of transwell solute flux assay of endothelial monolayers exposed to *T. pallidum*. HUVECs were seeded onto an artificial basement membrane in transwell inserts and grown to confluence. Prior to experimentation, barrier integrity was confirmed using transendothelial electrical resistance (TEER), where monolayer resistance >12Ωxcm^2 dictated an intact monolayer. Endothelial monolayers were treated with inhibitors of endocytosis, followed by addition of live *T. pallidum.* Barrier permeability was assessed with a transwell solute flux assay, where endothelial permeability in the presence *T. pallidum* was monitored with a FITC-dextran fluorescent tracer by sampling from the bottom compartment of the transwell for fluorescence measurements throughout the time course of the experiments. *Treponema pallidum* traversal was evaluated by collecting the media from the upper and lower compartment in each well and quantifying traversal with quantitative polymerase chain reaction (qPCR) detection of endoflagellar sheath gene *flaA*. **(B)** *Treponema pallidum* traversal across HUVEC monolayers in untreated control (blue) or in the presence of

inhibitors against lipid-raft mediated endocytosis (filipin, 5 μM, green), macropinocytosis (amiloride, 1 mM, red), or dynamin-dependent endocytosis (Dynasore, 80 μM, purple). Traversal was assessed using quantitative real-time PCR to measure *flaA* DNA concentrations in the bottom compartment of transwell plates. Results are presented as mean ± SEM percent *T. pallidum* traversal relative to the untreated control (set as 100% traversal, dashed red line) from two independent experiments. Statistical analysis was performed with one-way ANOVA with Tukey's post-test comparing *T. pallidum* traversal in the no inhibitor control to *T. pallidum* traversal in filipin (** p=0.0053), amiloride (ns p=0.240), and Dynasore (ns p=0.738) exposed treatments. (C) Solute permeability of HUVEC monolayers exposed to endocytosis inhibitors was evaluated with the fluorescent tracer FITC-dextran in the presence of *T. pallidum* and inhibitor treatments over four hours. Results are normalized to transwells containing artificial basement membrane without endothelial cells (set as 100% flux of FITC-dextran) and presented as mean ± SEM from two independent experiments with two biological replicates. Statistical analysis was performed with a two-way ANOVA (time factor ****p<0.001; treatment factor ns p=0.745).

Treponema pallidum transendothelial migration is blocked with a lipid raft/caveolae-mediated endocytosis inhibitor

To investigate whether *T. pallidum* traverses endothelial barriers using a transcellular mechanism, HUVEC monolayers were treated with endocytosis inhibitors and treponemal traversal was monitored using qPCR on the supernatant from the upper and lower chamber of transwell plates (Figure 24A). Endothelial cells were exposed to filipin, amiloride, or Dynasore which block lipid-raft/caveolae-mediated endocytosis, macropinocytosis, and dynamin-dependent endocytosis, respectively (Schnitzer et al. 1994; Koivusalo et al. 2010; Preta, Cronin, and Sheldon 2015; Vercauteren et al. 2010). A small proportion of *T. pallidum* crossed HUVEC monolayers in all treatments (Table 5) and a reduced traversal rate was observed in the presence of one endocytosis inhibitor. Quantification of *T. pallidum* from the lower compartment in untreated control samples revealed a traversal rate of 0.35% (Table 5); estimated traversal rates were calculated based on the starting inoculum added to the upper compartment. Quantification of treponemes from the upper

compartment was outside the linear range of the qPCR standard curve, thus the number of *T. pallidum* remaining in the upper compartment can only be estimated as $>6.1x10^5$ cells for all the treatments (Table 5). A statistically significant 60% reduction in *T. pallidum* transendothelial migration was observed in the presence of a lipid raft endocytosis inhibitor (Figure 24B; filipin; ** p=0.0053), whereas no significant difference was observed in the presence of the macropinocytosis inhibitor (Figure 24B; amilroide; p=0.240) or the dynamin inhibitor (Figure 21B; Dyansore; p=0.738). Control and inhibitor treated HUVECs were also subject to a transwell solute flux assay to monitor changes in barrier permeability. No statistically significant difference in endothelial barrier permeability was observed between the different inhibitor-treated monolayers at any time point (Figure 24C p=0.745).

Table 5 *Treponema pallidum* (*Tp*) transendothelial migration in the presence of endocytosis inhibitors.

Treatment	*Tp* upper compartment[1]	*Tp* lower compartment[2]	Traversal[3]
Tp + No inhibitor	$>6.1 \times 10^5$	$1.1 \times 10^5 \pm 1.4 \times 10^3$	0.35%
Tp + Filipin	$>6.1 \times 10^5$	$4.3 \times 10^4 \pm 1.3 \times 10^3$	0.14%
Tp + Amiloride	$>6.1 \times 10^5$	$8.1 \times 10^4 \pm 4.5 \times 10^4$	0.26%
Tp + Dynasore	$>6.1 \times 10^5$	$1.4 \times 10^5 \pm 1.1 \times 10^5$	0.50%

[1]qPCR of *flaA* from upper compartments to quantify *Tp* at the end of the 4 hour co-incubation with HUVECs in transwell plates. Values were outside of the linear range of the standard curve, thus are expressed as greater than the upper limit of the curve
[2]qPCR of *flaA* from lower compartments to quantify *Tp* at the end of the 4 hour co-incubation with HUVECs in transwell plates. Presented as mean ± SEM.
[3]Estimated percent traversal calculated based on starting inoculum (3.10×10^7 *Tp*/well) and *Tp* quantified in the lower compartment after 4 hour co-incubation with HUVECs

3.4 Discussion

Vascular dissemination of *T. pallidum* is central to the disease progression of this highly invasive organism. The diverse clinical manifestations observed during secondary and tertiary syphilis can be attributed to the ability of *T. pallidum* to seed into numerous host tissues and organs (Mahoney 1934; Stokes 1944; Cumberland MC 1949; Raiziss GW 1937). However, the specific molecular events that facilitate *T. pallidum* movement from the bloodstream into secondary infection sites are poorly understood. This work explores

the functional outcomes of Tp0751-mediated *T. pallidum* adhesion to endothelial cells to understand how *T. pallidum* modulates endothelial barriers to promote bacterial transendothelial migration. The findings presented herein establish that Tp0751 and *T. pallidum* modify endothelial adherens junctional architecture and that *T. pallidum* localizes to endothelial VE-cadherin at cell-cell borders. However, despite clear junctional modification by *T. pallidum* and recombinant Tp0751, no disruption of endothelial barrier permeability in transwell plate assays is observed after exposure to recombinant Tp0751 or live *T. pallidum.* Importantly, *T. pallidum* was able to traverse endothelial monolayers, while recombinant Tp0751 alone could not. Preliminary findings reveal that only a small subset of treponemes traverse across HUVEC monolayers, as indicated by a traversal rate of <1%. Furthermore, *T. pallidum* transendothelial migration is disrupted with an endocytosis inhibitor that targets raft-mediated endocytosis. These findings indicate that *T. pallidum* shares key elements of transendothelial migration with leukocytes and invasive extracellular bacteria including the spirochete *B. burgdorferi*, suggesting that parallel mechanisms could exist for endothelial traversal by diverse eukaryotic and prokaryotic cell types.

There are numerous mechanisms for the disassembly of VE-cadherin junctions in endothelial barriers, including phosphorylation of VE-cadherin and adherens junction adaptor proteins to weaken junctional bonds, clathrin-mediated endocytosis to internalize VE-cadherin, endothelial cell retraction via the actomyosin contractility apparatus to pull apart junctional bonds, and cleavage of VE-cadherin at cell borders as reviewed by Dejana, Orsenigo and Lampugnani *et al*. 2008. It is important to note that a reduction in strength of junctional bonds does not always translate to morphological changes and gap formation between endothelial cells, thus increased barrier permeability is not always a functional outcome of VE-cadherin modification (Dejana, Orsenigo, and Lampugnani 2008; Andriopoulou et al. 1999; Esser et al. 1998). For example, vascular permeability and leukocyte diapedesis are controlled via phosphorylation of separate tyrosine residues in the cytoplasmic tail of VE-cadherin, demonstrating that separate mechanisms exist for maintaining endothelial barrier function during leukocyte diapedesis versus modulation of vascular permeability (Wessel et al. 2014). While this body of work does not identify the mechanism underlying Tp0751-mediated modification of VE-cadherin junctional

architecture, it is hypothesized that the morphological changes in adherens junctions presented are a result of VE-cadherin internalization. This is based on the collective findings that mean fluorescence intensity of junctional VE-cadherin is reduced in non-permeabilized cells and that cytoplasmic VE-cadherin was observed in permeabilized cells treated with Tp0751, but not in cells treated with the negative control recombinant protein Tp0327. Future investigations should explore time-resolved disruption of VE-cadherin by Tp0751 and *T. pallidum* including inhibitors of clathrin-mediated endocytosis to definitively characterize the molecular events that underlie VE-cadherin modulation.

In this chapter, an *in vitro* transwell plate system was developed to investigate changes to endothelial barrier permeability. The growth of endothelial cells on porous filters of transwell inserts can be technically challenging; the development of this model was based on previous optimization of the growth of macrovascular HUVECs in the transwell inserts (Denchev 2014). However, future work should aim to develop a microvascular transwell model for *T. pallidum,* as the host microvasculature represents a more likely site for treponemal transendothelial migration *in vivo.* The dynamic nature of endothelial barriers poses a significant challenge to experimental determination of barrier integrity modulation *in vitro*. There are multiple techniques for evaluating endothelial barrier integrity. The data presented in this work relies on a permeability-based approach, in which the movement of a fluorescent tracer across endothelial barriers can be monitored at defined time intervals. For this approach, a FITC-labeled 40 kDa dextran tracer was selected. These dextrans are water soluble, membrane impermeant, and unable to be actively transported by cells across the monolayer (Wegener and Seebach 2014). These characteristics allow for the specific evaluation of paracellular permeability of endothelial monolayers, as FITC-dextran should not cross via a transcellular route. An alternative to the transwell solute flux approach is transendothelial electrical resistance (TEER), which measures endothelial permeability to small inorganic ions (Wegener and Seebach 2014). In this work, TEER was used initially to determine whether confluent endothelial monolayers seeded onto transwell filters had intact barrier integrity suitable for experimentation. However, this approach only allows discrete measurements of barrier resistance at defined time points, whereas macromolecular permeability provides a cumulative view of changes in the permeability. Furthermore, changes in TEER can also

reflect morphological changes in endothelial cells that occur independently of barrier disruption (Wegener and Seebach 2014; Claude 1978) and endothelial cells are known to have a naturally low TEER which can be technically challenging to measure accurately (Bischoff et al. 2016). Electrical cell-substrate impedance sensing (ECIS) is a more sensitive and comprehensive approach than TEER for studying barrier properties of endothelial cells. In ECIS, cells are grown on gold electrodes and an alternating current is applied. This allows for the measurement of resistance to the alternating currents; data acquisition can be automated, allowing for real-time barrier evaluation. Furthermore, in addition to evaluating barrier permeability, ECIS can also inform cell attachment, growth, morphology, and motility (Bischoff et al. 2016; Wegener and Seebach 2014). Although ECIS represents a robust method for evaluation of endothelial barriers, the specialized equipment required and the fact that cells must be grown directly on electrodes does not allow for detection of permeability in the context of a bacterial transendothelial migration assay. A comparative evaluation between macromolecular permeability using a 40 kDa FITC-dextran tracer and ECIS for monitoring changes in paracellular permeability in a human microvascular endothelial cell line revealed that while ECIS allowed for more sensitive detection of changes in permeability to certain agonists, there was general agreement for the evaluation of endothelial permeability between the two approaches (Bischoff et al. 2016).

Maintaining the integrity of the endothelium is essential for vascular homeostasis. The opening and closing of intercellular junctions is carefully regulated to prevent plasma leakage and thrombogenic events (Dejana, Orsenigo, and Lampugnani 2008); however, soluble inflammatory mediators, circulating immune cells, and bacteria can modify junctional integrity and vascular permeability using distinct but sometimes overlapping mechanisms (Lemichez et al. 2010; Dejana, Orsenigo, and Lampugnani 2008; Alon and van Buul 2017). Transendothelial migration by leukocytes occurs through two pathways: (1) transcellular traversal through endothelial cell bodies and (2) paracellular traversal where leukocytes cross through gaps in intercellular junctions. Paracellular traversal occurs via a highly coordinated process that involves a cascade of adhesive interactions at the endothelial-leukocyte interface and controlled disruption of intercellular junctions that allow for leukocyte transendothelial migration without a significant disruption of the

barrier permeability. While the detailed molecular mechanisms that protect the endothelium from vascular leakage during leukocyte paracellular traversal are not fully understood, it has been demonstrated that an F-actin-rich contractile ring forms at the traversal site (Heemskerk et al. 2016) to retain a minimum pore size of 1-2 μm that leukocytes must squeeze through (Heemskerk et al. 2016; Carman and Springer 2008; Vestweber 2015; Muller 2011). The finding that *T. pallidum* traversal across *in vitro* endothelial monolayers occurs independently of changes in barrier permeability could suggest that *T. pallidum* undergoes transcellular traversal through endothelial barriers. An alternative explanation is that *T. pallidum* uses a paracellular traversal mechanisms that mimics leukocyte transendothelial migration with transient junctional openings and F-actin contractile rings to maintain vascular integrity. While leukocytes must undergo significant actin reorganization ('squeezing') to fit through endothelial transcellular or paracellular pores of 1-2 μm, the 0.2 μm diameter of *T. pallidum* cells (Lafond and Lukehart 2006) would allow for traversal through even smaller pores. It is also plausible that *T. pallidum* could traverse endothelial barriers via both paracellular and transcellular mechanisms.

The meningitis-causing pathogens *Neisseria meningitidis, Escherichia coli* K1, *Haemophilus influenzae,* and *Streptococcus pneumoniae* all share a common endothelial receptor with *T. pallidum*: the 67 kDa laminin receptor (LamR). While *T. pallidum* and the meningitis-causing pathogens all interact with the same endothelial ligand, the transendothelial migration mechanisms that follow LamR adhesion are facilitated by distinct molecular events, though some intriguing parallels exist. The characterization of transendothelial migration mechanisms for other invasive bacteria has set a precedent for the disruption of intercellular junctions occurring in concert with transcellular traversal. *Neisseria meningitidis* traversal across the blood-brain barrier (BBB) occurs via a specialized transcellular route in which polarity complex and junctional proteins, including VE-cadherin, are recruited to sites of bacterial attachment, facilitating the opening of a traversal route below regions of meningococcal adhesion via the formation of new junctional sites. *In vitro,* this is accompanied by an increase in endothelial barrier permeability resulting from depletion of junctional proteins from cell margins (Coureuil et al. 2009; Coureuil et al. 2010). Conversely, *in vivo* meningococci invasion into the brain occurs without significant modulation of BBB permeability (Coureuil et al. 2017).

Transcellular traversal of neuroinvasive *E. coli* K1 across the BBB occurs via caveolae-mediated uptake and is paired with disruption of adherens junctions and increased endothelial barrier permeability (Sukumaran, Quon, and Prasadarao 2002; Krishnan et al. 2012; Sukumaran and Prasadarao 2003; Salmeri et al. 2013; Mittal and Prasadarao 2010). Similarly, *H. influenzae* traverses brain endothelial barriers via a transcellular route while disrupting VE-cadherin junctions and barrier permeability (Caporarello et al. 2018). Neuroinvasion of *S. pneumoniae* also occurs via transcytosis across brain endothelial cells, and while the specific mechanisms of traversal have yet to be delineated, numerous studies have reported that traversal occurs without disruption of intercellular junctions or barrier permeability (Iovino et al. 2013; Ring, Weiser, and Tuomanen 1998). It has been postulated that bacterial transendothelial migration could initially occur via transcellular routes, during which bacterial modulation of signaling pathways may induce opening of a paracellular route via junctional disruption (Dando et al. 2014). Of interest to the findings presented herein, with the exception of *S. pneumoniae,* the neuroinvasive LamR-binding pathogens all use a parallel strategy for transendothelial migration in which transcellular traversal is preceded by disruption of intercellular junctions.

The elements of *T. pallidum* and Tp0751 junctional modification and transendothelial migration presented in this chapter share interesting common elements with other invasive spirochetes. Despite distinct disease progression and pathologies, the spirochete pathogens *Borrelia burgdorferi* and *Leptospira interrogans*, the causative agents of Lyme disease and leptospirosis, respectively, are both highly invasive pathogens that exhibit widespread dissemination in their hosts (Hyde 2017; Galbe et al. 1993; Haake and Levett 2015). The molecular mechanisms of spirochete vascular dissemination have not been fully elucidated; however, spirochete-endothelial interactions have been studied most extensively for *B. burgdorferi*. Conflicting evidence has been presented for paracellular versus transcellular transendothelial migration of *B. burgdorferi*. Live imaging of *B. burgdorferi in vitro* and *in vivo* demonstrate that the *B. burgdorferi* traversal mechanism mimics leukocyte paracellular transendothelial migration with a multi-stage adhesion process followed by localization to endothelial intercellular junctions and subsequent paracellular traversal (Moriarty et al. 2008; Moriarty et al. 2012; Norman et al. 2008). Conversely, a transcellular traversal mechanism is supported by intracellular

localization of *B. burgdorferi* in endothelial cells (Wu et al. 2011; Comstock and Thomas 1989; Ma, Sturrock, and Weis 1991). Further to this, *B. burgdorferi* does not appear to modify VE-cadherin junctional architecture (Sato and Coburn 2017). Similar to the findings presented for *T. pallidum* barrier traversal, *B. burgdorferi* localizes to intercellular junctions and transendothelial migration *in vitro* occurs without modulation of barrier permeability (Grab et al. 2005). However, these results were based on single electrode TEER measurements, and a more recent investigation using ECIS, a technique that offers real-time monitoring of barrier permeability and endothelial morphology changes (Wegener and Seebach 2014), has since demonstrated increased permeability of endothelial monolayers upon exposure to *B. burgdorferi* (Grab et al. 2009). This discrepancy in barrier integrity after *B. burgdorferi* exposure suggests that ECIS is a more sensitive technique for studying barrier integrity, and further exploration of *T. pallidum*-endothelial interactions should utilize ECIS systems to explore changes in endothelial barrier properties.

Parallels can also be drawn between the endothelial interactions of *T. pallidum* and *L. interrogans.* Comparable to the findings presented in this work, *L. interrogans* disrupts the junctional architecture of VE-cadherin in endothelial monolayers, although this occurs independently of VE-cadherin internalization (Sato and Coburn 2017). There is also evidence for direct binding of VE-cadherin by *L. interrogans* (Evangelista et al. 2014), but localization to intercellular junctions has not been confirmed in the biological context of endothelial monolayers. Exploration of endothelial receptors for Tp0751 did not identify VE-cadherin as a receptor (Table 2, Table 3), which suggests that Tp0751-mediated modification of VE-cadherin does not occur through direct interactions between Tp0751 and VE-cadherin, but rather via signaling pathways induced by Tp0751 receptor engagement at the endothelial cell surface. However, the possibility remains that *T. pallidum* binds directly to VE-cadherin through another endothelial adhesin, as *T. pallidum* localization to endothelial intercellular regions implies a direct interaction with junctional proteins. *In vitro* modelling of *L. interrogans*-endothelial interactions has revealed that pathogenic leptospires traverse across endothelial barriers in transwell plate assays and induce actin remodeling that causes gap formation and cell rounding in confluent endothelial monolayers. However, in these investigations barrier integrity was not directly

monitored during transendothelial migration assays (Martinez-Lopez, Fahey, and Coburn 2010); therefore, it is plausible that *L. interrogans* could also traverse endothelial barriers without disrupting barrier permeability. In support of this, *L. interrogans* traversal across kidney epithelial cells occurs without affecting barrier permeability. Furthermore, the observation of leptospires at intracellular locales implies a transcellular mechanism for epithelial traversal (Barocchi et al. 2002). Two possibilities exist to explain these divergent results: (1) transendothelial and transepithelial migration of *L. interrogans* occur via distinct mechanisms or (2) *L. interrogans* disrupts endothelial monolayers without affecting barrier permeability, in parallel to our observations for *T. pallidum* transendothelial migration.

Little is known about the molecular mechanisms of *T. pallidum* dissemination, largely owing to the inherent difficulty of experimentation associated with research on this spirochete. In this chapter, it is revealed that *T. pallidum* localizes to intercellular junctions and modifies VE-cadherin junctional architecture; even with this junctional modification, *T. pallidum* traverses endothelial monolayers without disrupting barrier permeability. These findings corroborate previous observations that *T. pallidum* localizes to endothelial intercellular junctions and that *T. pallidum* transendothelial migration occurs without any discernable change in barrier permeability (Thomas et al. 1989; Thomas et al. 1988). A recent study using electron micrographs to evaluate *T. pallidum* interactions with human brain microvascular endothelial cells observed *T. pallidum* cells clustering at specific regions on endothelial surfaces and merging with endothelial cell surfaces. The identity of the treponemal clustering site on endothelial surfaces was not characterized or defined and the possibility that these sites were junctional regions was not explored (Wu, Zhang, and Wang 2017). The observation that *T. pallidum* merges with endothelial membranes is suggestive of a transcellular traversal mechanism for the spirochete, whereas localization to endothelial intercellular junctions implies a paracellular route of traversal.

Previous investigations have shown that *T. pallidum* is capable of activating cultured endothelial cells, which increases procoagulant activity and surface expression of leukocyte adhesion molecules and induces attachment and transendothelial migration of immune cells (Riley et al. 1992; Riley et al. 1994). Under normal conditions, the vascular endothelium mediates immune responses to agonists or alterations in the local environment

including changes in shear stress, minor trauma, and the presence of bacterial pathogens. This is referred to as endothelial cell activation, which can manifest as a broad range of responses to stimuli and is critical for maintaining vascular homeostasis. In general, activation results in the release of inflammatory mediators that further amplify the response to induce endothelial swelling, upregulation of leukocyte adhesion molecules, and increased leukocyte recruitment and transendothelial migration (Aird 2003). Of relevance to of the aims of this work, *T. pallidum*-mediated activation of endothelial cells occurs without modulating barrier permeability (Riley et al. 1992; Riley et al. 1994). Endothelial activation has been reported to be observed in response to the 47 kDa lipoprotein (Tp0574) purified directly from *T. pallidum* as well as numerous recombinant *T. pallidum* proteins, including Tp0574 (47 kDa lipoprotein), Tp0435 (Tp17), and Tp0965 (Zhang, Zhang, and Wang 2014; Zhang et al. 2015; Lee et al. 2000). In addition to activating endothelial cells, recombinant Tp0965 has also been reported to modify endothelial actin, reduce protein levels of the tight junction protein claudin-1, and increase the permeability of endothelial barriers *in vitro* (Zhang, Zhang, and Wang 2014). However, the finding that Tp0965 modulates endothelial barrier integrity disagrees with previous experiments using live *T. pallidum* (Thomas et al. 1988), as well as the results presented herein. It remains to be determined whether *T. pallidum* proteins are inherently immunogenic towards endothelial cells, as these recombinant protein studies failed to include a negative control recombinant protein or perform endotoxin removal on recombinant protein preparations, calling the biological relevance of the results into question. Additionally, Tp0965 is thought to localize to the periplasmic space as a predicted membrane fusion protein (The UniProt Consortium 2019), and the lipoproteins Tp0435 and Tp0574 are proposed to localize to the periplasmic face of the *T. pallidum* cytoplasmic membrane (Kubanov, Runina, and Deryabin 2017). Heterologous expression of Tp0435 in a model *B. burgdorferi* system results in multiple protein isoforms with predominant localization to the periplasm. However, Tp0435 was also confirmed to localize to the spirochete cell surface and confer a gain-of-function for attachment to a cultured epithelial cell line (Chan et al. 2016). While surface localization of Tp0435 would appropriately place the protein for endothelial activation by intact *T. pallidum*¸ the intracellular locale of Tp0965 and Tp0574 suggests that spirochetes would need to be degraded or coordinate the release of periplasmic contents to elicit such an

effect. Further to this, endothelial cell activation via Tp0435, Tp0965, and Tp0574 has not been confirmed in experiments with live *T. pallidum.* More experimental evidence will be required to understand if these proteins are important to the endothelial interaction of *T. pallidum.*

Endothelial dysfunction occurs when activation is uncontrolled and has negative consequences for the host. An example is sepsis, in which sustained activation of the endothelium occurs in response to pathogen invasion of endothelial cells (Volk and Kox 2000) or engagement of endothelial pattern recognition receptors by bacterial cell wall components such as lipopolysaccharide, peptidoglycan, or lipoproteins (Faure et al. 2001; Henneke and Golenbock 2002; Zhang et al. 1999; Zhao et al. 2001; Aird 2003). A key element of sepsis is the modification of endothelial barrier permeability, resulting in fluid leakage and tissue edema (Ferro et al. 2000; Ferro et al. 1997; Goldblum et al. 1993; Goldblum, Ding, and Campbell-Washington 1993). Sepsis can occur when an unbalanced immune response is initiated in response to bacterial pathogens like *Staphylococcus aureus, E. coli, Klebseiella* spp. *and Pseudomonas aeruginosa*; the imbalance can result in hyperinflammation leading to multisystem organ failure and early mortality or immune suppression leading to secondary infections and late onset mortality (Opal et al. 2003). Although *T. pallidum* undergoes rapid and widespread vascular dissemination, the spirochete does not induce an aberrant systemic inflammatory immune response in the host that is indicative of sepsis. This suggests that endothelial dysfunction and systemic modulation of barrier permeability do not occur during *T. pallidum* vascular dissemination. However, it is possible that limited activation of the endothelium could result in localized disruption of barrier permeability, but it is difficult to delineate whether this is an important event for *T. pallidum* dissemination or a natural endothelial immune response to *T. pallidum*. Taken in the context of previous investigations of *T. pallidum*-endothelial interactions (Thomas et al. 1988), the findings presented herein provide convincing evidence that *T. pallidum* transendothelial migration occurs independently of barrier permeability disruption. Further work will be required to understand the role of *T. pallidum*-mediated endothelial cell activation in the process of dissemination and to determine whether *T. pallidum* could induce localized, controlled barrier disruption in the vasculature.

It has long been assumed that *T. pallidum* traverses endothelial barriers via a paracellular mechanism based on the findings that treponemes localize to endothelial intercellular junctions (Thomas et al. 1988). However, this previous study (Thomas et al. 1988) and the results presented in herein both demonstrate that *T. pallidum* does not disrupt endothelial barrier permeability. Taken together, these findings suggest that *T. pallidum* transendothelial migration is likely to occur via a mechanism that mimics leukocytes by transcellular traversal or paracellular traversal that is tightly regulated to prevent vascular leakage. It is also possible that *T. pallidum* traverses via both mechanisms. While *T. pallidum* is generally understood to be an extracellular pathogen, electron micrographs have revealed instances of the spirochetes merging with endothelial cell surfaces (Wu, Zhang, and Wang 2017) and residing within intracellular sites of epithelial cells and fibroblasts (Sykes and Kalan 1975; Fitzgerald, Miller, and Sykes 1975). While currently there is no definitive evidence to support an intracellular locale for *T. pallidum,* the possibility remains that a transient intracellular stage could exist during *T. pallidum* transendothelial migration. In this chapter, the possibility of a transcellular barrier traversal mechanism was explored. Endothelial cells were exposed to endocytosis inhibitors prior to the addition of treponemes to disrupt lipid raft-mediated endocytosis, dynamin-dependent endocytosis, and macropinocytosis. These findings revealed a statistically significant 60% reduction in *T. pallidum* transendothelial migration in the presence of filipin, which binds cholesterol in plasma membranes, disrupting lipid rafts and caveolae (Schnitzer et al. 1994). However, no significant difference in *T. pallidum* traversal was observed in the presence of amiloride which blocks macropinocytosis by inhibiting Na+/H+ exchange at the cell surface (Koivusalo et al. 2010). Similarly, no change in *T. pallidum* traversal occurred in the presence of Dynasore, which prevents both clathrin- and caveolar-mediated endocytosis by inhibiting the GTPase dynamin, requires for vesicle fission in both of these endocytosis pathways. The fact that the endocytosis inhibitor filipin can reduce *T. pallidum* transendothelial migration provides a starting point to explore treponemal transcellular traversal mechanisms. More in-depth characterization will be required to confirm this temporary intracellular localization and delineate the specific endocytic pathway. Previous investigations have revealed an *in vitro* traversal rate of 5.4% for *T. pallidum* transendothelial migration across endothelial barriers after four hours (Thomas et al. 1988).

Based on this finding, it was anticipated that the *in vitro* traversal rates of *T. pallidum* in these investigations would also be low. Quantitative analysis using real-time qPCR revealed that only 0.35% of treponemes traversed HUVEC monolayers in untreated samples. While this traversal rate is substantially lower than expected, it is important to note that quantitation of the starting inoculum was based on darkfield microscopy counts, while qPCR was used for quantification of *T. pallidum* traversal. Therefore, this traversal rate discrepancy may be attributed to differences in the quantitation method. Furthermore, the previous evaluation of *T. pallidum* barrier traversal used a rabbit aortic endothelial cell line on gelatin-coated porous membranes, as well as a higher starting inoculum of 5.0 x 10^8 *T. pallidum* (Thomas et al. 1988). In this chapter, traversal was measured across HUVECs grown on Matrigel-coated porous transwell membranes with a starting inoculum of 3.1 x 10^7 *T. pallidum*. In addition, the bottom compartment in each well was supplemented with 50% NRS in endothelial growth medium to induce chemotaxis of the treponemes across the monolayer. Matrigel is a hydrogel basement membrane mimic composed of laminin, collagen IV, heparin sulfate, proteoglycans, entactin, nidogen, and additional growth factors. It is possible that this artificial basement membrane mimic was an additional impediment to *T. pallidum* traversal compared to the gelatin used in the previous investigation (Thomas et al. 1988). It is also possible that the differential traversal rates in these two studies can be attributed to differences in endothelial secretions or receptor expression of the different cell lines. During *T. pallidum* transendothelial migration *in vivo*, it is likely that chemoattractants on the tissue side are a strong driving force for traversal. The addition of extra serum in the studies presented herein may not facilitate significant treponemal chemotaxis to traverse endothelial monolayers. Further to this, the traversal rate for *T. pallidum in vivo* may occur with higher or lower frequency at different sites in the body depending on the type and abundance of chemoattractants, receptor expression, or the shear forces of the blood flow. Future investigations should measure the traversal rate using the same quantification technique for determining the starting inoculum and the transcellular migration and explore how *T. pallidum* traversal is impacted by starting inoculum, origin of the endothelial cell line and presence of different chemoattractants in the bottom compartment.

Although there is a broad diversity in cellular uptake mechanisms, and novel endocytosis pathways are still being discovered (Muro et al. 2003), endocytosis in non-phagocytic cells can generally be divided into two main groups: dynamin-dependent and dynamin-independent pathways. Dynamin-dependent pathways include clathrin- and caveolar-dependent endocytosis and share a reliance upon the GTPase dynamin to coordinate vesicle fission from the plasma membrane during uptake (McNiven 2005). Dynamin-independent pathways include macropinocytosis and dynamin-independent raft-mediated endocytosis (referred to as lipid raft-mediated endocytosis henceforth). Macropinocytosis is a form of endocytosis in which nonspecific uptake of extracellular fluid and membranes is coordinated by actin rich protrusions at cell surfaces (Swanson 2008). The resulting vacuoles (macropinosomes) can be 10 μm in diameter (El-Sayed and Harashima 2013) and have been observed to facilitate the uptake of bacterial cell wall components (Loh, Gao, and Tuomanen 2017), viruses (Mercer and Helenius 2009), necrotic cells (Hoffmann, deCathelineau, et al. 2001), and bacteria (Garcia-Perez et al. 2012; Baltierra-Uribe et al. 2014). There are numerous mechanisms of dynamin-independent lipid raft-mediated endocytosis, but they can generally be grouped into flotillin-dependent endocytosis and GTPase-dependent endocytosis. Flotillin-dependent endocytosis is characterized by uptake of vesicles enriched in flotillin-1 and flotillin-2; however, there is a limited understanding of how flotillins function in endothelial cells (Fork et al. 2014). The mechanisms for GTPase-dependent endocytosis are poorly characterized and include (1) GTPase regulator associated with focal adhesion kinase-1 (GRAF1)-dependent endocytosis and (2) adenosine diphosphate-ribosylation factor 6 (Arf6)-dependent (El-Sayed and Harashima 2013). GRAF1-dependent endocytosis coordinates the uptake of glycosylphosphatidylinositol-anchored protein (GPI-APs) to late endosomal compartment; the process is dependent on Cdc42-mediated actin polymerization and sensitive to cholesterol depletion (El-Sayed and Harashima 2013). However, this pathway can also be affected by the inhibitor amiloride via off-target effects on Cdc42 (Nonnenmacher and Weber 2011). No selective inhibitors exist for disruption of GRAF1-dependent endocytosis, thus siRNA is currently the only tool available to selectively disrupt trafficking via this pathway (El-Sayed and Harashima 2013). The Arf6 endocytosis pathway is proposed to be a raft-mediated endocytic pathway (El-Sayed and

Harashima 2013), but this has not been definitively determined. This pathway facilitates uptake of GPI-APs into actin-coated endocytic vesicles. Cargo includes adhesion molecules such as adherens junction proteins and integrins (Schweitzer, Sedgwick, and D'Souza-Schorey 2011). However, Arf6 is also involved in clathrin-mediated endocytosis, and clathrin knock-down studies have revealed that these two pathways are interconnected (Lau and Chou 2008). Of relevance to the current investigations, for each of these raft-dependent pathways there are conflicting reports as to whether they are truly dynamin-independent processes (El-Sayed and Harashima 2013). For example, different investigations have demonstrated the occurrence of dynamin-dependent and dynamin-independent flotillin-mediated endocytosis based on the use of the dynamin RNA interference (Vercauteren et al. 2011) and GTPase-null dynamin mutants (Glebov et al. 2006), respectively. Taken together, these investigations suggest that there may be multiple mechanisms of flotillin-mediated endocytosis that incorporate differential uses of dynamin. Overlap and crosstalk between different endocytosis pathways is likely to exist, which would be confounded by an inhibitor, mutant, or silencing based approach to delineating the pathways. Therefore, it is important to acknowledge that classification of endocytosis pathways based on their dependency of a specific protein can be misleading.

It is unlikely that *T. pallidum* utilizes a clathrin- or caveolar-mediated route of endocytosis, as Dynamin inhibition did not affect *T. pallidum* endothelial traversal. However, results from the two independent experiments were highly variable, which could be attributed to the off-target effects of this inhibitor. In addition to disrupting the GTPase activity of dynamin, Dynasore is also known to interfere with actin dynamics (Gu et al. 2010) and disrupt the organization of lipid rafts (Preta et al. 2015), which could inhibit dynamin-independent pathways including macropinocytosis and lipid raft-mediated endocytosis. Interference with normal functioning of actin impedes membrane ruffling (Park et al. 2013) which is required for initiation of macropinocytosis (Mercer and Helenius 2009). Importantly, these off-target effects occur in a dynamin-independent manner which is proposed to transpire via Dynasore-mediated disruption of cellular cholesterol affecting both lipid rafts and actin dynamics (Preta, Cronin, and Sheldon 2015). A non-significant trend toward decreased *T. pallidum* traversal was observed for the macropinocytosis inhibitor amiloride, which can also have off-target effects on actin (Lagana et al. 2000). A

statistically significant decrease in *T. pallidum* traversal was observed in the presence of filipin, which can inhibit dynamin-dependent caveolae-mediated endocytosis or dynamin-independent lipid raft-mediated endocytosis. However, filipin can be toxic at higher concentrations, and there are conflicting accounts as to whether filipin can also inhibit clathrin-mediated endocytosis (Rodal et al. 1999). While the off-target effects of endocytosis inhibitors make it challenging to accurately interpret the results, by considering the unintended effects of inhibitors, one can hypothesize which pathway(s) may be engaged by *T. pallidum.*

The results presented herein suggest that *T. pallidum* may utilize a lipid raft-dependent mechanism of endocytosis. However, it is important to note that *T. pallidum* has host-like cholesterol-rich membranes (Matthews, Yang, and Jenkin 1979). Since the mode of action for filipin is to bind cholesterol is it possible that there may have been unintended effects on the spirochetes that confounded the results. Lipid rafts are membrane microdomains that are enriched in cholesterol, function as cell signaling platforms and can facilitate endocytosis. While the existence and precise composition of lipid rafts is controversial (Munro 2003), flotillins have long been regarded as markers of these plasma membrane microdomains (Meister and Tikkanen 2014). Given that GRAF1-dependent endocytosis can be inhibited by amiloride (Nonnenmacher and Weber 2011) and Arf6-dependent endocytosis is not truly clathrin-independent (Lau and Chou 2008), it is unlikely that either of these raft-mediated endocytotic pathways are utilized by *T. pallidum.* With the current knowledge, it is impossible to definitively determine a transcellular traversal mechanism for *T. pallidum*, however based upon our findings the most probable mechanism for *T. pallidum* transendothelial migration is a flotillin-dependent pathway. Of relevance to this predicted traversal route, in Chapter 2 of this dissertation LamR and stomatin were identified as putative endothelial cell receptors for Tp0751; intriguingly, these proteins are both predicted to reside within lipid rafts. Furthermore, flotillin is known to co-localize with stomatin in lipid rafts of epithelial cell membranes (Snyers, Umlauf, and Prohaska 1999; Snyers, Thines-Sempoux, and Prohaska 1997). Taken together, these findings suggest that Tp0751 could mediate interactions with the endothelial receptors stomatin and LamR in lipid rafts to initiate transcellular traversal via flotillin-mediated endocytosis. Further investigation will be required to explore this possibility.

Although the prospect of a transcellular traversal mechanism for *T. pallidum* is exciting, it is important to consider the limitations of the experiment. Of significance to the findings presented in this chapter, *T. pallidum* has a unique, host-like lipid composition that contains 26.5% cholesterol (Matthews, Yang, and Jenkin 1979). Therefore, it is possible that filipin had unintended effects on *T. pallidum*. This presents a technical challenge for exploring lipid raft-mediated endocytosis, as the mechanism of action for inhibitors of lipid raft-dependent endocytosis target cholesterol via depletion or binding (El-Sayed and Harashima 2013). Future experiments should expand on the current findings, using varying doses of endocytosis inhibitors to further explore whether these pathways are utilized by *T. pallidum.* More in-depth investigations into endocytic pathways should employ live confocal microscopy to visualize interactions of *T. pallidum* with endothelial cells to look for treponemal endocytosis, localization to cholesterol-rich membrane microdomains on endothelial cells, and the dynamics of endothelial adherens junctions.

Chapter 4: Exploring Tp0751-induced alterations of signaling pathways in human endothelial cells

Contributions: Metabolic labeling, cell treatment and lysis, and data analysis were performed by KL. Phosphopeptide enrichment and LC-MS/MS was performed by Kyung-Mee Moon (Leonard Foster Laboratory, Department of Biochemistry, University of British Columbia)

4.1 Introduction

Protein phosphorylation is a dynamic and reversible modification that controls diverse processes at both cellular and molecular scales, including metabolism, growth, and apoptosis, as well as protein folding, localization, and degradation (Hunter 2000; Ubersax and Ferrell 2007). While phosphorylation can occur on a variety of amino acids, O-phosphates (serine, threonine, and tyrosine) are the most extensively studied. In mammalian cells, the majority of phosphorylation events occur on serine residues (90%) rather than threonine (9-10%) or tyrosine (0.05-1%) (Hunter and Sefton 1980; Olsen et al. 2006). Phosphorylation of these amino acids is coordinated by kinases that catalyze the transfer of a phosphate group from adenosine triphosphate (ATP) to create a phosphoester bond, while phosphatases hydrolyze the phosphoester bonds, removing the post-translational modification. The interplay of these enzymes through interconnected catalytic cascades permits tight control of cellular processes that underpins complex and often global signaling networks (Ardito et al. 2017). Importantly, phosphorylation is a sub-stoichiometric process, so not all copies of a phosphorylation site or protein are necessarily phosphorylated by the same trigger or modified at the same time (Eyrich, Sickmann, and Zahedi 2011). Aberrant signaling can contribute to cancer progression (Blume-Jensen and Hunter 2001; Clevenger 2004), diabetes, chronic inflammatory disease and neurodegenerative diseases, and host signaling cascades can also be exploited by pathogens during infection to promote invasion and persistence in the host (Krachler, Woolery, and Orth 2011). Investigating pathogen modulation of host signaling can provide a more in-depth understanding of host-pathogen interactions. Traditional methods for identifying signaling pathways manipulated by pathogenic bacteria utilize a reductionist approach, which includes the use of kinase and phosphatase inhibitors to target nodes and cascades

in characterized signaling networks to disrupt bacterial invasion (Krachler, Woolery, and Orth 2011)

Within the *T. pallidum* field, proteomics has been applied to identify receptors for *T. pallidum* adhesins (Houston et al. 2014), discover the identity of proteins that are reactive with patient serum (McGill et al. 2010), identify diagnostic markers for *T. pallidum* (Osbak et al. 2018) and investigate the *T. pallidum* proteome after *in vivo* propagation in rabbits (Osbak et al. 2016). However, mass spectrometry has never been harnessed to dissect host-pathogen interactions of *T. pallidum.* There are a myriad of clinical manifestations throughout the natural course of *T. pallidum* infection, contrasted by long periods of asymptomatic latency. The widespread systemic dissemination of *T. pallidum* allows for the seeding of treponemes into diverse secondary infection sites (Mahoney 1934; Stokes 1944; Cumberland MC 1949; Raiziss GW 1937). Within these tissues lies a poorly understood interplay between immune activation and immune evasion that facilitates inflammation or latency (Lafond and Lukehart 2006). Little is known about how *T. pallidum* coordinates this widespread dissemination, particularly during endothelial barrier traversal. Modulation of signaling networks to induce endothelial responses that facilitate bacterial invasion is a conserved process used for transendothelial migration by other invasive pathogens. Endothelial responses that are controlled by these signaling cascades include junctional changes, cytoskeletal reorganization and endocytosis (Lemichez et al. 2010). Mapping out the signaling pathways that are modified by *T. pallidum* and its adhesins could provide new insights into the mechanisms of transendothelial migration that will complement and guide *in vitro* investigations of barrier traversal. Furthermore, such investigations could uncover therapeutic targets that may prevent treponemal dissemination.

This chapter focusses upon workflow development for quantitative phosphoproteome analysis of endothelial cells utilizing stable isotope labeling by amino acids in cell culture (SILAC) with the end goal of exploring endothelial signaling networks that are modified by the *T. pallidum* adhesin, Tp0751. Metabolically labeled cells are subject to different treatments, followed by lysis, sample pooling and tryptic digestions. The resulting mixture is enriched for phosphorylated peptides and subject to liquid chromatography-tandem mass spectrometry (LC-MS/MS) to determine relative abundance

of phosphorylated peptides and the identity of the corresponding proteins (Figure 25). In this metabolic labeling approach, endothelial cells are grown in modified culture media supplemented with normal arginine and lysine ('light' R_0K_0) or non-radioactive, isotopically labeled forms of arginine and lysine ('medium' R_4K_6 or 'heavy' $R_{10}K_8$), necessitating isotope incorporation into cellular proteins. These isotopic labels produce predictable mass shifts in peptides. Cells must be grown in SILAC medium for a minimum of five cell divisions to ensure sufficient label incorporation (Hoedt, Zhang, and Neubert 2014).The availability of three different pairings of arginine and lysine isotopes allows for the implementation of a triplex experiment whereby Tp0751-treated cells can be compared to two controls: untreated or negative control recombinant protein-treated (Figure 25A). Since tryptic digestion occurs at sites that are carboxy-terminal to lysine or arginine residues, including isotopes of both arginine and lysine ensures that the majority of peptides will contain an isotopically labeled residue, improving the coverage and quantitative data.

The main advantage of SILAC is the early pooling of samples. Following cell treatment and prior to further processing, samples are pooled at a 1:1:1 ratio, based on the total amount of protein; this limits the variability that can arise from parallel sample handing. When pooled samples are subject to LC-MS/MS, the relative abundance of proteins is determined from the signal intensities of the same peptides derived from differentially treated samples, as indicated by a predictable shift in mass conferred by the isotopic label. Peptides that have the same sequences but unique isotopic labels are chemically identical and therefore co-elute from the reversed-phase HPLC (high performance liquid chromatography) column and enter the mass spectrometer at the same time. This allows for relative quantification based on peak height in the same MS/MS scan and determination of the sample origin based on a characteristic mass shift from the isotope label (Dephoure et al. 2013). From this data acquisition, an isotope pairing is generated for each peptide (heavy/light, medium/light, heavy/medium) that informs relative abundance of the corresponding protein. Sufficient coverage of the proteome is critical, as proper data interpretation requires the identification of at least one peptide from each of the light, medium and heavy samples.

The SILAC methodology can be adapted for evaluation of the phosphoproteome through relative quantitation of phosphorylated proteins as well as site-specific identification of phosphorylated residues. This technique provides information about the role of intracellular signaling networks in host-pathogen interactions. Although protein phosphorylation is thought to be the most abundant post-translational modification in mammalian cells, phosphorylation is a sub-stoichiometric process; thus, phosphopeptide enrichment is required to ensure that non-modified residues do not drown out the signal of phosphorylated peptides (Francavilla et al. 2014). To accomplish this, metal oxide affinity chromatography (MOAC) with titanium dioxide (TiO_2) was employed following tryptic digestion to enrich for phosphopeptides (Figure 25B). The basis of this enrichment approach relies upon the selective affinity of TiO_2 for phosphopeptides under acidic conditions; subsequent elution from TiO_2 can be achieved with an alkaline buffer (Thingholm and Larsen 2016).

In this chapter, an optimized method for the metabolic labeling of human endothelial cells by SILAC is presented. Different lysis conditions are explored to establish a protocol that will facilitate improved coverage of the phosphoproteome. Finally, a pipeline is developed for the analysis of quantitative phosphoproteomic data based on a data set yielded from a small-scale experiment. The results presented herein provide the framework for future large-scale experiments to be conducted to explore the signaling dynamics of *T. pallidum* adhesins and suggest a compelling mechanism of host signaling exploitation by *T. pallidum.*

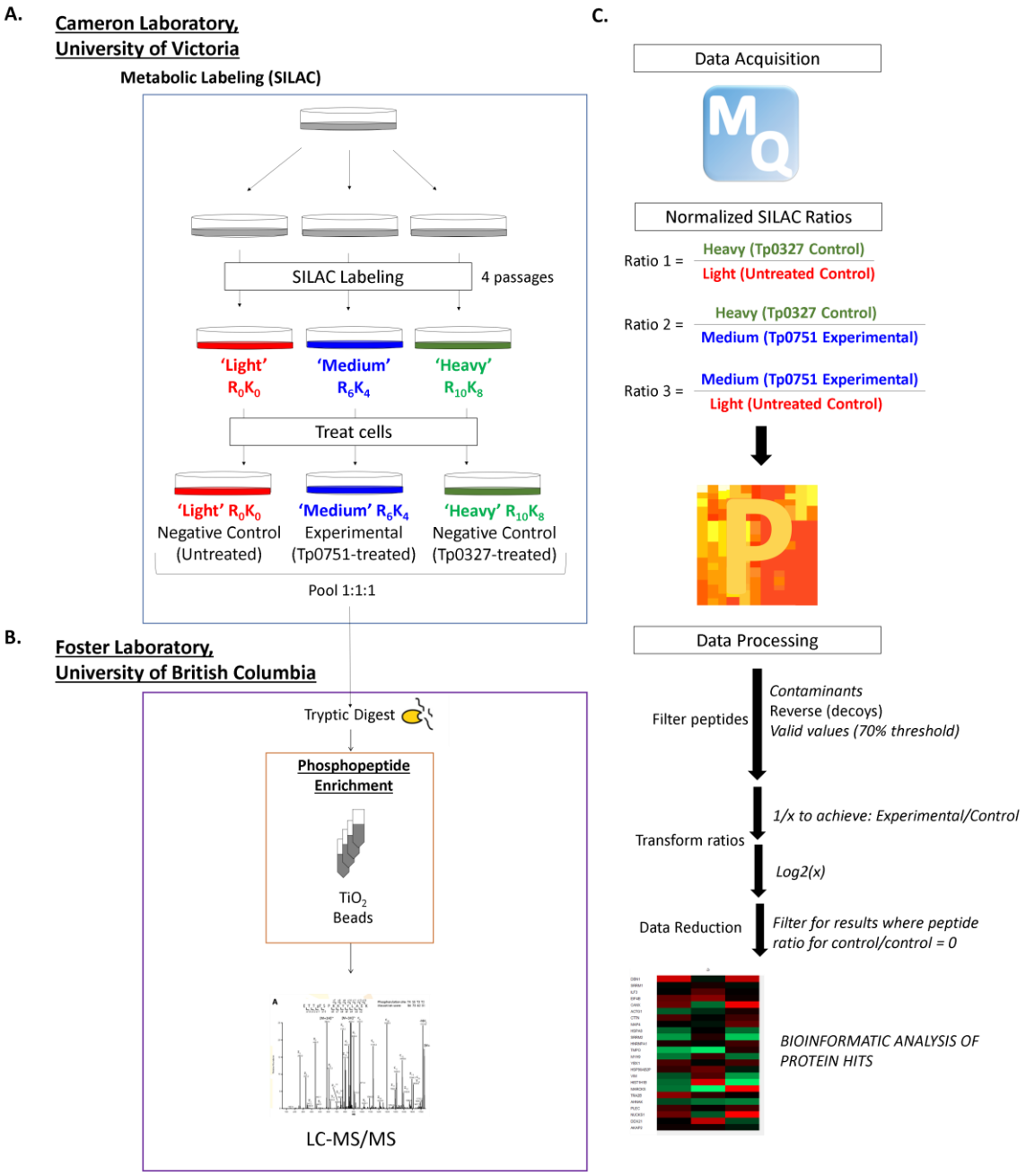

Figure 25: Schematic for stable isotope labeling by amino acids in cell culture (SILAC) based phosphoproteome analysis of endothelial cells treated with Tp0751. **(A)** Endothelial cells were metabolically labeled by passaging cells from normal growth media into media containing isotopes of arginine, denoted as light (R_0K_0), medium (R_6K_4), or heavy ($R_{10}K_8$). Cells were maintained in SILAC media for a minimum of three passages. Metabolically labeled cells were then treated for fifteen minutes at 37°C with Tp0751 (experimental treatment), negative control recombinant treponemal protein Tp0327, or left untreated.

Following incubation, cells were lysed, quantified and pooled at a 1:1:1 ratio. Metabolic labeling, cell treatment, and sample lysis, quantification and pooling were performed in the Cameron Lab at the University of Victoria. **(B)** In the Foster Lab at the University of British Columbia, pooled samples were subject to tryptic digestion followed by phosphopeptide enrichment using titanium dioxide (TiO_2) beads. Phosphorylated peptides were then subject to liquid chromatography tandem mass-spectrometry (LC-MS/MS). **(C)** Using Maxquant, SILAC ratios were generated for proteins with two or more peptide partners for each combination of labels (Heavy/Light, Medium/Light, and Heavy/Medium) and ratios were normalized to the median ratio of all peptide pairs for the protein group of a given label combination. Peptides were filtered for a false discovery rate (FDR) of 1% in MaxQuant. Data processing was performed in Perseus. Peptides were filtered to remove contaminants and false positives (reverse decoy peptides). The threshold for valid values was set at 70%, ratios were eliminated unless ≥2 unique peptides were identified in each sample (light, medium and heavy). Normalized SILAC ratios were transformed so that all ratios were experimental (Tp0751)/control(Tp0327 or Untreated) or control(Tp0327)/control(Untreated). Ratios were then log2(x) transformed to determine fold change between label partners. Data was visualized on a heatmap and filtered further to only include results where the log2-transformed control ratio (Tp0327/Untreated) equaled 0 ± 0.05, indicating that the negative controls did not have any effect on endothelial cell phosphorylation. Data was then visualized on heat maps and bioinformatic gene ontology analysis was performed on proteins that exhibited differential phosphorylation in Tp0751-treated endothelial cells.

4.2 Materials & Methods

Endothelial cell culture and metabolic labeling

Human umbilical vein endothelial cells (HUVECs; Lonza, Mississauga, ON) were cultured in endothelial growth medium-2 bulletkit (EGM-2; Lonza) and grown at 37°C in an atmosphere of 5% CO_2. Cerebral brain endothelial cells (hCMEC/d3; Millipore, Etobicoke, ON) were grown in EndoGro-MV (Millipore) supplemented with basic fibroblast growth factor (Millipore) at 37°C in an atmosphere of 5% CO_2. For HUVEC SILAC labeling, cells were split from normal growth media into arginine- and lysine-free Dulbecco's modified

Eagle's medium (DMEM, ThermoFisher, Burnaby, BC or Caisson Laboratories, Smithfield, UT) and supplemented with EGM-2 growth factors including hydrocortisone, human basic fibroblast growth factor, vascular endothelial growth factor, ascorbic acid, human epidermal growth factor, and heparin. For hCMEC/d3 SILAC labeling, cells were split from normal growth media into arginine- and lysine-free Dulbecco's modified Eagle's medium (DMEM; Caisson Laboratories Inc, Smithfield, UT) with the supplements from EndoGro-MV added; these included EndoGRO-LS supplement (0.2%), recombinant human epidermal growth factor (5 ng/mL rhEGF), L-Glutamine (10 mM), hyrdrocortisone hemisuccinate (1.0 μg/mL), heparin sulfate (0.75 U/mL), and ascorbic acid (5%). Medium for SILAC labeling of HUVECs and hCMEC/d3 was also supplemented with 8-15% (v/v) dialyzed fetal bovine serum (FBS; Gibco, Gaithersburg, MD or ThermoFisher Scientific) and L-lysine (36.5 mg/liter) and L-arginine (21 mg/liter) for light-labeled cells (Sigma-Aldrich, Oakville, ON), D_4-lysine (37.5 mg/liter) and $^{13}C_6$-arginine (21.75 mg/liter) for medium-labeled cells, and $^{13}C_6{}^{15}N_2$-lysine (38.5 mg/liter) and $^{13}C_6{}^{15}N_4$-arginine (22.25 mg/liter) for heavy-labeled cells (Cambridge Isotope Laboratories, Tewksbury, MA). Cells were maintained in the labelling medium for at least three passages and then seeded into T25 flasks at 6500 cells/cm^2 and grown to confluence for treatment with recombinant treponemal proteins.

Recombinant Protein Expression and Purification

Treponemal proteins Tp0327 [I23-S172] and Tp0751 [V99-P237] were cloned as previously described (Parker et al. 2016; Houston et al. 2014) and purified from *Escherichia coli* BL21-A1 or BL21*DE3, respectively, and subject to nickel affinity chromatography with HisTrap FF columns (GE Healthcare, Mississauga, ON). Proteins were further purified with size exclusion and cation exchange chromatography (HiLoad 16/60 Superdex 75; GE Healthcare, GE Healthcare) on an AKTA Prime Plus FPLC system (GE Healthcare) in a final gel filtration buffer of 20 mM HEPES, 150 mM NaCl, 1% glycerol, pH 7.0.

Endothelial Recombinant Protein Treatment

Metabolically labeled endothelial cells at 95-100% confluence were washed with room temperature (RT) HEPES buffered saline solution (HBSS; Lonza) and then treated with media (mock-treatment) or with 25 μM of the recombinant treponemal proteins – Tp0751 [V99-P237] or the negative control Tp0327 [I23-S172] and incubated for 15 minutes at 37°C, 5% CO_2. To calculate the concentration of the protein constructs, UV absorbance at 280 nm was measured prior to each experiment using a spectrophotometer. Molar concentrations of proteins were calculated based on the molecular weight of each recombinant protein construct in a defined volume to ensure the addition of equimolar amounts of protein.

Endothelial cell lysis

Following endothelial co-incubations with recombinant proteins or controls, cells were washed three times with RT HBSS and lysed. In the first SILAC experiment, cells were lysed by adding 4% SDS in 100 mM Tris (pH 8.8) to the flask ("in flask" lysis) and incubating on ice for 5 minutes. Lysates were then heated to 60°C for 30 minutes and protein concentrations were determined for each individual lysate sample using a standard bicinchoninic acid assay (BCA assay; ThermoFisher Scientific) and 100 μg per sample from paired samples (light-, med-, heavy-labeled) were combined for a final mass of 300 μg. Pooled samples were then acetone precipitated. In the second SILAC experiment, cells were lysed in flask with 1% (w/v) sodium deoxycholate (DOC) in 50 mM NH_4HCO_3 (pH 7.8) with a protease and phosphatase inhibitor cocktail (Abcam, Toronto, ON). In parallel, the third set of SILAC samples was lysed in flask in the absence of phosphatase inhibitors in 1% (w/v) sodium deoxycholate (DOC) in 50 mM NH_4HCO_3 (pH 7.8) and immediately heated to 99°C for five minutes. The protein concentration of each lysate was determined using a BCA assay (ThermoFisher Scientific) and 100 μg per sample from paired samples (light-, med-, heavy-labeled) were pooled for a final mass of 300 μg. For lysis optimization, monolayers of hCMEC/d3 were subject to in flask lysis (40 μl/cm^2) or lysis of pelleted cells that had been lifted by mechanical cell scraping or enzymatic trypsin removal (Lonza; 0.05%, 120 μl/cm^2) and centrifuged at 220 x g for five minutes at RT. Lysis efficiency was compared between in flask lysis versus lysis of cell pellets by determining the total protein

yield from each method with a BCA assay. For these optimization experiments, cells were lysed with 1% DOC/NH_4HCO_3 (50 mM/pH 7.8).

TiO_2 Enrichment of Phosphopeptides

Phosphopeptide enrichment was adapted from previous methods (Sugiyama et al. 2007; Kyono et al. 2008; Rappsilber, Mann, and Ishihama 2007). Construction of TiO_2 tips was accomplished by packing 0.5 mg TiO_2 beads (Titansphere, GL Science, Peterborough, ON) per 200 µl tip (Pack C8, 3M Empore, Charlotte, NC). Proteins were reduced and alkylated as previously described (Foster, De Hoog, and Mann 2003) and digested with a 1:50 ratio of trypsin (5µg; Promega) to protein at 37°C overnight. Peptides were purified by solid phase extraction and cleaned with C18 STAGE (Stop And Go Extraction) tips (3M Empore) and eluted with 0.1% trifluoroacetic acid (TFA) (ThermoFisher Scientific) in 80% acetonitrile (ACN) (ThermoFisher Scientific) as previously described (Ishihama et al. 2002). Peptides were then diluted with 0.1% TFA in 80% ACN to a concentration of 1 µg/µl, and an equal volume of DL-lactic acid solution (25% lactic acid, 60% ACN, 0.075% TFA; ThermoFisher Scientific) to a final concentration of 0.5 µg/µl. TiO_2 tips were washed with 50 µl of 0.1% TFA in 80% ACN followed by 50 µl of DL-lactic acid solution by centrifuging for 1000 x g for 1 minute for each wash. Peptide samples were then loaded into the TiO_2 tips (150 µg total pooled lysate per tip) and centrifuged for 800-1000 x g for 3 minutes, this was repeated until all of the sample was loaded. TiO_2 tips were then washed with 50 µl of DL-lactic acid solution followed by 50 µl of 0.1% TFA in 5% ACN to remove non-phosphorylated peptides. Phophopeptides were then eluted into fresh tubes with two consecutive elutions first with 5% NH_4OH (ThermoFisher Scientific), then with 0.5% pyrrolidine (Sigma Aldrich). Each elution was performed by centrifuging at 1000 x g for 2 minutes. Samples were then acidified and diluted with TFA to pH <2.5. Acidified samples were purified by solid phase extraction on C18 STAGE tips as previously described and resuspended for LC-MS/MS.

Liquid Chromatography Tandem Mass-Spectrometry (LC-MS/MS)

Purified phosphopeptide samples were analyzed by a quadropole-time of flight (QTOF) mass spectrometer (Impact II; Bruker, Billerica, MA) coupled to an Easy nano LC 1000

HPLC (ThermoFisher Scientific) with an analytical column that was 40-50 cm long with a 75 µm inner diameter fused silica with an integrated spray tip pulled with P-2000 laser puller (Sutter Instruments) packed with 1.9 µm diameter Reprosil-Pur C-18-AQ beads (Maisch, Ammerbuch, Germany) operated at 50°C with in-house built column heater. As previously described (Gibbs et al. 2017) standard 90-min peptide separation was performed with Buffer A (0.1 % aqueous formic acid) and Buffer B (0.1% formic acid, 80% [v/v] ACN in water), where the column wash washed with 100% Buffer B, then re-equilibrated with Buffer A. The QTOF Impact II was set to acquire in a data-dependent auto-MS/MS mode with inactive focus fragmenting the 20 most abundant ions (one at the time at an 18-Hz rate) after each full-range scan from *m/z*200 to *m/z* 2,000 at 5 Hz rate. The isolation window for MS/MS was 2–3 depending on the parent ion mass to charge ratio, and the collision energy ranged from 23 to 65 eV depending on ion mass and charge. Parent ions were then excluded from MS/MS for the next 0.4 min and reconsidered if their intensity increased more than five times. Singly charged ions were excluded from fragmentation.

Generation of Quantitative Phosphoproteome Data

Maxquant (version 1.6.1.0) was used to analyze raw mass spectrometric data files from LC-MS/MS. Human sequences were retrieved from Uniprot (June 13th, 2012; 86,749 entries plus common contaminants). Default setting were used unless stated otherwise, including the following parameters: fixed modification included carbamidomethyl, variable modifications included oxidation of methionine, acetyl (protein N-terminus), phosphorylation of serine, threonine, and tyrosine residues. The false discovery rate (FDR) was set at 0.01 for peptides proteins, and sites and the minimum peptide length was set at 7 amino acids.

Data analysis

Normalized median peptide SILAC ratios were imported into Perseus (version 1.6.5.0) for analysis. For each replicate, data was filtered for contaminants and reverse hits (decoys) and then filtered for valid values (threshold set at 70%). Data was transformed (1/x, where appropriate) to ensure that all ratios were presented as experimental/control. All data was log2(x) transformed to determine fold changes in treated samples. Data was filtered to

remove proteins where the normalized peptide ratio between control samples (Tp0327/Untreated) was within the threshold of log2 fold change 0 ± 0.05. Data was then visualized on heat maps and bioinformatic gene ontology analysis was performed on proteins that exhibited differential phosphorylation in Tp0751-treated endothelial cells.

4.3 Results

Optimizing the metabolic labeling of human endothelial cells

To investigate the phosphoproteome of Tp0751-treated endothelial cells, the growth of cultured endothelial cells in media containing 'light' arginine and lysine (K_0R_0; L-lysine and L-arginine) or isotopically labelled arginine and lysine for 'medium' (K_4R_6; D_4-lysine and $^{13}C_6$-arginine) and 'heavy' (K_8R_{10}; $^{13}C_6{}^{15}N_2$-lysine and $^{13}C_6{}^{15}N_4$-arginine) labels was optimized. The investigations of Tp0751-mediated functional changes in endothelial cells explored in Chapter 3 were performed using primary human umbilical vein endothelial cells (HUVECs). As a result, metabolic labeling was first attempted using this primary cell line. Endothelial cells were split from normal growth medium into arginine- and lysine-free Dulbecco's modified eagle medium (DMEM) supplemented with light, medium, or heavy arginine and lysine, as well as endothelial growth factors and dialyzed fetal bovine serum (dFBS) (Figure 25A). Limited growth of HUVECs was observed in SILAC medium supplemented with 8% dFBS or 10% dFBS (Figure 26, Table 6). Cells grown in SILAC media with K_4R_6 (medium arginine and lysine) exhibited the most stunted growth (Figure 26). For cells grown in K_4R_6 SILAC media supplemented with 8% dFBS, no expansion of the endothelial population was observed after day 6 where confluence reached a plateau at 30%. Intriguingly, in this growth trial, cells grown in SILAC media with light (K_0R_0) or heavy (K_8R_{10}) arginine and lysine grew to 70-80% confluence within 15 days after initial seeding into SILAC media (Figure 26A). As dFBS is an undefined component of the media recipe that can have a significant impact of growth of cultured cells, the concentration of dFBS was increased to 10% in order to promote HUVEC growth in SILAC medium. However, a similar trend was observed in which HUVECs grown in K_4R_6 (medium) SILAC media plateaued after six days and by day 14 most of the cells had lifted off. Conversely, HUVECs grown in with K_0R_0 (light) or K_8R_{10} (heavy) medium expanded to 80%

confluence by day 14 (Figure 26B). To ensure the limited growth could not be attributed to the batch of dFBS and the basal DMEM, dFBS and DMEM was acquired that had been validated to support cell growth at a collaborator's laboratory at the University of British Columbia; however, there was still no observed increase in HUVEC confluence in the SILAC media (Figure 26C).

Table 6 Optimizing growth conditions for the metabolic labeling of endothelial cells with stable isotopes of arginine and lysine.

Cell Line, Type	**DMEM Source**	**dFBS**		**Initial Seeding Density**	**Growth?**
		Source	*Conc (v/v%)*		
HUVEC, Primary	Thermo Fisher	Thermo Fisher	8%	6000 cells/cm^2	No
HUVEC, Primary	Thermo Fisher	Thermo Fisher	10%	6000 cells/cm^2	No
HUVEC, Primary	Caisson Labs*	Gibco*	10%	6000 cells/cm^2	No
hCMEC/d3, Immortalized	Caisson Labs	Gibco*	12%	6000 cells/cm^2	Yes – 3 passages
hCMEC/d3, Immortalized	Caisson Labs	Gibco*	12%	6000 cells/cm^2	No
hCMEC/d3, Immortalized	Caisson Labs	Gibco*	15%	6500 cells/cm^2	Yes – 4 passages

*previously tested in the Foster Laboratory, University of British Columbia to ensure reagent LOT numbers support growth of cultured cells

Because cell lines of primary origin often exhibit slower growth rates and more stringent growth requirements, an immortalized cerebral microvascular endothelial cell line hCMEC/d3 was tested for ability to grow in SILAC media. Results presented in Chapter 2 demonstrate that recombinant Tp0751 and live *T. pallidum* both adhere to hCMEC/d3 monolayers (Figure 5C; Figure 14). Immortalized endothelial cells were successfully grown in DMEM supplemented with light, medium, or heavy arginine and lysine and 12% (v/v) dFBS through three passages (Figure 27A, Table 6), allowing for sufficient label incorporation to proceed with sample processing for phosphoproteome

analysis (Figure 25). However, this growth was not replicated in a second attempt, where hCMEC/d3 confluence in light, medium, and heavy SILAC media began to decline six days after seeding into the media (Figure 27B). Growth of hCMEC/d3 in SILAC media was recovered by increasing the dFBS to 15% (v/v) and altering initial seeding density to 6500 cells/cm^2 (Figure 27C, Table 6).

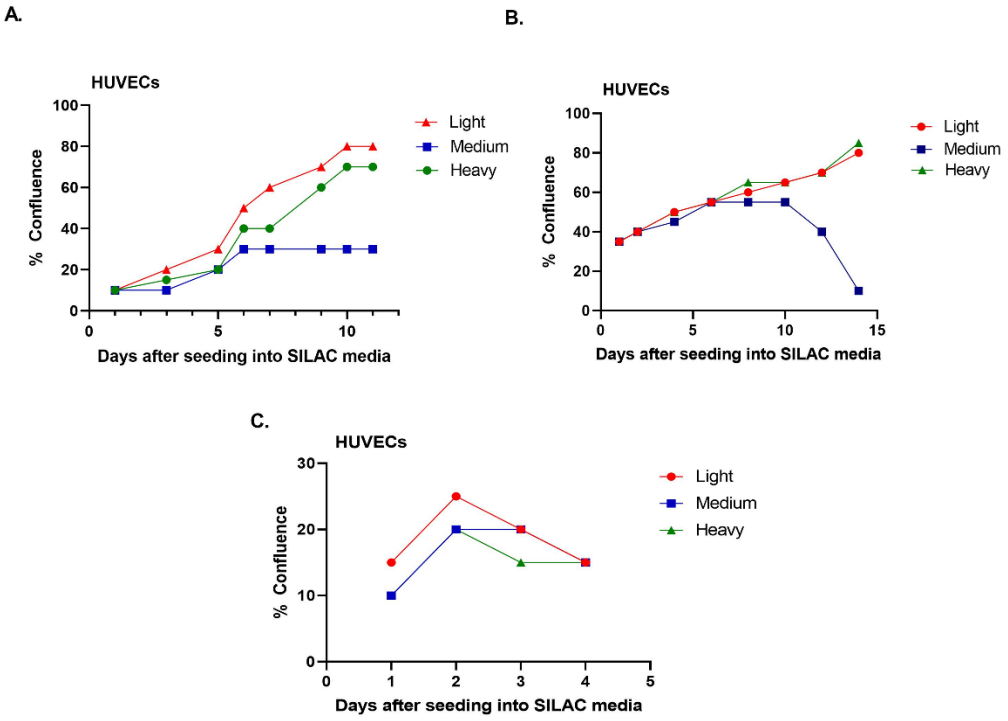

Figure 26: Growth of primary macrovascular HUVECs in SILAC media. Cells were split from normal culture medium into DMEM (arginine- and lysine-free) supplemented with endothelial growth factors, dialyzed FBS and normal arginine and lysine (K_0R_0), medium arginine and lysine (K_4R_6; $^{13}C_6$-arginine and D_4-lysine) or heavy arginine and lysine (K_8R_{10};$^{13}C_6{}^{15}N_4$-arginine and $^{13}C_6{}^{15}N_2$-lysine). Percent confluence of HUVECs in T25 flasks was estimated by inverted tissue microscopy after initial seeding into **(A)** SILAC DMEM media (ThermoFisher) supplemented with 8% dFBS (ThermoFisher) and light (red), medium (blue) or heavy (green) arginine and lysine at 6000 cells/cm^2 **(B)** SILAC DMEM media (ThermoFisher) supplemented with 10% dFBS (ThermoFisher) and light (red), medium (blue) or heavy (green) arginine and lysine at 6000 cells/cm^2 or **(C)** SILAC DMEM media (Caisson Laboratories) supplemented with 12% dFBS (Gibco, validated LOT#) at 6000 cells/cm^2. Dialyzed FBS had been validated to support the growth of *in*

vitro cells by collaborators at the University of British Columbia (Foster laboratory).

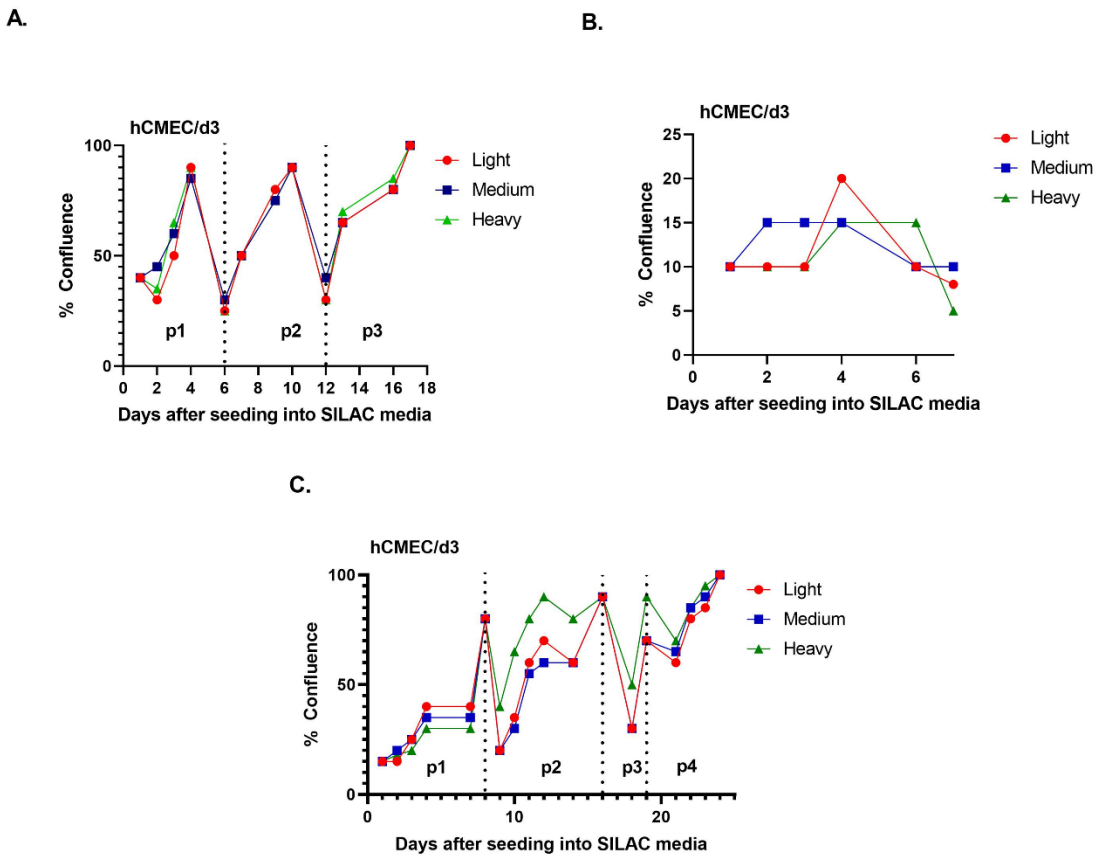

Figure 27: Growth of immortalized cerebral brain endothelial cells hCMEC/d3 in SILAC media.Cells were passaged from normal culture medium into DMEM (arginine- and lysine-free) supplemented with endothelial growth factors, dialyzed FBS and either normal arginine and lysine (K_0R_0), medium arginine and lysine (K_4R_6; $^{13}C_6$-arginine and D_4-lysine) or heavy arginine and lysine (K_8R_{10};$^{13}C_6{}^{15}N_4$-arginine and $^{13}C_6{}^{15}N_2$-lysine). Percent confluence of hCMEC/d3 in T25 flasks was estimated by inverted tissue microscopy after initial seeding into **(A)** SILAC DMEM media (Caisson Laboratories) supplemented with 12% dFBS (Gibco, validated LOT#) and light (red), medium (blue) or heavy (green) arginine and lysine at 6000 cells/cm^2, **(B)** SILAC DMEM media (Caisson Laboratories) supplemented with 12% dFBS (Gibco, validated LOT#) and light (red), medium (blue) or heavy (green) arginine and lysine at 6000 cells/cm^2 or **(C)** SILAC DMEM media (Caisson Laboratories) supplemented with 15% dFBS (Gibco, validated LOT#) and light (red), medium (blue) or heavy (green) arginine and lysine at 6500 cells/cm^2.

Optimizing endothelial cell lysis for downstream phosphoproteome analysis

Lysis of hCMEC/d3 cells following metabolic labeling and treatment with recombinant Tp0751 (Figure 25A) was initially performed using 4% sodium dodecyl sulfate (SDS) in 100 mM Tris, following by heating to 60°C to heat denature phosphatases. The samples were then acetone precipitated to remove SDS that would interfere with downstream steps, such as tryptic digestions, and pooled in equal µg amounts (100 µg/sample, 300 µg total). However, data acquisition from these samples resulted in low phosphoproteome coverage with only 262 total peptides identified, resulting in 50 normalized SILAC ratios for each pairing and the identification of 13 different proteins. Filtering for reverse hits (decoys), contaminants, and valid values eliminated all SILAC ratios from the analysis (Table 7). To improve coverage of the phosphoproteome, the methods for phosphatase inactivation and lysis of endothelial cells were optimized. For cell lysis, the total protein yield was compared between cells lysed in 4% SDS/100 mM tris followed by acetone precipitation and cells lysed with 1% (w/v) sodium deoxycholate (DOC) in 50 mM NH_4HCO_3 (pH 7.8). Lysis with 1% DOC resulted in a 10-fold increase in the total protein yield compared to SDS lysis with acetone precipitation (Figure 28A). Different methods of phosphatase inactivation were also tested to compare heat denaturation with addition of phosphatase inhibitors. As expected, no difference in the total protein yield was observed in cells lysed with 1% DOC with phosphatase inhibitor addition versus cells lysed with 1% DOC followed by heating at 99°C to heat denature phosphatases (Figure 28A). Cell lysis was further optimized by exploring lysis of pelleted cells removed from the flask via trypsinization or scraping and direct lysis of cells in the flask. From T25 flasks, a two-fold higher total protein yield was observed from cells lysed using the ‘in flask’ method (Figure 28B).

Table 7 The effect of lysis method and phosphatase inactivation on SILAC outputs.

Cell Line	Lysis Method	Phosphatase Inactivation	# of Peptides	# of Normalized SILAC Ratios[1]	# of Proteins Detected[2]
hCMEC/d3	4%SDS + acetone precipitation	Heat (60°C, 30 minutes)	262	50	0
hCMEC/d3	1% DOC	Heat (99°C, 5 minutes)	310	127	24
hCMEC/d3	1% DOC	Phosphatase Inhibitors	216	62	0

[1]Total count of all normalized SILAC ratios generated from identified peptides
[2]With valid SILAC ratios. Refined for proteins with 2 or more unique peptides in each sample (light, medium, and heavy) where valid value threshold was set at 70% and contaminants and reverse decoy hits were excluded

Improved phosphoproteome coverage with DOC lysis and phosphatase inactivation via heat denaturation

Three independent samples of endothelial cells were metabolically labeled, treated with recombinant Tp0751 or controls, and subject to TiO_2 phosphopeptide enrichment and mass spectrometry. As described in the previous section, the first set of samples yielded low phosphoproteome coverage (Table 7). An optimized method was used to lyse metabolically labeled hCMEC/d3 with DOC, and phosphatase inactivation was accomplished by heat denaturation (99°C) or addition of phosphatase inhibitors. Heat denaturation of phosphatases resulted in improved phosphoproteome coverage, with 310 total peptides identified corresponding to 127 normalized SILAC ratios that represent 89 different proteins. Filtering these results to include proteins with valid SILAC ratios for all three pairings (heavy/light, medium/light, and heavy/medium) resulted in identification of 24 unique proteins (Table 7). For accurate quantitation, there must be two or more unique peptide pairings for each protein to generate a ratio that establishes quantitative differences among samples. The addition of phosphatase inhibitors instead of heat inactivation yielded 216 total peptides and 62 normalized SILAC ratios that represented 21 different proteins; however, filtering the results for valid ratios resulted in zero proteins detected (Table 7).

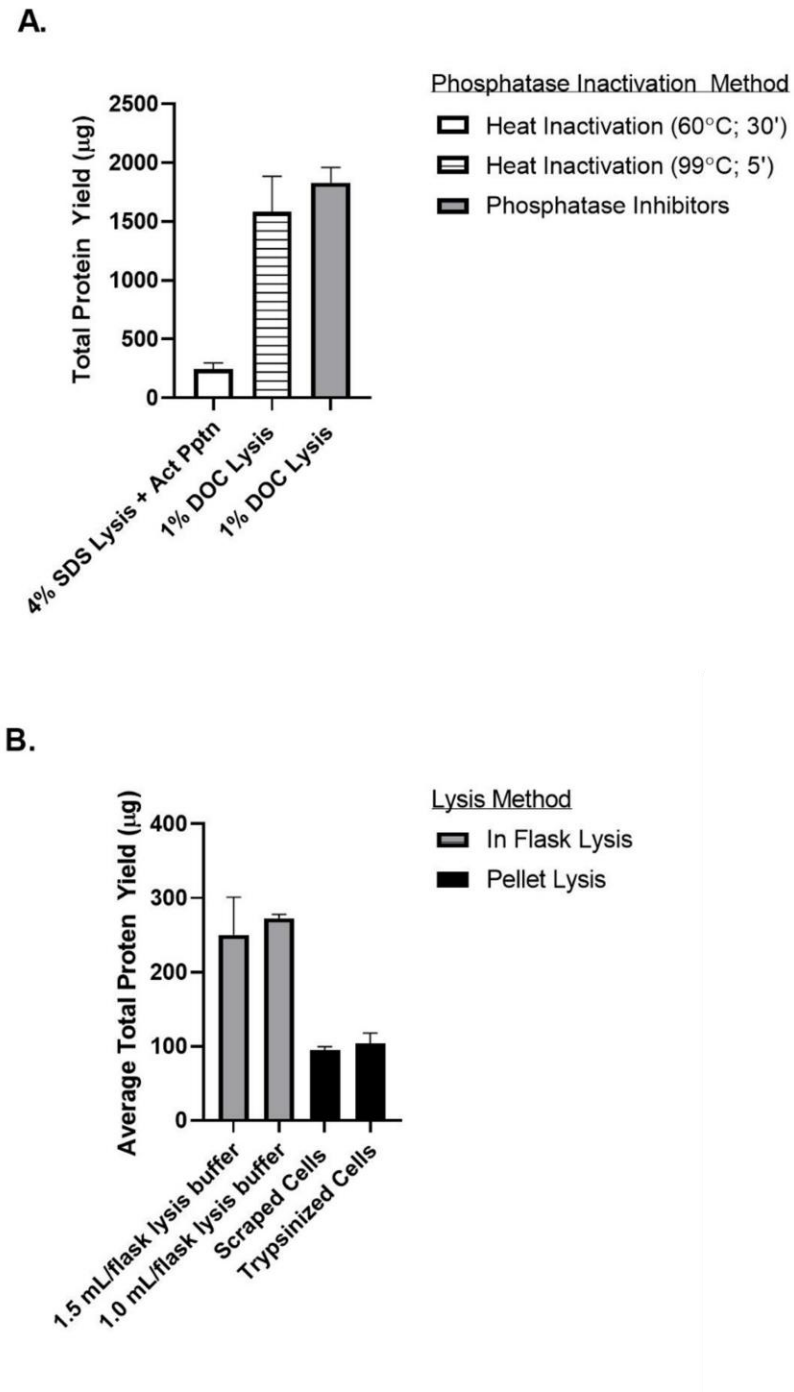

Figure 28: Optimizing lysis conditions for phosphoproteome evaluation of hCMEC/d3. **(A)** The total protein yield of lysates from confluent T25 flasks of hCMEC/d3 was determined with BCA assays after cells were lysed with 4% SDS in 100 mM Tris (pH 8.8) followed by heat inactivation of phosphatases at 60°C for 30 minutes and acetone precipitation (white bars), or lysed with 1% DOC in NH_4HCO_3 (pH 7.8) and heat inactivated at 99°C for

5 minutes (dashed bar) or lysed with 1% DOC in NH_4HCO_3 (pH 7.8) in the presence of phosphatase inhibitors (grey bar). **(B)** The total protein yield of lysates from confluent T25 flasks of hCMEC/d3 was determined with BCA assays after cells were lysed by addition of 1.5 mL or 1.0 mL of 1% DOC in in NH_4HCO_3 (pH 7.8) directly into the flask or after cells were removed from flasks via cell scraping or trypsinization, and centrifuged at 220 x g to pellet prior to lysis in 1% DOC in in NH_4HCO_3 (pH 7.8). Results are presented as mean ± SEM from two independent experiments.

Preliminary results for Tp0751-modified endothelial signaling

Usable data was acquired from one of the three SILAC experiments, where 24 different proteins were detected with valid SILAC ratios (Table 8). Although these results only represent a single technical replicate, data processing was carried out to establish a workflow for evaluating changes in the phosphoproteome. These preliminary results also provide intriguing insights into endothelial signaling changes during Tp0751 exposure that will be further explored. Data analysis was performed in Perseus, where peptides were filtered to remove contaminants and reverse hits (decoys). These data were further refined by setting the valid value threshold at 70% to generate a data set that includes proteins where SILAC ratios were detected for all three pairing groups in the triplex. The data was then transformed so that ratios including Tp0751 treated endothelial cells (medium) were expressed as Experimental (Tp0751)/Control (Untreated or Tp0327) and log2 transformed to evaluate as fold change relative to the control (Figure 25C). The log2 fold change for each SILAC pairing (Table 8) was plotted onto a heat map (Figure 29).

Table 8 Proteins identified from hCMEC/d3 with valid SILAC ratios for all sample pairings.

Gene Name	Sequence Coverage	Medium/Light (Tp0751/Untreated)		Heavy/Light (Tp0327/Untreated)		Medium/Heavy (Tp0751/Tp0327)	
		Log2 FC[1]	Peptide pairs[2]	Log2 FC[1]	Peptide pairs[2]	Log2 FC[1]	Peptide pairs[2]
DBN1	1.2%	0.285	2	**-0.036***	2	0.256	2
SRRM1	8.3%	-0.010	8	**0.037***	8	-0.019	8
ILF3	2.8%	-0.001	2	0.115	2	0.0094	2
EIF4B	6.0%	0.130	5	0.187	5	0.0223	5
CANX	6.4%	0.147	2	-0.203	2	0.329	2
ACTG1	17.7%	-0.173	6	-0.075	6	0.0377	6
CTTN	14.1%	0.105	2	**-0.003***	2	0.0884	2
MAP4	2.7%	0.005	2	**-0.034***	2	0.137	2
HSPA8	4.8%	-0.185	2	**0.004***	2	-0.200	2
SRRM2	1.7%	-0.291	**2**	0.051	2	-0.381	2
HNRNPA1	12.5%	0.043	4	**-0.011***	4	0.0881	4
TMPO	6.8%	-0.329	3	-0.443	3	0.052	3
MYH9	6.4%	-0.226	**3**	0.081	3	-0.216	3
YBX1	13.9%	0.103	**3**	**-0.008***	3	0.100	3
HSP90AB2P	4.5%	0.069	4	0.140	4	-0.045	4
VIM	15.7%	-0.153	6	0.113	6	-0.292	6
HIST1H1B	9.3%	-0.201	4	0.300	4	-0.454	4
MARCKS	9.9%	-0.220	2	-0.517	2	0.381	2
TRA2B	3.5%	0.193	2	0.068	2	0.010	2
AHNAK	0.7%	-0.138	4	-0.210	4	-0.241	4
PLEC	0.6%	0.091	2	**0.013***	2	0.093	2

[1]Fold change calculated by log2 transformation of normalized protein ratios

[2]Number of redundant peptides between samples used for quantification

*Indicates that the Log2 Fold Change between control groups (Tp0327 and Untreated) is within threshold 0 ± 0.05, demonstrating no change between control samples

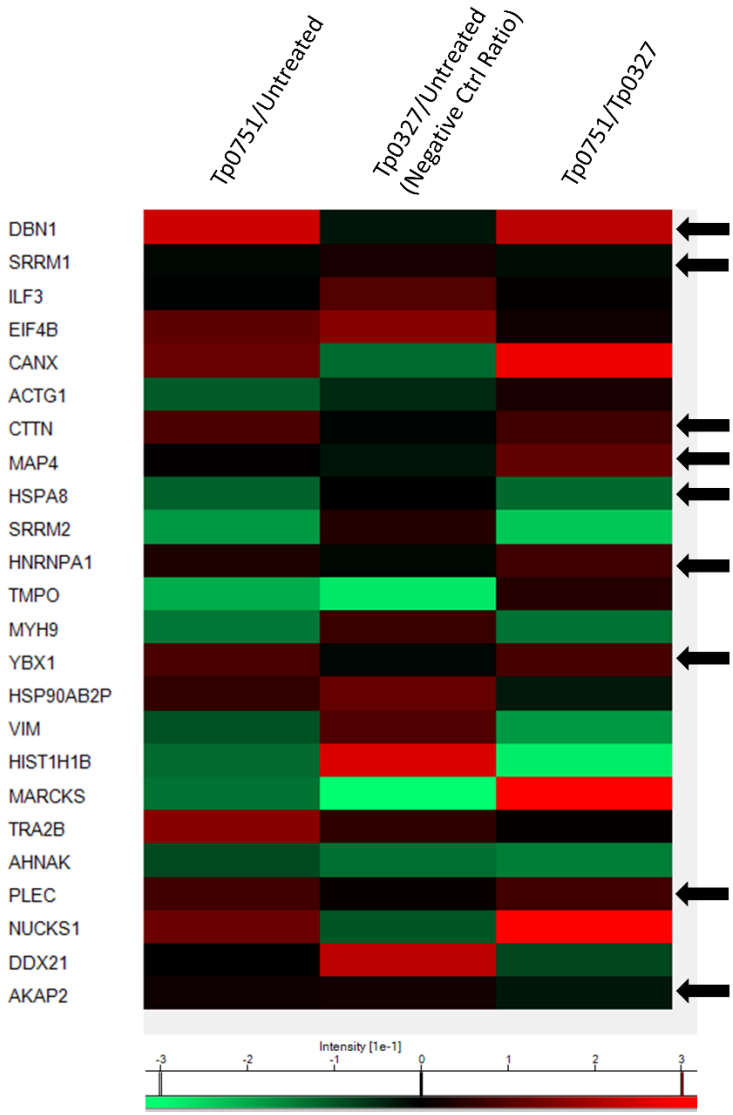

Figure 29: Heat map of proteins identified from hCMEC/d3 SILAC experiment with valid ratios for all sample pairings. The heat map reflects the value of log2 transformed normalized ratios of different proteins (gene names indicated left of the heat map) between Tp0751/Untreated (column 1), control samples Tp0327/Untreated (column 2), or Tp0751/Tp0327 (column 3), where increased phosphopeptide abundance in the Tp0751-treated samples is indicated in red (log2 fold change > 0.05) and decreased phosphopeptide abundance in the Tp0751-treated sample is indicated in green (log2 fold change <-0.05). Black indicates no change in phosphopeptide abundance (log2 = 0 ± 0.05). Black arrows indicate proteins where the phosphopeptide abundance does not differ between the two control treatments (column 2; Tp0327/Untreated). Perseus was used to generate the heat map.

Table 9 Proteins identified with valid SILAC ratios for all sample pairings where no change in phosphopeptide abundance is observed in the control heavy/light (Tp0327/Control) sample.

Gene Name	Medium/Light (Tp0751/Untreated)	Heavy/Light (Tp0327/Untreated)	Medium/Heavy (Tp0751/Tp0327)	Change in Tp0751-treated samples
	Log2 fold change[1]	**Log2 fold change[1]**	**Log2 fold change[1]**	
DBN1	+0.285	**-0.036***	+0.256	Increase
SRRM1	-0.010	+**0.037***	-0.019	No change[2]
CTTN	+0.105	**-0.003***	+0.088	Increase
MAP4	+0.005	**-0.034***	+0.137	N/A[2]
HSPA8	-0.185	+**0.004***	-0.200	Decrease
HNRNPA1	+0.043	**-0.011***	+0.0881	No change[2]
YBX1	+0.103	**-0.008***	+0.100	Increase
PLEC	+0.091	+**0.013***	+0.093	Increase
AKAP2	+0.022	+**0.030***	-0.040	N/A[2]

[1]Fold change calculated by log2 transformation of normalized protein ratios for each isotope pairing

[2]Fold change of experimental ratios is within 0 ± 0.05 threshold

[3]Not applicable, no agreement between Tp0751/Untreated and Tp0751/Tp0327 ratios

*Ratio within the log2 fold change threshold (0 ± 0.05)

Metabolically labelled endothelial cells were treated with two negative controls (light, untreated; heavy, control treponemal protein Tp0327) or recombinant Tp0751 (heavy) (Figure 25). This triplex experiment was designed to control for any nonspecific effects that recombinant protein in buffer may have on endothelial cells; thus, data were refined to only include proteins where the log2 fold change between control treatments (Untreated/Tp0327) was 0 ± 0.05 (Table 8 **ratios***, Figure 29 **black arrows**), which indicates no difference in peptide abundance between the two negative controls. This data reduction generated an assemblage of nine proteins (Table 9, Figure 30). Among these treatments, the log2 fold change ratio for two proteins exhibited disagreement in the two Tp0751/control ratios (Table 9, 'N/A'; Figure 30 MAP4, AKAP2), and two other

proteins had log2 fold change ratios within the control threshold of the untreated ratio (0 ± 0.05, Table 9 'No change', Figure 30 SRRM1, HNRNPA1), leading to the elimination of these four proteins from the analysis. Of the remaining proteins, five are putatively regulated by Tp0751 (Table 9, Figure 30) including four proteins with putative increased phosphorylation in Tp0751-treated samples (Table 10, Figure 30; DBN1, CTTN, YBX1 and PLEC) and one protein with a putative decrease in phosphorylation after Tp0751 treatment (Table 11, Figure 30 HSPA8).

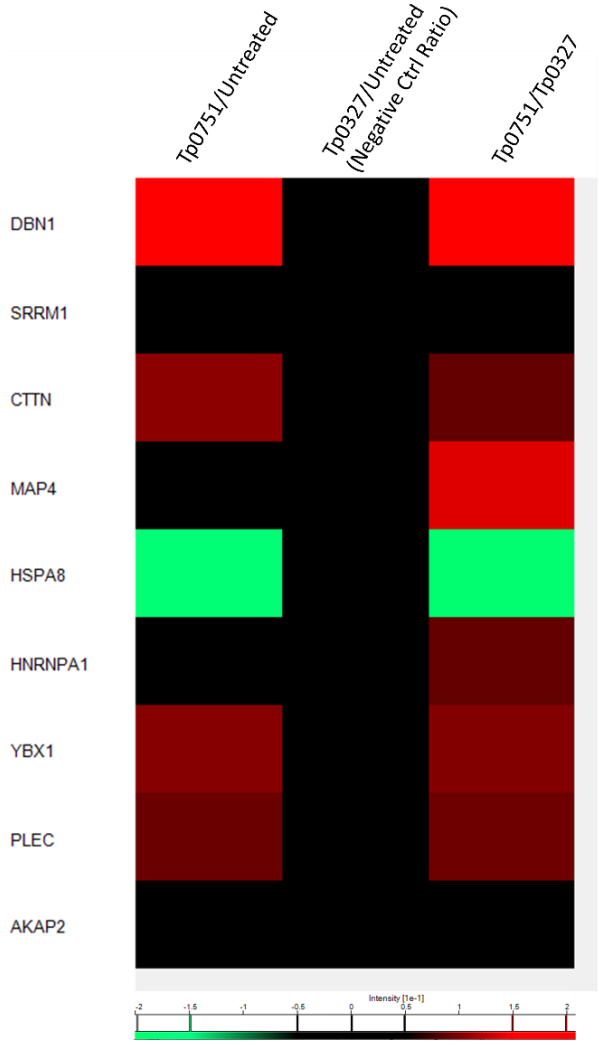

Figure 30: Heat map of proteins identified from hCMEC/d3 with valid SILAC ratios for all sample pairings that are not affected by control untreated or control Tp0327 treatments. The heat map reflects the value of log2 transformed normalized ratios of different proteins (gene names are indicated on the left side) between Tp0751/Untreated (column 1), control samples Tp0327/Untreated (column 2), or Tp0751/Tp0327 (column 3), where increased

phosphopeptide abundance in the Tp0751-treated samples is indicated in red (log2 fold change >0.05) and decreased phosphopeptide abundance in Tp0751-treated samples is indicated in green (log2 fold change <-0.05). Control SILAC ratio (column 2, Tp0327/Untreated) are all within the threshold 0 ± 0.05.

Table 10 Endothelial proteins with putative increased phosphopeptide abundance after Tp0751 treatment.

Gene Name	Protein Name	Molecular Function[1]	Subcellular Location[2]	KEGG Pathway[3]
DBN1	Drebrin	Actin, cadherin and profilin binding	Cytoplasm; cell cortex; cell junction	N/A
CTTN	Src substrate cortactin	Cadherin and profilin binding	Membrane; cytoskeleton; junctions; cell protrusions	Bacterial invasion of epithelial cells; Pathogenic *E. coli* infection
YBX1	Nuclease-sensitive element-binding protein 1	DNA, RNA and GTPase binding:	Secreted; nucleus; cytoplasm	N/A
PLEC	Plectin	Actin, ankyrin, cadherin and RNA binding	Cytoskeleton; hemidesmosome	N/A

[1]Gene ontology molecular function; [2]Uniprot subcellular location; [3]KEGG pathway database

Table 11 Endothelial protein with putative decreased phosphopeptide abundance after Tp0751 treatment.

Gene Name	Protein Name	Molecular Function[1]	Subcellular Location[2]	Pathway[3]
HSPA8	Heat shock cognate 71 kDa protein	ATPase activity; ATP binding; cadherin binding; chaperone binding; clathrin uncoating	Cell membrane, nucleolus, cytoplasm	N/A

[1]Gene ontology molecular function; [2]Uniprot subcellular location; [3]KEGG pathway database

Proteins with phosphorylation that is putatively regulated by Tp0751 include two actin-binding proteins (drebrin and plectin) and four cadherin binding proteins (drebrin, src substrate cortactin [cortactin], plectin, and heat shock cognate 71 kDa protein; Table 10, Table 11). Phosphorylation sites that are predicted to be regulated by Tp0751 were identified for drebrin (S^{141} and S^{142}) and src substrate cortactin (T^{401}, S^{405}) based upon the

highest phosphorylation site probability assigned by Maxquant for each peptide identified (Table 12). Phosphorylation sites could not be definitively determined for nuclease-sensitive element-binding protein 1, plectin, or heat shock cognate 71 kDa protein, as phosphorylated residues were not detected (YBX1, HSPA8) or Maxquant generated the same phosphorylation site probability for multiple residues within a single peptide (Table 12). Notably, two of the identified phosphorylation sites have known upstream kinases and a characterized associated function for the site. Phosphorylation of drebrin at S^{142} is coordinated by the cyclin-dependent kinase 5 (Cdk5) and promotes bundling of filamentous actin (F-actin; Worth et al. 2013). Cortactin is phosphorylated at S^{405} by the extracellular signal-regulated kinase 1/2 (ERK1/2), which promotes actin polymerization (Table 13) through activation of N-WASP (Neural Wiskott-Aldrich syndrome protein; Campbell, Sutherland, and Daly 1999; Kelley et al. 2010; Martinez-Quiles et al. 2004).

Table 12 Endothelial phosphorylation sites putatively regulated by Tp0751**.**

Gene Name	Local Prob[1]	# P-res[2]	Sequence Window[3]	P-site probabilities[4]	Site[5]
DBN1	0.65	1	AGAIGQRLSNGLARLSSPV LHRLRLREDENA	LS(0.93)S(0.07)PVL	S^{141}
	0.95	1	GAIGQRLSNGLARLSSPVL HRLRLREDENAE	LS(0.002)S(0.998)PVL	S^{142}
CTTN	0.99	2	KLEEQARAKTQTPPVSPAP QPTEERLPSSPV	T(0.031)QT(0.969)PPVS(1)	$T^{401}S^{405}$
	0.96	2	QEEARRKLEEQARAKTQT PPVSPAPQPTEER	T(0.5)QT(0.5)PPVS(0.995) PAPQPT(0.005)	S^{405} T^{x}
YBX1	N/A	N/A	N/A	N/A	N/A
PLEC	0.32	N/A	FADMLSGNAGGFRSRSSS VGSSSSYPISPAV	S(0.333)S(0.333)S(0.333)V	N/A
	0.32	N/A	ADMLSGNAGGFRSRSSSV GSSSSYPISPAVS	S(0.333)S(0.333)S(0.333)V	N/A
HSPA8	N/A	N/A	N/A	N/A	N/A

[1]Maxquant peptide phosphorylation site localization probability; [2]Number of phosphorylated residues on the peptide; [3]Full peptide sequence; [4]Maxquant phosphorylation site probability, max score=1; [5]Predicted phosphorylation site based on Maxquant phosphorylation site probabilities, where localization probability > 0.95

Table 13 Associated function of endothelial phosphorylation sites predicted to be regulated by Tp0751.

	Phosphosite	Phosphosite Function	Kinase	References
DBN1	S^{141}	Unknown	N/A	N/A
	S^{142}	Promotes F-actin bundling activity	Cdk5	(Tanabe et al. 2014; Worth et al. 2013)
CTTN	T^{401}	Unknown	N/A	N/A
	S^{405}	Promotes actin polymerization	ERK1/2	(Campbell, Sutherland, and Daly 1999; Kelley et al. 2010; Martinez-Quiles et al. 2004)

4.4 Discussion

Treponema pallidum is known to interact with host cells *in vitro* and during infection to coordinate vascular dissemination; however, the responses of host cells have not been extensively explored. Furthermore, quantitative proteomics has never been utilized to study host-pathogen interactions of *T. pallidum* or its adhesins. In this chapter a workflow is presented for the characterization of the endothelial phosphoproteome after exposure to the *T. pallidum* adhesin Tp0751 to explore whether signaling pathways are modulated by this protein. Despite the low phosphoproteome coverage yielded by this experiment, an exciting direction emerged in agreement with other data presented within this dissertation. The workflow established will guide future experiments that explore the modulation of signaling networks by Tp0751 and other *T. pallidum* proteins.

Previous investigations have demonstrated that primary HUVECs can be cultured in SILAC medium (Burghoff and Schrader 2011; Parker, Halligan, and Greene 2010; Bouyssie et al. 2007; Zanivan et al. 2013). In this chapter, HUVEC growth in SILAC medium supplemented with endothelial growth factors and isotopically labelled arginine and lysine was attempted, but this formulation could not support sustained growth of this primary cell line. Endothelial cells grown in EGM-2, a specialized medium for endothelial cells, can survive and proliferate with 2% FBS supplemented. However, endothelial cells grown in general culture medium such as DMEM, Medium 199 (M199), or RPMI (Rosewall Park Memorial Institute) must be supplemented with a higher concentration of FBS (20-30%) to support growth (Gimbrone, Cotran, and Folkman 1974). Previous studies have found that HUVECs can be grown in endothelial specific SILAC medium supplemented with 2% FBS (Burghoff and Schrader 2011) or in M199 or RPMI medium

supplemented with 20% FBS (Parker, Halligan, and Greene 2010; Zanivan et al. 2013). Of concern, the inclusion of high concentrations of FBS in SILAC media limits quantitative detection of peptides through masking (Shin et al. 2019). Growth of HUVECs was initially tested in DMEM (lysine- and arginine-free) supplemented in 8% or 10% dFBS and endothelial growth supplements, but this formulation did not support long-term growth of the endothelial cells. Fetal bovine serum is an undefined component in growth medium and varies in composition between batches, which can have significant affects on cell growth (Baker 2016). This is further exacerbated by the need to supplement SILAC medium with FBS that has been dialyzed to remove unlabelled amino acids that would contaminate results (Ong et al. 2002). To determine whether the lack of observed growth in SILAC medium was due to the specific batch of FBS, HUVEC growth was evaluated in SILAC medium supplemented with dFBS (10%) that had been previously validated to support growth of a non-endothelial cell line in a collaborating lab at the University of British Columbia (Foster Laboratory); however, HUVECs were still unable to grow in the SILAC medium.

Successful culturing of cells in SILAC medium requires highly proliferative cells and, due to the elimination of amino acids and peptides during dialysis, dFBS cannot always support the growth of primary cell lines (Cheruiyot et al. 2017). Therefore, an immortalized endothelial cell line of cerebral microvascular endothelial cells (hCMEC/d3) with a higher proliferation rate than primary HUVECs was tested for its capacity to grow in SILAC medium. In two separate experiments hCMEC/d3 successfully grew 3-4 passages in the SILAC medium supplemented with 12% or 15% dFBS.

To determine the ideal sample preparation conditions, three approaches were compared for cell lysis and phosphatase denaturation for downstream phosphoproteome analysis: (1) SDS-based lysis and heat denaturation at 60°C followed by acetone precipitation, (2) DOC-based lysis and heat denaturation at 99°C, and (3) DOC-based lysis with phosphatase and protease inhibitors. Since protein phosphorylation is reversible, preseveration of the modified residues must be carefully considered during phosphoproteome evaluation. Classically, this is accomplished with the incorporation of phosphatase inhibitors to inactivate phosphatases released from cells upon lysis. Select phosphatase inhibitors can improve phosphopeptide retention by 10-40% (Thingholm et

al. 2008). An alternative approach is harsh denaturation of proteins immediately following cell lysis in a chaotropic lysis buffer (Rogers, Fang, and Foster 2010). In these investigations sample preparation was initially conducted using a chaotropic lysis buffer (4% SDS in 100 mM tris pH 8.8) followed by heating at 60°C to denature phosphatases, and acetone precipitation, to remove SDS that would interfere with downstream tryptic digestions and LC-MS/MS. This method of sample preparation resulted in poor coverage of the phosphoproteome. Evaluation of total protein yields revealed a ten-fold increase in yield following lysis with 1% DOC in 50 mM NH_4HCO_3 (pH 7.8) versus the SDS lysis method. It is probable that sample loss occurred during the acetone precipitation step and that the heat denaturation temperature was not high enough to inactivate all active phosphatases and proteases. Similar to previous findings, the findings presented in this chapter suggest that the inclusion of phosphatase inhibitors negatively affected the phosphoproteome coverage (Rogers, Fang, and Foster 2010; Aryal and Ross 2010). Sodium deoxycholate is another effective chaotrope, but in contrast to SDS, does not interfere with downstream sample processing steps required for phosphoproteome evaluation (Rogers, Fang, and Foster 2010; Masuda, Tomita, and Ishihama 2008; Zhou et al. 2006). Superior phosphoproteome coverage was achieved by lysing cells with 1% DOC/NH_4HCO_3 followed immediately by heating to 99°C. This lysis and denaturation approach yielded 18% more phosphopeptides compared to the SDS lysis protocol and 44% more phosphopeptides compared to samples lysed in the presence of phosphatase inhibitors. Many phosphatase inhibitors have a high affinity for TiO_2, as their mechanism of action is to mimic phosphate and bind enzyme active sites. As a result, phosphatase inhibitors can outcompete phosphorylated peptides during TiO_2 enrichment steps (Rogers, Fang, and Foster 2010), decreasing phosphopeptide retention at this step in the protocol. Furthermore, previous studies have demonstrated that commonly used phosphatase inhibitors, such as calyculin A and sodium pervanadate, do not completely abolish enzyme activity (Thingholm et al. 2008; Pan et al. 2008), leaving the opportunity for enzymatic removal of phosphoryl groups from modified residues after cell lysis.

Although improved phosphoproteome coverage was achieved with a 1% DOC lysis/99°C denaturation, overall coverage of the phosphoproteome was still low. There are several adjustments that could be made to future experiments. First, serum starvation of

metabolically labeled cells prior to treatment and lysis could help eliminate contaminating proteins from FBS that may interfere with the signals from the endothelial phosphoproteome. Previous studies have also reported promising results using a combined approach of sample lysis in DOC with protease and phosphatase inhibitors followed by irreversible heat denaturation at 99°C (Rogers et al. 2011). This small-scale quantitative analysis focussed on optimizing sample preparation and generating a reliable workflow but increasing the scale of the experiment will be required to improve phosphoproteome coverage. Full scale quantitation of the proteome will require >10-fold more protein than was used in this study (Rogers et al. 2011). It is also important to note, that a natural limitation to a global phosphoproteome approach is that detection of low abundance proteins are limited, thus it is likely that in this experiment only phosphopeptides from highly abundant proteins were detected (Dephoure and Gygi 2012). Scaling up the experiment should improve the range of proteins detected, but especially with a triplex experiment, full coverage of the proteome is not anticipated. Finally, time-resolved samples, as well as biological and technical replicates with label swapping between replicates, will be critical for improving phosphoproteome coverage and producing a data set that can be evaluated by robust data exploration and statistical analysis.

Despite the stringent data analysis, conservative experimental design and small-scale of the experiment this exploration of endothelial signaling still identified two exciting phosphorylation targets that are putatively regulated by Tp0751. Duplex SILAC experiments are more commonly implemented over triplex experiments as they have decreased sample complexity which allows for higher performance identification and quantification (Dephoure and Gygi 2012). However, the experimental design of this investigation utilized a triplex approach that included two negative controls, allowing for stringent data refinement to generate a list of nine proteins where no difference was observed between untreated and control recombinant protein (Tp0327) treated samples. From the original list of 24 proteins with valid SILAC ratios, 62.5% (15/24) of the proteins did not exhibit agreement between Tp0327 and untreated controls, as indicated by a log2 fold change outside of 0 ± 0.05. This suggests that the negative control recombinant protein preparation had unintended impacts on certain endothelial proteins which may be attributed to the gel filtration buffer that the protein is prepared in. By using this dual control strategy,

we can improve the confidence that differences in relative abundance for proteins within the filtered list can be specifically attributed to modification by Tp0751. Of these nine proteins, five are putatively regulated by endothelial exposure to Tp0751. Increased fold changes in Tp0751-treated samples relative to the control ratio was observed for drebrin, cortactin, nuclease-sensitive element-binding protein 1, and plectin, while a decreased fold change was seen for heat shock cognate 71 kDa protein. Notably, four of these proteins are classified as cadherin binding proteins (DBN1, CTTN, PLEC, HSPA8) and three are constituents of the cytoskeleton or cell cortex (DBN1, CTTN, PLEC; The UniProt Consortium 2019). The corresponding phosphorylated residues were identified for drebrin (S^{141}, S^{142}) and cortactin (T^{401}, S^{405}). Drebrin S^{142} is phosphorylated by Cdk5, which facilitates a conformational change to promote binding to F-actin bundles in lamellipodia (Worth et al. 2013). Drebrin also links the adherens junction protein nectin to the cortical actin cytoskeleton to stabilize junctions and maintain vascular endothelial integrity, but regulation of this interaction is not yet understood (Rehm et al. 2013). Cortactin phosphorylation at S^{405} by ERK1/2 induces F-actin polymerization in lamellipodia by activating the effector protein N-WASP (Campbell, Sutherland, and Daly 1999; Kelley et al. 2010; Martinez-Quiles et al. 2004). Cortactin is involved in host cell invasion by *N. meningitidis* (Lambotin et al. 2005; Slanina et al. 2012; Hoffmann, Eugene, et al. 2001), *Rickettsia conorii* (Martinez and Cossart 2004), *Staphylococcus aureus* (Agerer et al. 2003), *Chlamydia trachomatis* (Fawaz et al. 1997), *and Shigella flexneri* (Bougneres et al. 2004; Dumenil, Sansonetti, and Tran Van Nhieu 2000), host cell actin pedestal formation by *E. coli* (Cantarelli et al. 2000; Cantarelli et al. 2006; Cantarelli et al. 2002), and both intracellular and intercellular actin-based motility by *S. flexneri* (Bougneres et al. 2004) and *Listeria monocytogenes* (Zettl and Way 2001; Frischknecht and Way 2001; Sousa et al. 2007). These processes are largely regulated by cortactin tyrosine phosphorylation at Y^{421}, Y^{466} and Y^{482} (Selbach and Backert 2005). However, during *Helicobacteri pylori* invasion of epithelial cells, ERK1/2 mediates cortactin S^{405} phosphorylation to promote interactions between cortactin and focal adhesin kinase (FAK) and disruption of cell-matrix adhesion (Tegtmeyer et al. 2011). Furthermore, ERK1/2 phosphorylation of cortactin S^{405} is required for membrane ruffling and epithelial cell invasion by *Campylobacter jejuni* (Samuelson and Konkel 2013). While the upstream kinases for the phosphorylation sites

identified in drebrin and cortactin are known, this investigation did not identify any kinases that were differentially phosphorylated as a result of exposure to Tp0751. This will be an important component of future large-scale experiments to understand which signaling nodes may be critical for Tp0751-mediated modulation of endothelial signaling.

Cytoskeletal modulation during transendothelial migration is common to leukocytes (Schimmel, Heemskerk, and van Buul 2017) and other invasive bacterial pathogens, such as *N. meningtidis* (Eugene et al. 2002) and *E. coli* (Loh et al. 2017). The formation of F-actin protrusions at endothelial cell surfaces is an initiating step of bacterial invasion via macropinocytosis (Loh et al. 2017). Additionally, F-actin protrusions can promote firm adhesion of bacteria and leukocytes to endothelial surfaces to resist shear stress of the blood flow (Schimmel, Heemskerk, and van Buul 2017; Eugene et al. 2002; Loh et al. 2017). In endothelial cells, actin forms a cortical rim at cell borders that links to cell-cell and cell-matrix adhesion complexes. The cortical actin binding protein, cortactin, acts in concert with N-WASP to promote polymerization of new branches of cortical F-actin, which stabilizes the cortical network and can induce assembly of adhesion complexes (Prasain and Stevens 2009). Importantly, both polymerization and depolymerization of cortical F-actin can lead to disruption of endothelial barriers (Moy et al. 2004; Bogatcheva et al. 2003; Benndorf et al. 1994), demonstrating that these processes must be tightly controlled to maintain endothelial barrier function (Prasain and Stevens 2009). Modulation of actin dynamics could also promote transendothelial migration by engaging the actomyosin contractility machinery to induce endothelial contraction and loosen junctions (Shen, Wu, and Yuan 2009). Another possibility is the formation of F-actin rich contractile rings around the site of transendothelial migration. This modification to actin organization occurs during leukocyte transendothelial migration and functions to prevent vascular leakage (Heemskerk et al. 2016). Additional investigations will be required to confirm Tp0751-mediated modification of the endothelial cytoskeleton and explore how these changes could relate to *T. pallidum* transendothelial migration.

The investigations presented in this chapter revealed optimized methods for the metabolic labeling of endothelial cells, lysis conditions, and inactivation of phosphatases. This provides the framework for future studies to explore changes in endothelial signaling induced by *T. pallidum* and its adhesins. Despite the limited phosphoproteome coverage,

increased phosphorylation of the cytoskeletal- and cadherin-binding proteins drebrin and cortactin was observed in Tp0751 treated samples. Intriguingly, both proteins are involved in regulating the dynamics of the cortical actin cytoskeleton (Weed and Parsons 2001; Rehm et al. 2013; Rehm and Linder 2017) and cortactin has been directly linked to host cell invasion by numerous pathogens (Selbach and Backert 2005). The exciting findings presented herein propose a clear direction for future studies to explore Tp0751-mediated induction of actin polymerization in endothelial cells.

5. Concluding Chapter

5.1 Mechanisms of *T. pallidum* vascular dissemination

Within hours of inoculation, *T. pallidum* disseminates through the vasculature gaining access to distant sites within the host where organisms penetrate tissue barriers including the placental and blood brain barriers (Mahoney 1934; Stokes 1944; Cumberland MC 1949; Raiziss GW 1937; Chapel 1981, 1980; Hira et al. 1987; Baughn and Musher 2005). These highly invasive organisms can evade the immune system, promoting asymptomatic infections that persist for decades and the clinical manifestations and disease progression of syphilis expose the highly invasive nature of this pathogen (Lafond and Lukehart 2006). Investigations into *T. pallidum* dissemination in the *in vivo* experimental rabbit model reveal that organisms can gain access to the bloodstream within minutes of intradermal or intratesticular inoculation (Cumberland MC 1949; Stokes 1944), while *in vitro* investigations demonstrate that *T. pallidum* adheres to intercellular junctions of endothelial cells and promotes endothelial cell activation (Thomas et al. 1988). More recent investigations have demonstrated that the *T. pallidum* adhesin Tp0751 can mediate attachment to endothelial cells *in vitro* under conditions of flow and *in vivo* in mouse post-capillary venules (Kao et al. 2017). The work described in this dissertation builds on these key findings and presents important advancements to the understanding of *T. pallidum* dissemination with respect to vascular adhesion and transendothelial migration.

5.1.1 Adhesion to the vascular endothelium

It has been well documented that *T. pallidum* attaches to a variety of host cells types (Fitzgerald et al. 1977; Hayes et al. 1977; Sandok et al. 1976; Thomas et al. 1989; Thomas et al. 1988; Wu, Zhang, and Wang 2017); however, there is limited understanding of the molecular machinery that facilitates these interactions. Previously identified *T. pallidum* adhesins that confer spirochete attachment to host cells include Tp0751 (Kao et al. 2017; Cameron et al. 2008) and Tp0435 (Chan et al. 2016). Numerous ECM binding adhesins have also been identified including Tp0750 (Houston et al. 2014), Tp0483, Tp0155, Tp0751 (Cameron et al. 2004) and Tp0136 (Brinkman et al. 2008; Ke et al. 2015). In Chapter 2 of this dissertation, the endothelial adhesive capacity of Tp0751 was validated

using three distinct approaches including endothelial binding assays with recombinant protein, a heterologous expression system, and live *T. pallidum.* In concert with previous investigations that demonstrate Tp0751 mediates spirochete adhesion to endothelial cells *in vitro* under physiological conditions of shear stress and *in vivo* in mouse post-capillary venules (Kao et al. 2017), this provides strong evidence to confirm that Tp0751 is a *T. pallidum* vascular adhesin.

In Chapter 2 of this dissertation, LamR was identified as an endothelial cell receptor for Tp0751. However, the fact that *T. pallidum* adhesion to endothelial monolayers cannot be completely abrogated with blocking antibodies specific to Tp0751 or LamR suggests that multiple *T. pallidum* adhesins act in concert to facilitate binding to a variety of distinct endothelial receptors. Identification of two lipid raft proteins, stomatin and LamR, as putative endothelial cell receptors for Tp0751, suggests that this adhesin may preferentially interact with receptors enriched in lipid raft subdomains of endothelial plasma membranes. While Tp0751 and Tp0435 are the only *T. pallidum* adhesins confirmed to mediate spirochete attachment to host cells (Kao et al. 2017; Chan et al. 2016), previous finding suggest that Tp0750 could also act as an endothelial adhesin. A functional linkage between Tp0751 and Tp0750 is supported by their genomic clustering and co-transcription in *T. pallidum* (Houston et al. 2014). Intriguingly, Tp0750 binds to the endothelial receptor annexin A2, which is known to colocalize with tight junction proteins at cell-cell borders (Lee et al. 2004). Although the interaction between Tp0750 and annexin A2 has not been explored with live endothelial cells, this interaction provides a putative molecular mechanism for the *T. pallidum* junctional localization presented in Chapter 3 of this dissertation.

Adhesin-ECM interactions are also likely to play a key role in *T. pallidum* attachment to the vascular endothelium as *T. pallidum* exhibits a functional redundancy of fibronectin binding proteins including Tp0483, Tp0751, Tp0750, Tp0155, Tp0136 (Cameron et al. 2004; Brinkman et al. 2008; Ke et al. 2015; Houston et al. 2014; Houston et al. 2015). Furthermore, *T. pallidum* attachment to host cells can be inhibited with anti-fibronectin antibodies (Peterson, Baseman, and Alderete 1983; Thomas, Baseman, and Alderete 1985). Fibronectin may support *T. pallidum* luminal attachment to endothelial cells via bridged interactions with integrins or direct subluminal binding to the basement

membrane. *Treponema pallidum* adhesion to the basement membrane may also be facilitated by interactions of Tp0751 and Tp0750 with the ECM proteins laminin and collagen (Houston et al. 2015).

Despite the inherent challenges associated with studying the molecular mechanisms of *T. pallidum* infection, inferences can be drawn by studying related organisms with physiological similarities. The vascular adhesion of the Lyme disease spirochete *Borrelia burgdorferi* is facilitated by distinct sequential molecular events including tethering, dragging, and stationary adhesion. Adhesin-mediated short-term tethering and dragging interactions with glycosaminoglycans in the endothelial glycocalyx layer facilitate the deceleration of *B. burgdorferi* in the vasculature. Subsequently, spirochetes mediate stationary interactions via direct binding to endothelial cells. This takes place within the glycocalyx exclusion layer, which protects the bacteria from the shear forces associated with the blood flow (Norman et al. 2008; Moriarty et al. 2008; Moriarty et al. 2012). Previous investigations with Tp0751-expressing *B. burgdorferi* demonstrate that Tp0751 can facilitate tethering interactions with endothelial surfaces *in vitro* and *in vivo* (Kao et al. 2017). The findings presented in Chapter 2 of this dissertation provide preliminary evidence for the involvement of plasma fibronectin in Tp0751-mediated tethering interactions with vascular surfaces. The remainder of the investigations in this body of work explore the stationary interactions of Tp0751 with endothelial cells to understand the molecular events that precede *T. pallidum* transendothelial migration.

Figure 31 presents a model whereby *T. pallidum* attachment to the luminal and subluminal faces of the vascular endothelium is coordinated by distinct sequential binding events involving specific endothelial receptors, ECM-bridged interactions with endothelial receptors, as well as direct adhesion to ECM proteins in the basement membrane.

(1) Tp0751 facilitates attachment to plasma fibronectin in the bloodstream which supports initial tethering interactions with vascular surfaces

(2) Tp0750 and Tp0751 act in concert to facilitate stationary adhesion of *T. pallidum* to the luminal surface of endothelial cells within the glycocalyx exclusion layer. While Tp0751 mediates spirochete attachment to lipid rafts enriched in LamR and

stomatin, Tp0750 promotes junctional localization of *T. pallidum* via adhesion to annexin A2;

(3) Endothelial attachment at the luminal surface is further supported by interactions between *T. pallidum* adhesins and integrins bridged by fibronectin;

(4) Subluminal endothelial attachment of *T. pallidum* is supported by direct interactions between Tp0751 and LamR, as well as LamR interactions bridged by laminin;

(5) Direct attachment to the basement membrane is facilitated by ECM-binding adhesins.

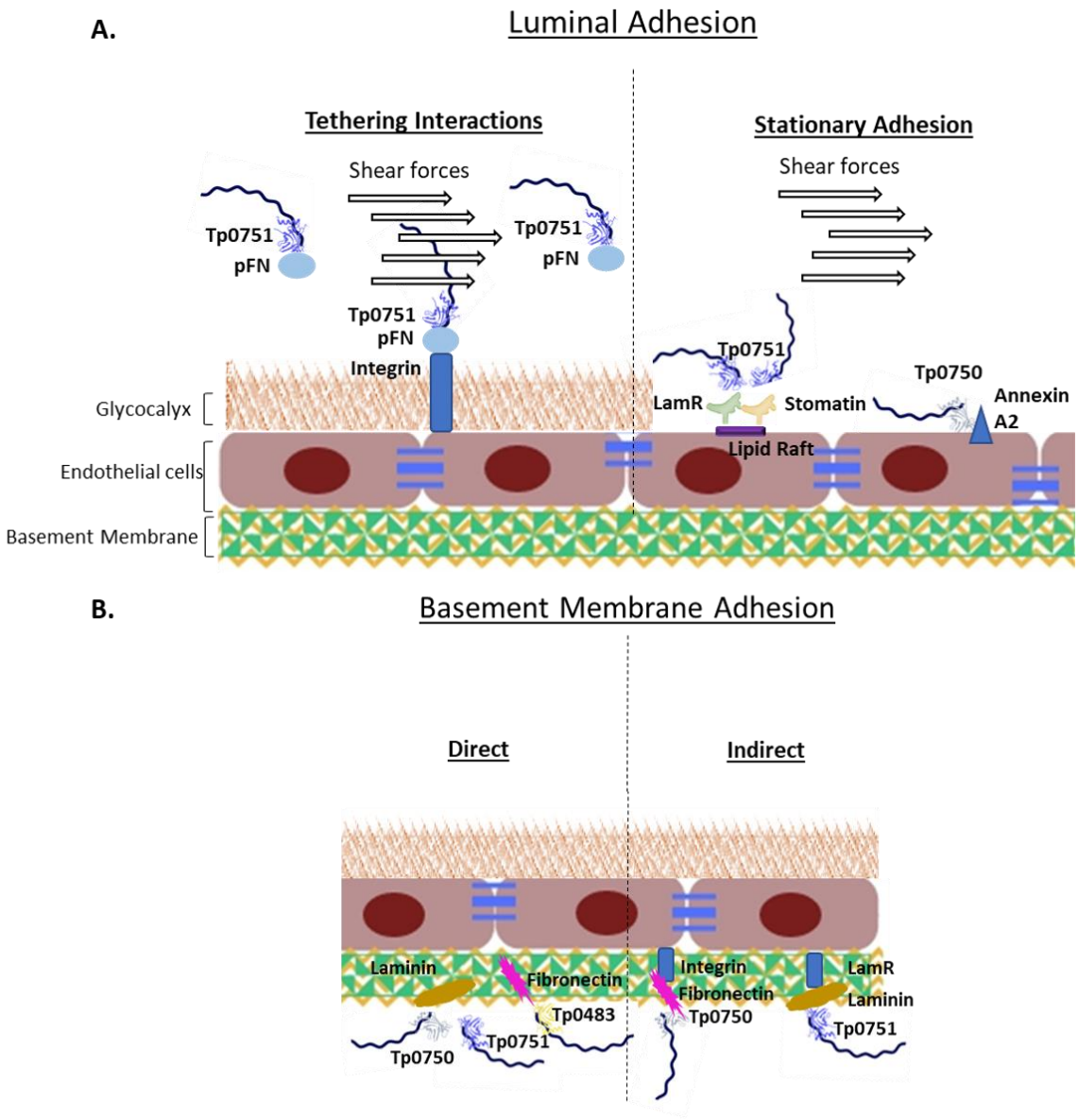

Figure 31: Proposed model for *T. pallidum* adhesion to the vascular endothelium. **(A)** *Treponema pallidum* attachment to the vascular endothelium in the lumen of the vasculature occurs via tethering interactions and stationary adhesion events. **Tethering interactions** between Tp0751 and pFN. Tp0751 binds to soluble pFN in the bloodstream, which facilitates pFN-bridged short-term transient interactions with integrins on vascular surface. These interactions function as molecular brakes to allow treponemes to overcome the shear forces of the blood flow to mediate more stable interactions with vascular surfaces. **Stationary interactions** between *T. pallidum* adhesins and endothelial receptors occurs within the glycocalyx exclusion layer, a protective niche where the bacteria are not

exposed to shear forces of the blood flow. **(B)** Adhesion to the subluminal basement membrane is facilitated by **direct** interactions between *T. pallidum* adhesins (Tp0751, Tp0483, Tp0155. Tp0136; not all shown in model) and ECM components including laminin and fibronectin. **Indirect** interactions between *T. pallidum* ECM-binding adhesins and endothelial integrins are bridged by ECM components such as fibronectin and laminin, while binding between Tp0751 and LamR is bridged by laminin.

5.1.2 Transendothelial migration

Knowledge regarding the molecular mechanisms of *T. pallidum* endothelial barrier traversal has been stunted by the technical complexities of *in vitro* investigations of both *T. pallidum* and endothelial barrier function. *Treponema pallidum* is known to mediate widespread vascular dissemination and invade into diverse secondary infection sites, but molecular characterization of this process was limited to the findings that *T. pallidum* could attach to endothelial cells, induce activation, and localize to intercellular junctions (Riley et al. 1992; Riley et al. 1994; Thomas et al. 1989; Thomas et al. 1988). The work presented in Chapter 3 of this dissertation represents significant progress towards understanding *T. pallidum* traversal of endothelial barriers, although there remains much to uncover about this process.

Treponema pallidum has a remarkable capacity to evade the host immune system, particularly during asymptomatic latent stages when treponemes reside in diverse secondary sites of infection without eliciting host immune response. This capacity has been attributed to the slow rate of *T. pallidum* replication (Magnuson, Eagle, and Fleischman 1948) and the lack of antigens present on the bacterial cell surface (Radolf, Norgard, and Schulz 1989). It has also been postulated that there is a minimum number of treponemes required to elicit an immune response in secondary infection sites (Lafond and Lukehart 2006). The *in vitro T. pallidum* transendothelial migration studies described in Chapter 3 revealed that only a small subpopulation of treponemes successfully traverse endothelial barriers. With a traversal rate of less than 1%, this finding suggests that the complex process of transendothelial migration represents a rate limiting step for treponemal seeding into secondary infection sites. In this scenario, only a small proportion of the treponemal population would express the necessary machinery to simultaneously avoid the immune

system while coordinating the complex adhesive interactions required to traverse across a given vascular endothelial barrier.

The localization of *T. pallidum* to intercellular junctions of endothelial cells described previously (Thomas et al. 1988) and in Chapter 3 of this dissertation implies a paracellular route of transendothelial migration. This is further supported by the observation that Tp0751 and *T. pallidum* can modify the architecture of endothelial junctions. However, a transcellular traversal mechanism for *T. pallidum* is suggested based on the finding that an inhibitor of lipid raft-mediated endocytosis reduced treponemal traversal by 60%. Taken together, these findings could indicate that *T. pallidum* has the capacity to facilitate endothelial barrier traversal via two distinct mechanisms. This suggests that *T. pallidum* may harness a modular approach to transendothelial migration that could facilitate traversal into a broader range of secondary infection sites. Substantial structural and functional heterogeneity exists for endothelial barriers based on the size of the blood vessel and site within the vasculature. This can extend to the dimensions of the glycocalyx and basement membrane, composition of junctional architecture and presence of pores between cells, and the predominance of transcytosis and endocytosis pathways (Aird 2007b). The fact that *T. pallidum* can seed into diverse tissue and organ sites that are separated from the vasculature by structurally distinct endothelial barriers including the heart, liver, and central nervous system, implies that diverse mechanisms are likely employed for invasion into different secondary infection sites. Transendothelial migration across the highly protected blood-brain, retinal or placental barriers would represent a vastly greater impediment to invasion compared to spirochete penetration of fenestrated or discontinuous endothelial barriers. The dissemination mechanisms explored in this body of work use a model macrovascular cell line (HUVECs) to explore *T. pallidum* transendothelial migration. Future investigations should utilize a variety of endothelial cell lines to explore how *T. pallidum* extravasation may differ in distinct sites of the vasculature.

It is impossible to distinguish the specific molecular mechanisms for *T. pallidum* transcellular and/or paracellular transendothelial migration based on the current state of knowledge. However, the findings presented herein inform a model to direct future investigations. Given that no change in barrier permeability was observed during *T.*

pallidum traversal *in vitro*, it is likely that paracellular traversal would occur via a parallel mechanism to leukocyte transendothelial migration as vascular leakage does not occur during this highly coordinated process. While the molecular events of this process are not fully understood, it is known that the paracellular traversal site retains a minimum pore size via an F-actin rich contractile ring that leukocytes must squeeze through (Heemskerk et al. 2016; Carman and Springer 2008; Vestweber 2015; Muller 2011). Transient disruption of VE-cadherin intercellular junctions also occurs during leukocyte transendothelial migration, but it has yet to be fully resolved whether VE-cadherin is internalized during this process (Muller 2016; Schimmel, Heemskerk, and van Buul 2017). The transcellular traversal mechanism of *T. pallidum* is likely a lipid raft-mediated endocytosis pathway. However, the off-target effects of the endocytosis inhibitors present a significant challenge for interpreting the results. The possibility of a raft-mediated endocytosis pathway is particularly intriguing given that both Tp0751 endothelial receptors identified in Chapter 2 are predicted to localize to lipid rafts. However, there is limited knowledge regarding the specific mechanisms of raft-mediated endocytosis, especially for abluminal exocytosis. Additional investigations are required to further explore the possibility of a transcellular traversal mechanism for *T. pallidum.*

The findings presented in Chapter 3 of this dissertation support a model (Figure 32) for *T. pallidum* transendothelial migration where:

(1) A subpopulation of *T. pallidum* localizes to regions of intercellular junctions in endothelial cells;
(2) *Treponema pallidum* modifies adherens junctional architecture to induce VE-cadherin internalization coordinated by Tp0751 modulation of intracellular signaling;
(3) A small proportion of the *T. pallidum* population traverses endothelial barriers. This occurs without disrupting barrier permeability via two distinct mechanisms:
    a. Paracellular traversal of junctional-localized *T. pallidum* through transient junctional pores that prevent vascular leakage
    b. Transcellular traversal of lipid raft-localized *T. pallidum* through a raft-mediated endocytosis pathway

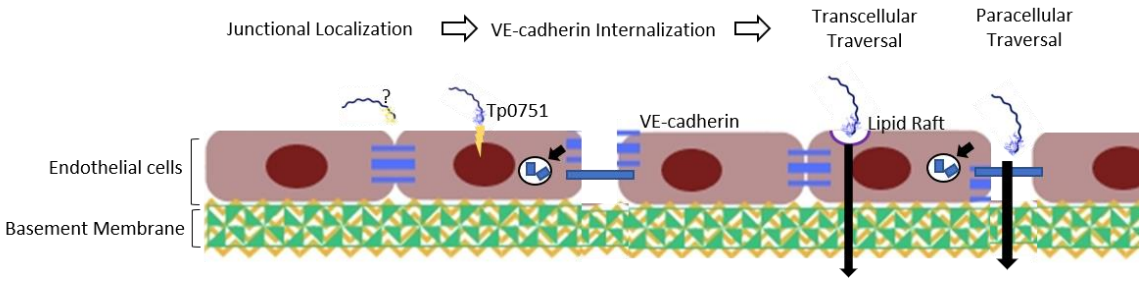

Figure 32: Proposed model for *T. pallidum* junctional disruption and transendothelial migration. A subpopulation of treponemal cells adheres to intercellular junctional regions of the endothelial barrier via an unknown receptor. The *T. pallidum* adhesin Tp0751 modifies endothelial signaling pathways to induce the internalization of VE-cadherin in clathrin-coated pits. Subsequently, *T. pallidum* can undergo endothelial transcellular traversal via lipid raft-mediated endocytosis or paracellular traversal through the openings in intercellular junctions.

5.1.3 Modulation of endothelial signaling pathways

Mass spectrometry-based techniques have previously been employed to study the proteome of *T. pallidum* (Osbak et al. 2016), but quantitative proteomics has never been harnessed to explore the host-pathogen interactions of *T. pallidum.* The results presented in Chapter 4 describe a workflow for quantitative analysis of changes to signaling networks facilitated by *T. pallidum* recombinant proteins. It is plausible that with additional optimization, this approach could be applied to investigate signaling networks modified by live *T. pallidum.*

Single-experiment discoveries from Chapter 4 include (1) bias toward Tp0751-regulation of cadherin and cytoskeletal proteins and (2) the identification of two intriguing endothelial signaling targets for Tp0751. Taken together, these preliminary findings suggest that Tp0751 adhesion to endothelial cells promotes junctional stabilization and cytoskeletal modulation. Two phosphorylated residues were identified for the F-actin binding protein drebrin: S^{141} and S^{142}, with increased phosphorylation observed in Tp0751-treated samples. Drebrin interacts with both cortical F-actin and afadin; these interactions establish a link between the actin cytoskeleton and intercellular junctions, since afadin is an intracellular adaptor for the adherens junction protein nectin (Rehm et al. 2013). The nectin/afadin/drebrin/F-actin complex is proposed to stabilize intercellular junctions, and

there is a growing body of knowledge that suggest such adaptor-mediated linkages between the cytoskeleton and intercellular junctions are critical for junctional stability and maintenance of endothelial barrier integrity (Rehm and Linder 2017; Lampugnani 2010). While the functional outcomes for drebrin S^{141} have not been explored, S^{142} phosphorylation is known to be carried out by the kinase Cdk5 to promote drebrin binding to F-actin bundles in lamellipodia (Worth et al. 2013). Protrusions of F-actin are commonly induced at the initiation phase of paracellular and transcellular traversal of leukocytes and invasive pathogens such as *N. meningitidis* and *E. coli*; thus, drebrin S^{142} phosphorylation may have important implications for the transendothelial migration of *T. pallidum.*

Endothelial cells treated with Tp0751 also exhibited increased phosphorylation of the F-actin binding protein cortactin at S^{405} and T^{401}. Cortactin is a key regulator of actin dynamics and is targeted by numerous bacterial pathogens for invasion of polarized cell barriers (Selbach and Backert 2005). These processes are largely coordinated by cortactin tyrosine phosphorylation. Less knowledge exists regarding serine phosphorylation of cortactin, though ERK1/2-mediated phosphorylation of S^{405} has been shown to potentiate cortactin interactions with N-WASP to induce polymerization of F-actin fibers (Campbell, Sutherland, and Daly 1999; Kelley et al. 2010; Martinez-Quiles et al. 2004). Furthermore, S^{405} phosphorylation plays a role in epithelial invasion by *Helicobacter pylori* by potentiating interactions with focal adhesion kinase (FAK) to modulate epithelial cell-matrix adhesion (Tegtmeyer et al. 2011). Like drebrin, cortactin localizes to lamellipodia, actin-based membrane protrusions (also referred to as membrane ruffles). The formation of membrane ruffles is an initiating step in macropinocytosis (Mercer and Helenius 2009) as well as *N. meningitidis* traversal of brain endothelial barriers (Lemichez et al. 2010). Furthermore, during the attachment stage of leukocyte and *N. meningitidis* transendothelial migration, F-actin membrane protrusions form around the cells to stabilize adhesion by providing a barrier to resist the forces of the blood flow (Lemichez et al. 2010; Schimmel, Heemskerk, and van Buul 2017; Mikaty et al. 2009). These results suggest that cortactin could play a role in actin polymerization at sites of *T. pallidum* adhesion to promote firm adhesion to the endothelium, promote endocytosis, or form F-actin rich contractile rings to prevent vascular leakage during *T. pallidum* paracellular transendothelial migration.

The involvement of ERK1/2 upstream of cortactin in Tp0751 mediated signaling pathways provides a possible link to Tp0751-mediated signaling through the endothelial receptor LamR. Previous investigations have demonstrated that LamR interacts directly with PED/PEA-15 (Phosphoprotein enriched in diabetes/phosphoprotein enriched in astrocytes-15), which contains an ERK binding site and two phosphorylation sites. LamR was shown to activate protein kinase C and CaMKII (Ca2+/calmodulin-dependent protein kinase) to induce phosphorylation of PED/PEA-15 at Ser^{104}. Although not directly observed in this study, phosphorylation of PED/PEA-15 at Ser^{104} induces the release of ERK and subsequent nuclear translocation to initiate transcriptional activity related to cell proliferation and prevention of apoptosis (Formisano et al. 2012). Such anti-apoptotic signals could be important for preserving vascular integrity during *T. pallidum* transendothelial migration. Conversely, to date there is no evidence for activation of drebrin downstream of LamR.

Taken together, these findings suggest that Tp0751 may induce the formation of F-actin polymerization to promote *T. pallidum* traversal of endothelial barriers, supporting a model (Figure 33) whereby Tp0751 induces:

(1) Stabilization of adherens junctions by linking the junctions to the actin cytoskeleton via protein complexes that include actin/drebrin/afadin/nectin. This stabilization may balance the junctional disruption of VE-cadherin to prevent vascular leakage during transendothelial migration;

(2) Cytoskeletal modulation to induce F-actin polymerization to assist in firm adhesion of the bacteria to the cell surface or formation of an F-actin rich contractile pore prevent vascular leakage during *T. pallidum* traversal of endothelial barriers.

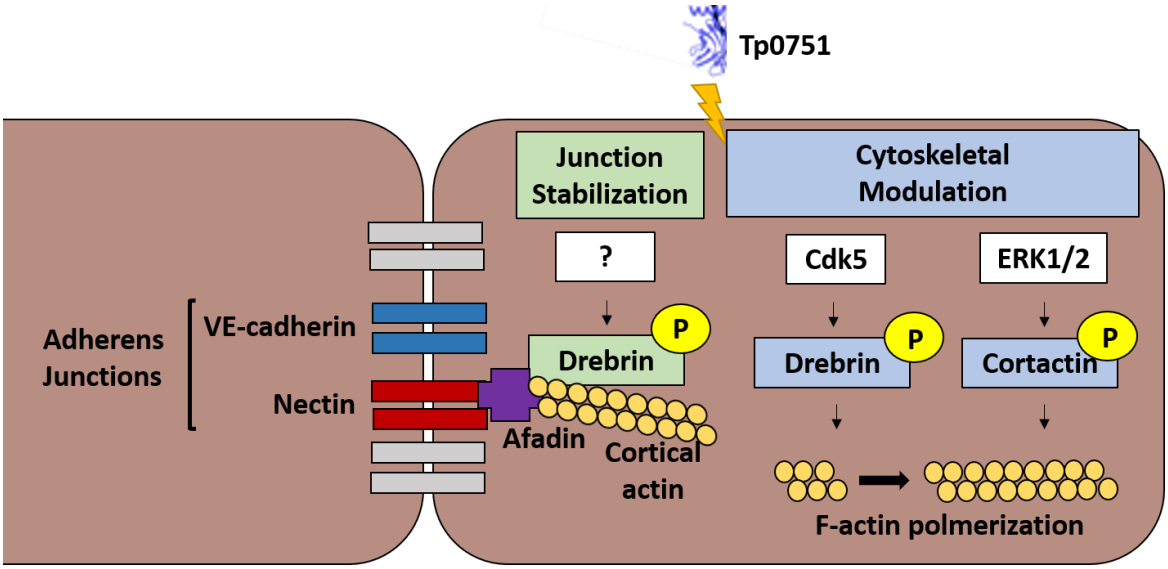

Figure 33: Proposed model for endothelial signaling pathways modified by Tp0751. Tp0751 adhesion to vascular surfaces results in increased phosphorylation of the F-actin binding proteins drebrin and cortactin. Junctional stabilization is facilitated by increased drebrin phosphorylation (unknown sites) which undergoes a conformational change to bind and link adherens junction complex nectin/afadin with the cortical actin cytoskeleton, preventing the full opening of adherens junctions during *T. pallidum* transendothelial migration. Increased phosphorylation of drebrin at S^{142} and cortactin at S^{405} is facilitated by Cdk5 and ERK1/2, respectively and induces the polymerization of F-actin. This promotes actin-based membrane protrusions that facilitate the uptake of *T. pallidum* during transendothelial migration, form F-actin contractile rings, or promote firm adhesion of the bacteria at the cell surface.

5.1.4 Proposed model for *T. pallidum* vascular adhesion and transendothelial migration

The combined body of work presented in this dissertation supports a model for *T. pallidum* transendothelial migration with elements that mimic key aspects of the traversal mechanisms of invasive bacteria and leukocytes. The phylogenetically distinct meningitis-causing pathogens *N. meningitidis, S. pneumoniae, H. influenzae,* and *T. pallidum* all interact with the same discrete region of LamR to facilitate adhesion to endothelial surfaces. Similar to other neuroinvasive pathogens, *T. pallidum* exhibits a functional redundancy in host binding adhesins, particularly fibronectin binding proteins. While there

is still much to be uncovered about the transendothelial migration process, *T. pallidum* shares common elements with invasive pathogens and leukocyte traversal that include (1) junctional disruption without altering vascular permeability, (2) modification of cortactin phosphorylation, and putatively, (3) the capacity to mediate both paracellular and transcellular traversal.

The combined findings presented in this dissertation support a modular model (Figure 34) for *T. pallidum* transendothelial migration, whereby different invasion strategies are utilized based upon the structural and phenotypic characteristics of the specific endothelial barrier:

(1) Transcellular traversal is employed for continuous endothelial barriers (e.g.: blood-brain barrier) and is facilitated by Tp0751 interactions with the endothelial lipid raft proteins stomatin and LamR that initiate a raft-mediated endocytosis pathway.

(2) Paracellular traversal is employed for fenestrated and discontinuous endothelial barriers (e.g.: liver) and is facilitated by Tp0750 interactions with annexin A2 at endothelial intercellular junctions. Tp0751 modifies intercellular junctions indirectly to open the paracellular route by modulating endothelial signaling pathways.

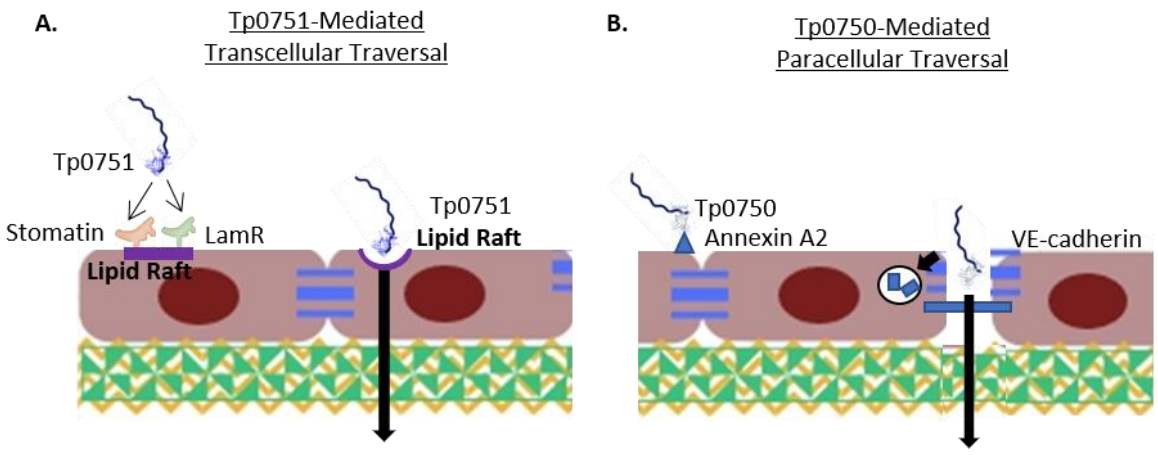

Figure 34: Proposed modular model for *T. pallidum* transendothelial migration. **(A)** Tp0751 facilitates *T. pallidum* transendothelial migration through a transcellular traversal mechanism. Tp0751 binds to lipid raft receptors, stomatin and LamR, to induce raft-mediated endocytosis. **(B)** Tp0750 facilitates *T. pallidum* transendothelial migration through a paracellular traversal mechanism. Tp0750 binds to Annexin A2 at intercellular junctions and traverses through junctional openings.

5.2 Understanding the molecular events of *T. pallidum* dissemination in the context of the disease progression of syphilis

Cardiovascular involvement in symptomatic stages of disease

There are drastic differences in the severity of symptoms that can occur during early versus late stage syphilis. Painless local and disseminated lesions that heal spontaneously are characteristic of the primary and secondary stages of early syphilis, while tertiary syphilis can include severe manifestations ranging from gummatous lesions to severe cardiovascular and neurological manifestations. Cardiovascular complications during tertiary syphilis were a predominant cause of patient mortality in the pre-antibiotic era, frequently manifesting as inflammation of localized regions within the heart or vasculature (Kampmeier 1946, 1948, 1972; Weinstein, Kampmeier, and Harwood 1957; Kampmeier 1964). Meningovascular syphilis is the inflammation of arterial blood vessels in the CNS which can result in blood clotting and vessel obstruction. Predicted to occur in up to 10% of modern neurosyphilis cases (Perdrup, Jorgensen, and Pedersen 1981; Danielsen et al. 2004), meningovascular syphilis often presents as headache or vertigo, but can also lead to

ischemic stroke (Ghanem 2010). In contrast to the localized inflammatory responses that underlie disease manifestations, systemic inflammation is not a sequela of syphilis despite the repeated rounds of vascular dissemination that occur throughout the course of infection.

At a molecular level, *T. pallidum* has been shown to activate endothelial cells, inducing the production of proinflammatory cytokines and upregulation of leukocyte adhesion molecules (Riley et al. 1992; Riley et al. 1994). This endothelial response functions to recruit immune cells to sites of infection or damage and has been attributed to *T. pallidum* proteins that localize to the periplasm including two lipoproteins: Tp0435 and Tp0574 (Riley et al. 1992; Zhang et al. 2015). While the surface of *T. pallidum* is antigenically inert owing to the lack of LPS and scarcity of outer membrane proteins, it has been postulated that when treponemes are degraded during opsonophagocytosis, lipopeptides become liberated from the periplasm and activate local immune cells to produce an inflammatory response. When Tp0435 is heterologously expressed in *B. burgdorferi,* two lipidated isoforms of the protein are produced and differentially localize to the periplasm and the cell surface (Chan et al. 2016). This presents the intriguing possibility that *T. pallidum* lipoproteins could exhibit stochastic or transient expression on the cell surface to activate the host immune system during symptomatic stages of infection, while periplasmic localization of lipoproteins would facilitate immune evasion during systemic dissemination and latent stages of the disease.

The results presented in this body of work demonstrate that *T. pallidum* transendothelial migration occurs without disrupting barrier permeability, which corroborates previous *in vitro* findings (Thomas et al. 1989; Thomas et al. 1988). While these *in vitro* studies have observed activation of endothelial cells, it is important to recognize that endothelial cell activation elicits a spectrum of responses. At one end of the spectrum is endothelial dysfunction, whereby sustained activation of the endothelium results in systemic inflammation and sepsis leading to modulation of endothelial barrier permeability, vascular leakage and tissue edema (Ferro et al. 2000; Ferro et al. 1997; Goldblum et al. 1993; Goldblum, Ding, and Campbell-Washington 1993). The lack of systemic inflammation or sepsis during disease progression of syphilis supports a transendothelial migration mechanism for *T. pallidum* where endothelial barrier permeability is not altered. A stealth mechanism for endothelial traversal is reinforced by

that fact that *T. pallidum* localizes to diverse anatomical sites and undergoes periods of latency during which no clinical manifestations are observed in the secondary infection sites (Lafond and Lukehart 2006). However, there are several clinical manifestations of syphilis that suggest endothelial pathology. Histological evaluation of primary and secondary lesions reveals that endothelial cell swelling is a common feature in these inflammatory sites (Rato 2018; Abell, Marks, and Jones 1975). Increased volume of endothelial cells is an initiating step in ischemic injury that results in reduced blood supply to underlying tissue sites (Corso et al. 1998). General paresis, a neurological manifestation of tertiary syphilis, can be accompanied by chronic meningitis, where *T. pallidum* can be found inside brain endothelial cells (Merritt, Adams, and Solomon 1946). It is not clear if endothelial invasion directly contributes to this clinical manifestation. Furthermore, during meningovascular syphilis, inflammation of arterial blood vessels in the meninges can result in thrombosis and vessel obstruction causing ischemic stroke (Ghanem 2010). The disease progression of syphilis manifests as a balance between inflammation during symptomatic active stages of infection and immune evasion during stages of latency. The data presented herein suggest that *T. pallidum*-endothelial interactions also contribute to this dichotomy.

A model for two distinct *T. pallidum*-endothelial cell interaction types

The findings in this body of work, taken in the context of previous investigations, suggest a model (Figure 35) for two distinct mechanisms of *T. pallidum*-endothelial cell interactions:

(A) Localized inflammation that occurs during active symptomatic infection is coordinated by endothelial cell responses to immunogenic lipoproteins stochastically expressed on the surface of *T. pallidum* or released from degraded *T. pallidum* cells during immune clearance. Local inflammation modulates barrier permeability in perivascular sites, providing an easy route for *T. pallidum* intravasation that facilitates systemic dissemination.

(B) During vascular dissemination and stages of asymptomatic latency, *T. pallidum* interactions with endothelial cells allow for non-inflammatory extravasation into secondary infection sites. This process may result in limited endothelial activation at the local site of extravasation but does not alter barrier

permeability, induce tissue damage, or potentiate abundant cellular infiltration. Early intravasation events out of the primary lesion occur without activating the immune system, since *T. pallidum* vascular dissemination takes place prior to the cellular infiltration and inflammation that underlies the formation of primary lesions.

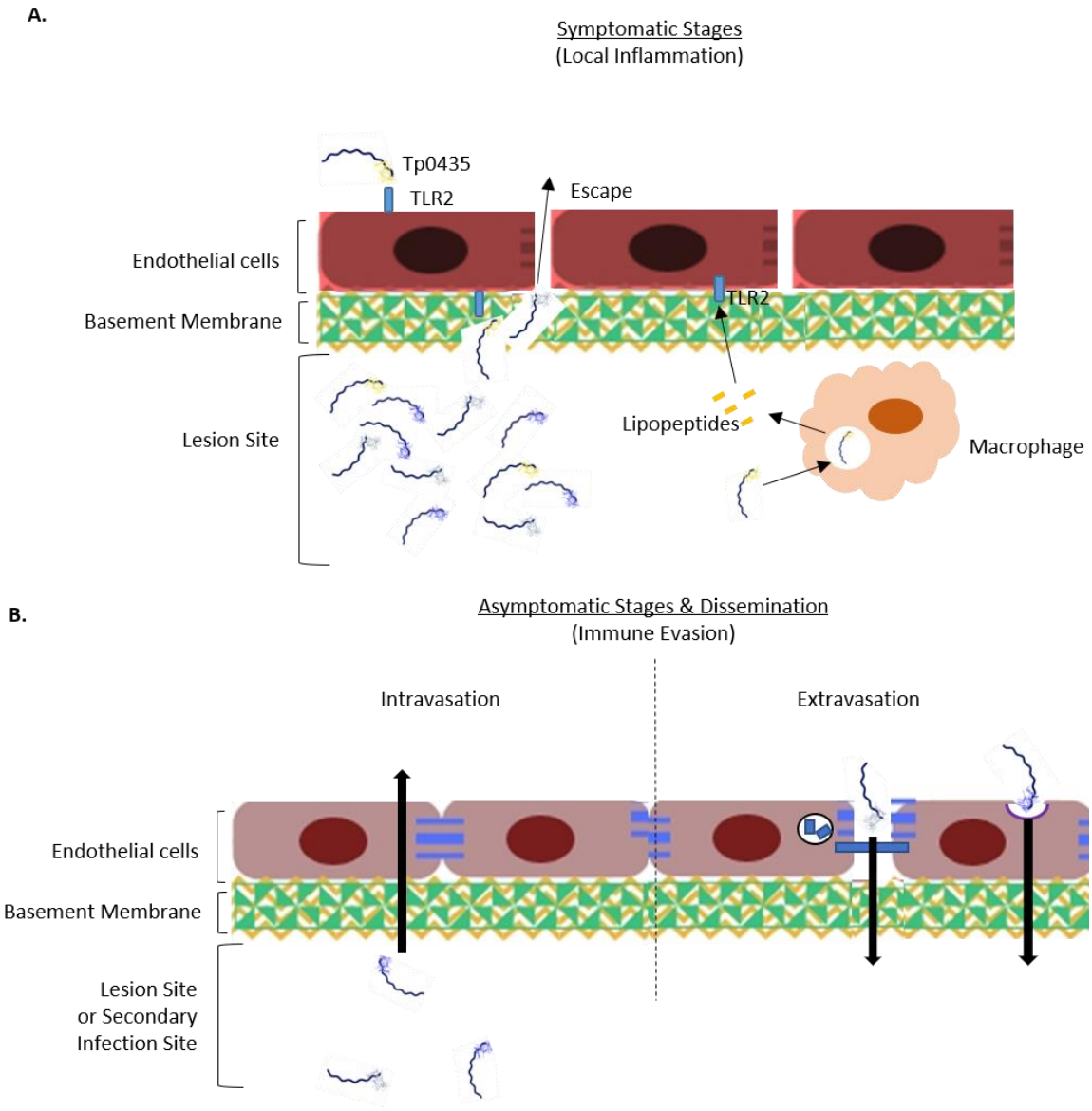

Figure 35: Proposed model for two distinct *T. pallidum*-endothelial interaction types. **(A)** During symptomatic stages of the disease progression, activation of the vascular endothelium is induced after treponemal proliferation and cellular infiltration has occurred.

Endothelial cells become activated (depicted in red) in response to *T. pallidum* lipoproteins (depicted in yellow) that are stochastically expressed on the spirochete surface or by lipopeptides released during macrophage opsonophagocytosis of *T. pallidum*. Endothelial activation may result in localized increases in barrier permeability (depicted as gaps between endothelial cells) that allow for treponemal escape into the vasculature to mediate systemic dissemination. **(B)** Immediately after infection and during asymptomatic stages of the disease progression, *T. pallidum* traverses the endothelial barrier using a stealth mechanism where endothelial cells do not become activated and there is no change in endothelial barrier permeability. Treponemes can undergo intravasation and extravasation using this stealth mechanism.

5.3 Implications for vaccine development

Informed vaccine design for the prevention of syphilis must target the active stages of infection, principally the formation of the primary chancre that facilitates transmission but must also impede treponemal escape from the initial infection site before bacteria can undergo systemic dissemination. An improved understanding of *T. pallidum*-endothelial interactions and the molecular machinery that drives adhesion and transendothelial migration is critical for developing an efficacious vaccine. Chapter 2 of this dissertation explored the molecular interface between Tp0751 and its endothelial receptor, LamR, revealing a putative charge-based interaction. Mapping the regions of Tp0751 that facilitate treponemal dissemination can guide vaccine development by informing antigen selection to design immunogens that will promote immune recognition of the discrete regions of Tp0751 that drive *T. pallidum* invasion. The findings in Chapter 2 of this dissertation revealed that endothelial binding localizes to the lipocalin region of the protein and that a discrete region (p10) of Tp0751 can interfere with spirochete adhesion *in vitro*. Future immunization protocols should use an antigen cocktail of Tp0751 (E115-P237) and peptide 10 (p10) to encourage immune recognition of regions of Tp0751 with a functional role in endothelial binding and dissemination. Furthermore, the knowledge that Tp0751 can facilitate adhesion to endothelial cell lines of diverse origin, including a cerebral brain microvascular endothelial cell line, suggests that Tp0751-mediated attachment is a

conserved mechanism for endothelial adhesion throughout heterogeneous sites in the vasculature.

5.4 Future perspectives

This body of work opens several new avenues for investigations of *T. pallidum*-host interactions. Additional work should explore the endothelial receptor interactions of Tp0751 with a focus on how lipid rafts contribute to the treponemal adhesion process. As *T. pallidum* exhibits redundancy in ECM-binding adhesins, it is also likely that this pathogen could employ numerous endothelial adhesins to facilitate vascular attachment and initiate transendothelial migration. The putative host cell binding adhesins Tp0750 and Tp0435 should be further explored to understand their contribution to treponemal dissemination. The interplay between Tp0751 and Tp0750 should also be investigated to determine if these proteins act in concert to drive *T. pallidum* attachment and traversal, or if these proteins each facilitate a distinct mechanism of adhesion and transendothelial migration. Identification of additional adhesins and receptors will provide an opportunity to explore whether the process of *T. pallidum* vascular adhesion and transendothelial migration occurs via coordinated sequential interactions between the bacteria and endothelial cells.

It is challenging to model true barrier properties of the vascular endothelium *in vitro*. In Chapter 2, Tp0751 adhesion to diverse endothelial cell types was evaluated. To extend the knowledge of whether a conserved transendothelial migration strategy exists for heterogeneous sites in the vasculature, *T. pallidum* traversal should be investigated across a broader range of endothelial cell types and in the presence of physiological shear stress that mimics conditions of the blood flow *in vivo.* Going forward, a major research focus should be developing techniques for the live imaging of *T. pallidum.* This method would allow for the assessment of *T. pallidum* transendothelial migration dynamics in an *in vitro* model system. Evaluating real-time changes in *T. pallidum* interactions with lipid rafts, modulation of actin dynamics, and visualization of transcellular or paracellular traversal of endothelial barriers could yield critical information about the dissemination mechanisms of this pathogen. A live imaging technique for *T. pallidum* could also be applied to observe

vascular interactions *in vivo* using intravital microscopy as previously described for *B. burgdorferi* (Moriarty et al. 2008).

The work presented in Chapter 4 presents an optimized workflow for the investigation of host signaling networks modified by Tp0751. By scaling up this experiment, future investigations could unravel the exact signaling network engaged by Tp0751. Further to this, the workflow could be applied to other *T. pallidum* host binding proteins as well as live *T. pallidum.* The *in vivo* propagation of *T. pallidum* presents numerous technical challenges for downstream experimentation, including the abundance of rabbit serum that contaminate the organisms extracted from the *in vivo* propagation. This abundance of serum would preclude a triplex SILAC experiment with live *T. pallidum*, as the excess serum would introduce unlabelled amino acids that would confound data analysis for the light channel. However, a duplex experiment with medium and heavy isotopically labelled amino acids could be employed. The excess serum would still have a masking effect during mass spectrometry, but this experimental approach could provide some initial insights into endothelial signaling networks modulated by *T. pallidum.*

Transendothelial migration is a highly complex process and experimental determination of the molecular events is a significant challenge. However, this process is best understood for immune cell traversal of endothelial barriers, and novel techniques developed for studying immune extravasation should be considered for exploring *T. pallidum* dissemination. Recent investigations in the leukocyte transendothelial migration field have demonstrated preferential use of transcellular or paracellular traversal depending of the immune cell extravasation site in the vasculature. This was accomplished using a "locked" VE-cadherin-catenin complex that prevents the opening of the paracellular pathway (Schulte et al. 2011; Kuppers, Vestweber, and Schulte 2013). Although these investigations were performed *in vivo* in genetically modified mice, a similar approach could be used with an *in vitro* endothelial barrier system.

This body of work represents significant advancements to the understanding of *T. pallidum*-endothelial cell interactions, an important step in vascular dissemination of bacterial pathogens. The findings presented herein demonstrate how *T. pallidum* and the adhesin Tp0751 mediate adherence to endothelial cells, alter endothelial junctional integrity without modifying barrier permeability, and induce changes in endothelial

signaling pathways. These investigations provide insight into the specific molecular mechanisms of *T. pallidum* dissemination and reveal intriguing parallels with other invasive bacterial pathogens that are phylogenetically distinct. Furthermore, key similarities can be observed for the transendothelial migration process of leukocytes and *T. pallidum.* This body of work combined with the future investigations proposed in this chapter provide a roadmap for the in-depth molecular characterization of *T. pallidum* traversal of endothelial barriers.

Bibliography

Abell, E., R. Marks, and E. W. Jones. 1975. 'Secondary syphilis: a clinico-pathological review', *Br J Dermatol*, 93: 53-61.

Abouseada, N. M., M. S. Assafi, J. Mahdavi, N. J. Oldfield, L. M. Wheldon, K. G. Wooldridge, and D. A. Ala'Aldeen. 2012. 'Mapping the laminin receptor binding domains of *Neisseria meningitidis* PorA and *Haemophilus influenzae* OmpP2', *PLoS One*, 7: e46233.

Abu Taha, A., and H. J. Schnittler. 2014. 'Dynamics between actin and the VE-cadherin/catenin complex: novel aspects of the ARP2/3 complex in regulation of endothelial junctions', *Cell Adh Migr*, 8: 125-35.

Agerer, F., A. Michel, K. Ohlsen, and C. R. Hauck. 2003. 'Integrin-mediated invasion of *Staphylococcus aureus* into human cells requires Src family protein-tyrosine kinases', *J Biol Chem*, 278: 42524-31.

Aird, W. C. 2003. 'The role of the endothelium in severe sepsis and multiple organ dysfunction syndrome', *Blood*, 101: 3765-77.

Aird, W. C. 2007a. 'Phenotypic heterogeneity of the endothelium: II. Representative vascular beds', *Circ Res*, 100: 174-90.

Aird, W. C. 2007b. 'Phenotypic heterogeneity of the endothelium: I. Structure, function, and mechanisms', *Circ Res*, 100: 158-73.

Akache, B., D. Grimm, K. Pandey, S. R. Yant, H. Xu, and M. A. Kay. 2006. 'The 37/67-kilodalton laminin receptor is a receptor for adeno-associated virus serotypes 8, 2, 3, and 9', *J Virol*, 80: 9831-6.

Alon, R., and J. D. van Buul. 2017. 'Leukocyte Breaching of Endothelial Barriers: The Actin Link', *Trends Immunol*, 38: 606-15.

Alderete, J.F. and J.B. Baseman. 1979. Surface-associated host proteins on virulent *Treponema pallidum*. *Infect Immun*, 26:1048–56.

Anand, A., A. Luthra, S. Dunham-Ems, M. J. Caimano, C. Karanian, M. LeDoyt, A. R. Cruz, J. C. Salazar, and J. D. Radolf. 2012. 'TprC/D (Tp0117/131), a trimeric, pore-forming rare outer membrane protein of *Treponema pallidum*, has a bipartite domain structure', *J Bacteriol*, 194: 2321-33.

Andriopoulou, P., P. Navarro, A. Zanetti, M. G. Lampugnani, and E. Dejana. 1999. 'Histamine induces tyrosine phosphorylation of endothelial cell-to-cell adherens junctions', *Arterioscler Thromb Vasc Biol*, 19: 2286-97.

Ardito, F., M. Giuliani, D. Perrone, G. Troiano, and L. Lo Muzio. 2017. 'The crucial role of protein phosphorylation in cell signaling and its use as targeted therapy (Review)', *Int J Mol Med*, 40: 271-80.

Aryal, U. K., and A. R. Ross. 2010. 'Enrichment and analysis of phosphopeptides under different experimental conditions using titanium dioxide affinity chromatography and mass spectrometry', *Rapid Commun Mass Spectrom*, 24: 219-31.

Baeyens, N. 2018. 'Fluid shear stress sensing in vascular homeostasis and remodeling: Towards the development of innovative pharmacological approaches to treat vascular dysfunction', *Biochem Pharmacol*, 158: 185-91.

Baker-Zander, S. A., J. M. Shaffer, and S. A. Lukehart. 1993. 'Characterization of the serum requirement for macrophage-mediated killing of *Treponema pallidum* ssp.

pallidum: relationship to the development of opsonizing antibodies', *FEMS Immunol Med Microbiol*, 6: 273-9.

Baker, M. 2016. 'Reproducibility: Respect your cells!', *Nature*, 537: 433-5.

Baltierra-Uribe, S. L., J. Garcia-Vasquez Mde, N. S. Castrejon-Jimenez, M. P. Estrella-Pinon, J. Luna-Herrera, and B. E. Garcia-Perez. 2014. 'Mycobacteria entry and trafficking into endothelial cells', *Can J Microbiol*, 60: 569-77.

Bansal, R. C., H. Cohn, K. Fani, and Y. L. Lynfield. 1978. 'Nephrotic syndrome and granulomatous hepatitis in secondary syphilis', *Arch Dermatol*, 114: 1228-9.

Barocchi, M. A., A. I. Ko, M. G. Reis, K. L. McDonald, and L. W. Riley. 2002. 'Rapid translocation of polarized MDCK cell monolayers by *Leptospira interrogans*, an invasive but nonintracellular pathogen', *Infect Immun*, 70: 6926-32.

Basagiannis, D., S. Zografou, K. Galanopoulou, and S. Christoforidis. 2017. 'Dynasore impairs VEGFR2 signalling in an endocytosis-independent manner', *Sci Rep*, 7: 45035.

Baughn, R. E., and D. M. Musher. 2005. 'Secondary syphilitic lesions', *Clin Microbiol Rev*, 18: 205-16.

Bendayan, M. 2002. 'Morphological and cytochemical aspects of capillary permeability', *Microsc Res Tech*, 57: 327-49.

Benndorf, R., K. Hayess, S. Ryazantsev, M. Wieske, J. Behlke, and G. Lutsch. 1994. 'Phosphorylation and supramolecular organization of murine small heat shock protein HSP25 abolish its actin polymerization-inhibiting activity', *J Biol Chem*, 269: 20780-4.

Bian, J., Y. Tu, S. M. Wang, X. Y. Wang, and C. Li. 2015. 'Evidence that TP_0144 of *Treponema pallidum* is a thiamine-binding protein', *J Bacteriol*, 197: 1164-72.

Bischoff, I., M. C. Hornburger, B. A. Mayer, A. Beyerle, J. Wegener, and R. Furst. 2016. 'Pitfalls in assessing microvascular endothelial barrier function: impedance-based devices versus the classic macromolecular tracer assay', *Sci Rep*, 6: 23671.

Bishop RE. 2000. The bacterial lipocalins. Biochim Biophys Acta. 1482(1–2): 73–83.

Blume-Jensen, P., and T. Hunter. 2001. 'Oncogenic kinase signalling', *Nature*, 411: 355-65.

Bogatcheva, N. V., A. D. Verin, P. Wang, A. A. Birukova, K. G. Birukov, T. Mirzopoyazova, D. M. Adyshev, E. T. Chiang, M. T. Crow, and J. G. Garcia. 2003. 'Phorbol esters increase MLC phosphorylation and actin remodeling in bovine lung endothelium without increased contraction', *Am J Physiol Lung Cell Mol Physiol*, 285: L415-26.

Bondarenko, E. I., E. V. Protopopova, S. N. Konovalova, A. V. Sorokin, A. V. Kachko, I. V. Surovtsev, and V. B. Loktev. 2003. '[Laminin-binding protein (LBP) as a cellular receptor for the virus of Venezuelan equine encephalomyelitis (VEE): Part 1. A study of the interaction between VEE virus virions and the human recombinant LBP]', *Mol Gen Mikrobiol Virusol*: 36-9.

Bondarenko, E. I., E. V. Protopopova, S. N. Konovalova, I. V. Surovtsev, V. P. Mal'tsev, and V. B. Loktev. 2004. '[Laminin-binding protein as a cellular receptor for the equine Venezuelan encephalomyelitis virus: Report 2. Inhibition of replication of equine Venezuelan encephalomyelitis virus by blocking laminin-binding protein on the surface of Vero cells]', *Mol Gen Mikrobiol Virusol*: 36-40.

Bougneres, L., S. E. Girardin, S. A. Weed, A. V. Karginov, J. C. Olivo-Marin, J. T. Parsons, P. J. Sansonetti, and G. T. Van Nhieu. 2004. 'Cortactin and Crk cooperate to trigger actin polymerization during Shigella invasion of epithelial cells', *J Cell Biol*, 166: 225-35.

Bouyssie, D., A. Gonzalez de Peredo, E. Mouton, R. Albigot, L. Roussel, N. Ortega, C. Cayrol, O. Burlet-Schiltz, J. P. Girard, and B. Monsarrat. 2007. 'Mascot file parsing and quantification (MFPaQ), a new software to parse, validate, and quantify proteomics data generated by ICAT and SILAC mass spectrometric analyses: application to the proteomics study of membrane proteins from primary human endothelial cells', *Mol Cell Proteomics*, 6: 1621-37.

Brautigam, C. A., R. K. Deka, Z. Ouyang, M. Machius, G. Knutsen, D. R. Tomchick, and M. V. Norgard. 2012. 'Biophysical and bioinformatic analyses implicate the *Treponema pallidum* Tp34 lipoprotein (Tp0971) in transition metal homeostasis', *J Bacteriol*, 194: 6771-81.

Brautigam, C. A., R. K. Deka, P. Schuck, D. R. Tomchick, and M. V. Norgard. 2012. 'Structural and thermodynamic characterization of the interaction between two periplasmic *Treponema pallidum* lipoproteins that are components of a TPR-protein-associated TRAP transporter (TPAT)', *J Mol Biol*, 420: 70-86.

Brinkman, M. B., M. A. McGill, J. Pettersson, A. Rogers, P. Matejkova, D. Smajs, G. M. Weinstock, S. J. Norris, and T. Palzkill. 2008. 'A novel *Treponema pallidum* antigen, TP0136, is an outer membrane protein that binds human fibronectin', *Infect Immun*, 76: 1848-57.

Buchacz, K., P. Patel, M. Taylor, P. R. Kerndt, R. H. Byers, S. D. Holmberg, and J. D. Klausner. 2004. 'Syphilis increases HIV viral load and decreases CD4 cell counts in HIV-infected patients with new syphilis infections', *AIDS*, 18: 2075-9.

Burghoff, S., and J. Schrader. 2011. 'Secretome of human endothelial cells under shear stress', *J Proteome Res*, 10: 1160-9.

Byard, R. W. 2018. 'Syphilis-Cardiovascular Manifestations of the Great Imitator', *J Forensic Sci*, 63: 1312-15.

Cameron, C. E. 2003. 'Identification of a *Treponema pallidum* laminin-binding protein', *Infect Immun*, 71: 2525-33.

Cameron, C. E., N. L. Brouwer, L. M. Tisch, and J. M. Kuroiwa. 2005. 'Defining the interaction of the *Treponema pallidum* adhesin Tp0751 with laminin', *Infect Immun*, 73: 7485-94.

Cameron, C. E., E. L. Brown, J. M. Kuroiwa, L. M. Schnapp, and N. L. Brouwer. 2004. '*Treponema pallidum* fibronectin-binding proteins', *J Bacteriol*, 186: 7019-22.

Cameron, C. E., C. Castro, S. A. Lukehart, and W. C. Van Voorhis. 1998. 'Function and protective capacity of *Treponema pallidum* subsp. *pallidum* glycerophosphodiester phosphodiesterase', *Infect Immun*, 66: 5763-70.

Cameron, C. E., J. M. Kuroiwa, M. Yamada, T. Francescutti, B. Chi, and H. K. Kuramitsu. 2008. 'Heterologous expression of the *Treponema pallidum* laminin-binding adhesin Tp0751 in the culturable spirochete *Treponema phagedenis*', *J Bacteriol*, 190: 2565-71.

Cameron, C. E., S. A. Lukehart, C. Castro, B. Molini, C. Godornes, and W. C. Van Voorhis. 2000. 'Opsonic potential, protective capacity, and sequence conservation

of the *Treponema pallidum* subspecies *pallidum* Tp92', *J Infect Dis*, 181: 1401-13.

Campbell, D. H., R. L. Sutherland, and R. J. Daly. 1999. 'Signaling pathways and structural domains required for phosphorylation of EMS1/cortactin', *Cancer Res*, 59: 5376-85.

Cantarelli, V. V., T. Kodama, N. Nijstad, S. K. Abolghait, T. Iida, and T. Honda. 2006. 'Cortactin is essential for F-actin assembly in enteropathogenic *Escherichia coli* (EPEC)- and enterohaemorrhagic *E. coli* (EHEC)-induced pedestals and the alpha-helical region is involved in the localization of cortactin to bacterial attachment sites', *Cell Microbiol*, 8: 769-80.

Cantarelli, V. V., A. Takahashi, Y. Akeda, K. Nagayama, and T. Honda. 2000. 'Interaction of enteropathogenic or enterohemorrhagic *Escherichia coli* with HeLa cells results in translocation of cortactin to the bacterial adherence site', *Infect Immun*, 68: 382-6.

Cantarelli, V. V., A. Takahashi, I. Yanagihara, Y. Akeda, K. Imura, T. Kodama, G. Kono, Y. Sato, T. Iida, and T. Honda. 2002. 'Cortactin is necessary for F-actin accumulation in pedestal structures induced by enteropathogenic *Escherichia coli* infection', *Infect Immun*, 70: 2206-9.

Cantini F, Veggi D, Dragonetti S, Savino S, Scarselli M, Romagnoli G, Pizza M, Banci L, and Rappuoli R. 2009. Solution structure of the factor H-binding protein, a survival factor and protective antigen of *Neisseria meningitidis*. J Biol Chem, 284(14): 9022–6.

Cao, J., M. Ehling, S. Marz, J. Seebach, K. Tarbashevich, T. Sixta, M. E. Pitulescu, A. C. Werner, B. Flach, E. Montanez, E. Raz, R. H. Adams, and H. Schnittler. 2017. 'Polarized actin and VE-cadherin dynamics regulate junctional remodelling and cell migration during sprouting angiogenesis', *Nat Commun*, 8: 2210.

Cao, J., and H. Schnittler. 2019. 'Putting VE-cadherin into JAIL for junction remodeling', *J Cell Sci*, 132.

Caporarello, N., M. Olivieri, M. Cristaldi, M. Scalia, M. A. Toscano, C. Genovese, A. Addamo, M. Salmeri, G. Lupo, and C. D. Anfuso. 2018. 'Blood-Brain Barrier in a *Haemophilus influenzae* Type a In Vitro Infection: Role of Adenosine Receptors A2A and A2B', *Mol Neurobiol*, 55: 5321-36.

Carlson, J. A., G. Dabiri, B. Cribier, and S. Sell. 2011. 'The immunopathobiology of syphilis: the manifestations and course of syphilis are determined by the level of delayed-type hypersensitivity', *Am J Dermatopathol*, 33: 433-60.

Carman, C. V., and T. A. Springer. 2008. 'Trans-cellular migration: cell-cell contacts get intimate', *Curr Opin Cell Biol*, 20: 533-40.

Casas, C.P.H., M. Martyn-St James, J. Hamilton, D. S. Marinho, R. Castro, and S. Harnan. 2018. 'Rapid diagnostic test for antenatal syphilis screening in low-income and middle-income countries: a systematic review and meta-analysis', *BMJ Open*, 8: e018132.

Cassels, S., and D. A. Katz. 2013. 'Seroadaptation among men who have sex with men: emerging research themes', *Curr HIV/AIDS Rep*, 10: 305-13.

Castronovo, V., G. Taraboletti, and M. E. Sobel. 1991. 'Functional domains of the 67-kDa laminin receptor precursor', *J Biol Chem*, 266: 20440-6.

Cendron L, Veggi D, Girardi E, Zanotti G. 2011. Structure of the uncomplexed *Neisseria meningitidis* factor H-binding protein fHbp (rLP2086). Acta Crystallogr Sect F Struct Biol Cryst Commun. 67(Pt 5): 531–5.

Centers for Disease Control and Prevention. 1998. 'HIV prevention through early detection and treatment of other sexually transmitted diseases--United States. Recommendations of the Advisory Committee for HIV and STD prevention', *MMWR Recomm Rep*, 47: 1-24.

Centers for Disease Control and Prevention. 2019. 'Sexually Transmitted Disease Surveillance 2017': 1-110. Available from: https://www.cdc.gov/std/stats17/toc.htm

Centurion-Lara, A., C. Castro, L. Barrett, C. Cameron, M. Mostowfi, W. C. Van Voorhis, and S. A. Lukehart. 1999. '*Treponema pallidum* major sheath protein homologue Tpr K is a target of opsonic antibody and the protective immune response', *J Exp Med*, 189: 647-56.

Centurion-Lara, A., R. E. LaFond, K. Hevner, C. Godornes, B. J. Molini, W. C. Van Voorhis, and S. A. Lukehart. 2004. 'Gene conversion: a mechanism for generation of heterogeneity in the tprK gene of *Treponema pallidum* during infection', *Mol Microbiol*, 52: 1579-96.

Cerutti, C., and A. J. Ridley. 2017. 'Endothelial cell-cell adhesion and signaling', *Exp Cell Res*, 358: 31-38.

Chan, K., T. Nasereddin, L. Alter, A. Centurion-Lara, L. Giacani, and N. Parveen. 2016. '*Treponema pallidum* Lipoprotein TP0435 Expressed in *Borrelia burgdorferi* Produces Multiple Surface/Periplasmic Isoforms and mediates Adherence', *Sci Rep*, 6: 25593.

Chapel, T. A. 1978. 'The variability of syphilitic chancres', *Sex Transm Dis*, 5: 68-70.

Chapel, T. A. 1980. 'The signs and symptoms of secondary syphilis', *Sex Transm Dis*, 7: 161-4.

Chapel, T. A. 1981. 'Physician recognition of the signs and symptoms of secondary syphilis', *JAMA*, 246: 250-1.

Chawla, V., K. Gupta, and M. B. Raghu. 1985. 'Congenital syphilis: a clinical profile', *J Trop Pediatr*, 31: 204-8.

Chen, G., Y. Cao, Y. Yao, M. Li, W. Tang, J. Li, G. R. Babu, Y. Jia, X. Huan, G. Xu, H. Yang, G. Fu, and L. Li. 2017. 'Syphilis incidence among men who have sex with men in China: results from a meta-analysis', *Int J STD AIDS*, 28: 170-78.

Chen, J., W. R. He, L. Shen, H. Dong, J. Yu, X. Wang, S. Yu, Y. Li, S. Li, Y. Luo, Y. Sun, and H. J. Qiu. 2015. 'The laminin receptor is a cellular attachment receptor for classical Swine Fever virus', *J Virol*, 89: 4894-906.

Cheruiyot, C., Z. Pataki, R. Williams, B. Ramratnam, and M. Li. 2017. 'SILAC Based Proteomic Characterization of Exosomes from HIV-1 Infected Cells', *J Vis Exp*.

Choudhri, Y., J. Miller, J. Sandhu, A. Leon, and J. Aho. 2018. 'Infectious and congenital syphilis in Canada, 2010-2015', *Can Commun Dis Rep*, 44: 43-48.

Christiansen S. 1963. Protective layer covering pathogenic treponemata, *Lancet*, 1:423–25.

Chung, J. W., S. J. Hong, K. J. Kim, D. Goti, M. F. Stins, S. Shin, V. L. Dawson, T. M. Dawson, and K. S. Kim. 2003. '37-kDa laminin receptor precursor modulates

cytotoxic necrotizing factor 1-mediated RhoA activation and bacterial uptake', *J Biol Chem*, 278: 16857-62.

Claude, P. 1978. 'Morphological factors influencing transepithelial permeability: a model for the resistance of the zonula occludens', *J Membr Biol*, 39: 219-32.

Clevenger, C. V. 2004. 'Roles and regulation of stat family transcription factors in human breast cancer', *Am J Pathol*, 165: 1449-60.

Collart, P., P. Franceschini, and P. Durel. 1971. 'Experimental rabbit syphilis', *Br J Vener Dis*, 47: 389-400.

Comstock, L. E., and D. D. Thomas. 1989. 'Penetration of endothelial cell monolayers by *Borrelia burgdorferi*', *Infect Immun*, 57: 1626-8.

Corso, C. O., S. Okamoto, R. Leiderer, and K. Messmer. 1998. 'Resuscitation with hypertonic saline dextran reduces endothelial cell swelling and improves hepatic microvascular perfusion and function after hemorrhagic shock', *J Surg Res*, 80: 210-20.

Coureuil, M., H. Lecuyer, S. Bourdoulous, and X. Nassif. 2017. 'A journey into the brain: insight into how bacterial pathogens cross blood-brain barriers', *Nat Rev Microbiol*, 15: 149-59.

Coureuil, M., H. Lecuyer, M. G. Scott, C. Boularan, H. Enslen, M. Soyer, G. Mikaty, S. Bourdoulous, X. Nassif, and S. Marullo. 2010. 'Meningococcus Hijacks a beta2-adrenoceptor/beta-Arrestin pathway to cross brain microvasculature endothelium', *Cell*, 143: 1149-60.

Coureuil, M., G. Mikaty, F. Miller, H. Lecuyer, C. Bernard, S. Bourdoulous, G. Dumenil, R. M. Mege, B. B. Weksler, I. A. Romero, P. O. Couraud, and X. Nassif. 2009. 'Meningococcal type IV pili recruit the polarity complex to cross the brain endothelium', *Science*, 325: 83-7.

Cox, D. L., D. R. Akins, S. F. Porcella, M. V. Norgard, and J. D. Radolf. 1995. '*Treponema pallidum* in gel microdroplets: a novel strategy for investigation of treponemal molecular architecture', *Mol Microbiol*, 15: 1151-64.

Cox, D. L., P. Chang, A. W. McDowall, and J. D. Radolf. 1992. 'The outer membrane, not a coat of host proteins, limits antigenicity of virulent *Treponema pallidum*', *Infect Immun*, 60: 1076-83.

Cox, D. L., A. Luthra, S. Dunham-Ems, D. C. Desrosiers, J. C. Salazar, M. J. Caimano, and J. D. Radolf. 2010. 'Surface immunolabeling and consensus computational framework to identify candidate rare outer membrane proteins of *Treponema pallidum*', *Infect Immun*, 78: 5178-94.

Cruz, A. R., L. G. Ramirez, A. V. Zuluaga, A. Pillay, C. Abreu, C. A. Valencia, C. La Vake, J. L. Cervantes, S. Dunham-Ems, R. Cartun, D. Mavilio, J. D. Radolf, and J. C. Salazar. 2012. 'Immune evasion and recognition of the syphilis spirochete in blood and skin of secondary syphilis patients: two immunologically distinct compartments', *PLoS Negl Trop Dis*, 6: e1717.

Cumberland MC, Turner TB. 1949. 'The rate of multiplication of *Treponema pallidum* in normal and immune rabbits', *Am J Syph Gonorrhea Vener Dis*, 33 201-12.

Dando, S. J., A. Mackay-Sim, R. Norton, B. J. Currie, J. A. St John, J. A. Ekberg, M. Batzloff, G. C. Ulett, and I. R. Beacham. 2014. 'Pathogens penetrating the central nervous system: infection pathways and the cellular and molecular mechanisms of invasion', *Clin Microbiol Rev*, 27: 691-726.

Danielsen, A. G., K. Weismann, B. B. Jorgensen, M. Heidenheim, and A. M. Fugleholm. 2004. 'Incidence, clinical presentation and treatment of neurosyphilis in Denmark 1980-1997', *Acta Derm Venereol*, 84: 459-62.

Dejana, E. 2004. 'Endothelial cell-cell junctions: happy together', *Nat Rev Mol Cell Biol*, 5: 261-70.

Dejana, E., F. Orsenigo, and M. G. Lampugnani. 2008. 'The role of adherens junctions and VE-cadherin in the control of vascular permeability', *J Cell Sci*, 121: 2115-22.

Deka, R. K., L. Neil, K. E. Hagman, M. Machius, D. R. Tomchick, C. A. Brautigam, and M. V. Norgard. 2004. 'Structural evidence that the 32-kilodalton lipoprotein (Tp32) of *Treponema pallidum* is an L-methionine-binding protein', *J Biol Chem*, 279: 55644-50.

Denchev, Y. 2014. Investigating the role of pallilysin in the dissemination of the syphilis spirochete, *Treponema pallidum* [master's thesis]. University of Victoria.

Dephoure, N., K. L. Gould, S. P. Gygi, and D. R. Kellogg. 2013. 'Mapping and analysis of phosphorylation sites: a quick guide for cell biologists', *Mol Biol Cell*, 24: 535-42.

Dephoure, N., and S. P. Gygi. 2012. 'Hyperplexing: a method for higher-order multiplexed quantitative proteomics provides a map of the dynamic response to rapamycin in yeast', *Sci Signal*, 5: rs2.

Desrosiers, D. C., A. Anand, A. Luthra, S. M. Dunham-Ems, M. LeDoyt, M. A. Cummings, A. Eshghi, C. E. Cameron, A. R. Cruz, J. C. Salazar, M. J. Caimano, and J. D. Radolf. 2011. 'TP0326, a *Treponema pallidum* beta-barrel assembly machinery A (BamA) orthologue and rare outer membrane protein', *Mol Microbiol*, 80: 1496-515.

Dewi, B. E., T. Takasaki, and I. Kurane. 2004. 'In vitro assessment of human endothelial cell permeability: effects of inflammatory cytokines and dengue virus infection', *J Virol Methods*, 121: 171-80.

Dickerson, M. T., M. B. Abney, C. E. Cameron, M. Knecht, L. G. Bachas, and K. W. Anderson. 2012. 'Fibronectin binding to the *Treponema pallidum* adhesin protein fragment rTp0483 on functionalized self-assembled monolayers', *Bioconjug Chem*, 23: 184-95.

DiGiacomo, V., and D. Meruelo. 2016. 'Looking into laminin receptor: critical discussion regarding the non-integrin 37/67-kDa laminin receptor/RPSA protein', *Biol Rev Camb Philos Soc*, 91: 288-310.

Doulet, N., E. Donnadieu, M. P. Laran-Chich, F. Niedergang, X. Nassif, P. O. Couraud, and S. Bourdoulous. 2006. '*Neisseria meningitidis* infection of human endothelial cells interferes with leukocyte transmigration by preventing the formation of endothelial docking structures', *J Cell Biol*, 173: 627-37.

Du, Z. P., B. L. Wu, X. Wu, X. H. Lin, X. Y. Qiu, X. F. Zhan, S. H. Wang, J. H. Shen, C. P. Zheng, Z. Y. Wu, L. Y. Xu, D. Wang, and E. M. Li. 2015. 'A systematic analysis of human lipocalin family and its expression in esophageal carcinoma', *Sci Rep*, 5: 12010.

Dumenil, G., P. Sansonetti, and G. Tran Van Nhieu. 2000. 'Src tyrosine kinase activity down-regulates Rho-dependent responses during Shigella entry into epithelial cells and stress fibre formation', *J Cell Sci*, 113 (Pt 1): 71-80.

Dvorak, A. M., S. Kohn, E. S. Morgan, P. Fox, J. A. Nagy, and H. F. Dvorak. 1996. 'The vesiculo-vacuolar organelle (VVO): a distinct endothelial cell structure that provides a transcellular pathway for macromolecular extravasation', *J Leukoc Biol*, 59: 100-15.

Ebady, R., A. F. Niddam, A. E. Boczula, Y. R. Kim, N. Gupta, T. T. Tang, T. Odisho, H. Zhi, C. A. Simmons, J. T. Skare, and T. J. Moriarty. 2016. 'Biomechanics of *Borrelia burgdorferi* Vascular Interactions', *Cell Rep*, 16: 2593-604.

Edmondson, D. G., B. Hu, and S. J. Norris. 2018. 'Long-Term In Vitro Culture of the Syphilis Spirochete *Treponema pallidum* subsp. pallidum', *MBio*, 9.

El-Sayed, A., and H. Harashima. 2013. 'Endocytosis of gene delivery vectors: from clathrin-dependent to lipid raft-mediated endocytosis', *Mol Ther*, 21: 1118-30.

Esser, S., M. G. Lampugnani, M. Corada, E. Dejana, and W. Risau. 1998. 'Vascular endothelial growth factor induces VE-cadherin tyrosine phosphorylation in endothelial cells', *J Cell Sci*, 111 (Pt 13): 1853-65.

Eugene, E., I. Hoffmann, C. Pujol, P. O. Couraud, S. Bourdoulous, and X. Nassif. 2002. 'Microvilli-like structures are associated with the internalization of virulent capsulated *Neisseria meningitidis* into vascular endothelial cells', *J Cell Sci*, 115: 1231-41.

Evangelista, K., R. Franco, A. Schwab, and J. Coburn. 2014. '*Leptospira interrogans* binds to cadherins', *PLoS Negl Trop Dis*, 8: e2672.

Eyrich, B., A. Sickmann, and R. P. Zahedi. 2011. 'Catch me if you can: mass spectrometry-based phosphoproteomics and quantification strategies', *Proteomics*, 11: 554-70.

Faure, E., L. Thomas, H. Xu, A. Medvedev, O. Equils, and M. Arditi. 2001. 'Bacterial lipopolysaccharide and IFN-gamma induce Toll-like receptor 2 and Toll-like receptor 4 expression in human endothelial cells: role of NF-kappa B activation', *J Immunol*, 166: 2018-24.

Fawaz, F. S., C. van Ooij, E. Homola, S. C. Mutka, and J. N. Engel. 1997. 'Infection with *Chlamydia trachomatis* alters the tyrosine phosphorylation and/or localization of several host cell proteins including cortactin', *Infect Immun*, 65: 5301-8.

Fears, M. B., and V. Pope. 2001. 'Syphilis fast latex agglutination test, a rapid confirmatory test', *Clin Diagn Lab Immunol*, 8: 841-2.

Ferro, T. J., N. Gertzberg, L. Selden, P. Neumann, and A. Johnson. 1997. 'Endothelial barrier dysfunction and p42 oxidation induced by TNF-alpha are mediated by nitric oxide', *Am J Physiol*, 272: L979-88.

Ferro, T., P. Neumann, N. Gertzberg, R. Clements, and A. Johnson. 2000. 'Protein kinase C-alpha mediates endothelial barrier dysfunction induced by TNF-alpha', *Am J Physiol Lung Cell Mol Physiol*, 278: L1107-17.

Fitzgerald, T. J., R. C. Johnson, J. A. Sykes, and J. N. Miller. 1977. 'Interaction of *Treponema pallidum* (Nichols strain) with cultured mammalian cells: effects of oxygen, reducing agents, serum supplements, and different cell types', *Infect Immun*, 15: 444-52.

Fitzgerald, T. J., J. N. Miller, and J. A. Sykes. 1975. '*Treponema pallidum* (Nichols strain) in tissue cultures: cellular attachment, entry, and survival', *Infect Immun*, 11: 1133-40.

Fitzgerald, T. J., and L. A. Repesh. 1985. 'Interactions of fibronectin with *Treponema pallidum*', *Genitourin Med*, 61: 147-55.

Fitzgerald, T. J., L. A. Repesh, D. R. Blanco, and J. N. Miller. 1984. 'Attachment of *Treponema pallidum* to fibronectin, laminin, collagen IV, and collagen I, and blockage of attachment by immune rabbit IgG', *Br J Vener Dis*, 60: 357-63.

Fitzgerald T.J. amd R.C. Johnson. 1979. Surface mucopolysaccharides of *Treponema pallidum*, *Infect Immun*, 24:244–51.

Fork, C., J. Hitzel, B. J. Nichols, R. Tikkanen, and R. P. Brandes. 2014. 'Flotillin-1 facilitates toll-like receptor 3 signaling in human endothelial cells', *Basic Res Cardiol*, 109: 439.

Formisano, P., Ragno, P., Pesapane, A., Alfano, D., Alberobello, A.T., Rea, V.E.A., Giusto, R., Rossi, F.W., Beguinot, F., Rossi, G., and N. Montuori. 2012. 'PED/PEA-15 interacts with the 67 kD laminin receptor and regulates cell adhesion, migration, prolifersion and apoptosis', *J Cell Mol Med*, 16(7): 1435-46.

Foster, L. J., C. L. De Hoog, and M. Mann. 2003. 'Unbiased quantitative proteomics of lipid rafts reveals high specificity for signaling factors', *Proc Natl Acad Sci U S A*, 100: 5813-8.

Francavilla, C., O. Hekmat, B. Blagoev, and J. V. Olsen. 2014. 'SILAC-based temporal phosphoproteomics', *Methods Mol Biol*, 1188: 125-48.

Fraser, C. M., S. J. Norris, G. M. Weinstock, O. White, G. G. Sutton, R. Dodson, M. Gwinn, E. K. Hickey, R. Clayton, K. A. Ketchum, E. Sodergren, J. M. Hardham, M. P. McLeod, S. Salzberg, J. Peterson, H. Khalak, D. Richardson, J. K. Howell, M. Chidambaram, T. Utterback, L. McDonald, P. Artiach, C. Bowman, M. D. Cotton, C. Fujii, S. Garland, B. Hatch, K. Horst, K. Roberts, M. Sandusky, J. Weidman, H. O. Smith, and J. C. Venter. 1998. 'Complete genome sequence of *Treponema pallidum*, the syphilis spirochete', *Science*, 281: 375-88.

Frischknecht, F., and M. Way. 2001. 'Surfing pathogens and the lessons learned for actin polymerization', *Trends Cell Biol*, 11: 30-38.

Fujimura, Y., D. Umeda, Y. Kiyohara, Y. Sunada, K. Yamada, and H. Tachibana. 2006. 'The involvement of the 67 kDa laminin receptor-mediated modulation of cytoskeleton in the degranulation inhibition induced by epigallocatechin-3-O-gallate', *Biochem Biophys Res Commun*, 348: 524-31.

Fujimura, Y., K. Yamada, and H. Tachibana. 2005. 'A lipid raft-associated 67kDa laminin receptor mediates suppressive effect of epigallocatechin-3-O-gallate on FcepsilonRI expression', *Biochem Biophys Res Commun*, 336: 674-81.

Fung, K. Y. Y., G. D. Fairn, and W. L. Lee. 2018. 'Transcellular vesicular transport in epithelial and endothelial cells: Challenges and opportunities', *Traffic*, 19: 5-18.

Gal-Mor, O., and B. B. Finlay. 2006. 'Pathogenicity islands: a molecular toolbox for bacterial virulence', *Cell Microbiol*, 8: 1707-19.

Galbe, J. L., E. Guy, J. M. Zapatero, E. I. Peerschke, and J. L. Benach. 1993. 'Vascular clearance of *Borrelia burgdorferi* in rats', *Microb Pathog*, 14: 187-201.

Garcia-Perez, B. E., J. J. De la Cruz-Lopez, J. I. Castaneda-Sanchez, A. R. Munoz-Duarte, A. D. Hernandez-Perez, H. Villegas-Castrejon, E. Garcia-Latorre, A. Caamal-Ley, and J. Luna-Herrera. 2012. 'Macropinocytosis is responsible for the uptake of pathogenic and non-pathogenic mycobacteria by B lymphocytes (Raji cells)', *BMC Microbiol*, 12: 246.

Gavard, J. 2014. 'Endothelial permeability and VE-cadherin: a wacky comradeship', *Cell Adh Migr*, 8: 158-64.

GBD DALYs and Hale Collaborators. 2016. 'Global, regional, and national disability-adjusted life-years (DALYs) for 315 diseases and injuries and healthy life expectancy (HALE), 1990-2015: a systematic analysis for the Global Burden of Disease Study 2015', *Lancet*, 388: 1603-58.

Ghanem, K. G. 2010. 'REVIEW: Neurosyphilis: A historical perspective and review', *CNS Neurosci Ther*, 16: e157-68.

Giacani, L., S. Lukehart, and A. Centurion-Lara. 2007. 'Length of guanosine homopolymeric repeats modulates promoter activity of subfamily II tpr genes of *Treponema pallidum* ssp. *pallidum*', *FEMS Immunol Med Microbiol*, 51: 289-301.

Gibbs, M. R., K. M. Moon, M. Chen, R. Balakrishnan, L. J. Foster, and K. Fredrick. 2017. 'Conserved GTPase LepA (Elongation Factor 4) functions in biogenesis of the 30S subunit of the 70S ribosome', *Proc Natl Acad Sci U S A*, 114: 980-85.

Gimbrone, M. A., Jr., R. S. Cotran, and J. Folkman. 1974. 'Human vascular endothelial cells in culture. Growth and DNA synthesis', *J Cell Biol*, 60: 673-84.

Gjestland, T. 1955. 'The Oslo study of untreated syphilis; an epidemiologic investigation of the natural course of the syphilitic infection based upon a re-study of the Boeck-Bruusgaard material', *Acta Derm Venereol Suppl (Stockh)*, 35: 3-368; Annex I-LVI.

Glebov, O.O., Bright, N.A., and B.J. Nichols. 2006. 'Flotillin-1 defines a clathrin-independent endocytic pathway in mammalian cells', *Nat Cell Biol*, 8:46-54.

Goldblum, S. E., X. Ding, T. W. Brann, and J. Campbell-Washington. 1993. 'Bacterial lipopolysaccharide induces actin reorganization, intercellular gap formation, and endothelial barrier dysfunction in pulmonary vascular endothelial cells: concurrent F-actin depolymerization and new actin synthesis', *J Cell Physiol*, 157: 13-23.

Goldblum, S. E., X. Ding, and J. Campbell-Washington. 1993. 'TNF-alpha induces endothelial cell F-actin depolymerization, new actin synthesis, and barrier dysfunction', *Am J Physiol*, 264: C894-905.

Grab, D. J., E. Nyarko, O. V. Nikolskaia, Y. V. Kim, and J. S. Dumler. 2009. 'Human brain microvascular endothelial cell traversal by *Borrelia burgdorferi* requires calcium signaling', *Clin Microbiol Infect*, 15: 422-6.

Grab, D. J., G. Perides, J. S. Dumler, K. J. Kim, J. Park, Y. V. Kim, O. Nikolskaia, K. S. Choi, M. F. Stins, and K. S. Kim. 2005. '*Borrelia burgdorferi*, host-derived proteases, and the blood-brain barrier', *Infect Immun*, 73: 1014-22.

Greenblatt, R. M., S. A. Lukehart, F. A. Plummer, T. C. Quinn, C. W. Critchlow, R. L. Ashley, L. J. D'Costa, J. O. Ndinya-Achola, L. Corey, A. R. Ronald, and et al. 1988. 'Genital ulceration as a risk factor for human immunodeficiency virus infection', *AIDS*, 2: 47-50.

Gu, C., S. Yaddanapudi, A. Weins, T. Osborn, J. Reiser, M. Pollak, J. Hartwig, and S. Sever. 2010. 'Direct dynamin-actin interactions regulate the actin cytoskeleton', *EMBO J*, 29: 3593-606.

Haake, D. A., and P. N. Levett. 2015. 'Leptospirosis in humans', *Curr Top Microbiol Immunol*, 387: 65-97.

Handsfield, H. H., S. A. Lukehart, S. Sell, S. J. Norris, and K. K. Holmes. 1983. 'Demonstration of *Treponema pallidum* in a cutaneous gumma by indirect immunofluorescence', *Arch Dermatol*, 119: 677-80.

Hawley, K. L., A. R. Cruz, S. J. Benjamin, C. J. La Vake, J. L. Cervantes, M. LeDoyt, L. G. Ramirez, D. Mandich, M. Fiel-Gan, M. J. Caimano, J. D. Radolf, and J. C. Salazar. 2017. 'IFNgamma Enhances CD64-Potentiated Phagocytosis of *Treponema pallidum* Opsonized with Human Syphilitic Serum by Human Macrophages', *Front Immunol*, 8: 1227.

Hayes, N. S., K. E. Muse, A. M. Collier, and J. B. Baseman. 1977. 'Parasitism by virulent *Treponema pallidum* of host cell surfaces', *Infect Immun*, 17: 174-86.

Hazlett, K. R., D. L. Cox, M. Decaffmeyer, M. P. Bennett, D. C. Desrosiers, C. J. La Vake, M. E. La Vake, K. W. Bourell, E. J. Robinson, R. Brasseur, and J. D. Radolf. 2005. 'TP0453, a concealed outer membrane protein of *Treponema pallidum*, enhances membrane permeability', *J Bacteriol*, 187: 6499-508.

Heemskerk, N., L. Schimmel, C. Oort, J. van Rijssel, T. Yin, B. Ma, J. van Unen, B. Pitter, S. Huveneers, J. Goedhart, Y. Wu, E. Montanez, A. Woodfin, and J. D. van Buul. 2016. 'F-actin-rich contractile endothelial pores prevent vascular leakage during leukocyte diapedesis through local RhoA signalling', *Nat Commun*, 7: 10493.

Henneke, P., and D. T. Golenbock. 2002. 'Innate immune recognition of lipopolysaccharide by endothelial cells', *Crit Care Med*, 30: S207-13.

Herbert, L. J., and S. I. Middleton. 2012. 'An estimate of syphilis incidence in Eastern Europe', *J Glob Health*, 2: 010402.

Hilario, E., F. Unda, G. Perez-Yarza, A. Alvarez, M. Garcia-Sanz, and S. F. Allno. 1996. 'Presence of laminin and 67KDa laminin-receptor on endothelial surface of lung capillaries. An immunocytochemical study', *Histol Histopathol*, 11: 915-8.

Hira, S. K., J. S. Patel, S. G. Bhat, K. Chilikima, and N. Mooney. 1987. 'Clinical manifestations of secondary syphilis', *Int J Dermatol*, 26: 103-7.

Hoedt, E., G. Zhang, and T. A. Neubert. 2014. 'Stable isotope labeling by amino acids in cell culture (SILAC) for quantitative proteomics', *Adv Exp Med Biol*, 806: 93-106.

Hoffmann, I., E. Eugene, X. Nassif, P. O. Couraud, and S. Bourdoulous. 2001. 'Activation of ErbB2 receptor tyrosine kinase supports invasion of endothelial cells by *Neisseria meningitidis*', *J Cell Biol*, 155: 133-43.

Hoffmann, P. R., A. M. deCathelineau, C. A. Ogden, Y. Leverrier, D. L. Bratton, D. L. Daleke, A. J. Ridley, V. A. Fadok, and P. M. Henson. 2001. 'Phosphatidylserine (PS) induces PS receptor-mediated macropinocytosis and promotes clearance of apoptotic cells', *J Cell Biol*, 155: 649-59.

Hook, E. W., 3rd. 2017. 'Syphilis', *Lancet*, 389: 1550-57.

Hook, E. W., 3rd, and C. M. Marra. 1992. 'Acquired syphilis in adults', *N Engl J Med*, 326: 1060-9.

Hourihan, M., H. Wheeler, R. Houghton, and B. T. Goh. 2004. 'Lessons from the syphilis outbreak in homosexual men in east London', *Sex Transm Infect*, 80: 509-11.

Houston, S., R. Hof, T. Francescutti, A. Hawkes, M. J. Boulanger, and C. E. Cameron. 2011. 'Bifunctional role of the *Treponema pallidum* extracellular matrix binding adhesin Tp0751', *Infect Immun*, 79: 1386-98.

Houston, S., R. Hof, L. Honeyman, J. Hassler, and C. E. Cameron. 2012. 'Activation and proteolytic activity of the *Treponema pallidum* metalloprotease, pallilysin', *PLoS Pathog*, 8: e1002822.

Houston, S., K. V. Lithgow, K. K. Osbak, C. R. Kenyon, and C. E. Cameron. 2018. 'Functional insights from proteome-wide structural modeling of *Treponema pallidum* subspecies *pallidum*, the causative agent of syphilis', *BMC Struct Biol*, 18: 7.

Houston, S., S. Russell, R. Hof, A. K. Roberts, P. Cullen, K. Irvine, D. S. Smith, C. H. Borchers, M. L. Tonkin, M. J. Boulanger, and C. E. Cameron. 2014. 'The multifunctional role of the pallilysin-associated *Treponema pallidum* protein, Tp0750, in promoting fibrinolysis and extracellular matrix component degradation', *Mol Microbiol*, 91: 618-34.

Houston, S., J. S. Taylor, Y. Denchev, R. Hof, R. L. Zuerner, and C. E. Cameron. 2015. 'Conservation of the Host-Interacting Proteins Tp0750 and Pallilysin among Treponemes and Restriction of Proteolytic Capacity to *Treponema pallidum*', *Infect Immun*, 83: 4204-16.

Hudetz, A. G., G. Feher, D. E. Knuese, and J. P. Kampine. 1994. 'Erythrocyte flow heterogeneity in the cerebrocortical capillary network', *Adv Exp Med Biol*, 345: 633-42.

Hundt, C., J. M. Peyrin, S. Haik, S. Gauczynski, C. Leucht, R. Rieger, M. L. Riley, J. P. Deslys, D. Dormont, C. I. Lasmezas, and S. Weiss. 2001. 'Identification of interaction domains of the prion protein with its 37-kDa/67-kDa laminin receptor', *EMBO J*, 20: 5876-86.

Hunter, T. 2000. 'Signaling--2000 and beyond', *Cell*, 100: 113-27.

Hunter, T., and B. M. Sefton. 1980. 'Transforming gene product of Rous sarcoma virus phosphorylates tyrosine', *Proc Natl Acad Sci U S A*, 77: 1311-5.

Hyde, J. A. 2017. '*Borrelia burgdorferi* Keeps Moving and Carries on: A Review of Borrelial Dissemination and Invasion', *Front Immunol*, 8: 114.

Hynes, R. O. 2009. 'The extracellular matrix: not just pretty fibrils', *Science*, 326: 1216-9.

Iovino, F., C. J. Orihuela, H. E. Moorlag, G. Molema, and J. J. Bijlsma. 2013. 'Interactions between blood-borne *Streptococcus pneumoniae* and the blood-brain barrier preceding meningitis', *PLoS One*, 8: e68408.

Ishihama, Y., J. Rappsilber, J. S. Andersen, and M. Mann. 2002. 'Microcolumns with self-assembled particle frits for proteomics', *J Chromatogr A*, 979: 233-9.

Jarzebowski, W., E. Caumes, N. Dupin, D. Farhi, A. S. Lascaux, C. Piketty, P. de Truchis, M. A. Bouldouyre, O. Derradji, J. Pacanowski, D. Costagliola, S. Grabar, and Fhdh-Anrs Co Study Team. 2012. 'Effect of early syphilis infection on plasma viral load and CD4 cell count in human immunodeficiency virus-infected men: results from the FHDH-ANRS CO4 cohort', *Arch Intern Med*, 172: 1237-43.

Jepsen, O. B., K. H. Hougen, and A. Birch-Andersen. 1968. 'Electron microscopy of *Treponema pallidum* Nichols', *Acta Pathol Microbiol Scand*, 74: 241-58.

Johnson R.C., Ritzi D.M., and B.P. Livermore. 1973. Outer envelope of virulent *Treponema pallidum*, *Infect Immun*, 8:291–95.

Kadler, K. E., A. Hill, and E. G. Canty-Laird. 2008. 'Collagen fibrillogenesis: fibronectin, integrins, and minor collagens as organizers and nucleators', *Curr Opin Cell Biol*, 20: 495-501.

Kampmeier, R. H. 1946. 'The diagnosis and treatment of cardiovascular syphilis', *Clinics*, 5: 135-66.
Kampmeier, R. H. 1948. 'Cardiovascular syphilis', *Tex State J Med*, 44: 23-8.
Kampmeier, R. H. 1964. 'The late manifestations of syphilis: skeletal, visceral and cardiovascular', *Med. Clin. N. Am.*, 48: 667-97.
Kampmeier, R. H. 1972. 'The Tuskegee study of untreated syphilis', *South Med J*, 65: 1247-51.
Kao, W. A., H. Petrosova, R. Ebady, K. V. Lithgow, P. Rojas, Y. Zhang, Y. E. Kim, Y. R. Kim, T. Odisho, N. Gupta, A. Moter, C. E. Cameron, and T. J. Moriarty. 2017. 'Identification of Tp0751 (Pallilysin) as a *Treponema pallidum* Vascular Adhesin by Heterologous Expression in the Lyme disease Spirochete', *Sci Rep*, 7: 1538.
Kazmin, D. A., T. R. Hoyt, L. Taubner, M. Teintze, and J. R. Starkey. 2000. 'Phage display mapping for peptide 11 sensitive sequences binding to laminin-1', *J Mol Biol*, 298: 431-45.
Ke, W., B. J. Molini, S. A. Lukehart, and L. Giacani. 2015. '*Treponema pallidum* subsp. *pallidum* TP0136 protein is heterogeneous among isolates and binds cellular and plasma fibronectin via its NH2-terminal end', *PLoS Negl Trop Dis*, 9: e0003662.
Kelley, L. C., K. E. Hayes, A. G. Ammer, K. H. Martin, and S. A. Weed. 2010. 'Cortactin phosphorylated by ERK1/2 localizes to sites of dynamic actin regulation and is required for carcinoma lamellipodia persistence', *PLoS One*, 5: e13847.
Kenyon, C., L. Lynen, E. Florence, S. Caluwaerts, M. Vandenbruaene, L. Apers, P. Soentjens, M. Van Esbroeck, and E. Bottieau. 2014. 'Syphilis reinfections pose problems for syphilis diagnosis in Antwerp, Belgium - 1992 to 2012', *Euro Surveill*, 19: 20958.
Kenyon, C., K. K. Osbak, and L. Apers. 2018. 'Repeat Syphilis Is More Likely to Be Asymptomatic in HIV-Infected Individuals: A Retrospective Cohort Analysis With Important Implications for Screening', *Open Forum Infect Dis*, 5: ofy096.
Kenyon, C., K. K. Osbak, T. Crucitti, and L. Kestens. 2018. 'Syphilis reinfection is associated with an attenuated immune profile in the same individual: a prospective observational cohort study', *BMC Infect Dis*, 18: 479.
Kidd, S.E., J.A. Grey, E.T. Torrone, and M.D. Weinstock. 2019. 'Increased Methamphetamine, Injection Drug, and Heroin Use Among Women and Heterosexual Men with Primary and Secondary Syphilis — United States, 2013–2017', *Morbidity and Mortality Weekly Report*, 68: 144-48.
Kim, K. J., J. W. Chung, and K. S. Kim. 2005. '67-kDa laminin receptor promotes internalization of cytotoxic necrotizing factor 1-expressing *Escherichia coli* K1 into human brain microvascular endothelial cells', *J Biol Chem*, 280: 1360-8.
Kim, M. H., F. R. Curry, and S. I. Simon. 2009. 'Dynamics of neutrophil extravasation and vascular permeability are uncoupled during aseptic cutaneous wounding', *Am J Physiol Cell Physiol*, 296: C848-56.
Koivusalo, M., C. Welch, H. Hayashi, C. C. Scott, M. Kim, T. Alexander, N. Touret, K. M. Hahn, and S. Grinstein. 2010. 'Amiloride inhibits macropinocytosis by lowering submembranous pH and preventing Rac1 and Cdc42 signaling', *J Cell Biol*, 188: 547-63.

Kojima, N., D. J. Davey, and J. D. Klausner. 2016. 'Pre-exposure prophylaxis for HIV infection and new sexually transmitted infections among men who have sex with men', *AIDS*, 30: 2251-2.

Krachler, A. M., A. R. Woolery, and K. Orth. 2011. 'Manipulation of kinase signaling by bacterial pathogens', *J Cell Biol*, 195: 1083-92.

Krishnan, S., G. E. Fernandez, D. B. Sacks, and N. V. Prasadarao. 2012. 'IQGAP1 mediates the disruption of adherens junctions to promote *Escherichia coli* K1 invasion of brain endothelial cells', *Cell Microbiol*, 14: 1415-33.

Kubanov, A., A. Runina, and D. Deryabin. 2017. 'Novel *Treponema pallidum* Recombinant Antigens for Syphilis Diagnostics: Current Status and Future Prospects', *Biomed Res Int*, 2017: 1436080.

Kuppers, V., D. Vestweber, and D. Schulte. 2013. 'Locking endothelial junctions blocks leukocyte extravasation, but not in all tissues', *Tissue Barriers*, 1: e23805.

Kyono, Y., N. Sugiyama, K. Imami, M. Tomita, and Y. Ishihama. 2008. 'Successive and selective release of phosphorylated peptides captured by hydroxy acid-modified metal oxide chromatography', *J Proteome Res*, 7: 4585-93.

LaFond, R. E., A. Centurion-Lara, C. Godornes, A. M. Rompalo, W. C. Van Voorhis, and S. A. Lukehart. 2003. 'Sequence diversity of *Treponema pallidum* subsp. *pallidum* tprK in human syphilis lesions and rabbit-propagated isolates', *J Bacteriol*, 185: 6262-8.

Lafond, R. E., and S. A. Lukehart. 2006. 'Biological Basis for Syphilis', *Clinical Microbiology Reviews*, 19: 29-49.

LaFond, R. E., B. J. Molini, W. C. Van Voorhis, and S. A. Lukehart. 2006. 'Antigenic variation of TprK V regions abrogates specific antibody binding in syphilis', *Infect Immun*, 74: 6244-51.

Lagana, A., J. Vadnais, P. U. Le, T. N. Nguyen, R. Laprade, I. R. Nabi, and J. Noel. 2000. 'Regulation of the formation of tumor cell pseudopodia by the Na(+)/H(+) exchanger NHE1', *J Cell Sci*, 113 (Pt 20): 3649-62.

Lambotin, M., I. Hoffmann, M. P. Laran-Chich, X. Nassif, P. O. Couraud, and S. Bourdoulous. 2005. 'Invasion of endothelial cells by *Neisseria meningitidis* requires cortactin recruitment by a phosphoinositide-3-kinase/Rac1 signalling pathway triggered by the lipo-oligosaccharide', *J Cell Sci*, 118: 3805-16.

Lampugnani, M. G. 2010. 'Endothelial adherens junctions and the actin cytoskeleton: an 'infinity net'?', *J Biol*, 9: 16.

Landowski, T. H., E. A. Dratz, and J. R. Starkey. 1995. 'Studies of the structure of the metastasis-associated 67 kDa laminin binding protein: fatty acid acylation and evidence supporting dimerization of the 32 kDa gene product to form the mature protein', *Biochemistry*, 34: 11276-87.

Landowski, T. H., S. Uthayakumar, and J. R. Starkey. 1995. 'Control pathways of the 67 kDa laminin binding protein: surface expression and activity of a new ligand binding domain', *Clin Exp Metastasis*, 13: 357-72.

Lau, A. W., and M. M. Chou. 2008. 'The adaptor complex AP-2 regulates post-endocytic trafficking through the non-clathrin Arf6-dependent endocytic pathway', *J Cell Sci*, 121: 4008-17.

Leader, B. T., K. Hevner, B. J. Molini, L. K. Barrett, W. C. Van Voorhis, and S. A. Lukehart. 2003. 'Antibody responses elicited against the *Treponema pallidum*

repeat proteins differ during infection with different isolates of *Treponema pallidum* subsp. *pallidum*', *Infect Immun*, 71: 6054-7.

Lee, D. B., N. Jamgotchian, S. G. Allen, F. W. Kan, and I. L. Hale. 2004. 'Annexin A2 heterotetramer: role in tight junction assembly', *Am J Physiol Renal Physiol*, 287: F481-91.

Lee, J. H., H. J. Choi, J. Jung, M. G. Lee, J. B. Lee, and K. H. Lee. 2003. 'Receptors for *Treponema pallidum* attachment to the surface and matrix proteins of cultured human dermal microvascular endothelial cells', *Yonsei Med J*, 44: 371-78.

Lee, K. H., H. J. Choi, M. G. Lee, and J. B. Lee. 2000. 'Virulent *Treponema pallidum* 47 kDa antigen regulates the expression of cell adhesion molecules and binding of T-lymphocytes to cultured human dermal microvascular endothelial cells', *Yonsei Med J*, 41: 623-33.

Lemichez, E., M. Lecuit, X. Nassif, and S. Bourdoulous. 2010. 'Breaking the wall: targeting of the endothelium by pathogenic bacteria', *Nat Rev Microbiol*, 8: 93-104.

Leng X, Lin H, Ding T, Wang Y, Wu Y, Klumpp S, Sun T, Zhou Y, Monaco P, Belmont J, Aderem A, Akira S, Strong R, and Arlinghaus R. 2008. Lipocalin 2 is required for BCR-ABL-induced tumorigenesis. *Oncogene*, 27: 6110–9.

Lesot, H., U. Kuhl, and K. Mark. 1983. 'Isolation of a laminin-binding protein from muscle cell membranes', *EMBO J*, 2: 861-5.

Lewis, R. E., and H. J. Granger. 1988. 'Diapedesis and the permeability of venous microvessels to protein macromolecules: the impact of leukotriene B4 (LTB4)', *Microvasc Res*, 35: 27-47.

Lewis, R. E., R. A. Miller, and H. J. Granger. 1989. 'Acute microvascular effects of the chemotactic peptide N-formyl-methionyl-leucyl-phenylalanine: comparisons with leukotriene B4', *Microvasc Res*, 37: 53-69.

Li, H. H., J. Li, K. J. Wasserloos, C. Wallace, M. G. Sullivan, P. M. Bauer, D. B. Stolz, J. S. Lee, S. C. Watkins, C. M. St Croix, B. R. Pitt, and L. M. Zhang. 2013. 'Caveolae-dependent and -independent uptake of albumin in cultured rodent pulmonary endothelial cells', *PLoS One*, 8: e81903.

Lithgow, K. V., R. Hof, C. Wetherell, D. Phillips, S. Houston, and C. E. Cameron. 2017. 'A defined syphilis vaccine candidate inhibits dissemination of *Treponema pallidum* subspecies *pallidum*', *Nat Commun*, 8: 14273.

Liu, A. Y., S. E. Cohen, E. Vittinghoff, P. L. Anderson, S. Doblecki-Lewis, O. Bacon, W. Chege, B. S. Postle, T. Matheson, K. R. Amico, T. Liegler, M. K. Rawlings, N. Trainor, R. W. Blue, Y. Estrada, M. E. Coleman, G. Cardenas, D. J. Feaster, R. Grant, S. S. Philip, R. Elion, S. Buchbinder, and M. A. Kolber. 2016. 'Preexposure Prophylaxis for HIV Infection Integrated With Municipal- and Community-Based Sexual Health Services', *JAMA Intern Med*, 176: 75-84.

Loh, L. N., G. Gao, and E. I. Tuomanen. 2017. 'Dissecting Bacterial Cell Wall Entry and Signaling in Eukaryotic Cells: an Actin-Dependent Pathway Parallels Platelet-Activating Factor Receptor-Mediated Endocytosis', *MBio*, 8.

Loh, L. N., E. M. C. McCarthy, P. Narang, N. A. Khan, and T. H. Ward. 2017. '*Escherichia coli* K1 utilizes host macropinocytic pathways for invasion of brain microvascular endothelial cells', *Traffic*, 18: 733-46.

Loscalzo, Joseph, and Andrew I. Schafer. 2003. *Thrombosis and hemorrhage* (Lippincott Williams & Wilkins: Philadelphia).

Ludwig, G. V., J. P. Kondig, and J. F. Smith. 1996. 'A putative receptor for Venezuelan equine encephalitis virus from mosquito cells', *J Virol*, 70: 5592-9.

Lukehart, S. A., C. Godornes, B. J. Molini, P. Sonnett, S. Hopkins, F. Mulcahy, J. Engelman, S. J. Mitchell, A. M. Rompalo, C. M. Marra, and J. D. Klausner. 2004. 'Macrolide resistance in *Treponema pallidum* in the United States and Ireland', *N Engl J Med*, 351: 154-8.

Lukehart, S. A., and C. M. Marra. 2007. 'Isolation and laboratory maintenance of *Treponema pallidum*', *Curr Protoc Microbiol*, Chapter 12: Unit 12A 1.

Lukehart, S. A., and J. N. Miller. 1978. 'Demonstration of the in vitro phagocytosis of *Treponema pallidum* by rabbit peritoneal macrophages', *J Immunol*, 121: 2014-24.

Lukehart, S. A., J. M. Shaffer, and S. A. Baker-Zander. 1992. 'A subpopulation of *Treponema pallidum* is resistant to phagocytosis: possible mechanism of persistence', *J Infect Dis*, 166: 1449-53.

Lukehart SA, Hook EW 3rd, Baker-Zander SA, Collier AC, Critchlow CW, Handsfield HH. 1988. 'Invasion of the central nervous system by *Treponema pallidum*: implications for diagnosis and treatment', *Ann Intern Med*, 109(11):855–62: 955-62.

Luthra, A., A. Anand, and J. D. Radolf. 2015. '*Treponema pallidum* in Gel Microdroplets: A Method for Topological Analysis of BamA (TP0326) and Localization of Rare Outer Membrane Proteins', *Methods Mol Biol*, 1329: 67-75.

Ma, Y., A. Sturrock, and J. J. Weis. 1991. 'Intracellular localization of Borrelia burgdorferi within human endothelial cells', *Infect Immun*, 59: 671-8.

Magnuson, H. J., H. Eagle, and R. Fleischman. 1948. 'The minimal infectious inoculum of *Spirochaeta pallida* (Nichols strain) and a consideration of its rate of multiplication in vivo', *Am J Syph Gonorrhea Vener Dis*, 32: 1-18.

Mahajan-Miklos, S., L. G. Rahme, and F. M. Ausubel. 2000. 'Elucidating the molecular mechanisms of bacterial virulence using non-mammalian hosts', *Mol Microbiol*, 37: 981-8.

Mahoney, J. F., Bryant, K.K. 1934. 'The time element in the penetration of the genital mucosa of the rabbit by the *Treponema pallidum'*, *Vener. Dis. Inf.*, 15: 1-5.

Mairey, E., A. Genovesio, E. Donnadieu, C. Bernard, F. Jaubert, E. Pinard, J. Seylaz, J. C. Olivo-Marin, X. Nassif, and G. Dumenil. 2006. 'Cerebral microcirculation shear stress levels determine *Neisseria meningitidis* attachment sites along the blood-brain barrier', *J Exp Med*, 203: 1939-50.

Malinoff, H. L., and M. S. Wicha. 1983. 'Isolation of a cell surface receptor protein for laminin from murine fibrosarcoma cells', *J Cell Biol*, 96: 1475-9.

Malygin, A. A., E. I. Bondarenko, V. A. Ivanisenko, E. V. Protopopova, G. G. Karpova, and V. B. Loktev. 2009. 'C-terminal fragment of human laminin-binding protein contains a receptor domain for venezuelan equine encephalitis and tick-borne encephalitis viruses', *Biochemistry (Mosc)*, 74: 1328-36.

Marcus, U., A. J. Schmidt, and O. Hamouda. 2011. 'HIV serosorting among HIV-positive men who have sex with men is associated with increased self-reported incidence of bacterial sexually transmissible infections', *Sex Health*, 8: 184-93.

Marra, C. M., C. L. Maxwell, S. L. Smith, S. A. Lukehart, A. M. Rompalo, M. Eaton, B. P. Stoner, M. Augenbraun, D. E. Barker, J. J. Corbett, M. Zajackowski, C. Raines, J. Nerad, R. Kee, and S. H. Barnett. 2004. 'Cerebrospinal fluid abnormalities in patients with syphilis: association with clinical and laboratory features', *J Infect Dis*, 189: 369-76.

Martinez-Lopez, D. G., M. Fahey, and J. Coburn. 2010. 'Responses of human endothelial cells to pathogenic and non-pathogenic Leptospira species', *PLoS Negl Trop Dis*, 4: e918.

Martinez-Quiles, N., H. Y. Ho, M. W. Kirschner, N. Ramesh, and R. S. Geha. 2004. 'Erk/Src phosphorylation of cortactin acts as a switch on-switch off mechanism that controls its ability to activate N-WASP', *Mol Cell Biol*, 24: 5269-80.

Martinez, J. J., and P. Cossart. 2004. 'Early signaling events involved in the entry of Rickettsia conorii into mammalian cells', *J Cell Sci*, 117: 5097-106.

Masuda, T., M. Tomita, and Y. Ishihama. 2008. 'Phase transfer surfactant-aided trypsin digestion for membrane proteome analysis', *J Proteome Res*, 7: 731-40.

Matthews, H. M., T. K. Yang, and H. M. Jenkin. 1979. 'Unique lipid composition of *Treponema pallidum* (Nichols virulent strain)', *Infect Immun*, 24: 713-9.

McGill, M. A., D. G. Edmondson, J. A. Carroll, R. G. Cook, R. S. Orkiszewski, and S. J. Norris. 2010. 'Characterization and serologic analysis of the *Treponema pallidum* proteome', *Infect Immun*, 78: 2631-43.

McNiven, M. A. 2005. 'Dynamin in disease', *Nat Genet*, 37: 215-6.

Meister, M., and R. Tikkanen. 2014. 'Endocytic trafficking of membrane-bound cargo: a flotillin point of view', *Membranes (Basel)*, 4: 356-71.

Menard, S., V. Castronovo, E. Tagliabue, and M. E. Sobel. 1997. 'New insights into the metastasis-associated 67 kD laminin receptor', *J Cell Biochem*, 67: 155-65.

Menard, S., E. Tagliabue, and M. I. Colnaghi. 1998. 'The 67 kDa laminin receptor as a prognostic factor in human cancer', *Breast Cancer Res Treat*, 52: 137-45.

Mercer, J., and A. Helenius. 2009. 'Virus entry by macropinocytosis', *Nat Cell Biol*, 11: 510-20.

Merritt, H.H., R.D. Adams, and H.C. Solomon. 1946. 'Neurosyphilis', *New York: Oxford University Press*.

Mikaty, G., M. Soyer, E. Mairey, N. Henry, D. Dyer, K. T. Forest, P. Morand, S. Guadagnini, M. C. Prevost, X. Nassif, and G. Dumenil. 2009. 'Extracellular bacterial pathogen induces host cell surface reorganization to resist shear stress', *PLoS Pathog*, 5: e1000314.

Millan, J., L. Hewlett, M. Glyn, D. Toomre, P. Clark, and A. J. Ridley. 2006. 'Lymphocyte transcellular migration occurs through recruitment of endothelial ICAM-1 to caveola- and F-actin-rich domains', *Nat Cell Biol*, 8: 113-23.

Mindel, A., S. J. Tovey, D. J. Timmins, and P. Williams. 1989. 'Primary and secondary syphilis, 20 years' experience. 2. Clinical features', *Genitourin Med*, 65: 1-3.

Mittal, R., and N. V. Prasadarao. 2010. 'Nitric oxide/cGMP signalling induces *Escherichia coli* K1 receptor expression and modulates the permeability in human brain endothelial cell monolayers during invasion', *Cell Microbiol*, 12: 67-83.

Miyasaka, M., and T. Tanaka. 2004. 'Lymphocyte trafficking across high endothelial venules: dogmas and enigmas', *Nat Rev Immunol*, 4: 360-70.

Morgan, C. A., S. A. Lukehart, and W. C. Van Voorhis. 2003. 'Protection against syphilis correlates with specificity of antibodies to the variable regions of *Treponema pallidum* repeat protein K', *Infect Immun*, 71: 5605-12.

Morgan, C. A., B. J. Molini, S. A. Lukehart, and W. C. Van Voorhis. 2002. 'Segregation of B and T cell epitopes of *Treponema pallidum* repeat protein K to variable and conserved regions during experimental syphilis infection', *J Immunol*, 169: 952-7.

Moriarty, T. J., M. U. Norman, P. Colarusso, T. Bankhead, P. Kubes, and G. Chaconas. 2008. 'Real-time high resolution 3D imaging of the lyme disease spirochete adhering to and escaping from the vasculature of a living host', *PLoS Pathog*, 4: e1000090.

Moriarty, T. J., M. Shi, Y. P. Lin, R. Ebady, H. Zhou, T. Odisho, P. O. Hardy, A. Salman-Dilgimen, J. Wu, E. H. Weening, J. T. Skare, P. Kubes, J. Leong, and G. Chaconas. 2012. 'Vascular binding of a pathogen under shear force through mechanistically distinct sequential interactions with host macromolecules', *Mol Microbiol*, 86: 1116-31.

Morla, A., Z. Zhang, and E. Ruoslahti. 1994. 'Superfibronectin is a functionally distinct form of fibronectin', *Nature*, 367: 193-6.

Moy, A. B., K. Blackwell, N. Wang, K. Haxhinasto, M. K. Kasiske, J. Bodmer, G. Reyes, and A. English. 2004. 'Phorbol ester-mediated pulmonary artery endothelial barrier dysfunction through regulation of actin cytoskeletal mechanics', *Am J Physiol Lung Cell Mol Physiol*, 287: L153-67.

Muller, W. A. 2011. 'Mechanisms of leukocyte transendothelial migration', *Annu Rev Pathol*, 6: 323-44.

Muller, W. A. 2016. 'Transendothelial migration: unifying principles from the endothelial perspective', *Immunol Rev*, 273: 61-75.

Munro, S. 2003. 'Lipid rafts: elusive or illusive?', *Cell*, 115: 377-88.

Muro, S., M. Koval, and V. Muzykantov. 2004. 'Endothelial endocytic pathways: gates for vascular drug delivery', *Curr Vasc Pharmacol*, 2: 281-99.

Muro, S., R. Wiewrodt, A. Thomas, L. Koniaris, S. M. Albelda, V. R. Muzykantov, and M. Koval. 2003. 'A novel endocytic pathway induced by clustering endothelial ICAM-1 or PECAM-1', *J Cell Sci*, 116: 1599-609.

Newman, L., M. Kamb, S. Hawkes, G. Gomez, L. Say, A. Seuc, and N. Broutet. 2013. 'Global estimates of syphilis in pregnancy and associated adverse outcomes: analysis of multinational antenatal surveillance data', *PLoS Med*, 10: e1001396.

Newman, L., J. Rowley, S. Vander Hoorn, N. S. Wijesooriya, M. Unemo, N. Low, G. Stevens, S. Gottlieb, J. Kiarie, and M. Temmerman. 2015. 'Global Estimates of the Prevalence and Incidence of Four Curable Sexually Transmitted Infections in 2012 Based on Systematic Review and Global Reporting', *PLoS One*, 10: e0143304.

Nonnenmacher, M., and T. Weber. 2011. 'Adeno-associated virus 2 infection requires endocytosis through the CLIC/GEEC pathway', *Cell Host Microbe*, 10: 563-76.

Norman, M. U., T. J. Moriarty, A. R. Dresser, B. Millen, P. Kubes, and G. Chaconas. 2008. 'Molecular mechanisms involved in vascular interactions of the Lyme disease pathogen in a living host', *PLoS Pathog*, 4: e1000169.

Norgard, M.V., and J.N. Miller. 1983. ‘Cloning and expression of *Treponema pallidum* (Nichols) antigen genes in *Escherichia coli’, Infect Immun,* 42: 435-45.

Norris, S.J., Alderete, J.F., Axelsen, N.H., Bailey, M.J., Baker-Zander, S.A., Baseman, J.B., Bassford, P.J., Baughn, R.E., Cockayne, A., Hanff, P.A., Hindersson, P., Larsen, S.A., Lovett, M.A., Lukehart, S.A., Miller, J.N., Moskophidis, M.A., Muller, F., Norgard, M.V., Penn, C.W., Stamm, L.V., van Embden, J.D., and K. Wicher. 'Identity of *Treponema pallidum* subsp. *pallidum* polypeptides: correlation of sodium dodecyl sulfate-polyacrylamide gel electrophoresis results from different laboratories', *Electrophoresis*, 8(2):

Norris, S. J., and D. G. Edmondson. 1986. 'Factors affecting the multiplication and subculture of *Treponema pallidum* subsp. *pallidum* in a tissue culture system', *Infect Immun*, 53: 534-9.

Nurse-Findlay, S., M. M. Taylor, M. Savage, M. B. Mello, S. Saliyou, M. Lavayen, F. Seghers, M. L. Campbell, F. Birgirimana, L. Ouedraogo, M. Newman Owiredu, N. Kidula, and L. Pyne-Mercier. 2017. 'Shortages of benzathine penicillin for prevention of mother-to-child transmission of syphilis: An evaluation from multi-country surveys and stakeholder interviews', *PLoS Med*, 14: e1002473.

O'Regan, S., J. S. Fong, J. P. de Chadarevian, J. R. Rishikof, and K. N. Drummond. 1976. 'Treponemal antigens in congenital and acquired syphilitic nephritis: demonstration by immunofluorescence studies', *Ann Intern Med*, 85: 325-7.

Olsen, J. V., B. Blagoev, F. Gnad, B. Macek, C. Kumar, P. Mortensen, and M. Mann. 2006. 'Global, in vivo, and site-specific phosphorylation dynamics in signaling networks', *Cell*, 127: 635-48.

Ong, S. E., B. Blagoev, I. Kratchmarova, D. B. Kristensen, H. Steen, A. Pandey, and M. Mann. 2002. 'Stable isotope labeling by amino acids in cell culture, SILAC, as a simple and accurate approach to expression proteomics', *Mol Cell Proteomics*, 1: 376-86.

Opal, S. M., G. E. Garber, S. P. LaRosa, D. G. Maki, R. C. Freebairn, G. T. Kinasewitz, J. F. Dhainaut, S. B. Yan, M. D. Williams, D. E. Graham, D. R. Nelson, H. Levy, and G. R. Bernard. 2003. 'Systemic host responses in severe sepsis analyzed by causative microorganism and treatment effects of drotrecogin alfa (activated)', *Clin Infect Dis*, 37: 50-8.

Orihuela, C. J., J. Mahdavi, J. Thornton, B. Mann, K. G. Wooldridge, N. Abouseada, N. J. Oldfield, T. Self, D. A. Ala'Aldeen, and E. I. Tuomanen. 2009. 'Laminin receptor initiates bacterial contact with the blood brain barrier in experimental meningitis models', *J Clin Invest*, 119: 1638-46.

Osbak, K. K., S. Houston, K. V. Lithgow, C. J. Meehan, M. Strouhal, D. Smajs, C. E. Cameron, X. Van Ostade, C. R. Kenyon, and G. A. Van Raemdonck. 2016. 'Characterizing the Syphilis-Causing *Treponema pallidum* ssp. *pallidum* Proteome Using Complementary Mass Spectrometry', *PLoS Negl Trop Dis*, 10: e0004988.

Osbak, K. K., G. A. Van Raemdonck, M. Dom, C. E. Cameron, C. J. Meehan, D. Deforce, X. V. Ostade, C. R. Kenyon, and M. Dhaenens. 2018. 'Candidate *Treponema pallidum* biomarkers uncovered in urine from individuals with syphilis using mass spectrometry', *Future Microbiol*, 13: 1497-510.

Ouedraogo, H. G., I. B. Meda, I. Zongo, O. Ky-Zerbo, A. Grosso, B. C. Samadoulougou, G. Tarnagda, K. Cisse, A. Sondo, N. Sawadogo, Y. Traore, N. Barro, S. Baral, and S. Kouanda. 2018. 'Syphilis among Female Sex Workers: Results of Point-of-

Care Screening during a Cross-Sectional Behavioral Survey in Burkina Faso, West Africa', *Int J Microbiol*, 2018: 4790560.

Ould-Abeih, M. B., I. Petit-Topin, N. Zidane, B. Baron, and H. Bedouelle. 2012. 'Multiple folding states and disorder of ribosomal protein SA, a membrane receptor for laminin, anticarcinogens, and pathogens', *Biochemistry*, 51: 4807-21.

Pan, C., F. Gnad, J. V. Olsen, and M. Mann. 2008. 'Quantitative phosphoproteome analysis of a mouse liver cell line reveals specificity of phosphatase inhibitors', *Proteomics*, 8: 4534-46.

Park, R. J., H. Shen, L. Liu, X. Liu, S. M. Ferguson, and P. De Camilli. 2013. 'Dynamin triple knockout cells reveal off target effects of commonly used dynamin inhibitors', *J Cell Sci*, 126: 5305-12.

Parker, M. L., S. Houston, H. Petrosova, K. V. Lithgow, R. Hof, C. Wetherell, W. C. Kao, Y. P. Lin, T. J. Moriarty, R. Ebady, C. E. Cameron, and M. J. Boulanger. 2016. 'The Structure of *Treponema pallidum* Tp0751 (Pallilysin) Reveals a Non-canonical Lipocalin Fold That Mediates Adhesion to Extracellular Matrix Components and Interactions with Host Cells', *PLoS Pathog*, 12: e1005919.

Parker, S. J., B. D. Halligan, and A. S. Greene. 2010. 'Quantitative analysis of SILAC data sets using spectral counting', *Proteomics*, 10: 1408-15.

Patti, J. M., B. L. Allen, M. J. McGavin, and M. Hook. 1994. 'MSCRAMM-mediated adherence of microorganisms to host tissues', *Annu Rev Microbiol*, 48: 585-617.

Patton, M. E., J. R. Su, R. Nelson, H. Weinstock, Control Centers for Disease, and Prevention. 2014. 'Primary and secondary syphilis--United States, 2005-2013', *MMWR Morb Mortal Wkly Rep*, 63: 402-6.

Pei H, Li L, Fridley BL, Jenkins GD, Kalari KR, Lingle W, Petersen G, Lou Z, Wang L. 2009. FKBP51 affects cancer cell response to chemotherapy by negatively regulating Akt. *Cancer Cell*. 16: 259–66.

Penn, C. W., A. Cockayne, and M. J. Bailey. 1985. 'The outer membrane of *Treponema pallidum*: biological significance and biochemical properties', *J Gen Microbiol*, 131: 2349-57.

Perdrup, A., B. B. Jorgensen, and N. S. Pedersen. 1981. 'The profile of neurosyphilis in Denmark A clinical and serological study of all patients in Denmark with neurosyphilis disclosed in the years 1971-1979 incl. by Wassermann reaction (CWRM) in the cerebrospinal fluid', *Acta Derm Venereol Suppl (Stockh)*, 96: 1-14.

Perez, F., and P. Mayaud. 2019. 'One step in the right direction: improving syphilis screening and treatment in pregnant women in Africa', *Lancet Glob Health*.

Peterson, K. M., J. B. Baseman, and J. F. Alderete. 1983. '*Treponema pallidum* receptor binding proteins interact with fibronectin', *J Exp Med*, 157: 1958-70.

Petrosova, H., P. Pospisilova, M. Strouhal, D. Cejkova, M. Zobanikova, L. Mikalova, E. Sodergren, G. M. Weinstock, and D. Smajs. 2013. 'Resequencing of *Treponema pallidum* ssp. *pallidum* strains Nichols and SS14: correction of sequencing errors resulted in increased separation of syphilis treponeme subclusters', *PLoS One*, 8: e74319.

Prasain, N., and T. Stevens. 2009. 'The actin cytoskeleton in endothelial cell phenotypes', *Microvasc Res*, 77: 53-63.

Preta, G., J. G. Cronin, and I. M. Sheldon. 2015. 'Dynasore - not just a dynamin inhibitor', *Cell Commun Signal*, 13: 24.

Preta, G., V. Lotti, J. G. Cronin, and I. M. Sheldon. 2015. 'Protective role of the dynamin inhibitor Dynasore against the cholesterol-dependent cytolysin of *Trueperella pyogenes*', *FASEB J*, 29: 1516-28.

Public Health Agency of Canada. 2017. ' Public Health Agency of Canada. Report on Sexually Transmitted Infections in Canada: 2013 - 2014.'. Available from: https://www.canada.ca/en/public-health/services/publications/diseases-conditions/report-sexually-transmitted-infections-canada-2013-14.html

Public Health England. 2015. 'Infection Report: Sexually Transmitted Infections', *Public Health England, London*.

Purcell, D. W., D. Higa, Y. Mizuno, and C. Lyles. 2017. 'Quantifying the Harms and Benefits from Serosorting Among HIV-Negative Gay and Bisexual Men: A Systematic Review and Meta-analysis', *AIDS Behav*, 21: 2835-43.

Radolf, J. D. 1995. '*Treponema pallidum* and the quest for outer membrane proteins', *Mol Microbiol*, 16: 1067-73.

Radolf, J. D., R. K. Deka, A. Anand, D. Smajs, M. V. Norgard, and X. F. Yang. 2016. '*Treponema pallidum*, the syphilis spirochete: making a living as a stealth pathogen', *Nat Rev Microbiol*, 14: 744-59.

Radolf, J. D., and S. Kumar. 2018. 'The *Treponema pallidum* Outer Membrane', *Curr Top Microbiol Immunol*, 415: 1-38.

Radolf, J. D., M. V. Norgard, and W. W. Schulz. 1989. 'Outer membrane ultrastructure explains the limited antigenicity of virulent *Treponema pallidum*', *Proc Natl Acad Sci U S A*, 86: 2051-5.

Radolf J.D., Fehniger T.E., Silverblatt F.J., Miller J.N., and M.A. Lovett. 1986. The surface of virulent *Treponema pallidum*: resistance to antibody binding in the absence of complement and surface association of recombinant antigen 4D, *Infect Immun*, 52:579–85

Raiziss GW, Severac M. 1937. 'Rapidity with which *Spirochaeta pallida* invades the blood stream', *Arch Dermatol Syph*, 35: 1101-09.

Rao, N. C., S. H. Barsky, V. P. Terranova, and L. A. Liotta. 1983. 'Isolation of a tumor cell laminin receptor', *Biochem Biophys Res Commun*, 111: 804-8.

Rappsilber, J., M. Mann, and Y. Ishihama. 2007. 'Protocol for micro-purification, enrichment, pre-fractionation and storage of peptides for proteomics using StageTips', *Nat Protoc*, 2: 1896-906.

Rato, M., Luis, P., Vale, E., Viana, I., . 2018. 'Syphilis: Relevance of immunohistochemistry for the diagnosis', *Journal of the American Academy of Dermatology*, 79: AB277.

Rehm, K., and S. Linder. 2017. 'Drebrin's Role in the Maintenance of Endothelial Integrity', *Adv Exp Med Biol*, 1006: 347-60.

Rehm, K., L. Panzer, V. van Vliet, E. Genot, and S. Linder. 2013. 'Drebrin preserves endothelial integrity by stabilizing nectin at adherens junctions', *J Cell Sci*, 126: 3756-69.

Reitsma, S., D. W. Slaaf, H. Vink, M. A. van Zandvoort, and M. G. oude Egbrink. 2007. 'The endothelial glycocalyx: composition, functions, and visualization', *Pflugers Arch*, 454: 345-59.

Riley, B. S., N. Oppenheimer-Marks, E. J. Hansen, J. D. Radolf, and M. V. Norgard. 1992. 'Virulent *Treponema pallidum* activates human vascular endothelial cells', *J Infect Dis*, 165: 484-93.

Riley, B. S., N. Oppenheimer-Marks, J. D. Radolf, and M. V. Norgard. 1994. 'Virulent *Treponema pallidum* promotes adhesion of leukocytes to human vascular endothelial cells', *Infect Immun*, 62: 4622-5.

Ring, A., J. N. Weiser, and E. I. Tuomanen. 1998. 'Pneumococcal trafficking across the blood-brain barrier. Molecular analysis of a novel bidirectional pathway', *J Clin Invest*, 102: 347-60.

Rodal, S. K., G. Skretting, O. Garred, F. Vilhardt, B. van Deurs, and K. Sandvig. 1999. 'Extraction of cholesterol with methyl-beta-cyclodextrin perturbs formation of clathrin-coated endocytic vesicles', *Mol Biol Cell*, 10: 961-74.

Rogers, L. D., N. F. Brown, Y. Fang, S. Pelech, and L. J. Foster. 2011. 'Phosphoproteomic analysis of Salmonella-infected cells identifies key kinase regulators and SopB-dependent host phosphorylation events', *Sci Signal*, 4: rs9.

Rogers, L. D., Y. Fang, and L. J. Foster. 2010. 'An integrated global strategy for cell lysis, fractionation, enrichment and mass spectrometric analysis of phosphorylated peptides', *Mol Biosyst*, 6: 822-9.

Rompalo, A. M., J. Lawlor, P. Seaman, T. C. Quinn, J. M. Zenilman, and E. W. Hook, 3rd. 2001. 'Modification of syphilitic genital ulcer manifestations by coexistent HIV infection', *Sex Transm Dis*, 28: 448-54.

Rothberg, K. G., Y. S. Ying, B. A. Kamen, and R. G. Anderson. 1990. 'Cholesterol controls the clustering of the glycophospholipid-anchored membrane receptor for 5-methyltetrahydrofolate', *J Cell Biol*, 111: 2931-8.

Salmeri, M., C. Motta, C. D. Anfuso, A. Amodeo, M. Scalia, M. A. Toscano, M. Alberghina, and G. Lupo. 2013. 'VEGF receptor-1 involvement in pericyte loss induced by *Escherichia coli* in an in vitro model of blood brain barrier', *Cell Microbiol*, 15: 1367-84.

Samuelson, D. R., and M. E. Konkel. 2013. 'Serine phosphorylation of cortactin is required for maximal host cell invasion by *Campylobacter jejuni*', *Cell Commun Signal*, 11: 82.

Sandok, P. L., H. M. Jenkin, S. R. Graves, and S. T. Knight. 1976. 'Retention of motility of *Treponema pallidum* (Nichols virulent strain) in an anaerobic cell culture system and in a cell-free system', *J Clin Microbiol*, 3: 72-4.

Sato, H., and J. Coburn. 2017. '*Leptospira interrogans* causes quantitative and morphological disturbances in adherens junctions and other biological groups of proteins in human endothelial cells', *PLoS Negl Trop Dis*, 11: e0005830.

Savage, E. J., G. Hughes, C. Ison, C. M. Lowndes, and network European Surveillance of Sexually Transmitted Infections. 2009. 'Syphilis and gonorrhoea in men who have sex with men: a European overview', *Euro Surveill*, 14.

Savage, E. J., K. Marsh, S. Duffell, C. A. Ison, A. Zaman, and G. Hughes. 2012. 'Rapid increase in gonorrhoea and syphilis diagnoses in England in 2011', *Euro Surveill*, 17.

Schimmel, L., N. Heemskerk, and J. D. van Buul. 2017. 'Leukocyte transendothelial migration: A local affair', *Small GTPases*, 8: 1-15.

Schnitzer, J. E., P. Oh, E. Pinney, and J. Allard. 1994. 'Filipin-sensitive caveolae-mediated transport in endothelium: reduced transcytosis, scavenger endocytosis, and capillary permeability of select macromolecules', *J Cell Biol*, 127: 1217-32.

Schroder, A., B. Schroder, B. Roppenser, S. Linder, B. Sinha, R. Fassler, and M. Aepfelbacher. 2006. '*Staphylococcus aureus* fibronectin binding protein-A induces motile attachment sites and complex actin remodeling in living endothelial cells', *Mol Biol Cell*, 17: 5198-210.

Schulte, D., V. Kuppers, N. Dartsch, A. Broermann, H. Li, A. Zarbock, O. Kamenyeva, F. Kiefer, A. Khandoga, S. Massberg, and D. Vestweber. 2011. 'Stabilizing the VE-cadherin-catenin complex blocks leukocyte extravasation and vascular permeability', *EMBO J*, 30: 4157-70.

Schwarz-Linek, U., J. M. Werner, A. R. Pickford, S. Gurusiddappa, J. H. Kim, E. S. Pilka, J. A. Briggs, T. S. Gough, M. Hook, I. D. Campbell, and J. R. Potts. 2003. 'Pathogenic bacteria attach to human fibronectin through a tandem beta-zipper', *Nature*, 423: 177-81.

Schweitzer, J. K., A. E. Sedgwick, and C. D'Souza-Schorey. 2011. 'ARF6-mediated endocytic recycling impacts cell movement, cell division and lipid homeostasis', *Semin Cell Dev Biol*, 22: 39-47.

Seebach, J. Cao, J, Schnittler, H J. 2016. 'Quantitative dynamics of VE-cadherin at endothelial cell junctions at a glance: basic requirements and current concepts', *DISCOVERIES*, 4: E63.

Seebach, J., A. A. Taha, J. Lenk, N. Lindemann, X. Jiang, K. Brinkmann, S. Bogdan, and H. J. Schnittler. 2015. 'The CellBorderTracker, a novel tool to quantitatively analyze spatiotemporal endothelial junction dynamics at the subcellular level', *Histochem Cell Biol*, 144: 517-32.

Selbach, M., and S. Backert. 2005. 'Cortactin: an Achilles' heel of the actin cytoskeleton targeted by pathogens', *Trends Microbiol*, 13: 181-9.

Shechter, R., A. London, and M. Schwartz. 2013. 'Orchestrated leukocyte recruitment to immune-privileged sites: absolute barriers versus educational gates', *Nat Rev Immunol*, 13: 206-18.

Sheffield, J. S., P. J. Sanchez, G. Morris, M. Maberry, F. Zeray, D. D. McIntire, and G. D. Wendel, Jr. 2002. 'Congenital syphilis after maternal treatment for syphilis during pregnancy', *Am J Obstet Gynecol*, 186: 569-73.

Shen, Q., M. H. Wu, and S. Y. Yuan. 2009. 'Endothelial contractile cytoskeleton and microvascular permeability', *Cell Health Cytoskelet*, 2009: 43-50.

Shin, J., J. Rhim, Y. Kwon, S. Y. Choi, S. Shin, C. W. Ha, and C. Lee. 2019. 'Comparative analysis of differentially secreted proteins in serum-free and serum-containing media by using BONCAT and pulsed SILAC', *Sci Rep*, 9: 3096.

Sidebottom, D., A. M. Ekstrom, and S. Stromdahl. 2018. 'A systematic review of adherence to oral pre-exposure prophylaxis for HIV - how can we improve uptake and adherence?', *BMC Infect Dis*, 18: 581.

Sidibe, M., and P. K. Singh. 2016. 'Thailand eliminates mother-to-child transmission of HIV and syphilis', *Lancet*, 387: 2488-9.

Simms, I., K. A. Fenton, M. Ashton, K. M. Turner, E. E. Crawley-Boevey, R. Gorton, D. R. Thomas, A. Lynch, A. Winter, M. J. Fisher, L. Lighton, H. C. Maguire, and M.

Solomou. 2005. 'The re-emergence of syphilis in the United Kingdom: the new epidemic phases', *Sex Transm Dis*, 32: 220-6.

Singh, B., C. Fleury, F. Jalalvand, and K. Riesbeck. 2012. 'Human pathogens utilize host extracellular matrix proteins laminin and collagen for adhesion and invasion of the host', *FEMS Microbiol Rev*, 36: 1122-80.

Slanina, H., S. Hebling, C. R. Hauck, and A. Schubert-Unkmeir. 2012. 'Cell invasion by *Neisseria meningitidis* requires a functional interplay between the focal adhesion kinase, Src and cortactin', *PLoS One*, 7: e39613.

Snyers, L., D. Thines-Sempoux, and R. Prohaska. 1997. 'Colocalization of stomatin (band 7.2b) and actin microfilaments in UAC epithelial cells', *Eur J Cell Biol*, 73: 281-5.

Snyers, L., E. Umlauf, and R. Prohaska. 1999. 'Association of stomatin with lipid-protein complexes in the plasma membrane and the endocytic compartment', *Eur J Cell Biol*, 78: 802-12.

Sousa, S., D. Cabanes, L. Bougneres, M. Lecuit, P. Sansonetti, G. Tran-Van-Nhieu, and P. Cossart. 2007. 'Src, cortactin and Arp2/3 complex are required for E-cadherin-mediated internalization of Listeria into cells', *Cell Microbiol*, 9: 2629-43.

Srinivasan, B., A. R. Kolli, M. B. Esch, H. E. Abaci, M. L. Shuler, and J. J. Hickman. 2015. 'TEER measurement techniques for in vitro barrier model systems', *J Lab Autom*, 20: 107-26.

Stamm, L.V., Folds, J.D., and P.J. Bassford. 1982. ‘Expression of *Treponema pallidum* antigens in *Escherichia coli* K-12’, *Infect Immun* 36: 1238-41.

Stamm, L. V., and H. L. Bergen. 2000. 'A point mutation associated with bacterial macrolide resistance is present in both 23S rRNA genes of an erythromycin-resistant *Treponema pallidum* clinical isolate', *Antimicrob Agents Chemother*, 44: 806-7.

Stamm, W. E., H. H. Handsfield, A. M. Rompalo, R. L. Ashley, P. L. Roberts, and L. Corey. 1988. 'The association between genital ulcer disease and acquisition of HIV infection in homosexual men', *JAMA*, 260: 1429-33.

Stebeck, C. E., J. M. Shaffer, T. W. Arroll, S. A. Lukehart, and W. C. Van Voorhis. 1997. 'Identification of the *Treponema pallidum* subsp. *pallidum* glycerophosphodiester phosphodiesterase homologue', *FEMS Microbiol Lett*, 154: 303-10.

Stokes, J. H., Beerman H., Ingraham N. R. 1944. 'Modern clinical syphilology', *The W.B. Saunders Co., Philadelphia, Pa*.

Stoltey, J. E., and S. E. Cohen. 2015. 'Syphilis transmission: a review of the current evidence', *Sex Health*, 12: 103-9.

Sugiyama, N., T. Masuda, K. Shinoda, A. Nakamura, M. Tomita, and Y. Ishihama. 2007. 'Phosphopeptide enrichment by aliphatic hydroxy acid-modified metal oxide chromatography for nano-LC-MS/MS in proteomics applications', *Mol Cell Proteomics*, 6: 1103-9.

Sukumaran, S. K., and N. V. Prasadarao. 2003. '*Escherichia coli* K1 invasion increases human brain microvascular endothelial cell monolayer permeability by disassembling vascular-endothelial cadherins at tight junctions', *J Infect Dis*, 188: 1295-309.

Sukumaran, S. K., M. J. Quon, and N. V. Prasadarao. 2002. '*Escherichia coli* K1 internalization via caveolae requires caveolin-1 and protein kinase Calpha

interaction in human brain microvascular endothelial cells', *J Biol Chem*, 277: 50716-24.

Sun, E. S., B. J. Molini, L. K. Barrett, A. Centurion-Lara, S. A. Lukehart, and W. C. Van Voorhis. 2004. 'Subfamily I *Treponema pallidum* repeat protein family: sequence variation and immunity', *Microbes Infect*, 6: 725-37.

Swanson, J. A. 2008. 'Shaping cups into phagosomes and macropinosomes', *Nat Rev Mol Cell Biol*, 9: 639-49.

Sykes, J. A., and J. Kalan. 1975. 'Intracellular *Treponema pallidum* in cells of a syphilitic lesion of the uterine cervix', *Am J Obstet Gynecol*, 122: 361-7.

Tanabe, K., H. Yamazaki, Y. Inaguma, A. Asada, T. Kimura, J. Takahashi, M. Taoka, T. Ohshima, T. Furuichi, T. Isobe, K. Nagata, T. Shirao, and S. Hisanaga. 2014. 'Phosphorylation of drebrin by cyclin-dependent kinase 5 and its role in neuronal migration', *PLoS One*, 9: e92291.

Taylor, M. M., X. Zhang, S. Nurse-Findlay, L. Hedman, and J. Kiarie. 2016. 'The amount of penicillin needed to prevent mother-to-child transmission of syphilis', *Bull World Health Organ*, 94: 559-59A.

Tegtmeyer, N., R. Wittelsberger, R. Hartig, S. Wessler, N. Martinez-Quiles, and S. Backert. 2011. 'Serine phosphorylation of cortactin controls focal adhesion kinase activity and cell scattering induced by *Helicobacter pylori*', *Cell Host Microbe*, 9: 520-31.

The UniProt Consortium. 2019. 'UniProt: a worldwide hub of protein knowledge', *Nucleic Acids Res*, 47: D505-15.

Thepparit, C., and D. R. Smith. 2004. 'Serotype-specific entry of dengue virus into liver cells: identification of the 37-kilodalton/67-kilodalton high-affinity laminin receptor as a dengue virus serotype 1 receptor', *J Virol*, 78: 12647-56.

Thingholm, T. E., and M. R. Larsen. 2016. 'The Use of Titanium Dioxide for Selective Enrichment of Phosphorylated Peptides', *Methods Mol Biol*, 1355: 135-46.

Thingholm, T. E., M. R. Larsen, C. R. Ingrell, M. Kassem, and O. N. Jensen. 2008. 'TiO(2)-based phosphoproteomic analysis of the plasma membrane and the effects of phosphatase inhibitor treatment', *J Proteome Res*, 7: 3304-13.

Thomas, D. D., J. B. Baseman, and J. F. Alderete. 1985. 'Fibronectin mediates *Treponema pallidum* cytadherence through recognition of fibronectin cell-binding domain', *J Exp Med*, 161: 514-25.

Thomas, D. D., A. M. Fogelman, J. N. Miller, and M. A. Lovett. 1989. 'Interactions of *Treponema pallidum* with endothelial cell monolayers', *Eur J Epidemiol*, 5: 15-21.

Thomas, D. D., M. Navab, D. A. Haake, A. M. Fogelman, J. N. Miller, and M. A. Lovett. 1988. '*Treponema pallidum* invades intercellular junctions of endothelial cell monolayers', *Proc Natl Acad Sci U S A*, 85: 3608-12.

Tio, P. H., W. W. Jong, and M. J. Cardosa. 2005. 'Two dimensional VOPBA reveals laminin receptor (LAMR1) interaction with dengue virus serotypes 1, 2 and 3', *Virol J*, 2: 25.

To, W. S., and K. S. Midwood. 2011. 'Plasma and cellular fibronectin: distinct and independent functions during tissue repair', *Fibrogenesis Tissue Repair*, 4: 21.

Tong Z, Kunnumakkara AB, Wang H, Matsuo Y, Diagaradjane P, Harikumar KB, Ramachandran V, Sung B, Chakraborty A, Bresalier RS, Logsdon C, Aggarwal

BB, Krishnan S, Guha S. 2008. Neutrophil gelatinase-associated lipocalin: a novel suppressor of invasion and angiogenesis in pancreatic cancer. *Cancer Res*. 68: 6100–8.

Tourville, D. R., L. H. Byrd, D. U. Kim, D. Zajd, I. Lee, L. B. Reichman, and S. Baskin. 1976. 'Treponemal antigen in immunopathogenesis of syphilitic glomerulonephritis', *Am J Pathol*, 82: 479-92.

Truong, H. M., T. Kellogg, J. D. Klausner, M. H. Katz, J. Dilley, K. Knapper, S. Chen, R. Prabhu, R. M. Grant, B. Louie, and W. McFarland. 2006. 'Increases in sexually transmitted infections and sexual risk behaviour without a concurrent increase in HIV incidence among men who have sex with men in San Francisco: a suggestion of HIV serosorting?', *Sex Transm Infect*, 82: 461-6.

Tucker, J. D., X. S. Chen, and R. W. Peeling. 2010. 'Syphilis and social upheaval in China', *N Engl J Med*, 362: 1658-61.

Tucker, J. D., and M. S. Cohen. 2011. 'China's syphilis epidemic: epidemiology, proximate determinants of spread, and control responses', *Curr Opin Infect Dis*, 24: 50-5.

Tucker, J. D., J. Z. Li, G. K. Robbins, B. T. Davis, A. M. Lobo, J. Kunkel, G. N. Papaliodis, M. L. Durand, and D. Felsenstein. 2011. 'Ocular syphilis among HIV-infected patients: a systematic analysis of the literature', *Sex Transm Infect*, 87: 4-8.

Ubersax, J. A., and J. E. Ferrell, Jr. 2007. 'Mechanisms of specificity in protein phosphorylation', *Nat Rev Mol Cell Biol*, 8: 530-41.

Valeski, J. E., and A. L. Baldwin. 1999. 'Effect of early transient adherent leukocytes on venular permeability and endothelial actin cytoskeleton', *Am J Physiol*, 277: H569-75.

Veggi D, Gentile MA, Cantini F, Lo Surdo P, Nardi-Dei V, Seib KL, Pizza M, Rappuoli R, Banci L, Savino S, and Scarselli M. 2012. The factor H binding protein of *Neisseria meningitidis* interacts with xenosiderophores in vitro. Biochemistry.;51(46):9384–93.

Venning, F. A., L. Wullkopf, and J. T. Erler. 2015. 'Targeting ECM Disrupts Cancer Progression', *Front Oncol*, 5: 224.

Venkatesha S, Hanai J, Seth P, Karumanchi SA, Sukhatme VP. 2006. Lipocalin 2 antagonizes the proangiogenic action of ras in transformed cells. *Mol Cancer Res*, 4: 821–829.

Vercauteren, D., R. E. Vandenbroucke, A. T. Jones, J. Rejman, J. Demeester, S. C. De Smedt, N. N. Sanders, and K. Braeckmans. 2010. 'The use of inhibitors to study endocytic pathways of gene carriers: optimization and pitfalls', *Mol Ther*, 18: 561-9.

Vercauteren, D., Piest, M., van der Aa, L.J., Soraj, M.A., Jones, A.W., Engbersen, J.F.J, De Smedt, S.C., and K. Braeckmans. 2011. 'Flotillin-dependent endocytosis and a phagocytosis-like mechanism for cellular itnernalization of disulfide-based poly(amido amine)/DNA polyplexes', *Biomaterials*, 32(11): 3072-84.

Vestweber, D. 2015. 'How leukocytes cross the vascular endothelium', *Nat Rev Immunol*, 15: 692-704.

Villringer, A., A. Them, U. Lindauer, K. Einhaupl, and U. Dirnagl. 1994. 'Capillary perfusion of the rat brain cortex. An in vivo confocal microscopy study', *Circ Res*, 75: 55-62.

Voigt, J., J. Christensen, and V. P. Shastri. 2014. 'Differential uptake of nanoparticles by endothelial cells through polyelectrolytes with affinity for caveolae', *Proc Natl Acad Sci U S A*, 111: 2942-7.

Volk, J. E., J. L. Marcus, T. Phengrasamy, D. Blechinger, D. P. Nguyen, S. Follansbee, and C. B. Hare. 2015. 'No New HIV Infections With Increasing Use of HIV Preexposure Prophylaxis in a Clinical Practice Setting', *Clin Infect Dis*, 61: 1601-3.

Volk, T., and W. J. Kox. 2000. 'Endothelium function in sepsis', *Inflamm Res*, 49: 185-98.

von Andrian, U. H., and T. R. Mempel. 2003. 'Homing and cellular traffic in lymph nodes', *Nat Rev Immunol*, 3: 867-78.

Walfied, A.M., Hanff, P.A., and M.A. Lovett. 1982. 'Expression of *Treponema pallidum* antigens in *Escherichia coli*', *Science*, 216: 522-23.

Walker, E. M., G. A. Zampighi, D. R. Blanco, J. N. Miller, and M. A. Lovett. 1989. 'Demonstration of rare protein in the outer membrane of *Treponema pallidum* subsp. *pallidum* by freeze-fracture analysis', *J Bacteriol*, 171: 5005-11.

Wang, H., L. Zhang, Y. Zhou, K. Wang, X. Zhang, J. Wu, and G. Wang. 2018. 'The use of geosocial networking smartphone applications and the risk of sexually transmitted infections among men who have sex with men: a systematic review and meta-analysis', *BMC Public Health*, 18: 1178.

Wang, K. S., R. J. Kuhn, E. G. Strauss, S. Ou, and J. H. Strauss. 1992. 'High-affinity laminin receptor is a receptor for Sindbis virus in mammalian cells', *J Virol*, 66: 4992-5001.

Watts, P. J., H. L. Greenberg, and A. Khachemoune. 2016. 'Unusual primary syphilis: Presentation of a likely case with a review of the stages of acquired syphilis, its differential diagnoses, management, and current recommendations', *Int J Dermatol*, 55: 714-28.

Weed, S. A., and J. T. Parsons. 2001. 'Cortactin: coupling membrane dynamics to cortical actin assembly', *Oncogene*, 20: 6418-34.

Wegener, J., and J. Seebach. 2014. 'Experimental tools to monitor the dynamics of endothelial barrier function: a survey of in vitro approaches', *Cell Tissue Res*, 355: 485-514.

Weinstein, A., R. H. Kampmeier, and T. R. Harwood. 1957. 'Complete heart block due to syphilis', *AMA Arch Intern Med*, 100: 90-100.

Wessel, F., M. Winderlich, M. Holm, M. Frye, R. Rivera-Galdos, M. Vockel, R. Linnepe, U. Ipe, A. Stadtmann, A. Zarbock, A. F. Nottebaum, and D. Vestweber. 2014. 'Leukocyte extravasation and vascular permeability are each controlled in vivo by different tyrosine residues of VE-cadherin', *Nat Immunol*, 15: 223-30.

White, E. S. 2015. 'Lung extracellular matrix and fibroblast function', *Ann Am Thorac Soc*, 12 Suppl 1: S30-3.

Wijesooriya, N. S., R. W. Rochat, M. L. Kamb, P. Turlapati, M. Temmerman, N. Broutet, and L. M. Newman. 2016. 'Global burden of maternal and congenital syphilis in

2008 and 2012: a health systems modelling study', *Lancet Glob Health*, 4: e525-33.

Wimley, W. C. 2003. 'The versatile beta-barrel membrane protein', *Curr Opin Struct Biol*, 13: 404-11.

Wolgemuth, C. W. 2015. 'Flagellar motility of the pathogenic spirochetes', *Semin Cell Dev Biol*, 46: 104-12.

Woolston, S., S. E. Cohen, R. N. Fanfair, S. C. Lewis, C. M. Marra, and M. R. Golden. 2015. 'A Cluster of Ocular Syphilis Cases - Seattle, Washington, and San Francisco, California, 2014-2015', *MMWR Morb Mortal Wkly Rep*, 64: 1150-1.

Woolston, S. L., S. Dhanireddy, and J. Marrazzo. 2016. 'Ocular Syphilis: a Clinical Review', *Curr Infect Dis Rep*, 18: 36.

Workowski, K. A. 2015. 'Centers for Disease Control and Prevention Sexually Transmitted Diseases Treatment Guidelines', *Clin Infect Dis*, 61 Suppl 8: S759-62.

World Health Organization. 2012. 'Investment case for eliminating mother-to-child transmission of syphilis: Promoting better maternal and child health and stronger health systems.' Geneva, Switzerland. Available from: https://www.who.int/reproductivehealth/publications/rtis/9789241504348/en/

World Health Organization. 2016a. 'Report on global sexually transmitted infection surveillance 2015.' Geneva, Switzerland. Available from: https://www.who.int/reproductivehealth/publications/rtis/stis-surveillance-2015/en/

World Health Organization. 2016b. 'Sixty-ninth World Health Assembly closes', Geneva, Switzerland. Available from: https://www.who.int/en/news-room/detail/28-05-2016-sixty-ninth-world-health-assembly-closes

Worth, D. C., C. N. Daly, S. Geraldo, F. Oozeer, and P. R. Gordon-Weeks. 2013. 'Drebrin contains a cryptic F-actin-bundling activity regulated by Cdk5 phosphorylation', *J Cell Biol*, 202: 793-806.

Wu, F., J. P. Zhang, and Q. Q. Wang. 2017. 'Scanning electron microscopy of the adhesion of *Treponema pallidum* subspecies *pallidum* (Nichol strain) to human brain microvascular endothelial cells in vitro', *J Eur Acad Dermatol Venereol*, 31: e221-e23.

Wu, H. J., A. H. Wang, and M. P. Jennings. 2008. 'Discovery of virulence factors of pathogenic bacteria', *Curr Opin Chem Biol*, 12: 93-101.

Wu, J., E. H. Weening, J. B. Faske, M. Hook, and J. T. Skare. 2011. 'Invasion of eukaryotic cells by *Borrelia burgdorferi* requires beta(1) integrins and Src kinase activity', *Infect Immun*, 79: 1338-48.

Wurmbach E, Chen YB, Khitrov G, Zhang W, Roayaie S, Schwartz M, Fiel I, Thung S, Mazzaferro V, Bruix J, Bottinger E, Friedman S, Waxman S, and Llovet JM. 2007. Genome-wide molecular profiles of HCV-induced dysplasia and hepatocellular carcinoma. *Hepatology*. 45: 938–47.

Yan L, Borregaard N, Kjeldsen L, Moses MA. 2001. The high molecular weight urinary matrix metalloproteinase (MMP) activity is a complex of gelatinase B/MMP-9 and neutrophil gelatinase-associated lipocalin (NGAL). Modulation of MMP-9 activity by NGAL. *J Biol Chem*; 276: 37258–65.

Yousif, L. F., J. Di Russo, and L. Sorokin. 2013. 'Laminin isoforms in endothelial and perivascular basement membranes', *Cell Adh Migr*, 7: 101-10.

Yuan, S. Y., and R. R. Rigor. 2010. Regulation of Endothelial Barrier Function. San Rafael (CA): Morgan & Claypool Life Sciences.

Zanivan, Sara, Federica Maione, Marco Y. Hein, Juan Ramon Hernández-Fernaud, Pawel Ostasiewicz, Enrico Giraudo, and Matthias Mann. 2013. 'SILAC-Based Proteomics of Human Primary Endothelial Cell Morphogenesis Unveils Tumor Angiogenic Markers', 12: 3599-611.

Zettl, M., and M. Way. 2001. 'New tricks for an old dog?', *Nat Cell Biol*, 3: E74-5.

Zhang, F. X., C. J. Kirschning, R. Mancinelli, X. P. Xu, Y. Jin, E. Faure, A. Mantovani, M. Rothe, M. Muzio, and M. Arditi. 1999. 'Bacterial lipopolysaccharide activates nuclear factor-kappaB through interleukin-1 signaling mediators in cultured human dermal endothelial cells and mononuclear phagocytes', *J Biol Chem*, 274: 7611-4.

Zhang, L., Y. Tao, J. Woodring, K. Rattana, S. Sovannarith, T. Rathavy, K. Cheang, S. Hossain, L. Ferradini, S. Deng, C. Sokun, C. Samnang, M. Nagai, Y. R. Lo, and N. Ishikawa. 2019. 'Integrated approach for triple elimination of mother-to-child transmission of HIV, hepatitis B and syphilis is highly effective and cost-effective: an economic evaluation', *Int J Epidemiol*.

Zhang, R. L., Q. Q. Wang, J. P. Zhang, and L. J. Yang. 2015. 'Tp17 membrane protein of *Treponema pallidum* activates endothelial cells in vitro', *Int Immunopharmacol*, 25: 538-44.

Zhang, R. L., J. P. Zhang, and Q. Q. Wang. 2014. 'Recombinant *Treponema pallidum* protein Tp0965 activates endothelial cells and increases the permeability of endothelial cell monolayer', *PLoS One*, 9: e115134.

Zhao, B., R. A. Bowden, S. A. Stavchansky, and P. D. Bowman. 2001. 'Human endothelial cell response to gram-negative lipopolysaccharide assessed with cDNA microarrays', *Am J Physiol Cell Physiol*, 281: C1587-95.

Zhao, Y., N. S. Mangalmurti, Z. Xiong, B. Prakash, F. Guo, D. B. Stolz, and J. S. Lee. 2011. 'Duffy antigen receptor for chemokines mediates chemokine endocytosis through a macropinocytosis-like process in endothelial cells', *PLoS One*, 6: e29624.

Zhou, J., T. Zhou, R. Cao, Z. Liu, J. Shen, P. Chen, X. Wang, and S. Liang. 2006. 'Evaluation of the application of sodium deoxycholate to proteomic analysis of rat hippocampal plasma membrane', *J Proteome Res*, 5: 2547-53.

Appendix

Copyright permissions for manuscripts and figures adapted in this dissertation:

(1) Cerutti, C., and A. J. Ridley. 2017. 'Endothelial cell-cell adhesion and signaling', *Exp Cell Res*, 358: 31-38.

-No permission required from Elselvier (Open access).

"This article is available under the terms of the Creative Commons Attribution License (CC BY). You may copy and distribute the article, create extracts, abstracts and new works from the article, alter and revise the article, text or data mine the article and otherwise reuse the article commercially (including reuse and/or resale of the article) without permission from Elsevier. You must give appropriate credit to the original work, together with a link to the formal publication through the relevant DOI and a link to the Creative Commons user license above. You must indicate if any changes are made but not in any way that suggests the licensor endorses you or your use of the work. Permission is not required for this type of reuse."

Accessed April 02, 2019. Article available from:

doi: 10.1016/j.yexcr.2017.06.003

(2) Aird, W. C. 2007b. 'Phenotypic heterogeneity of the endothelium: I. Structure, function, and mechanisms', *Circ Res*, 100: 158-73.

-Printed with permission from Wolters Kluwer Health, Inc.

Accessed April 02, 2019. Article available from:

doi: 10.1161/01.RES.0000255691.76142.4a

(3) Schimmel, L., N. Heemskerk, and J. D. van Buul. 2017. 'Leukocyte transendothelial migration: A local affair', *Small GTPases*, 8: 1-15.

-Printed with permission from Taylor & Francis

"Taylor & Francis is pleased to offer reuses of its content for a thesis or dissertation free of charge contingent on resubmission of permission request if work is published."

Accessed April 02, 2019. Article available from:

doi: 10.1080/21541248.2016.1197872

(4) Kao, W. A., H. Petrosova, R. Ebady, K. V. Lithgow, P. Rojas, Y. Zhang, Y. E. Kim, Y. R. Kim, T. Odisho, N. Gupta, A. Moter, C. E. Cameron, and T. J. Moriarty. 2017. 'Identification of Tp0751 (Pallilysin) as a Treponema pallidum Vascular Adhesin by Heterologous Expression in the Lyme disease Spirochete', *Sci Rep*, 7: 1538.
-Open access journal (no permission required)

(5) Parker, M. L., S. Houston, H. Petrosova, K. V. Lithgow, R. Hof, C. Wetherell, W. C. Kao, Y. P. Lin, T. J. Moriarty, R. Ebady, C. E. Cameron, and M. J. Boulanger. 2016. 'The Structure of Treponema pallidum Tp0751 (Pallilysin) Reveals a Non-canonical Lipocalin Fold That Mediates Adhesion to Extracellular Matrix Components and Interactions with Host Cells', *PLoS Pathog*, 12: e1005919.
-Open access journal (no permission required)